

Thèse de doctorat

NNT : 2024UPASI014



Climate uncertainties

Incertitudes climatiques

Thèse de doctorat de l'Université Paris-Saclay

École doctorale n°630 Droit, Économie, Management (DEM)
Spécialité de doctorat : Sciences Économiques
Graduate school : Economics & Management

Thèse préparée dans les UMR **Paris-Saclay Applied Economics** (INRAE, Université Paris-Saclay - AgroParisTech) & **CIRED** (CNRS, Cirad, EHESS, Institut Polytechnique de Paris - École des Ponts, Université Paris Saclay - AgroParisTech)

sous la direction de **Vincent Martinet**,
Directeur de recherche INRAE - Université Paris-Saclay, AgroParisTech

et la codirection de **Céline Guivarch**,
Directrice de recherche - Institut Polytechnique de Paris, École des Ponts

Thèse présentée et soutenue à Nogent-sur-Marne, le 9 décembre 2024, par

Romain Fillon

Composition du Jury

Marc Fleurbaey
Directeur de Recherche CNRS
Paris School of Economics & École Normale Supérieure Président

Fanny Henriet
Directrice de Recherche CNRS
Aix Marseille School of Economics Rapportrice

Frank Venmans
Associate Professor
London School of Economics, Grantham Institute Rapporteur

Frances Moore
Associate Professor
University of California at Davis Examinatrice

Vincent Martinet
Directeur de recherche INRAE
Université Paris-Saclay, AgroParisTech Directeur de thèse

Céline Guivarch
Directrice de recherche
Institut Polytechnique de Paris, École des Ponts Codirectrice de thèse

Titre : Incertitudes climatiques**Mots clés :** Politiques climatiques, risques, choix social, modélisation dynamique sto-chastique économie-climat, approches spatiales

Résumé : J'étudie les incertitudes climatiques et leurs impacts économiques. Dans le premier chapitre, nous discutons des limites et alternatives aux critères habituels de choix social intertemporel. Si ces critères sont bien adaptés aux risques standards, leur usage devrait être discuté en présence de risques irréversibles de changement de régime tels que les points de basculement climatiques, où le risque agrégé sur le bien-être des générations présentes et futures est important. En effet, ces modèles font l'hypothèse que le planificateur est neutre vis-à-vis de ce risque agrégé. Au contraire, nous montrons qu'introduire de l'aversion temporelle au risque agrégé implique une augmentation importante du coût social du carbone (SCC) en présence de risques catastrophiques irréversibles de points de basculement. Dans le deuxième chapitre, nous décomposons le module climatique des modèles économiques pour analyser et quantifier comment les interactions dynamiques entre le risque climatique global et des sous-systèmes climatiques affectent la politique climatique mondiale et la gestion régionale de ces sous-systèmes. Nous appliquons notre cadre théorique au sort controversé de la forêt amazonienne. Notre approche aboutit à deux résultats méthodologiques clés. Premièrement, le SCC doit inclure l'impact qu'a une augmentation marginale des émissions cumulées à l'échelle mondiale sur la dynamique de la forêt amazonienne. Cela inclut à la fois une mise à l'échelle des politiques actuelles en tenant compte des émissions de carbone de la forêt amazonienne sous un climat changeant, ainsi qu'un canal d'assurance, le « beta amazonien », car la va-

leur sociale des émissions de carbone varie selon les états du monde dans lesquels elles se produisent. Deuxièmement, la valeur sociale de la forêt amazonienne en tant que stock de carbone ne peut se réduire à la quantité de carbone qu'elle contient : le coût social du système dynamique est également important, c'est-à-dire le coût d'une diminution marginale dans l'état du sous-système qui réduit sa capacité à se perpétuer. Dans le troisième chapitre, nous quantifions dans quelle mesure l'agrégation spatiale et temporelle des données de température lors de la projection des impacts climatiques futurs pourrait masquer les incertitudes scientifiques entre les projections climatiques et sous-estimer les dommages climatiques futurs. Dans le quatrième chapitre, je quantifie l'impact des canaux bio-physiques (albédo, évapotranspiration, rugosité) sur la distribution et les impacts agrégés du changement climatique sur le bien-être le long du scénario SSP2-4.5 à l'échelle globale et à une résolution de 1° grillée. Ces canaux sont endogènes aux activités économiques régionales en raison des changements d'utilisation des terres agricoles et urbaines et ils interagissent avec les stratégies d'adaptation comme la migration ou le changement structurel. En conclusion, ma thèse suit trois directions : documenter les conséquences économiques des incertitudes climatiques, contribuer méthodologiquement à l'étude de l'incertitude à l'interface des systèmes humains et naturels, et enrichir la littérature sur le choix social normatif intertemporel avec des modèles numériques utilisés pour la quantification.

Title : Climate uncertainties

Keywords : Climate policies, risks, social choice, dynamic stochastic climate-economy modelling, spatial approaches

Abstract : I study climate uncertainties and their economic impacts. In the first chapter, we discuss the limitations and alternatives to the standard criteria for intertemporal social choice. While these criteria are well-suited for standard risks, their use should be reconsidered in the presence of irreversible regime-shift risks, such as climate tipping points, where the aggregate risk to the welfare of present and future generations is significant. Indeed, these models assume that the planner is risk-neutral regarding this aggregate risk. In contrast, we show that introducing risk aversion over time significantly increases the social cost of carbon (SCC) in the presence of irreversible catastrophic tipping point risks. In the second chapter, we decompose the climate module of economic models to analyze and quantify how the dynamic interactions between global climate risk and climate subsystems affect global climate policy and the regional management of these subsystems. We apply our theoretical framework to the controversial fate of the Amazon rainforest. Our approach yields two key methodological insights. First, the SCC should include the impact that a marginal increase in cumulative global emissions has on the dynamics of the Amazon rainforest. This includes scaling current policies to account for carbon emissions from the Amazon under a changing climate, as well as an insurance channel—the "Amazonian beta"—as the social value of carbon emis-

sions varies according to the states of the world in which they occur. Second, the social value of the Amazon rainforest as a carbon stock cannot be reduced to the quantity of carbon it contains; the social cost of the dynamic system is also crucial, that is, the cost of a marginal decline in the state of the subsystem that reduces its capacity to persist. In the third chapter, we quantify the extent to which the spatial and temporal aggregation of temperature data in climate impact projections might obscure scientific uncertainties between climate projections and underestimate future climate damages. In the fourth chapter, I quantify the impact of biophysical channels (albedo, evapotranspiration, roughness) on the distribution and aggregate impacts of climate change on welfare along the Shared Concentration Pathway SSP2-4.5 at a global scale and at 1° resolution. These channels are endogenous to regional economic activities due to land use changes from agriculture and urbanization, and they interact with adaptation strategies such as migration or structural change. Thus, my dissertation follows three directions : documenting the economic consequences of climate uncertainties, contributing methodologically to the study of uncertainty at the interface of human and natural systems, and enriching the literature on intertemporal normative social choice through numerical models used for quantification.

Remerciements

Je tiens d'abord à remercier Céline et Vincent : votre complémentarité a été précieuse. Je mesure la chance d'avoir reçu un encadrement bienveillant qui m'a accordé beaucoup de confiance et de liberté dans mes projets de recherche, tout en étant rigoureux sur le fond! Au-delà des aspects scientifiques, vous m'avez beaucoup facilité la vie dans tous les aspects de la vie de doctorant et tout au long de la thèse, ce qui m'a permis de me concentrer sur la recherche. Cette thèse vous doit beaucoup! Merci à l'Université Paris-Saclay, au CIRED et à PSAE. Many thanks to Marc Fleurbaey, Fanny Henriet, Frances Moore and Frank Venmans for doing me the honor of serving on the jury.

J'ai eu la chance de pouvoir travailler avec des personnes passionnantes. Merci à Céline (encore!) et Nicolas, notamment pour ce projet mené ensemble au cours duquel j'ai beaucoup appris. Pour Céline, c'est un mentorat qui a débuté avant la thèse, avec ce stage qui a ensuite ouvert la porte à trois années passionnantes : nos entretiens fréquents vont me manquer! Merci à Philippe Ciais et Thomas Gasser, pour leur aide essentielle sur le deuxième chapitre. Thank you Gernot, for hosting me at Columbia, and Manuel, who joined the team! Merci à Fulbright d'avoir financé ce séjour américain. J'ai reçu de nombreux conseils de collègues plus expérimentés : je les en remercie vivement! Je remercie aussi mon comité de suivi : Johannes Emmerling, Aurélie Méjean, Natacha Raffin et Stéphane Zuber. Enfin, j'ai eu beaucoup de plaisir à discuter et débattre avec mes collègues doctorant·e·s au CIRED et à PSAE surtout, mais également dans les séminaires et conférences, ou lors de mon séjour américain. Je ne vais pas tenter un inventaire de ces personnes : elles sont le cœur de mon attachement à ce métier. Beaucoup sont désormais des ami·e·s. Enfin, dans la dernière ligne droite, la compagnie du petit équipage cirédiens du bout du couloir a été essentielle.

Merci à mes proches adorés, rencontrés durant ces années aux quatre coins de l'Île-de-France (notamment BL, cachanais·es, rêveurs·ses) et au-delà (Shanghai notamment!). J'ai une pensée émue pour le groupe d'une quinzaine d'hurluberlu·e·s avec qui j'ai grandi, presque quotidiennement à mes côtés en coévolution depuis plus ou moins quinze années : 'puisse qu'on puisse faire C X'! Merci à mon grand frère et ma grande sœur : pousser à l'ombre de vos branches a été bien confortable! Chacun à votre manière, vous avez contribué à teindre mon rouge (mon rose?) de vert. Merci enfin et surtout à mes chers parents pour leur goût des livres et du débat contradictoire, ainsi que pour leur amour formidable avec lequel on peut soulever toutes les montagnes et dont je tire ma sérénité.

Table des matières

Table des figures	viii
Liste des tableaux	xiii
Introduction [in english]	1
1 Four dimensions : time, space, risk and scientific uncertainty	2
1 Time	2
2 Space	4
3 Risk	5
4 Scientific uncertainties	8
5 This thesis	8
2 Climate policies : normative and positive approaches	9
1 Normative approaches	9
2 Positive approaches	10
3 Thesis description	11
1 Time, risk and scientific uncertainty	12
2 Time and space	14
3 List of research work	16
Introduction [en français]	17
1 Quatre dimensions : temps, espace, risque et incertitude scientifique	18
1 Temps	18
2 Espace	20
3 Risque	22
4 Incertitudes scientifiques	25
5 Cette thèse	25
2 Politiques climatiques : approches positives et normatives	26
1 Approches normatives	26
2 Approches positives	28
3 Description de la thèse	29
1 Temps, risque et incertitude scientifique	29

2	Temps et espace	33
3	Liste des travaux de recherche	35
	Bibliographie	37
1	Optimal climate policy under tipping risk and temporal risk aversion	40
1	Introduction	41
2	A dynamic climate-economy stochastic model	44
1	A simple illustration	44
2	The model	46
3	Social preferences	48
4	Comparison with alternative social preferences	49
3	How does temporal risk aversion affect optimal policy under a tipping risk?	51
4	A numerical investigation	56
1	Calibration	56
2	A comparison of the two social welfare functions under risk .	58
5	Discussion	61
6	Annex	64
1	Analytical decomposition details	64
2	Numerical resolution	65
3	Risk-sensitive preferences and the risk premium	66
4	Time paths	66
5	Sensitivities	70
	Bibliographie	72
2	The need for regulation of climate subsystems	76
1	Introduction	78
2	Modeling approach	84
1	A dynamic climate-economy model	84
2	Social choice criteria	86
3	Analytical definitions	88
3	A quantitative application : the Amazon rainforest	94
1	Model specification	95
2	Calibration	97
3	Results	100
4	Conclusion	106
5	Appendix	110
1	Analytical decomposition - SCC	110

2	Analytical decomposition - SCDS	113
3	Resolution of the model	113
4	Procedure for the calibration	115
5	Calibration	115
6	Consistency of the coefficients	121
7	Stochastic paths for some variables of interest	123
	Bibliographie	125
3	Climate shift uncertainty and economic damages	130
1	Introduction	131
2	Climate and economic data	134
1	Warming patterns	134
2	Econometric estimates of climate damages	136
3	Descriptive statistics	137
3	Quantification	139
1	Missing shape-related growth effect of climate change	139
2	Aggregate impacts	140
3	Distributional impacts	142
4	Conclusion	144
5	Annex	147
1	Building climate landscapes	147
	Bibliographie	148
4	The biophysical channels of climate impacts	150
1	Introduction	151
2	Motivation	157
1	Regional biophysical channels and their impacts	157
2	Impact of economic activities on LULC changes	160
3	Theoretical Model	162
1	Households	162
2	Production	164
3	Estimation of dose-response functions	167
4	Numerical results	172
1	Model resolution	172
2	Counterfactual climates and policies	174
3	Benchmark biogeochemical climate impacts (SSP2-4.5)	175
4	Counterfactual exogenous biophysical impacts (SSP2-4.5)	179
5	Discussion	181

6	Appendix	183
1	Migration in hat algebra	183
2	Profit maximization	183
3	Prices and bilateral trade flows in exact hat algebra	184
4	Welfare	185
5	Dose-response functions	185
6	Migration data	185
7	Algorithm	187
	Bibliographie	189
	Conclusion [in english]	193
	Conclusion [en français]	199
	Bibliographie	205

Table des figures

1.1	Climate tipping elements. Illustration taken from (Armstrong McKay et al., 2022)	3
1.2	Biophysical climate impacts of human activities. Illustration taken from Masson-Delmotte et al. (2019)	5
1.3	Éléments de basculement dans le système climatique. Illustration reprise de Armstrong McKay et al. (2022)	20
1.4	Impacts biophysiques des activités humaines. Illustration reprise de Masson-Delmotte et al. (2019)	22
1.1	Absolute values of the additive and risk-sensitive SCC (in \$ per tC) at initial time (left) and ratio of the risk-sensitive SCC to the additive SCC (right).	58
1.2	Equivalence in ρ (left) and J (right) needed to obtain the same SCC at initial time under additive and risk-sensitive preferences under our benchmark calibration	60
1.3	Marginal contributions to the SCC at initial time (in \$) of the complete <i>MHE</i> (left) and the complete <i>DWI</i> (right) under risk-sensitive preferences for various J and ϵ	61
1.4	Share of the stochastic SCC that is explained by expected damages (in %) (Left) Share of the risk-sensitive risk premium that is already priced under additive preferences (Right).	67
1.5	Time paths of the mean temperature increase until 2100 under additive (left) and risk-sensitive (right) preferences.	68
1.6	Time paths of the SCC until 2100 under additive (left) and risk-sensitive (right) preferences.	68
1.7	Time paths of the abatement rate until 2100 under additive (left) and risk-sensitive (right) preferences.	69
1.8	Mean time paths of the temperature increase in °C with respect to preindustrial era (left), the SCC (middle) and the abatement rate (in %) (right) until 2100.	69

1.9	Ratio of risk-sensitive to additive SCC for a benchmark $\epsilon = 0.133$, $J = 20\%$ and various upper temperature threshold.	70
1.10	Ratio of risk-sensitive to additive SCC at initial time for a benchmark $\epsilon = 0.133$ and various J	70
1.11	Ratio of the SCC at initial time under risk-sensitive preferences on the additive SCC. The graph is for benchmark calibration and for different J and η	71
1.12	Marginal contribution to the SCC at initial time (in \$) of the immediate mhe (left) and the immediate dwi (right) under risk-sensitive preferences. Graph is for various J and ϵ . Results based on 1000 stochastic runs.	71
2.13	Mean net cumulative carbon losses (in GtC) from the Amazon rainforest along mean temperature increases with respect to preindustrial era from various extended concentration pathways (SSP1-1.9, SSP1-2.6, SSP4-3.4, SSP5-3.4, SSP2-4.5, SSP4-6.0, SSP3-7.0, SSP5-8.5), from 2000 to 2200, under our calibration.	99
2.14	Left Increase (in %) from SCC to SCDS when the Amazon rainforest is added to the dynamics system, under stochastic aggregate climate risk (left), under both stochastic aggregate climate risk and idiosyncratic amazon risk (right). Right Share (in %) of each channel in this increase (scaling, insurance & subsystem channels) under aggregate climate risk (left) and both aggregate climate and idiosyncratic amazon risks (right).	102
2.15	Left Share (in %) of SCDS in the SCC under expected utility with stochastic climate risk under deterministic and stochastic specifications for the rainforest, i.e. without (left) and with (right) idiosyncratic amazon risk. Right Share (in %) of each channel in the SCDS (temperature and subsystem channels) under aggregate climate risk (left) and both aggregate climate risk and idiosyncratic amazon risk (right).	104
2.16	Increase (in %) from low to high risk aversion parameter values under smooth ambiguity when the amazon rainforest is accounted for (Top) $SCDS^{SA}$ (Down) $SCCDS^{SA}$	106

2.17	Spatial cumulative distribution at 0.5° resolution of maximum cumulative water deficit anomaly with respect to historical baseline for RCP 8.5 over the Amazon rainforest. Left shows that over all climate models, the average MCWD anomaly shifts to more extreme and frequent droughts from 2010-2050 to 2050-2090. Right shows how the distribution of average MCWD anomaly over 2050-2090 depends on the climate model used	116
2.18	Cumulative distribution function of $\tilde{\epsilon}$ with red mean $\mathbb{E}(\epsilon) \approx 0.0431$ and blue median $\mathbb{P}(\epsilon > 0.0462) = 50\%$	121
2.19	Time horizon Mean cumulative carbon losses (in GtC) from the Amazon rainforest along various extended concentration pathways (in $^\circ\text{C}$) from 2000 to 2200 under no tipping risk (A), a tipping risk (B), and in our model (C).	122
2.20	Phase diagram. Dynamics of the forest under no tipping risk for various $\tilde{\epsilon}$ and for a low, medium and a high temperature corridor. $\mathbb{E}(\epsilon) \approx 0.0431$ and $\mathbb{P}(\epsilon > 0.0462) = 50\%$	122
2.21	Phase diagram. Dynamics of the forest under a tipping risk, i.e. $Y \neq 0$, for various $\tilde{\epsilon}$ and for a low, medium and a high temperature corridor. $\mathbb{E}(\epsilon) \approx 0.0431$ and $\mathbb{P}(\epsilon > 0.0462) = 50\%$	123
2.22	Stochastic optimized paths under aggregate climate risk, without endogenous amazon dynamics.	123
2.23	Stochastic optimized paths under aggregate climate risk, with endogenous amazon dynamics, without amazon idiosyncratic risk.	124
2.24	Stochastic optimized paths under aggregate climate risk, with endogenous amazon dynamics, with amazon idiosyncratic risk.	124
3.1	Left Distribution of daily mean temperatures for four climate landscapes. Middle Distribution of climate shift, i.e. difference in distribution of daily mean temperatures under projection vs. a synthetic-model climate. Right Change in growth rate from one day in this bin relative to one additional day in $[20^\circ\text{C} : 22^\circ\text{C}]$	138

3.2	Double difference DD estimates for year 2050, all SSP and climatic regions. Left Top For each ESM vs. average, using synthetic-model and regional damage Right Top For synthetic-model vs. synthetic-general, using regional damage, averaging over ESM Left Bottom For global vs. regional damage, using synthetic-model, averaging over ESM Right Bottom For central, minimum and maximum estimates of regional damage, using synthetic-model, averaging over ESM.	141
3.3	Left Global DD under synthetic-model approach for each ESM and the average over ESM with regional dose-response function Right Global DD for each dose-response function, synthetic-model approach and average climate model with regional dose-response function.	142
3.4	Left Distribution of impacts (in % of current estimates) across DOSE regions Right Distribution of impacts across and within 2015 USD GDP per capita quantiles of DOSE regions.	143
3.5	Map of DOSE regions with their associated missing-shaped related climate impacts, as a share of 2050 estimated growth impacts along SSP5-8.5.	144
3.6	Köppen climatic zones.	147
4.1	13 Köppen-Geiger climate reference regions in 2015.	159
4.2	1° locations who change Köppen-Geiger classification between 2015 and 2100 under SSP2-4.5.	160
4.3	Non-linear marginal effect (in %) of an additional day in the 1°C temperature bin on regional amenities. Estimates are computed with 95% confidence intervals. The regression is done with 95% winsorized bins [-2°C : 31°C] for 194.032 observations.	168
4.4	Non-linear marginal effect of an additional day in the 1°C temperature bin on regional sectoral productivities	171
4.5	Left Synthetic global annual distributions of daily mean temperatures in 2015 (in blue) and 2100 (in red), under SSP2-4.5, for all gridded locations studied in the paper. Right Shifts from 2015 to 2100 in the frequency of daily mean temperatures per temperature bin (in number of days) for climate projections (in red) and for a synthetic shape-preserving approximate annual mean shift.	176

4.6	Ratio of amenity (left), agricultural productivity (middle), non-agricultural productivity (right) changes between scenario 2 with SSP2-4.5 forced with biogeochemical anthropogenic impacts and scenario 1 without climate change.	177
4.7	Ratio of welfare changes between scenario 2 with SSP2-4.5 climate impacts and counterfactual scenario 1 without climate change, plotted on a map (left) and on an histogram (right).	178
4.8	Share of welfare changes (in %) between scenario 3 with both SSP2-4.5 biogeochemical and biophysical channels and counterfactual scenario 2 without biophysical channels in the change between scenario 1 and scenario 2, plotted on a map (left) and on an histogram (right).	179
4.9	Distributional impacts of biogeochemical and biophysical channels along SSP2-4.5 Left Biogeochemical only with respect to no climate change (scenario 2 and scenario 1) Middle Both biogeochemical and biophysical impacts with respect to no climate change (scenario 3 and scenario 1). Right Deviation between scenario 2 and scenario 3 (scenario 3 and scenario 2).	180

Liste des tableaux

1.1	Table of Tipping Elements, Warming Thresholds, and sign of impacts (in °C), taken from Armstrong McKay et al. (2022)	7
1.2	Correspondence between the four dimensions and my chapters	9
1.3	Table des éléments de basculement, avec leurs seuils probables de déclenchement et le signe de leurs impacts (en °C). Tableau repris de Armstrong McKay et al. (2022)	24
1.4	Correspondance entre ces dimensions et mes chapitres	26
4.1	Change in monthly (January/July for illustration) mean daily surface temperature (in °C) for various Köppen-Geiger climatic zones for a 1% absolute change in land use for two net transitions of interest : from forests to croplands, from shrublands to croplands. 1% absolute change over 1° gridded regions represents around 123km ² at Equator and 87km ² on the French mainland. Data is missing for some combinations.	158
4.2	Change in mean daily temperature (in °C) for various Köppen-Geiger zones for a 1% absolute change in impervious surfaces over 1° regions.	159
4.3	Cumulative net change (as a share of total cell extent, in %) between 2015 and 2100 in LUMIP MESSAGE-Globiom SSP2 4-5 for the 1° gridded locations used in the simulations, from forests to croplands (left), from rangelands to croplands (middle), from non-impervious to urban impervious surfaces (right).	161

Introduction

Public debate about climate change has fortunately shifted from questioning its anthropogenic origins to discussing its potential magnitude, its impacts on economic growth and welfare, and the most efficient adaptation and mitigation strategies given debated ethical principles. Because of economic, physical, and scientific uncertainties and their interactions, society faces a spectrum of possible futures across time and space, across scientific models, and within a given model, necessitating informed decision-making. But it is precisely these uncertainties that make decision making more complex. Our inclination often skews towards one end of this spectrum : for instance, techno-optimists favor best-case scenarios on the left of the distribution, while collapsologists focus on worst-case outcomes on the right. I believe that such polarized views are not reasonable guides for public action. **This thesis advocates for a comprehensive approach, considering the entire distributions rather than focusing on a single aspect of risk, a specific scientific model, a particular location, or a moment in time.** By encompassing the full range of possible distributions across time, space, risk, and scientific uncertainty, we lay the backbone of models that incorporate the best available scientific knowledge. On this foundation, decisions can then be made, accounting for temporal and risk preferences, as well as aversion to inequalities, which should be publicly debated. In this way, **we can sequence the decision-making process and adopt a two-step approach that explicitly differentiates the object from our attitude towards it** : separating risk within models from our aversion to risk, scientific uncertainty between models from our aversion to scientific uncertainty, and the distribution of possible futures in time and space from our aversion to intra- and inter-temporal inequalities.

Box 1 - stochastic risk and scientific uncertainty

What is usually referred to as risk encompasses two different concepts : standard risk, where probabilities associated to each possible future states of the world are known, and uncertain (ambiguous) situations, i.e. situations in which there is

no unanimous probability assignment due to insufficient information or competing datasets, models, or expert opinions.

1 Four dimensions : time, space, risk and scientific uncertainty

Defining the spatio-temporal spectrum of possible futures, accounting for stochastic risk within models and scientific uncertainty between models, is challenging due to uncertainties in each dimension and their dynamic interactions. Before detailing these challenges and presenting my contributions to addressing them, I offer this personal perspective on climate policy : the significant magnitude of these uncertainties should inspire humility and lead us to favor minimal disruption of systems beyond our control. While my study focuses on climate change, perturbations of other planetary limits are also a significant concern. The average scenario of future economic damage should not be the only guide to action : it is the deep uncertainty about the earth system's reaction to our disturbances that should drive us to take the most decisive actions in the short term. In the medium term, we can hope to reduce the cost of our intense mitigation efforts by further exploring and reducing these uncertainties. In other words, I do not believe that the worst should be disregarded simply because it is not certain, nor do I believe that the worst is certain simply because it is possible. However, **I do lean towards the cautious approach of considering the worst-case scenarios more seriously, both in their modeling and in our attitude towards them.**

1 Time

Time is a crucial dimension of the climate issue, raising two main challenges. The first challenge, recognized since at least Frank Ramsey's time, involves solving problems with long or infinite time horizons, presenting both ethical and numerical difficulties. In normative settings, the practice of pure time discounting is still commonly used, a practice that is 'ethically indefensible and arising merely from the weakness of the imagination' ([Ramsey, 1928](#)). Numerical optimization of present and future generations' welfare is often achieved at the expense of unequal treatment of these generations. In positive settings, e.g. in spatial integrated assessment models ([Cruz and Rossi-Hansberg, 2024](#)), the challenge of a long horizon is sidestepped by assuming a stationary equilibrium and the conver-

gence of fundamentals for model closure, a bold assumption with no empirical foundation. The second problem, less frequently discussed in economics due to simplifications in system modeling, often using fixed stock depletion models, is the impact of the passage of time on the dynamics of these systems due to temporal autocorrelation. The climate system and its components, disrupted by human activities, have for instance their own independent dynamics due to feedback effects, inertia, or nonlinearities that can generate abrupt and qualitative changes in their regime (Ritchie et al., 2021) simply by the passage of time.

Box 2 - The Economics of Climate Tipping Elements

Tipping elements are large-scale components of the Earth system that may pass a tipping point. A tipping point is a critical threshold at which a tiny perturbation can qualitatively alter the state of the system (Lenton et al., 2008). Examples of tipping elements include the Amazon rainforest, the Greenland ice sheet, or the Atlantic Meridional Overturning Circulation, which might be classified by the Earth domain to which they belong : respectively biosphere, cryosphere or the ocean and atmosphere.

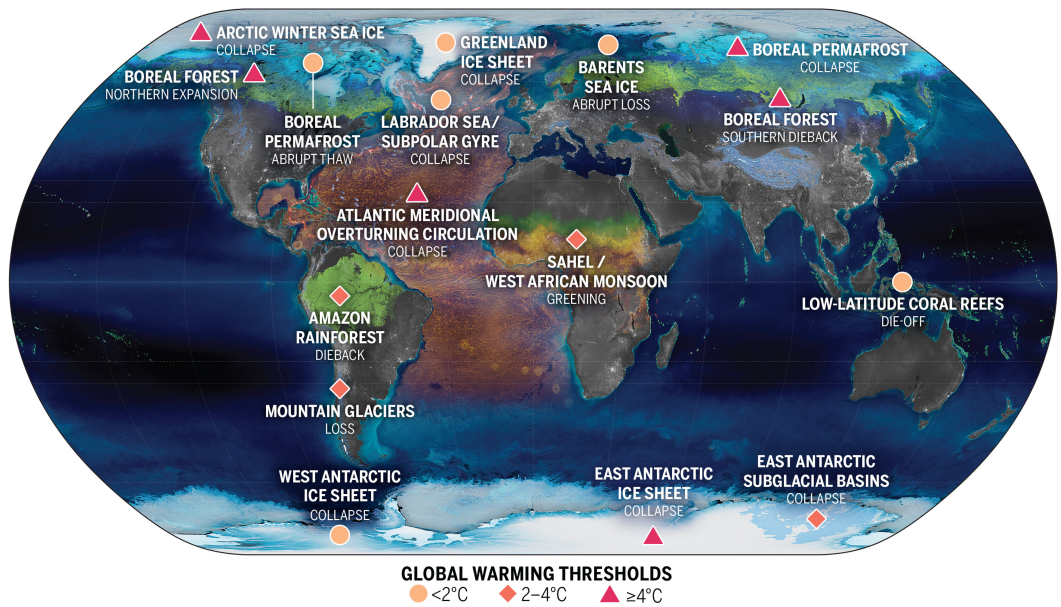


FIGURE 1.1 – Climate tipping elements. Illustration taken from (Armstrong McKay et al., 2022).

2 Space

Space is another essential dimension of the problem, as the impacts of climate change and the capacity to mitigate and adapt are highly heterogeneous across different regions over time. This dimension raises a major challenge : spatial aggregation. The increasing granularity available in gridded socio-economic and climate data allows for a better understanding of phenomena at different scales. However, this finer granularity can pose three main problems. First, some phenomena may be non-linear on a micro scale but linear on a macro scale, and *vice versa* (Burke et al., 2015). The second problem is the explosion in the dimension of numerical problems when the number of locations is increased, especially if decisions in one location influence all the others (Desmet and Rossi-Hansberg, 2024). Finally, the third problem is spatial autocorrelation, which becomes increasingly problematic as granularity increases (Hsiang, 2016). Space and time interact, raising additional challenges, such as the articulation of inter- and intratemporal inequality, or the interaction of spatial and temporal autocorrelations, which can lead to propagating effects that are harder to estimate, more unstable to predict, and more complex to model and calibrate.

I believe that we need to move back and forth between the stylized and the detailed, constantly ensuring that our acceptance of the stylized as a good first approximation holds when we introduce other aspects of the problem or when we change the scale. For instance, the cumulative stock of global emissions is probably a good first approximation when considering the seminal DICE model and its global scale (Nordhaus, 2008). But once we disaggregate spatially to examine the distributional impacts of climate change as in the recent quantitative spatial literature, I believe that we should consider other mechanisms, for instance impacts of biophysical channels via land use and land cover changes on regional climates, as these mechanisms bring nonlinearities in the earth-human interactions and interact with the first-order climate change adaptation strategies usually modeled, such as migration and population concentration, change in trade patterns and relative prices or regional structural change.

Box 3 - Biogeochemical and biophysical climate impacts

At the local and regional scales, land use and land cover changes such as urbanization or transition from and to croplands have impacts on regional climates because of *biophysical* channels (Masson-Delmotte et al., 2019). Examples of biophysical channels are changes in albedo, changes in evapotranspiration, or

changes in roughness. Albedo is the fraction of solar radiation reflected by a surface. Evapotranspiration is the combined process of evaporation from the Earth's surface and transpiration from vegetation. Roughness length refers to the measure of a surface's roughness, which influences how air moves above that surface. These changes in regional land conditions affect regional climate. Authors from the burgeoning spatial integrated assessment modelling literature ([Desmet and Rossi-Hansberg, 2024](#)) omit these mechanisms in their assessments of climate impacts : they focus on the *biogeochemical* channel of global cumulative carbon emissions from which they infer local impacts with time-invariant downscaling.

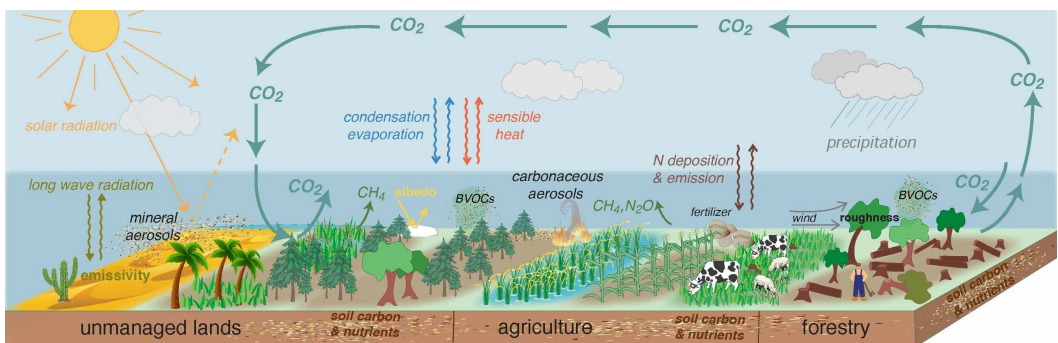


FIGURE 1.2 – Biophysical climate impacts of human activities. Illustration taken from [Masson-Delmotte et al. \(2019\)](#).

3 Risk

Risky social situations are those in which the probabilities of events' occurrences are known; that is, the whole distribution of future possible states of the world is known but the event is not deterministic. Incorporating stochastic risk in the frameworks raises four main challenges.

First, it is challenging to calibrate and define risk. The notion can encompass various concepts : for instance parametric risk, such as the true value of transient climate response to cumulative emissions, differs from trajectory risk, which stems from multiple possible realizations from a model with perturbed initial conditions ([Rising et al., 2022](#)). A standard representation of economic and climate risk in the macroeconomics literature, e.g. in [Hong et al. \(2023\)](#), represents volatility with possible reversible jumps along a smooth economic trend and representative concentration pathway, with Poisson and Wiener processes, rather than considering more abrupt regime changes, nonlinearities and catastrophes. And yet, some climate risks have been characterized by climate scientists, such as the risk of climate tipping points. We know too much about these tangible

risks to be fully satisfied by the modelling of generic catastrophic or extinction risks : [Ritchie et al. \(2021\)](#) suggest reduced-form equations for these systems as a first approximation. Characterizing the catastrophe as an emergent property of the dynamic system rather than defining a probability of collapse *ad hoc* can teach us a lot about optimal economic policy. This requires interdisciplinary work that should go beyond using climate model outputs ([Folini et al., 2024](#)) but would incorporate credible geophysical mechanisms and processes ([Dietz et al., 2021](#)), even reduced-form.

A second challenge is the multiple sources of climate and economic risk that interact across space and time, a correlation that might increase or decrease aggregate risk. For instance, regarding climate risks, various climate subprocesses have dynamics that interact in different ways with global climate change and macroeconomic activity. These subprocesses have diverse insurance values ([Le-moine and Rudik, 2017](#); [Dietz et al., 2018](#)). In the table below, I reproduce data from [Armstrong McKay et al. \(2022\)](#) on tipping elements, their warming threshold and the sign of the feedback they might have on global or regional climates (in °C). Some tipping elements reduce the temperature, but this decrease in average temperature does not have the same impact depending on the threshold at which the tipping point is triggered. Equivalently, tipping elements that bring a positive feedback on climate, i.e. further increase temperature, at low warming threshold do not have the same value as tipping elements that increase the temperatures at high temperatures, without even considering the expected value of the impact from the tipping element. One could also consider the precise mechanisms by which the tipping points are triggered and their timescales of occurrence once triggered. This correlation also matters for systems with non-tipping behavior, for instance the south-eastern asian rainforest, that stores and releases carbon. The social planner might have aversion to this correlation, which means for instance that the planner might put more weight on subprocesses that have the largest impacts on intertemporal welfare in the states of the world where intertemporal welfare is low.

Tipping element	Warming threshold	Sign of impacts
Boreal Permafrost (abrupt thaw)	<2°C	+
Greenland & West Antarctic Ice Sheets	<2°C	+
Barents Sea Ice	<2°C	+
Labrador-Irminger Seas / SPG Convection	<2°C	-
Amazon Rainforest	2-4°C	+
East Antarctic Subglacial Basins	2-4°C	+
Mountain Glaciers	2-4°C	+
Sahel and W. African Monsoon	2-4°C	+
Boreal Permafrost (collapse)	≥ 4°C	+
Arctic Winter Sea Ice	≥ 4°C	+
Boreal Forest (northern expansion)	≥ 4°C	+
East Antarctic Ice Sheet	≥ 4°C	+
Atlantic Meridional Overturning Circulation	≥ 4°C	-
Boreal Forest (southern dieback)	≥ 4°C	-

TABLE 1.1 – Table of Tipping Elements, Warming Thresholds, and sign of impacts (in °C), taken from [Armstrong McKay et al. \(2022\)](#)

A third challenge is the resolution of risk over time and the possibility of learning. When calculating welfare impacts, should we assume that the future risk distribution will likely narrow around its mean over time, and should the social planner have a preference with respect to the resolution of risk over time? These preferences with respect to temporal resolution of risk and uncertainty underlie most recursive models ([Kreps and Porteus, 1978](#); [Strzalecki, 2013](#)), and interact with temporal and atemporal risk and uncertainty aversions ([Stanca, 2023](#)) in ways that are often overlooked in applied research.

The last challenge is to take risk seriously, which means defining optimal social choice under true stochastic risk, i.e. settings in which the decision maker acknowledges the full set of possible future trajectories in every period, rather than averaging over deterministic realizations *à la Monte Carlo* ([Crost and Traeger, 2013](#); [Lemoine and Rudik, 2017](#)). This raises numerical challenges, as there is currently no global solution for solving optimization problems with more than a few state variables, depending on the complexity of the dynamics and risk ([Cai, 2019](#); [Cai and Lontzek, 2019](#)). On the one hand, recent advances using deep neural networks ([Azinovic et al., 2022](#); [Friedl et al., 2023](#)) might raise ethical questions, if the underlying social choice criterion is not explicit. On the other hand, perturbation methods ([Van den Bremer and Van der Ploeg, 2021](#); [Bilal, 2023](#); [Bilal and Rossi-Hansberg, 2023](#)) are only adapted for small risks around the equilibrium solution.

4 Scientific uncertainties

Uncertain scientific situations are those in which there is no unanimous probability assignment due to insufficient information or competing datasets, models, or expert opinions (Berger and Marinacci, 2020). This uncertainty differs from standard stochastic risk, as does its potential resolution over time. The difficulty, however, is calibrating the resolution of scientific uncertainty in a world where scientific progress is non-linear and scientific theories are under-determined (Quine, 1970). For economic policy, it is crucial to consider scientific disagreements within a single framework, as optimal social choice is usually not the average of optimal choices made based on competing models. We could even delve deeper and consider the reasons why individuals agree or disagree (Bommier et al., 2021) rather than focusing only on the outcome. This scientific uncertainty matters especially for debated catastrophic risks. For instance, while it is often assumed that the probability of catastrophic events is known and unanimously accepted, there are fierce scientific debates about their likelihood of occurrence, their timescale once triggered, their consequences, etc. (Armstrong McKay et al., 2022). The IPCC articulates quantitative and qualitative judgements of confidence on these assertions; we could imagine taking both of them into account in our decisions (Bradley et al., 2017).

5 This thesis

I first worked on climate uncertainties because I believed they could shape the way we define mitigation and adaptation policies. Then, I realized that studying dynamic systems with risky and uncertain dynamics at the earth-human interface can come with methodological advances for the field of economics. Finally, I discovered that examining these climate risks and uncertainties could provide new insights into how we should approach normative social choice in economics, particularly in intertemporal contexts. Thus, my thesis follows three directions : documenting the economic consequences of climate uncertainties, contributing methodologically to the study of uncertainty at the interface of human and natural systems, and enriching the literature on normative intertemporal social choice with numerical models for quantification. To contribute to this literature, I investigate alternatively the different dimensions highlighted above and navigate between normative and positive approaches, each with its own advantages, disadvantages, and assumptions.

Dimension	Chapter 1	Chapter 2	Chapter 3	Chapter 4
Time				
Space				
Risk				
Scientific uncertainty				

TABLE 1.2 – Correspondence between the four dimensions and my chapters

Black indicates that the dimension is the main focus of the chapter while **gray** indicates that the chapter addresses but does not focus on the dimension.

2 Climate policies : normative and positive approaches

1 Normative approaches

The Brundtland Commission of the United Nations provides a framework that prompts more questions than actionable guidance : ‘sustainable development is development that meets the needs of the present without compromising the ability of future generations to meet their own needs’. Meeting this criterion across all four dimensions highlighted above is theoretically and numerically challenging. Indeed, each dimension involves ethical considerations crucial for social choice.

First, in the temporal dimension, we must decide how much consumption to sacrifice today for future welfare. This extends to a deeper trade-off involving the social value of reducing catastrophic risks : how much consumption should we forgo today to lower the probability of an uncontrollable climate catastrophe tomorrow ([Bommier et al., 2015](#))?

Second, in the spatial dimension, there are existing inequalities within and between countries that we may wish to address, such as inequalities in greenhouse gas emissions (cause) and disparities in exposure to climate impacts (consequence). For political economy reasons, such as the assumed impracticality of global wealth transfer programs for income equalization across regions without having been tried, economists have often chosen utility weighting, like Negishi weights ([Nordhaus and Yang, 1996](#)). In my view, this approach reflects a lack of imagination similar to that seen in pure time discounting. These spatial inequalities interact with temporal inequalities, as future generations may be wealthier on average, but today’s richest are richer than tomorrow’s poorest, depending on assumptions about climate impacts and future total factor productivity growth.

Third, there are inequalities in risk exposure ([Beck, 1986](#)). A key ethical question in risky contexts is whether to prefer *ex-post* catastrophe avoidance (a pre-

ference for concentrating the distribution of catastrophes, such as deaths from climate disasters) or *ex-ante* risk equity (a preference for equalizing the probability of dying across agents), two conflicting concepts (Keeney, 1980; Bernard et al., 2018). Whatever the ethical stance taken between these two options, incorporating risk exposure implies that the policy question becomes an *ex ante* issue, and not just an *ex post* redistribution issue if and once the risk has materialized, as is the case with the compensation for natural disasters from the Federal Emergency Management Agency in the USA.

Fourth, the same question arises concerning unequal exposure to scientific uncertainty (Blicharska et al., 2017). This reflects the scientific community's lack of interest in certain research questions, a scarcity of data and fewer climate scientists and economists outside OECD countries and China. Furthermore, faced with scientific uncertainty, scientific research and economic policies try to make the environment more predictable for economic agents, but this effort might have a distributional effect if some agents benefit from scientific uncertainty. Unequal exposure to scientific uncertainty raises the question of the distributional effects of the resolution of this uncertainty.

2 Positive approaches

Even though the distinction between normative and positive approaches is somewhat overplayed, as value judgments are always involved, certain elements do not directly relate to a social choice criterion, even if they guide it. This is the case with our hypotheses about agents' adaptation to climate change, future growth, and so on. Social choice optimization models, due to the complexity of solving high-dimensional problems with risk, have often chosen not to model adaptation explicitly. This is a significant assumption and is subject to some form of Lucas's critique. Recent spatial Integrated Assessment Models (IAMs) are evolving to model agents' migration, changes in economic specialization, and other adaptations endogenously (Desmet and Rossi-Hansberg, 2024). However, they deviate from the social planner's ethical framework that maximizes social welfare, shifting the focus to impact scenarios. This represents a significant loss when considering optimal policy today because the optimal choice criterion is not explicit. Indeed, optimization is not global but arises merely from the combinations of many decentralized choices from rational agents driven by perfect forward-looking expectations and utility maximization.

The notable challenge in this positive approach, strongly highlighted by Popper (1945), is historicism in the social sciences : 'Let it suffice for me to say that

by [historicism] I mean a theory, affecting all the social sciences, which makes historical prediction its principal aim, and which teaches that this aim can be achieved if one discovers the ‘rhythms’ or ‘patterns’, the ‘laws’, or the ‘general tendencies’ which underlie historical developments’. This relates to the criticism of most economists assuming ergodicity of socioeconomic processes, an anhistoric assumption according to [North \(2005\)](#). This is the trap that modeling economic behavior such as climate adaptation and extrapolating past weather impacts into future climate impacts can lead us into. The first issue is claiming to identify laws in the social sciences and projecting them for prospective modeling. The second issue is the political power of these so-called laws that might be dubious, generating false oppositions among proponents of similar solutions. This might arise, for instance, in the hypothesis of future economic growth in total factor productivity (TFP) being exponential, whereas recent work suggests it is additive ([Philippon, 2022](#)). Digging deeper into these positive assumptions could help reconcile certain views between green growth and degrowth, without resorting to strong ethical positions, such as strong preference for redistribution and strong aversion to risk, or an overestimation of catastrophic climate risks compared to other possible states of the world. Regarding the merits of these positive approaches in the economics of climate change, I remain cautious even though I adopt them, be it by scientific conformism or due to their appeals, the main ones being the growing availability of rich gridded datasets, the attempt to start answering Lucas’s critique and the numerical tractability of high-dimensional positive problems in comparison to the global solution methods applied to normative intertemporal optimization frameworks.

3 Thesis description

How do the uncertainties arising from these four dimensions (time, space, risk, scientific uncertainty) affect optimal social choice at the Earth-Human interface? The first two papers of my thesis are normative and focus on defining optimal policy within dynamic stochastic optimization models that account for endogenous climate change. This approach feeds discussions on choosing a rational and consistent intertemporal social choice criterion when dealing with irreversible catastrophic risks (Project 1) and modeling the uncertain dynamics of Earth subsystems and their interactions with the macroeconomy and aggregate climate uncertainty (Project 2).

1 Time, risk and scientific uncertainty

In the first chapter, we develop a dynamic stochastic climate-economy model (Cai and Lontzek, 2019) to examine and quantify a critical assumption in the standard model used to define optimal climate policy : temporal risk-neutrality under discounted expected utility. How does this assumption hold when society faces large, irreversible risks such as climate tipping points, e.g., Amazon rainforest dieback, Greenland Ice Sheet disintegration (Lenton et al., 2008)? Once a tipping point is crossed, the welfare of all subsequent generations is adversely affected and positively correlated. Just as a risk-averse portfolio manager considers the aggregate risk of a portfolio rather than summing individual asset risks—because positive correlations among asset risks increase overall risk—it may be optimal for a social planner to put more weight on social situations where aggregate risk bearing on intertemporal utility is large, for instance if the welfare of different generations is low and positively correlated. The social planner under additive expected utility does not put more weight on this aggregate risk bearing on intertemporal utility. We employ risk-sensitive social preferences (Bommier et al., 2017), which are well-behaved and monotone with respect to first-order dominance, unlike the Epstein-Zin-Weil framework, and compare optimal policy under this criterion to the standard expected utility model, both analytically and numerically. Our numerical results show that temporal risk aversion leads to a 30% increase in the social cost of carbon (SCC) for a large 10% irreversible rise in economic damage from climate change. Assuming temporal risk neutrality is not benign for climate policy, particularly if we anticipate significant damage from catastrophic events, as the SCC rises sharply with the level of damage. If one believes that major catastrophes bearing large multiplier effects such as irreversible regime shifts are possible, aversion towards those risks bearing on intertemporal utility should be accounted for. On the other hand, if there is no such risk or if the possible damage is low, then we should stick to the additive model as it does not come with the ethical drawbacks catastrophe aversion bears.

A limitation of our approach is that it is stylized, especially the modelling of a generic tipping risk. We did not model a tipping element and its dynamics, as well as the consequences of a climate risk, instead representing it as a stochastic process with an irreversible jump. My aim was to develop a model that provides a more accurate representation of climate uncertainties with an explicit calibration. Specifically, I wanted the catastrophic outcome to be an emergent property of the dynamic system, rather than an *ad hoc* specification, in line with bifurcation

theory (Ritchie et al., 2021). Furthermore, I intended to study the interaction of a specific catastrophic climate risk with aggregate climate risk impacting intertemporal welfare within a framework that incorporates scientific uncertainties.

In the second chapter, we examine how economists' simplified models of climate uncertainties can distort optimal economic policy, particularly when considering Earth's subsystems. These subsystems have three key characteristics. First, global climate change affects their dynamics. Second, these subsystems impact global climate change. Both effects that can be either positive or negative. Third, the dynamics of these subsystems are not solely a linear function of climate change; they also involve inertia, self-sustaining processes, or feedback effects. Examples include climate tipping elements and subsystems without tipping behavior, such as the South-Eastern Asian rainforest. The interactions between these subsystems and global climate change are stochastic in nature. A central question for economists is to determine if and how the idiosyncratic risks associated with these subsystems affect aggregate climate risk and intertemporal welfare. We analytically explore the channels through which these interactions influence optimal climate policy. Additionally, we investigate how regional management of these subsystems could be guided by a reduced-form representation of their geophysical dynamics. We apply our framework to a calibrated quantitative model of the Amazon rainforest, a subject of intense debate. Aside from standard risk scenarios, where future state probabilities are known, there are substantial scientific uncertainties concerning both subsystem dynamics and their interaction with global climate change, due to competing datasets and climate models. Decision theory offers tools to integrate these uncertainties into our social choice criterion. The methodological approach in this paper involves solving an optimization program with a state variable that exhibits curvature due to tipping risks in rainforest dynamics, using simplicial Chebyshev polynomials for value function approximation on parallel CPUs (Cai, 2019). Our approach yields two key economic insights to the literature on tropical deforestation (Balboni et al., 2023). First, the social cost of carbon (SCC) must account for the effects of a marginal increase in global cumulative emissions on the dynamics of the rainforest. This includes adjusting current policies for carbon releases from the Amazon rainforest under changing climate conditions and incorporating an 'Amazon beta' insurance channel, as the social value of carbon releases varies depending on the state of the world where they occur. Second, the social value of the Amazon rainforest as a carbon sink should not be limited to its current carbon content alone; the social cost of the

dynamic system (SCDS) is also crucial. This cost reflects the marginal decrease in the subsystem's state due to its diminished capacity for self-regulation. These insights lead to two important policy implications. First, the social cost of carbon should be increased to reflect the impact of global marginal emissions on the Amazon rainforest, which further releases carbon. This adjustment ensures that emitters worldwide compensate for the welfare impacts of their emissions. In our benchmark calibration, this adjustment yields a 15% increase in the standard SCC. The disparity between standard SCC and SCC with endogenous Amazon feedback could be leveraged to fund coasian ecosystem service payments for rainforest preservation in a double dividend perspective. Second, the valuation of a hectare of rainforest should include not only the standard SCC but also the Amazon-augmented SCC and a share of the SCDS. A reduction in forest cover impacts welfare both directly, through carbon release, and indirectly, by affecting future subsystem dynamics. In our benchmark calibration, the SCDS represents 16% of the standard SCC. Our theoretical framework can thus be applied to local cost-benefit analyses of deforestation and complements recent advances in quantifying carbon storage using satellite observations. Thus, in our best guess, we estimate that a 24% increase in the marginal value of a tCO₂ stored in the rainforest should be applied in local cost-benefit analysis, for instance for infrastructure projects in Brazil. We believe that our analytical approach applied to the quantitative model of the Amazon rainforest could also be applied to other dynamic geophysical systems to inform policy decisions at both global and regional levels.

The normative approach has limitations, as it becomes intractable when the complexity of the dynamic stochastic optimization problem increases. As a result, analyzing distributional effects of climate change, such as including numerous regions or accounting for individual agent adaptations, becomes impractical. A positive approach that dispenses with social choice might be the way forward on these issues until high-dimensional optimization methods become tractable and accessible without message passing interface on high performance clusters.

2 Time and space

How do the uncertainties arising from the four dimensions highlighted above (time, space, risk, scientific uncertainty) affect our estimations of climate impacts at the Earth-Human interface? While the approach in the two first papers of my thesis is stylized and global in scale, focusing on modeling stochastic risk and its impact on optimal policy, the second part of my thesis addresses

the spatial dimension of climate uncertainties. I aimed to work with increasingly available gridded climatic and socio-economic data, which can provide valuable insights into the economic impacts of climate change. In chapter 3, we analyze the aggregation of these data over time and space. In my fourth chapter, the job market paper, I develop a dynamic sectoral spatial equilibrium model and apply it to 1° gridded data to quantify the nonlinear impact of omitted biophysical channels (albedo, evapotranspiration, and surface roughness), driven by land use and land cover (LULC) changes, on regional climate impacts and adaptation decisions.

In the third chapter, we demonstrate how the current aggregation of climate and economic data to compute annual global dose-response functions can obscure some climate uncertainties between climate models and skew our estimates of climate impacts. This global annual approach is commonly used in both standard climate-economy models and newer quantitative spatial models. We employ downscaled and bias-corrected regional climate projections of daily mean temperatures and combine them with empirically estimated global and regional dose-response functions of GDP growth rates to daily mean temperature levels. We disentangle how much of the missing impacts are due to heterogeneous warming versus heterogeneous damage patterns across space and time for various shared socio-economic pathways (SSPs). Accounting for the shift in the entire distribution of daily mean temperatures at the regional scale reveals that global damages in 2050 could be around 25% higher. Differences in the shape of daily temperature distributions between climate models transform standard risk rankings based on temperature anomalies and increase uncertainty across climate models. Differences in the shape of daily temperature distributions also affect the geography of future climate impacts, with a lot of damages that have been so far overlooked because of the spatio-temporal aggregation procedure, especially in continental areas from the northern hemisphere.

In the fourth chapter, I contribute to the growing literature in spatial economics which models economic activity at the regional scale using spatial data, particularly in assessing the economic impacts of climate change (Desmet Rossit-Hansberg, 2024). This literature reveals significant uncertainty regarding the interaction between economic activity and climate change. Some of this uncertainty, such as linear downscaling from global climate change to local impacts, can be addressed with Monte Carlo approaches. However, some uncertainty is endogenous and results directly from regional economic activities and adaptation stra-

tegies, such as the feedback of economic activity on regional climate through LULC changes. Downscaling from global to regional climate change is uncertain and cannot be considered stable and linear across time and space; it is influenced by regional economic activities. These regional distributions shift with agents' decisions (urbanization, agricultural expansion) and, in turn, affect those decisions (sectoral specialization, migration). In this research project, I model a qualitatively distinct mechanism linking economic activity and climate impacts and quantify how much this channel matters for the aggregate and distributional intertemporal welfare impacts of climate change within a dynamic spatial framework. Human activity affects LULC through agricultural expansion and urbanization. The biophysical channels (albedo, evapotranspiration, roughness) resulting from these LULC changes provide feedback on regional climate conditions (annual distribution of daily temperatures), impacting current linear climate downscaling and interacting with regional activity. These regional feedbacks also interact with adaptation decisions and may reduce the expected welfare gains from adaptation mechanisms. I first estimate reduced-form relations between changes in agricultural intensity and LULC, and changes in urban land demand and LULC. Leveraging gridded estimates from climate science linking changes in regional LULC to temperatures, I build a dynamic spatial model with multiple locations, two sectors (agricultural and non-agricultural), and individuals who adapt through trade, migration, and sectoral specialization. Climate change affects regional productivities and amenities heterogeneously. For internal validity, I use recent developments in climate adaptive response estimation and the model's equilibrium conditions to estimate dose-response functions of regional amenities and sectoral productivities to the annual distribution of daily mean temperatures. Finally, I apply the model to 1° gridded data globally and solve it with exact hat algebra to avoid computing fundamental initial productivities and amenities. In my baseline SSP2-4.5 simulation, without biophysical impacts, almost all locations experience negative welfare changes from nonlinear regional intra-annual warming patterns interacted with nonlinear binned damage patterns. My results suggest that there are no benefits to be expected from climate change in the Northern Hemisphere. Adding biophysical channels, i.e. a non-linear and time-varying downscaling from global to regional temperature distributions, accounts for 2.4% of the aggregate biogeochemical welfare impacts of climate change. Both biogeochemical and biophysical climate impacts are regressive, decreasing with 2015 income per capita levels. Regional economic activity shapes regional climate impacts and has non-negligible aggregate and distributional consequences.

3 List of research work

In this PhD thesis, spanning over more than three years, I have strived to address climate uncertainties and their implications for economic policy. This endeavor led me to critically examine the limitations of our standard models. Throughout my research, I have explored the validity of our social choice criteria (Chapter 1), the accuracy of our stylized representations of the climate system and its subcomponents (Chapter 2), the effectiveness of our data aggregation methods across space and time (Chapter 3), and the modelling of regional biophysical impacts (Chapter 4). I am the first author of all these research projects, though I am deeply grateful for the invaluable contributions of my co-authors. I recommend focusing on Chapters 2 and 4, which, in my view, make the most original contributions to the scientific literature and public debate among all chapters.

Research papers :

Chapter 1 : Fillon, Guivarch, Taconet, 2023. 'Optimal climate policy under tipping risk and temporal risk aversion', *Journal of Environmental Economics and Management*.

Chapter 2 : Fillon, Guivarch, 2024. 'The need for regulation of climate subsystems'.

Chapter 3 : Fillon, Linsenmeier, Wagner, 2024. 'Climate shift uncertainty and economic damages'.

Chapter 4 : Fillon, 2024. 'The biophysical channels of climate impacts'.

Presentations :

2024 FAERE conference (BETA, U. de Strasbourg), EAERE conference (KU Leuven), LAGV conference (AMSE), iRisk invited seminar (IESEG, LEM, U. de Lille), CIRED (internal PhD seminar), U. Paris-Saclay (Economics & Management, PhD).

2023 MIT (CEEPR, weekly lunch talk), Columbia U. (SIPA, Sustainable Development Colloquium), Duke U. (Nicholas & Sanford Schools, UPEP PhD seminar), Yale U. (School of the Environment, PhD seminar), U. Paris-Saclay (Economics & Management, PhD seminar).

2022 CIRED (PhD seminar, internal), ENS Paris-Saclay (CEPS PhD seminar), Modeling Uncertainty in Social, Economic, and Environmental Sciences MUSEES Conference (EM Lyon), 12th FAERE Workshop (ENS Paris-Saclay), International Conference on Public Economic Theory PET 2022 (AMSE), EAERE conference (U. di Bologna), FAERE conference (U. de Rouen).

Introduction

Le débat public sur le changement climatique a évolué : il ne porte plus sur la remise en question de ses origines anthropiques, mais sur l'ampleur potentielle du phénomène, ses impacts sur la croissance économique et le bien-être, ainsi que sur les stratégies d'adaptation et d'atténuation les plus efficientes en tenant compte de principes éthiques débattus. En raison des incertitudes économiques, physiques et scientifiques et de leurs interactions, la société est confrontée à un éventail de futurs possibles à travers le temps et l'espace, entre différents modèles scientifiques et pour un modèle donné, ce qui nécessite une prise de décision éclairée. Mais ce sont précisément ces incertitudes qui rendent la prise de décision plus complexe. Notre penchant naturel nous pousse à une extrémité de ce spectre : par exemple, les techno-optimistes favorisent les meilleurs scénarios à gauche de la distribution, tandis que les collapsologues se concentrent sur les pires résultats à droite. Je pense que de tels points de vue polarisés ne sont pas des guides raisonnables pour l'action publique. **Cette thèse plaide en faveur d'une approche globale, qui considère l'ensemble des distributions plutôt que de se concentrer sur un seul aspect du risque, un modèle scientifique spécifique, un lieu particulier ou un moment dans le temps.** En englobant l'ensemble des distributions possibles dans le temps, l'espace, le risque et l'incertitude scientifique, nous jetons les bases de modèles qui intègrent les meilleures connaissances scientifiques disponibles. Sur cette fondation, des décisions peuvent alors être prises, en tenant compte des préférences temporelles et en matière de risque, ainsi que de l'aversion pour les inégalités, qui devraient faire l'objet d'un débat public ouvert. De cette manière, **nous pouvons séquencer le processus de prise de décision et adopter une approche en deux étapes qui différencie explicitement l'objet de notre attitude à son égard** : séparer le risque au sein des modèles de notre aversion pour le risque, l'incertitude scientifique entre les modèles de notre aversion pour l'incertitude scientifique, et la distribution des futurs possibles dans le temps et l'espace de notre aversion pour les inégalités intra- et inter-temporelles.

Box 1 - risque stochastique et incertitudes scientifiques

Ce que l'on appelle généralement le risque englobe deux concepts différents en économie : le risque standard, où les probabilités associées à chaque état futur possible du monde sont connues, et les situations incertaines (ambiguës), c'est-à-dire les situations dans lesquelles il n'y a pas d'attribution unanime de probabilité en raison d'informations insuffisantes ou d'ensembles de données, de modèles ou d'avis d'experts concurrents.

1 Quatre dimensions : temps, espace, risque et incertitude scientifique

Définir le spectre spatio-temporel des futurs possibles, en tenant compte du risque stochastique au sein des modèles et de l'incertitude scientifique entre les modèles, est un défi en raison des incertitudes dans chaque dimension et de leurs interactions dynamiques. Avant de détailler ces défis et de présenter mes contributions pour les relever, je propose ce point de vue personnel sur la politique climatique : l'ampleur significative de ces incertitudes devrait nous inspirer de l'humilité et nous amener à favoriser une perturbation minimale de systèmes qui échappent à notre contrôle. Si mon étude se concentre sur le changement climatique, les perturbations d'autres limites planétaires constituent également une préoccupation majeure. Le scénario moyen des dommages économiques futurs ne doit pas être le seul guide pour agir : c'est la profonde incertitude quant à la réaction du système terrestre à nos perturbations qui doit nous pousser à prendre les mesures les plus décisives à court terme. À moyen terme, nous pouvons espérer réduire le coût de nos efforts intenses d'atténuation en explorant et en réduisant davantage ces incertitudes. En d'autres termes, je ne crois pas que le pire doive être ignoré simplement parce qu'il n'est pas certain, ni que le pire soit certain simplement parce qu'il est possible. Cependant, je penche en faveur d'une approche prudente consistant à envisager les pires scénarios avec plus de sérieux, tant dans leur modélisation que dans notre attitude à leur égard.

1 Temps

Le temps est une dimension cruciale de la question climatique, qui soulève deux défis principaux. Le premier défi, reconnu depuis l'époque de Frank Ramsey au moins, consiste à résoudre des problèmes avec des horizons temporels

longs ou infinis, ce qui présente des difficultés à la fois éthiques et numériques. Dans un cadre normatif, la pratique de l'actualisation temporelle pure est encore couramment utilisée, une pratique qui est "indéfendable d'un point de vue éthique et qui découle simplement de la faiblesse de l'imagination". L'optimisation numérique du bien-être des générations présentes et futures est souvent réalisée au prix d'un traitement inégal de ces générations. Dans des contextes positifs, par exemple dans les modèles d'évaluation spatiale intégrée ([Cruz and Rossi-Hansberg, 2024](#)) économique, le défi d'un long horizon est contourné en supposant un équilibre stationnaire et la convergence des fondamentaux pour la clôture du modèle, une hypothèse audacieuse sans fondement empirique. Le second problème, moins souvent abordé en économie en raison des simplifications de la modélisation des systèmes, qui utilisent souvent des modèles d'épuisement de stocks fixes, est l'impact du passage du temps sur la dynamique de ces systèmes en raison de l'auto-corrélation temporelle. Le système climatique et ses composantes, perturbés par les activités humaines, ont par exemple leur propre dynamique indépendante due à des effets de rétroaction, à l'inertie ou à des non-linéarités qui peuvent générer des changements abrupts et qualitatifs de leur régime par le simple passage du temps.

Box 2 - éléments de basculement dans le système climatique

Les éléments de basculement sont des composantes à grande échelle du système terrestre susceptibles de passer un point de basculement. Un point de basculement est un seuil critique à partir duquel une perturbation minime peut modifier qualitativement l'état du système. Parmi les exemples d'éléments de basculement figurent la forêt amazonienne, la calotte glaciaire du Groenland ou la circulation méridienne de retournement de l'Atlantique, qui peuvent être classés en fonction du domaine terrestre auquel ils appartiennent : respectivement la biosphère, la cryosphère ou l'océan et l'atmosphère.

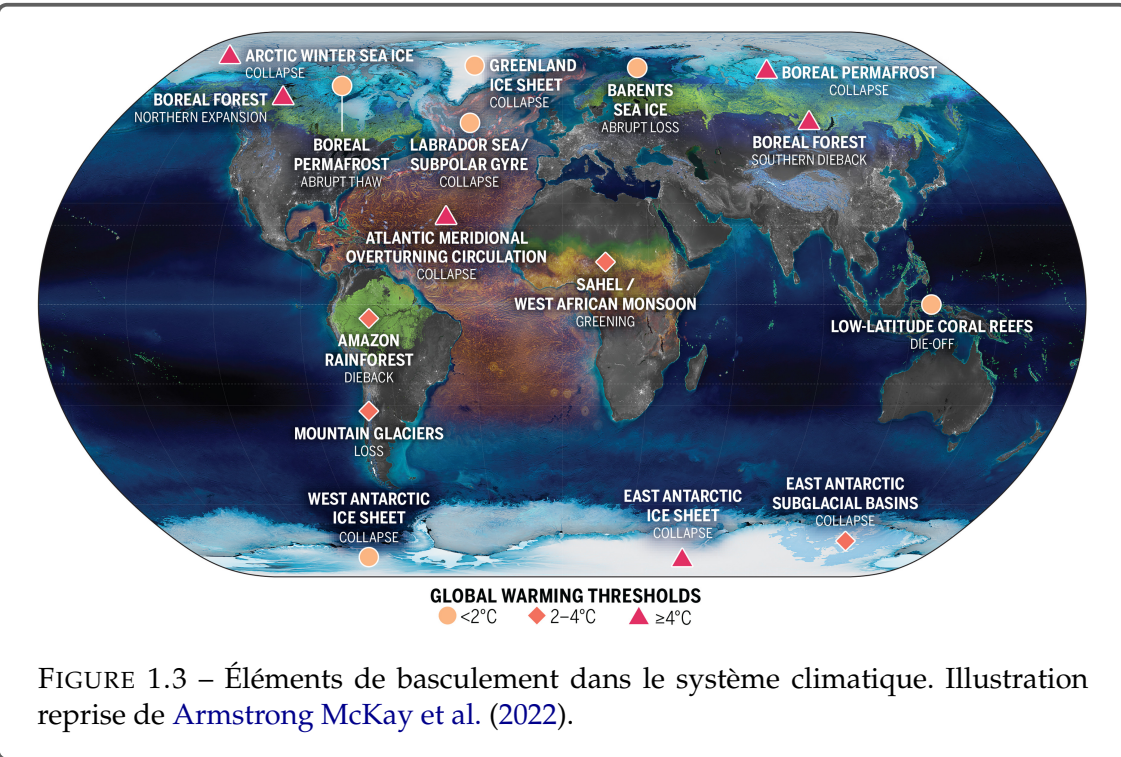


FIGURE 1.3 – Éléments de basculement dans le système climatique. Illustration reprise de Armstrong McKay et al. (2022).

2 Espace

L'espace est une autre dimension essentielle du problème, car les effets du changement climatique et la capacité d'atténuation et d'adaptation sont très hétérogènes d'une région à l'autre au fil du temps. Cette dimension soulève un défi majeur : l'agrégation spatiale. La granularité croissante des données socio-économiques et climatiques permet de mieux comprendre les phénomènes à différentes échelles. Cependant, cette granularité plus fine peut poser trois problèmes principaux. Premièrement, certains phénomènes peuvent être non linéaires à une échelle micro-économique mais linéaires à une échelle macroéconomique, et *vice versa* (Burke et al., 2015). Le deuxième problème est l'explosion de la dimension des problèmes numériques lorsque le nombre de lieux augmente, en particulier si les décisions prises dans une localisation influencent tous les autres (Desmet and Rossi-Hansberg, 2024). Enfin, le troisième problème est l'auto-corrélation spatiale, qui devient de plus en plus problématique à mesure que la granularité augmente (Hsiang, 2016). L'espace et le temps interagissent, soulevant des défis supplémentaires, tels que l'articulation de l'inégalité inter- et intra-temporelle, ou l'interaction des auto-corrélations spatiales et temporelles, qui peuvent conduire à des effets de propagation qui sont plus difficiles à estimer, plus instables à prédirer, et plus complexes à modéliser et à calibrer.

Je crois que nous devons aller et venir entre le stylisé et le détaillé, en

veillant constamment à ce que notre acceptation du stylisé comme une bonne première approximation se maintienne lorsque nous introduisons d'autres aspects du problème ou lorsque nous changeons d'échelle dans une des dimensions évoquées. Par exemple, le stock cumulé d'émissions mondiales est probablement une bonne première approximation si l'on considère le modèle DICE ([Nordhaus, 2008](#)) et son échelle globale. Mais une fois que nous désagrégons l'espace pour examiner les impacts distributifs du changement climatique, comme dans la récente littérature spatiale quantitative, je pense que nous devrions considérer d'autres mécanismes, par exemple les impacts des canaux biophysiques *via* les changements d'utilisation et de couverture des sols sur les climats régionaux, car ces mécanismes apportent des non-linéarités dans les interactions terre-homme et interagissent avec les stratégies d'adaptation au changement climatique de premier ordre généralement modélisées, telles que la migration et la concentration de la population, le changement des schémas commerciaux et des prix relatifs ou le changement structurel régional.

Box 3 - Impacts climatiques biophysiques et biogéochimiques

À l'échelle locale et régionale, les modifications de l'occupation des sols, telles que l'urbanisation ou la transition des terres cultivées vers d'autres types d'usages, ont un impact sur les climats régionaux en raison des canaux *biophysiques* ([Masson-Delmotte et al., 2019](#)). Des exemples de canaux biophysiques sont les changements d'albédo, les changements d'évapotranspiration ou les changements de rugosité. L'albédo est la fraction du rayonnement solaire réfléchie par une surface. L'évapotranspiration est le processus combiné de l'évaporation de la surface de la Terre et de la transpiration de la végétation. La longueur de rugosité est la mesure de la rugosité d'une surface, qui influence la façon dont l'air se déplace au-dessus de cette surface. Ces changements dans les conditions terrestres régionales affectent le climat régional. Les modèles d'évaluation spatiale intégrée ([Desmet and Rossi-Hansberg, 2024](#)) omettent ces mécanismes dans leurs évaluations des impacts climatiques : ils se concentrent sur le canal *biogéochimique* des émissions cumulées de carbone à l'échelle mondiale, dont ils déduisent les impacts locaux à l'aide d'un facteur invariant dans le temps.

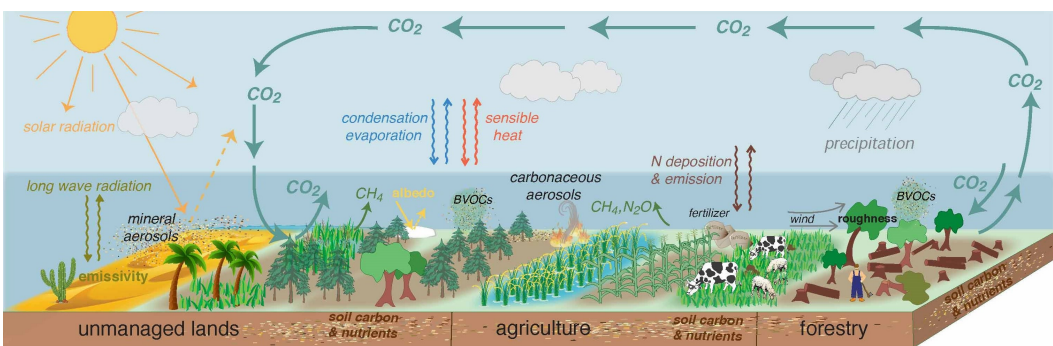


FIGURE 1.4 – Impacts biophysiques des activités humaines. Illustration reprise de Masson-Delmotte et al. (2019).

3 Risque

Les situations sociales risquées sont des situations dans lesquelles les probabilités d'occurrence des événements sont connues ; c'est-à-dire que l'ensemble de la distribution des états futurs possibles du monde est connu mais que l'état du monde n'est pas déterministe. L'intégration du risque stochastique dans les modèles économiques appliqués au changement climatique soulève quatre défis principaux.

Premièrement, il est difficile de calibrer et de définir le risque. La notion englobe différents concepts : par exemple, le risque paramétrique, tel que la valeur réelle de la réponse transitoire du climat aux émissions cumulées, diffère du risque de trajectoire, qui découle des multiples réalisations possibles d'un modèle dont les conditions initiales sont perturbées. Une représentation standard du risque économique et climatique dans la littérature macroéconomique, par exemple dans Hong et al. (2023), représente la volatilité avec des sauts réversibles le long d'une tendance économique lisse et d'une trajectoire de concentration représentative (SSP), avec des processus de Poisson et de Wiener, plutôt que de considérer des changements de régime plus abrupts, des non-linéarités et des catastrophes. Pourtant, certains risques climatiques ont été caractérisés par les climatologues, comme le risque de points de basculement climatique. Nous en savons trop sur ces risques tangibles pour être pleinement satisfaits de la modélisation des risques génériques de catastrophe ou d'extinction : Ritchie et al. (2021) propose des équations de forme réduite pour ces systèmes en première approximation. Caractériser la catastrophe comme une propriété émergente du système dynamique plutôt que de définir une probabilité d'effondrement *ad hoc* peut nous apprendre beaucoup sur la politique économique optimale. Cela nécessite un tra-

vail interdisciplinaire qui devrait aller au-delà de l'utilisation des résultats des modèles climatiques (Folini et al., 2024) en intégrant des mécanismes et des processus géophysiques crédibles (Dietz et al., 2021), même de forme réduite.

Un deuxième défi concerne les multiples sources de risques climatiques et économiques qui interagissent dans l'espace et dans le temps, une corrélation qui pourrait augmenter ou diminuer le risque global. Par exemple, en ce qui concerne les risques climatiques, divers sous-processus climatiques ont une dynamique qui interagit de différentes manières avec le changement climatique mondial et l'activité macroéconomique. Ces sous-processus ont des valeurs d'assurance diverses (Lemoine and Rudik, 2017; Dietz et al., 2018). Dans le tableau ci-dessous, je reproduis les données de Armstrong McKay et al. (2022) sur les éléments de basculement, leur seuil de réchauffement et le signe de la rétroaction qu'ils pourraient avoir sur les climats mondiaux ou régionaux (en °C). Certains éléments de basculement réduisent la température, mais cette diminution de la température moyenne n'a pas le même impact selon le seuil auquel le point de basculement est déclenché. De même, les éléments de basculement qui entraînent une rétroaction positive sur le climat, c'est-à-dire une nouvelle augmentation de la température, à un seuil de réchauffement bas, n'ont pas la même valeur que les éléments de basculement qui augmentent les températures à des températures élevées, sans même tenir compte de la valeur escomptée de l'impact de l'élément de basculement. On pourrait également examiner les mécanismes précis par lesquels les points de basculement sont déclenchés et le temps que mettent leurs conséquences physiques à se manifester une fois qu'ils sont déclenchés. Cette corrélation est également importante pour les systèmes qui n'ont pas de comportement de basculement, par exemple la forêt tropicale du sud-est de l'Asie, qui stocke et libère du carbone et dont la dynamique interagit donc avec le changement climatique global. Le planificateur social peut avoir une aversion pour cette corrélation, ce qui signifie par exemple qu'il peut accorder plus d'importance aux sous-processus qui ont le plus d'impact sur le bien-être inter-temporel dans les états du monde où le bien-être inter-temporel est faible.

Éléments de basculement climatique	Seuil de déclenchement (°C)	Signe de l'impact
Pergélisol boréal (dégel brutal)	<2°C	+
Inlandsis du Groenland et de l'Antarctique occidental	<2°C	+
Mer de glace de Barents	<2°C	+
Mers du Labrador et d'Irminger / Convection SPG	<2°C	-
Amazonie	2-4°C	+
Bassins sous-glaciaires de l'Antarctique de l'Est	2-4°C	+
Glaciers de montagne	2-4°C	+
Sahel et mousson ouest-africaine	2-4°C	+
Pergélisol boréal (effondrement)	≥ 4°C	+
Glace de mer arctique hivernale	≥ 4°C	+
Forêt boréale (expansion septentrionale)	≥ 4°C	+
Inlandsis de l'Antarctique Est	≥ 4°C	+
Circulation méridienne de retournement de l'Atlantique	≥ 4°C	-
Forêt boréale (déperissement austral)	≥ 4°C	-

TABLE 1.3 – Table des éléments de basculement, avec leurs seuils probables de déclenchement et le signe de leurs impacts (en °C). Tableau repris de [Armstrong McKay et al. \(2022\)](#)

Un troisième défi est la résolution du risque dans le temps et la possibilité d'apprentissage. Lors du calcul de l'impact sur le bien-être, devons-nous supposer que la distribution future des risques se resserrera probablement autour de sa moyenne au fil du temps ? Le planificateur social doit-il avoir une préférence en ce qui concerne la résolution des risques dans le temps ? Ces préférences en matière de résolution temporelle du risque et de l'incertitude sous-tendent la plupart des modèles récursifs ([Kreps and Porteus, 1978](#); [Strzalecki, 2013](#)), et interagissent avec les aversions temporelles et atemporelles au risque et à l'incertitude ([Stanca, 2023](#)) d'une manière qui est souvent négligée dans la recherche appliquée.

Le dernier défi consiste à prendre le risque au sérieux, ce qui implique de définir un choix social optimal en présence d'un véritable risque stochastique, c'est-à-dire dans des contextes où le décideur prend en compte l'ensemble des trajectoires futures possibles à chaque période, plutôt que de faire la moyenne des réalisations déterministes *à la Monte Carlo* ([Crost and Traeger, 2013](#); [Lemoine and Rudik, 2017](#)). Cela pose des défis numériques, car il n'existe actuellement aucune solution globale pour résoudre les problèmes d'optimisation avec plus de quelques variables d'état, en fonction de la complexité de la dynamique et du risque ([Cai, 2019](#); [Cai and Lontzek, 2019](#)). D'une part, les progrès récents dans l'utilisation des réseaux neuronaux profonds ([Azinovic et al., 2022](#); [Friedl et al., 2023](#)) peuvent soulever des questions éthiques, si le critère de choix social sous-jacent n'est plus explicite. D'autre part, les méthodes de perturbation ([Van den Bremer and Van der Ploeg, 2021](#); [Bilal, 2023](#); [Bilal and Rossi-Hansberg, 2023](#)) ne

sont adaptées qu’aux petits risques autour de la solution d’un équilibre qui est présupposé.

4 Incertitudes scientifiques

Les situations scientifiques incertaines sont celles dans lesquelles il n’y a pas d’attribution unanime de probabilité en raison d’informations insuffisantes ou d’ensembles de données, de modèles ou d’avis d’experts concurrents. Cette incertitude diffère du risque stochastique standard, tout comme sa résolution potentielle dans le temps. La difficulté, cependant, est de calibrer la résolution de l’incertitude scientifique dans un monde où le progrès scientifique n’est pas linéaire et où les théories scientifiques sont sous-déterminées (Quine, 1970). Pour la politique économique, il est crucial de prendre en compte les désaccords scientifiques dans un cadre unique, car le choix social optimal n’est généralement pas la moyenne des choix optimaux effectués sur la base de modèles concurrents. Nous pourrions même aller plus loin et examiner les raisons pour lesquelles les scientifiques sont d’accord ou en désaccord (Bommier et al., 2021) plutôt que de nous concentrer uniquement sur le résultat. Cette incertitude scientifique est particulièrement importante pour les risques catastrophiques très débattus. Par exemple, alors que l’on suppose souvent que la probabilité d’événements catastrophiques est connue et unanimement acceptée, il existe des débats scientifiques importants sur leur probabilité d’occurrence, leur échelle de temps une fois qu’ils sont déclenchés, leurs conséquences, etc. (Armstrong McKay et al., 2022). Le Groupe d’experts intergouvernemental sur l’évolution du climat (GIEC) articule des jugements de confiance quantitatifs et qualitatifs sur ces affirmations ; nous pourrions imaginer de prendre en compte les deux dans nos décisions (Bradley et al., 2017).

5 Cette thèse

J’ai d’abord travaillé sur les incertitudes climatiques parce que je pensais qu’elles pouvaient influencer la manière dont nous définissons les politiques d’atténuation et d’adaptation. Ensuite, j’ai réalisé que l’étude des systèmes dynamiques comportant des risques et des incertitudes à l’interface entre la terre et l’homme pouvait apporter des avancées méthodologiques au domaine de l’économie. Enfin, j’ai découvert que l’examen de ces risques et incertitudes climatiques pouvait apporter de nouvelles perspectives sur la manière dont nous devrions aborder le choix social normatif en économie, en particulier dans des contextes inter-

temporels. Ainsi, ma thèse suit trois directions : documenter les conséquences économiques des incertitudes climatiques, contribuer d'un point de vue méthodologique à l'étude de l'incertitude à l'interface des systèmes humains et naturels, et enrichir la littérature sur le choix social normatif inter-temporel avec des modèles numériques pour la quantification. Pour contribuer à cette littérature, j'étudie alternativement les différentes dimensions soulignées ci-dessus et navigue entre les approches normatives et les approches positives, chacune avec ses propres avantages, inconvénients et hypothèses.

Dimension	Chapitre 1	Chapitre 2	Chapitre 3	Chapitre 4
Temps				
Espace				
Risque				
Incertitude scientifique				

TABLE 1.4 – Correspondance entre ces dimensions et mes chapitres

Le **noir** indique que cette dimension est l'enjeu clef du chapitre tandis que le **gris** indique que cette dimension est traitée dans le chapitre mais n'est pas centrale.

2 Politiques climatiques : approches positives et normatives

1 Approches normatives

La Commission Brundtland des Nations Unies fournit un cadre qui nourrit plus d'interrogations nouvelles que de conseils pratiques : "le développement durable est un développement qui répond aux besoins du présent sans compromettre la capacité des générations futures à répondre à leurs propres besoins". Le respect de ce critère dans les quatre dimensions susmentionnées représente un défi théorique et numérique. En effet, chaque dimension implique des considérations éthiques cruciales pour le choix social.

Premièrement, dans la dimension temporelle, nous devons décider de la quantité de consommation à sacrifier aujourd'hui pour le bien-être futur. Cela s'étend à un arbitrage plus profond impliquant la valeur sociale de la réduction des risques catastrophiques : à quelle consommation devrions-nous renoncer aujourd'hui pour réduire la probabilité d'une catastrophe climatique incontrôlable demain (Bommier et al., 2015) ?

Deuxièmement, dans la dimension spatiale, il existe des inégalités au sein des pays et entre eux que nous pourrions souhaiter aborder, telles que les inégalités

dans les émissions de gaz à effet de serre (cause) et les disparités dans l'exposition aux impacts climatiques (conséquence). Pour des raisons d'économie politique, telles que l'impossibilité supposée de mettre en œuvre des programmes de transfert de richesses à l'échelle mondiale en vue d'une égalisation des revenus entre les régions sans avoir été essayés, les économistes ont souvent opté pour une pondération de l'utilité, telle que la pondération de Negishi. À mon avis, cette approche reflète un manque d'imagination similaire à celui observé dans l'actualisation temporelle pure. Ces inégalités spatiales interagissent avec les inégalités temporelles, car les générations futures peuvent être plus riches en moyenne, mais les plus riches d'aujourd'hui sont plus riches que les plus pauvres de demain, en fonction des hypothèses sur les impacts climatiques et la croissance future de la productivité totale des facteurs.

Troisièmement, il existe des inégalités dans l'exposition au risque. Une question éthique clé dans les contextes risqués est de savoir s'il faut préférer l'évitement des catastrophes *ex-post* (une préférence pour la concentration de la distribution des catastrophes, telles que les décès dus aux catastrophes climatiques) ou l'équité *ex-ante* face aux risques (une préférence pour l'égalisation de la probabilité de mourir entre les agents), deux concepts contradictoires (Keeney, 1980; Bernard et al., 2018). Quelle que soit la position éthique adoptée entre ces deux options, l'intégration de l'exposition au risque implique que la question politique devient une question *ex ante*, et pas seulement une question *ex post* de redistribution si et une fois que le risque s'est matérialisé, comme c'est le cas avec l'indemnisation pour les catastrophes naturelles de l'Agence fédérale de gestion des urgences aux États-Unis.

Quatrièmement, la même question se pose concernant l'exposition inégale à l'incertitude scientifique. Cela reflète le manque d'intérêt de la communauté scientifique pour certaines questions de recherche, la rareté des données et le faible nombre de climatologues et d'économistes en dehors des pays de l'OCDE et de la Chine. De plus, face à l'incertitude scientifique, la recherche scientifique et les politiques économiques tentent de rendre l'environnement plus prévisible pour les agents économiques, mais cet effort peut avoir un effet distributif si certains agents bénéficient de l'incertitude scientifique. L'exposition inégale à l'incertitude scientifique soulève la question des effets distributifs de la résolution de cette incertitude.

2 Approches positives

Même si la distinction entre approches normatives et approches positives est quelque peu sur-jouée, car il s'agit toujours de jugements de valeur, certains éléments ne relèvent pas directement d'un critère de choix social, même s'ils l'orientent. C'est le cas de nos hypothèses sur l'adaptation des agents au changement climatique, sur la croissance future, etc. Les modèles d'optimisation de choix social, en raison de la complexité de la résolution de problèmes en grande dimension avec du risque, ont souvent choisi de ne pas modéliser l'adaptation de manière explicite. Il s'agit d'une hypothèse importante qui peut faire l'objet d'une forme de critique à la Lucas. Les modèles d'évaluation intégrée spatiaux récents évoluent pour modéliser la migration des agents, les changements dans la spécialisation économique et d'autres adaptations endogènes ([Desmet and Rossi-Hansberg, 2024](#)). Cependant, ils s'écartent du cadre éthique du planificateur social qui maximise le bien-être social, en mettant l'accent sur les scénarios d'impact. Cela représente une perte importante lorsque l'on considère la politique optimale aujourd'hui, car le critère de choix optimal n'est pas explicite. En effet, l'optimisation n'est pas globale mais résulte simplement de la combinaison de nombreux choix décentralisés d'agents rationnels motivés par des anticipations parfaites et la maximisation de l'utilité.

Le défi majeur de cette approche positive, souligné par [Popper \(1945\)](#), est l'historicisme dans les sciences sociales : "Qu'il me suffise de dire que par [historicisme] j'entends une théorie, affectant toutes les sciences sociales, qui fait de la prédiction historique son objectif principal, et qui enseigne que cet objectif peut être atteint si l'on découvre les "rythmes" ou "modèles", les "lois", ou les "tendances générales" qui sous-tendent les développements historiques". Ceci est lié à la critique de la plupart des économistes qui supposent l'ergodicité des processus socio-économiques, une hypothèse an-historique selon [North \(2005\)](#). C'est le piège dans lequel la modélisation du comportement économique, comme l'adaptation au climat et l'extrapolation des impacts météorologiques passés en impacts climatiques futurs, peut nous conduire. Le premier problème est de prétendre identifier des lois dans les sciences sociales et de les projeter pour une modélisation prospective. Le deuxième problème est le pouvoir politique de ces soi-disant lois qui pourraient être douteuses, générant de fausses oppositions parmi les partisans de solutions similaires. C'est le cas, par exemple, de l'hypothèse selon laquelle la croissance économique future de la productivité totale des facteurs est exponentielle, alors que des travaux récents suggèrent qu'elle est additive ([Philippon, 2022](#)). L'approfondissement de ces hypothèses positives pourrait aider

à réconcilier certains points de vue entre la croissance verte et la décroissance, sans recourir à des positions éthiques fortes, telles qu'une préférence marquée pour la redistribution et une forte aversion pour le risque, ou une surestimation des risques climatiques catastrophiques par rapport à d'autres états possibles du monde. En ce qui concerne les mérites de ces approches positives dans l'économie du changement climatique, je reste prudent même si je les adopte, que ce soit par conformisme scientifique ou en raison de leurs attraits, les principaux étant la disponibilité croissante de riches ensembles de données maillées, la tentative de commencer à répondre à la critique de Lucas et la tractabilité numérique des problèmes positifs en grande dimension par rapport aux méthodes de solution globale appliquées aux cadres d'optimisation inter-temporelle normatifs.

3 Description de la thèse

Comment les incertitudes découlant de ces quatre dimensions (temps, espace, risque, incertitude scientifique) affectent-elles les choix sociaux optimaux à l'interface entre les systèmes naturels et humains ? Les deux premiers articles de ma thèse sont normatifs et se concentrent sur la définition d'une politique optimale dans le cadre de modèles dynamiques d'optimisation stochastique qui tiennent compte du changement climatique endogène. Cette approche alimente les discussions sur le choix d'un critère de choix social inter-temporel rationnel et cohérent face à des risques catastrophiques irréversibles (Projet 1) et sur la modélisation de la dynamique incertaine des sous-systèmes terrestres et de leurs interactions avec la macroéconomie et l'incertitude climatique globale (Projet 2).

1 Temps, risque et incertitude scientifique

Dans le premier chapitre, nous développons un modèle dynamique stochastique économie-climat ([Cai and Lontzek, 2019](#)) pour examiner et quantifier une hypothèse critique dans le modèle standard utilisé pour définir la politique climatique optimale : la neutralité temporelle au risque agrégé dans le cadre de l'utilité escomptée actualisée. Cette hypothèse peut-elle tenir lorsque la société est confrontée à des risques importants et irréversibles tels que les points de basculement climatiques, par exemple le dépérissement de la forêt amazonienne ou la désintégration de la calotte glaciaire du Groenland ? Une fois qu'un point de basculement est franchi, le bien-être de toutes les générations suivantes est affecté négativement et corrélé positivement. Tout comme un gestionnaire de por-

tefeuille financier averse au risque considère le risque global d'un portefeuille plutôt que d'additionner les risques des actifs individuels (parce que les corrélations positives entre les risques des actifs augmentent le risque global) il peut être optimal pour un planificateur social d'accorder plus d'importance aux situations sociales où le risque global qui pèse sur l'utilité inter-temporelle est important, par exemple si le bien-être des différentes générations est faible et positivement corrélé. Le planificateur social dans le cadre du modèle d'espérance d'utilité escomptée additif n'accorde pas plus d'importance à ce risque global pesant sur l'utilité inter-temporelle. Nous utilisons des préférences sociales sensibles au risque ([Bommier et al., 2017](#)), qui sont monotones et respectent la dominance stochastique de premier ordre, contrairement au cadre d'Epstein-Zin-Weil, et comparons la politique optimale selon ce critère au modèle standard d'utilité espérée, à la fois analytiquement et numériquement. Nos résultats numériques montrent que l'aversion au risque temporel entraîne une augmentation de 30% du coût social du carbone (SCC) pour une forte augmentation irréversible de 10% des dommages économiques dus au changement climatique. L'hypothèse d'une neutralité temporelle à l'égard du risque n'est alors pas adaptée à la politique climatique, en particulier si nous prévoyons des dommages importants dus à des événements catastrophiques, car le coût social du carbone augmente fortement avec le niveau des dommages. Si l'on pense que des catastrophes majeures ayant des effets multiplicateurs importants, tels que des changements de régime irréversibles, sont possibles, alors l'aversion du planificateur social à l'égard de ces risques ayant une incidence sur l'utilité inter-temporelle doit être prise en compte. En revanche, si ce risque n'existe pas ou si les dommages possibles sont faibles, nous devrions nous en tenir au modèle additif, qui ne présente pas les inconvénients éthiques de l'aversion pour les catastrophes.

L'une des limites de notre approche est qu'elle est très stylisée, en particulier la modélisation d'un risque de basculement générique. Nous n'avons pas modélisé un élément de basculement et sa dynamique, ni les conséquences d'un risque climatique, mais nous l'avons représenté comme un processus stochastique avec un saut irréversible. Mon objectif était donc de développer un modèle qui fournit une représentation plus précise des incertitudes climatiques avec une calibration explicite. Plus précisément, je voulais que le résultat catastrophique soit une propriété émergente du système dynamique, plutôt qu'une spécification *ad hoc*, conformément à la théorie de la bifurcation ([Ritchie et al., 2021](#)). En outre, j'avais l'intention d'étudier l'interaction d'un risque climatique catastrophique spécifique avec le risque climatique global ayant un impact sur le bien-être inter-

temporel dans un cadre qui incorpore les incertitudes scientifiques.

Dans le deuxième chapitre, nous examinons comment les modèles simplifiés d'incertitudes climatiques utilisés par les économistes peuvent fausser la politique économique optimale, en particulier lorsque l'on considère les sous-systèmes de la Terre. Ces sous-systèmes présentent trois caractéristiques essentielles. Premièrement, le changement climatique mondial affecte leur dynamique. Deuxièmement, ces sous-systèmes ont un impact sur le changement climatique mondial. Ces deux effets peuvent être positifs ou négatifs. Troisièmement, la dynamique de ces sous-systèmes n'est pas uniquement une fonction linéaire du changement climatique ; elle implique également une inertie, des processus auto-entretenus ou des effets de rétroaction. Des exemples notoires de sous-systèmes climatiques sont les éléments de basculement climatique. Mais il existe également d'autres sous-systèmes sans comportement de basculement, tels que la forêt tropicale d'Asie du Sud-Est. Les interactions entre ces sous-systèmes et le changement climatique mondial sont de nature stochastique. Une question centrale pour les économistes est de déterminer si et comment les risques idiosyncratiques associés à ces sous-systèmes affectent le risque climatique global et le bien-être inter-temporel. Nous explorons analytiquement les canaux par lesquels ces interactions influencent la politique climatique optimale. En outre, nous étudions comment la gestion régionale de ces sous-systèmes pourrait être guidée par une représentation même stylisée de leur dynamique géophysique. Nous appliquons notre cadre à un modèle quantitatif calibré de la forêt amazonienne, dont la dynamique future fait l'objet d'un débat intense. En dehors des scénarios de risque standard, pour lesquels les probabilités d'état du monde futur sont connues, il existe des incertitudes scientifiques substantielles concernant la dynamique des sous-systèmes et leur interaction avec le changement climatique mondial, en raison d'ensembles de données et de modèles climatiques concurrents. La théorie de la décision offre des outils permettant d'intégrer ces incertitudes dans notre critère de choix social. L'approche méthodologique de cet article implique la résolution d'un programme d'optimisation avec une variable d'état qui présente une courbure due aux risques de basculement dans la dynamique de la forêt tropicale, en utilisant des polynômes de Chebyshev simpliciaux pour l'approximation de la fonction de valeur sur des processeurs (CPU) parallèles ([Cai, 2019](#)). Notre approche apporte deux informations économiques essentielles à la littérature sur la déforestation tropicale ([Balboni et al., 2023](#)). Premièrement, le coût social du carbone doit tenir compte des effets d'une augmentation marginale des émissions cumulées mondiales sur la dynamique de la forêt tropicale. Il s'agit notamment d'adapter les politiques ac-

tuelles aux émissions de carbone de la forêt amazonienne dans des conditions climatiques changeantes et d'intégrer un canal d'assurance, un « Amazon beta », étant donné que la valeur sociale des émissions de carbone varie en fonction de l'état du monde où elles se produisent. Deuxièmement, la valeur sociale de la forêt amazonienne en tant que puits de carbone ne doit pas se limiter à sa seule teneur actuelle en carbone ; le coût social du système dynamique (SCDS) est également crucial. Ce coût reflète la diminution marginale de l'état du sous-système due à la diminution de sa capacité d'autorégulation. Ces idées conduisent à deux implications politiques importantes. Premièrement, le coût social du carbone devrait être augmenté pour refléter l'impact des émissions marginales mondiales sur la forêt amazonienne, qui libère davantage de carbone. Cet ajustement garantit que les émetteurs du monde entier compensent les effets de leurs émissions sur le bien-être. Dans notre calibration centrale, nous estimons que cet ajustement représente une hausse de 15% dans le niveau de SCC standard qui serait appliqué seulement en présence de risque climatique agrégé. La disparité entre le SCC standard et le SCC avec rétroaction endogène de l'Amazonie pourrait être mise à profit pour financer les systèmes coasiens pour la préservation de la forêt tropicale dans une perspective de double dividende. Deuxièmement, l'évaluation d'un hectare de forêt tropicale devrait inclure non seulement le SCC standard, mais aussi le SCC élargi à l'Amazonie et une partie du SCDS. Une réduction de la couverture forestière a un impact sur le bien-être à la fois direct, par la libération de carbone, et indirect, en affectant la dynamique future du sous-système. Nous estimons que le SCDS représente environ 16% de la valeur standard du SCC. Notre cadre théorique peut donc être appliqué aux analyses locales des coûts et bénéfices de la déforestation et complète les avancées récentes dans la quantification du stockage du carbone à l'aide d'observations par satellite. Notre modélisation nous permet d'estimer qu'une hausse de 24% de la valeur de la tonne de carbone stockée dans la forêt amazonienne devrait être appliquée pour valoriser un hectare marginal de forêt dans le cadre des analyses coûts-bénéfices, par exemple pour des projets d'infrastructure au Brésil. Nous pensons que notre approche analytique appliquée ici à un modèle quantitatif de la forêt amazonienne pourrait également être appliquée à d'autres systèmes géophysiques dynamiques afin d'éclairer les décisions politiques aux niveaux mondial et régional.

L'approche normative a des limites, car elle devient difficile à résoudre lorsque la complexité du problème d'optimisation dynamique stochastique augmente. Par conséquent, l'analyse des effets distributifs du changement climatique, comme

l'inclusion de nombreuses régions ou la prise en compte des adaptations individuelles des agents, devient impraticable. Une approche positive qui se passe de choix social pourrait être la voie à suivre sur ces questions jusqu'à ce que les méthodes d'optimisation en grande dimension deviennent accessibles sans interface de passage de messages sur des *clusters* à haute performance.

2 Temps et espace

Comment les incertitudes découlant des quatre dimensions mises en évidence ci-dessus (temps, espace, risque, incertitude scientifique) affectent-elles nos estimations des impacts climatiques à l'interface entre les systèmes naturels et humains? Alors que l'approche des deux premiers articles de ma thèse est stylisée et globale, se concentrant sur la modélisation du risque stochastique et son impact sur la politique optimale, la deuxième partie de ma thèse aborde la dimension spatiale des incertitudes climatiques. J'ai cherché à travailler avec des données climatiques et socio-économiques maillées de plus en plus disponibles, qui peuvent fournir des informations précieuses sur les impacts économiques du changement climatique. Dans le chapitre 3, nous analysons l'agrégation de ces données dans le temps et l'espace. Dans mon quatrième chapitre, je développe un modèle d'équilibre spatial sectoriel dynamique et l'applique à des données maillées de 1° afin de quantifier l'impact non linéaire des canaux biophysiques souvent omis dans cette littérature (albédo, évapotranspiration et rugosité de surface), entraînés par les changements d'utilisation et d'occupation des sols (LULC), sur les impacts climatiques régionaux et les décisions d'adaptation.

Dans le troisième chapitre, nous démontrons comment l'agrégation actuelle des données climatiques et économiques dans le temps (au niveau annuel) et l'espace (à l'échelle globale) peut masquer certaines incertitudes climatiques entre les modèles climatiques et fausser nos estimations des impacts climatiques. Cette approche annuelle globale est couramment utilisée dans les modèles intégrés économie-climat standard et dans les nouveaux modèles spatiaux quantitatifs. Nous utilisons des projections climatiques régionales de distributions annuelles de température quotidiennes moyennes *downscalées* et corrigées des biais et les combinons avec des fonctions dose-réponse mondiales et régionales estimées empiriquement. Nous distinguons dans quelle mesure les impacts manquants du fait de l'agrégation dans le temps et dans l'espace des données sont dus à l'hétérogénéité dans les projections régionales du changement climatique par rapport à l'hétérogénéité régionale des dommages pour diverses trajectoires socio-économiques (SSP). La prise en compte de l'évolution de l'ensemble de la forme

de la distribution des températures moyennes journalières à l'échelle régionale révèle que les dommages mondiaux en 2050 pourraient être supérieurs d'environ 25% par rapport à une distribution synthétique où la forme de ces distributions régionales resterait la même quand la moyenne des températures change. Les différences dans la forme de la distribution des températures journalières entre les modèles climatiques transforment les classements de risque standard basés sur les anomalies de température et augmentent l'incertitude entre les modèles climatiques. Notre procédure montre que ces agrégations dissimulent également des impacts distributifs hétérogènes à travers le monde, avec des régions continentales de l'hémisphère nord particulièrement touchées par ces incertitudes sur la forme de la distribution intra-annuelle des dommages.

Dans le quatrième chapitre, je contribue à la littérature bourgeonnante en économie spatiale qui modélise l'activité économique à l'échelle régionale en utilisant des données spatiales, en particulier dans l'évaluation des impacts économiques du changement climatique ([Desmet and Rossi-Hansberg, 2024](#)). Cette littérature révèle une grande incertitude quant à l'interaction entre l'activité économique et le changement climatique. Certaines de ces incertitudes, telles que la réduction linéaire de l'échelle du changement climatique mondial aux impacts locaux, peuvent être traitées par des approches de type *Monte Carlo*. Cependant, une partie de l'incertitude est endogène et résulte directement des activités économiques régionales et des stratégies d'adaptation, comme la rétroaction de l'activité économique sur le climat régional par le biais des changements d'usage des terres. Le *downscaling* du changement climatique global au changement climatique régional est incertain et ne peut être considéré comme stable et linéaire dans le temps et l'espace ; il est influencé par les activités économiques régionales. Les climats régionaux évoluent en effet en fonction des décisions des agents (urbanisation, expansion agricole) et, à leur tour, ces climats régionaux affectent leurs décisions (spécialisation sectorielle, migration). Dans ce projet de recherche, je modélise un mécanisme qualitativement distinct reliant l'activité économique et les impacts climatiques et je quantifie l'importance de ce canal pour les impacts intertemporels agrégés et distributifs du changement climatique sur le bien-être dans un cadre spatial dynamique. Dans mon modèle, l'activité humaine affecte l'usage des terres par le biais de l'expansion agricole et de l'urbanisation. Les canaux biophysiques (albédo, évapotranspiration, rugosité) résultant de ces changements d'usage des sols ont un effet sur les conditions climatiques régionales (mesurées par les distributions annuelles des températures quotidiennes moyennes). Ces rétroactions régionales interagissent également avec les décisions d'adapta-

tion et peuvent réduire les gains de bien-être attendus des mécanismes d'adaptation. Je commence par estimer des relations de forme réduite entre l'activité économique régionale et les impacts biophysiques régionaux *via* les demandes de terres urbaines et agricoles. Je construis ensuite un modèle spatial dynamique à l'échelle mondial, avec deux secteurs (agricole et non agricole) et des individus qui s'adaptent par le biais du commerce, de la migration et de la spécialisation sectorielle. Le changement climatique affecte de manière hétérogène les productivités régionales sectorielles et les aménités régionales. Pour la validité interne du modèle, j'utilise les conditions d'équilibre du modèle pour estimer les fonctions dose-réponse des aménités régionales et des productivités sectorielles à la distribution annuelle semi-paramétrique des températures moyennes journalières. Enfin, j'applique le modèle à des données maillées à 1° à l'échelle mondiale et je le résous en algèbre à chapeau dynamique afin d'éviter de calculer les productivités et les aménités initiales fondamentales. Dans ma simulation de référence SSP2-4.5, sans impacts biophysiques, presque toutes les régions subissent des changements négatifs de bien-être en raison des schémas non linéaires de réchauffement intra-annuel régional, combinés à des dommages non-linéaires par bins de température. D'après mes résultats, aucun bénéfice notable n'est à attendre du changement climatique dans l'hémisphère Nord. L'ajout de canaux biophysiques, c'est-à-dire un down-scaling non linéaire, endogène aux activités régionales et variable dans le temps des distributions de température globale à régionale, représente 2.4 % des impacts biogéochimiques standard du changement climatique sur le bien-être. Les impacts climatiques biogéochimiques et biophysiques sont tous deux régressifs, décroissant en fonction des niveaux de revenu par habitant de 2015. L'activité économique régionale façonne clairement les impacts climatiques physiques régionaux et entraîne des conséquences agrégées et distributionnelles non négligeables.

3 Liste des travaux de recherche

Dans cette thèse de doctorat, qui s'étend sur plus de trois ans, je me suis efforcé d'étudier les incertitudes climatiques et leurs implications pour la politique économique. Tout au long de mes recherches, j'ai étudié la validité de nos critères de choix social en présence de risques irréversibles (chapitre 1), la précision de nos représentations stylisées du système climatique et de ses composantes (chapitre 2), l'efficacité de nos méthodes d'agrégation des données dans l'espace et dans le temps (chapitre 3) et l'importance des canaux biophysiques régionaux du changement climatique (chapitre 4). Je suis le premier auteur de tous ces projets de

recherche, mais je suis profondément reconnaissant à mes coauteurs pour leurs contributions inestimables. Je recommande de se concentrer sur les chapitres 2 et 4 qui, à mon avis, apportent les contributions les plus originales à la littérature scientifique et au débat public parmi tous les chapitres.

Documents de travail :

Chapter 1 : Fillon, Guivarch, Taconet, 2023. 'Optimal climate policy under tipping risk and temporal risk aversion', *Journal of Environmental Economics and Management*.

Chapter 2 : Fillon, Guivarch, 2024. 'The need for regulation of climate subsystems'.

Chapter 3 : Fillon, Linsenmeier, Wagner, 2024. 'Climate shift uncertainty and economic damages'.

Chapter 4 : Fillon, 2024. 'The biophysical channels of climate impacts'.

2024 FAERE conference (BETA, U. de Strasbourg), EAERE conference (KU Leuven), LAGV conference (AMSE), iRisk invited seminar (IESEG, LEM, U. de Lille), CIRED (internal PhD seminar), U. Paris-Saclay (Economics & Management, PhD).

2023 MIT (CEEPR, weekly lunch talk), Columbia U. (SIPA, Sustainable Development Colloquium), Duke U. (Nicholas & Sanford Schools, UPEP PhD seminar), Yale U. (School of the Environment, PhD seminar), U. Paris-Saclay (Economics & Management, PhD seminar).

2022 CIRED (PhD seminar, internal), ENS Paris-Saclay (CEPS PhD seminar), Modeling Uncertainty in Social, Economic, and Environmental Sciences MUSEES Conference (EM Lyon), 12th FAERE Workshop (ENS Paris-Saclay), International Conference on Public Economic Theory PET 2022 (AMSE), EAERE conference (U. di Bologna), FAERE conference (U. de Rouen).

Bibliographie

- D. I. Armstrong McKay, A. Staal, J. F. Abrams, R. Winkelmann, B. Sakschewski, S. Loriani, I. Fetzer, S. E. Cornell, J. Rockström, and T. M. Lenton. Exceeding 1.5 °C global warming could trigger multiple climate tipping points. *Science*, 377(6611) :eabn7950, 2022.
- M. Azinovic, L. Gaegau, and S. Scheidegger. Deep equilibrium nets. *International Economic Review*, 63(4) :1471–1525, 2022.
- C. Balboni, A. Berman, R. Burgess, and B. A. Olken. The economics of tropical deforestation. *Annual Review of Economics*, 15 :723–754, 2023.
- U. Beck. *Risk Society : Towards a New Modernity*. 1986.
- L. Berger and M. Marinacci. Model uncertainty in climate change economics : A review and proposed framework for future research. *Environmental and Resource Economics*, 77(3) :475–501, 2020.
- C. Bernard, C. M. Rheinberger, and N. Treich. Catastrophe aversion and risk equity in an interdependent world. *Management Science*, 64(10) :4490–4504, 2018.
- A. Bilal. Solving heterogeneous agent models with the master equation. Technical report, National Bureau of Economic Research, 2023.
- A. Bilal and E. Rossi-Hansberg. Anticipating climate change across the united states. Technical report, National Bureau of Economic Research, 2023.
- M. Blicharska, R. J. Smithers, M. Kuchler, G. K. Agrawal, J. M. Gutiérrez, A. Hassanali, S. Huq, S. H. Koller, S. Marjit, H. M. Mshinda, et al. Steps to overcome the north–south divide in research relevant to climate change policy and practice. *Nature Climate Change*, 7(1) :21–27, 2017.
- A. Bommier, B. Lanz, and S. Zuber. Models-as-usual for unusual risks? on the value of catastrophic climate change. *Journal of Environmental Economics and Management*, 74 :1–22, 2015.
- A. Bommier, A. Kochov, and F. Le Grand. On monotone recursive preferences. *Econometrica*, 85 (5) :1433–1466, 2017.
- A. Bommier, A. Fabre, A. Goussebaïle, and D. Heyen. Disagreement aversion. Available at SSRN 3964182, 2021.
- R. Bradley, C. Helgeson, and B. Hill. Climate change assessments : Confidence, probability, and decision. *Philosophy of Science*, 84(3) :500–522, 2017.
- M. Burke, S. M. Hsiang, and E. Miguel. Global non-linear effect of temperature on economic production. *Nature*, 527(7577) :235–239, 2015.
- Y. Cai. Computational methods in environmental and resource economics. *Annual Review of Resource Economics*, 11(1) :59–82, 2019.

- Y. Cai and T. S. Lontzek. The social cost of carbon with economic and climate risks. *Journal of Political Economy*, 127(6) :2684–2734, 2019.
- B. Crost and C. P. Traeger. Optimal climate policy : uncertainty versus monte carlo. *Economics Letters*, 120(3) :552–558, 2013.
- J.-L. Cruz and E. Rossi-Hansberg. The economic geography of global warming. *Review of Economic Studies*, 91(2) :899–939, 2024.
- K. Desmet and E. Rossi-Hansberg. Climate change economics over time and space. *Annual Review of Economics*, 16, 2024.
- S. Dietz, C. Gollier, and L. Kessler. The climate beta. *Journal of Environmental Economics and Management*, 87 :258–274, 2018.
- S. Dietz, J. Rising, T. Stoerk, and G. Wagner. Economic impacts of tipping points in the climate system. *Proceedings of the National Academy of Sciences*, 118(34) :e2103081118, 2021.
- D. Folini, A. Friedl, F. Kübler, and S. Scheidegger. The climate in climate economics. *Review of Economic Studies*, page rdae011, 2024.
- A. Friedl, F. Kübler, S. Scheidegger, and T. Usui. Deep uncertainty quantification : with an application to integrated assessment models. Technical report, Working Paper University of Lausanne, 2023.
- H. Hong, N. Wang, and J. Yang. Mitigating disaster risks in the age of climate change. *Econometrica*, 91(5) :1763–1802, 2023.
- S. Hsiang. Climate econometrics. *Annual Review of Resource Economics*, 8(1) :43–75, 2016.
- R. L. Keeney. Equity and public risk. *Operations research*, 28(3-part-i) :527–534, 1980.
- D. M. Kreps and E. L. Porteus. Temporal resolution of uncertainty and dynamic choice theory. *Econometrica : journal of the Econometric Society*, pages 185–200, 1978.
- D. Lemoine and I. Rudik. Managing climate change under uncertainty : Recursive integrated assessment at an inflection point. *Annual Review of Resource Economics*, 9(1) :117–142, 2017.
- T. M. Lenton, H. Held, E. Kriegler, J. W. Hall, W. Lucht, S. Rahmstorf, and H. J. Schellnhuber. Tipping elements in the earth’s climate system. *Proceedings of the national Academy of Sciences*, 105(6) :1786–1793, 2008.
- V. Masson-Delmotte, H. Pörtner, J. Skea, E. Buendía, P. Zhai, and D. Roberts. Climate change and land. *IPCC Report*, 2019.
- W. Nordhaus. *A question of balance : Weighing the options on global warming policies*. Yale University Press, 2008.
- W. D. Nordhaus and Z. Yang. A regional dynamic general-equilibrium model of alternative climate-change strategies. *The American Economic Review*, pages 741–765, 1996.

- D. North. *Understanding The Process Of Economic Change*. Princeton University Press, 2005.
- T. Philippon. Additive growth. Technical report, National Bureau of Economic Research, 2022.
- K. Popper. *The Open Society and Its Enemies*. Routledge, London, 1945.
- W. V. Quine. On the reasons for indeterminacy of translation. *The Journal of Philosophy*, 67(6) : 178–183, 1970.
- F. P. Ramsey. A mathematical theory of saving. *Economic Journal*, 38(152) :543–559, 1928.
- J. Rising, M. Tedesco, F. Piontek, and D. A. Stainforth. The missing risks of climate change. *Nature*, 610(7933) :643–651, 2022.
- P. D. Ritchie, J. J. Clarke, P. M. Cox, and C. Huntingford. Overshooting tipping point thresholds in a changing climate. *Nature*, 592(7855) :517–523, 2021.
- L. M. Stanca. Recursive preferences, correlation aversion, and the temporal resolution of uncertainty. *arXiv preprint arXiv* :2304.04599, 2023.
- T. Strzalecki. Temporal resolution of uncertainty and recursive models of ambiguity aversion. *Econometrica*, 81(3) :1039–1074, 2013.
- T. S. Van den Bremer and F. Van der Ploeg. The risk-adjusted carbon price. *American Economic Review*, 111(9) :2782–2810, 2021.

Chapitre 1

Optimal climate policy under tipping risk and temporal risk aversion

This article^a is a joint work with Céline Guivarch (École des Ponts, CIRED) and Nicolas Taconet (École des Ponts, CIRED & PIK), published in *Journal of Environmental Economics and Management*, 2023.

We investigate the implications of absolute risk aversion with respect to intertemporal utility, i.e. *temporal* risk aversion, in the presence of a stylized climate tipping risk affecting productivity irreversibly. Optimal climate policy is more stringent under temporal risk aversion, in order to reduce all present and future probabilities of crossing the tipping point and avoid a situation where all generations are badly off. Temporal risk aversion implies a 30% increase in the social cost of carbon (SCC) under our benchmark calibration and for a 10% irreversible increase in the level of economic damage from climate change. The optimal SCC under temporal risk aversion increases sharply with the level of damage brought by a potential tipping point.

Keywords : stochastic climate-economy modelling, risk-sensitive recursive preferences, environmental policy, risk aversion.

JEL classification : D61, D63, D71, D81, Q54, Q58.

^a. We thank two anonymous referees for their invaluable help in improving the manuscript. We also thank Thomas Douenne, Johannes Emmerling, Simon Jean, Vincent Martinet, Aurelie Méjean, Eddy H.F. Tam and Stephane Zuber for comments on earlier versions of this work. Any remaining errors are ours. Céline Guivarch received funding from the European Union's Horizon Europe research and innovation programme under grant agreement No. 101081604 (PRISMA). Corresponding author : Romain Fillon.

1 Introduction

When it comes to decision-making, risk is all around. But the concept is equivocal. First, it can refer to a univariate risk bearing on a single prospect. The seminal work from [Pratt \(1964\)](#) and [Arrow \(1971\)](#) introduced this risk into the analysis of decision-making through univariate measures of absolute and relative risk aversion within expected utility theory. A substantial body of literature has developed to generalise these measures of risk aversion to multivariate risks ([Kihlstrom and Mirman, 1974](#)). A risk-averse portfolio manager does not sum the risk of each asset, but considers the aggregate risk bearing on the portfolio. Indeed, a positive correlation between these asset risks increases the aggregate risk. In intertemporal settings, the absolute risk aversion with respect to aggregate intertemporal risk is called the *temporal risk aversion* ([Bommier et al., 2015](#)). The standard discounted expected utility model assumes temporal risk-neutrality ([Ahn, 1989](#)). This assumption has large implications as it implies that the decision-maker has no preference on the correlation between individual risks. Introducing absolute risk aversion with respect to intertemporal utility, i.e. temporal risk aversion, on the other hand, allows to consider risk bearing on aggregate intertemporal utility. It can explain agent's intertemporal decisions ([Bommier, 2013](#); [Bommier and Grand, 2019](#)). It is also of interest from a normative point of view, to define optimal policies in risky social situations that involve several successive generations whose welfare is correlated.

A prominent example of intertemporal social risk management is climate policy-making. A major concern of climate policy-making is the possibility of non-linearities such as tipping points in the climate system. Once some thresholds for greenhouse gas concentrations in the atmosphere are exceeded, the state of the climate system could be radically and irreversibly altered. Tipping elements with significant economic implications have been identified, including the slowdown of the Atlantic Meridional Overturning Circulation, the West Antarctic ice sheet disintegration, the Amazon rainforest dieback, or the Greenland ice sheet disintegration ([Arias et al., 2021](#)). In the states of the world where the tipping point occurs, the welfare of all subsequent generations is affected by this qualitative regime change. Consequently, considering absolute risk aversion with respect to intertemporal utility becomes imperative due to the substantial impact on intertemporal welfare.

Temporal risk aversion can be interpreted as positive intertemporal correlation aversion ([Richard, 1975](#)), as positive intertemporal correlation implies a lar-

ger aggregate risk over intertemporal utility. A temporally risk-averse social planner prefers the welfare of different generations to be negatively or not correlated rather than positively correlated, in order to lower the risk on the aggregate outcome. In other words, the temporally risk averse social planner would be ready to give up some social welfare to prevent a situation where the tipping point is crossed and all subsequent generations are badly off. Thus, this social diversification strategy is appealing from a normative point of view when facing irreversible catastrophic tipping risks. Also, from a positive point of view, empirical elicitations of individual preferences suggest that individual agents might exhibit positive correlation aversion ([Ebert and van de Kuilen, 2015](#); [Andersen et al., 2018](#); [Gangadharan et al., 2019](#); [Rohde and Yu, 2022](#); [Lanier et al., 2024](#)).

In this article, we investigate how temporal risk aversion may affect optimal climate policy. We analyze both analytically and numerically why, how and by how much two social planners, i.e. a temporally risk-neutral and a temporally risk-averse planner, differ in their optimal policy under risk. We focus on a specific type of risk : a climate tipping risk. We use a dynamic stochastic climate-economy model ([Guivarch and Pottier, 2018](#); [Taconet et al., 2021](#)) and extend it to an alternative social welfare function which allows the analysis of temporal risk aversion : the risk-sensitive preferences axiomatized in [Hansen and Sargent \(1995\)](#). By comparing optimal climate policies under risk-sensitive preferences with those under the standard additive form of expected discounted utility, which assumes temporal risk-neutrality, we shed light on the implications of temporal risk aversion for policy design.

We find that, in the presence of a tipping risk, climate policy is more stringent under risk-sensitive preferences. The social planner under risk-sensitive preferences is willing to sacrifice more today to reduce all present and future probabilities of crossing the tipping point to avoid a situation of low overall intertemporal utility level. The difference in optimal climate policy between the two planners increases more than proportionally to the increase in the possible shock or in the temporal risk aversion. Under our benchmark calibration, a change from additive to risk-sensitive preferences implies a 30% increase in the social cost of carbon (SCC) for a 10% irreversible increase in the damage factor. Switching from additive to risk-sensitive preferences under a 10% possible shock is equivalent to a 5 percentage points increase in the shock if we keep additive preferences. The difference between the two social choice criteria increases steeply with risk. Furthermore, other things being equal, a 50% decrease in pure time preference (from

1.5% to 1% yearly) is needed to obtain the same optimal policy under additive preferences as under risk-sensitive preferences for a 10% tipping risk and under our benchmark calibration. Thus, a change in the structure of the social welfare function can be directly compared to a change in the value of some parameters that have been highly debated. Finally, we use an analytical decomposition of our optimal policy program to derive the key channels through which a tipping risk affects optimal policy under both social welfare functions.

Our work contributes to the literature aiming to enhance the integration of different types of risk, particularly the risk of climate tipping points ([Lemoine and Traeger, 2014](#); [van der Ploeg and de Zeeuw, 2019](#); [Cai and Lontzek, 2019](#)), into stochastic integrated assessment models (IAM). The first integrated climate-economy models were deterministic, e.g. [Nordhaus \(2008\)](#). These models did not allow for a proper consideration of risk and uncertainty in planner's decisions, even when Monte Carlo analyses were conducted ([Crost and Traeger, 2013](#)). In parallel, contributions to modeling endogenous catastrophic environmental risk were mostly stylized ([Clarke and Reed, 1994](#); [Tsur and Zemel, 1996](#); [Bommier et al., 2015](#)). In particular, these models are based on the assumption that welfare after the catastrophic event is exogenous and independent of the planner's actions. Tipping points are less extreme than catastrophes after which production and consumption would be exogenous and independent of the planner's decisions. Indeed, these are ecological regime shifts with large economic consequences rather than complete economic or institutional collapses. These events are also different from reversible extreme events that occur as one-off catastrophes along a smoothly evolving climate regime with fluctuations, traditionally modelled with Poisson and Wiener processes in the macroeconomics literature on disasters, e.g. in [Bretschger and Vinogradova \(2019\)](#). Departing from the assumption of a geometric Brownian motion with rare and reversible catastrophic events, we study irreversible regime changes. This modelling approach has counterparts in the real business cycles literature studying markov switching rational expectations models with Bayesian learning, e.g. in [Bullard and Singh \(2012\)](#).

Our contribution confronts the standard discounted expected utility model with an alternative criterion : a risk-sensitive criterion stemming from social choice theory and axiomatized in [Bommier et al. \(2017\)](#). Exploration of alternative social choice criteria under endogenous climate change was undertaken to introduce relative risk aversion under Epstein-Zin-Weil preferences ([Belaia et al., 2017](#);

van der Ploeg and de Zeeuw, 2018), a robust control penalty (Rudik, 2020) and ambiguity aversion under isoelastic preferences in a setting with uncertainty (Lemoine and Traeger, 2016). In comparison with EZW preferences, risk-sensitive preferences are the only recursive preferences axiomatized by Kreps and Porteus (1978) that admit a separation of risk and intertemporal attitudes, while being monotone (Bommier et al., 2017). This desirable normative property ensures that a more risk-averse planner consistently prioritizes risk reduction. Those preferences can be defined through the following recursion (Hansen and Sargent, 1995; Bommier et al., 2017) :

$$V_t = \begin{cases} (1 - \beta) u_t + \beta \mathbb{E}[V_{t+1}] & \text{if } \epsilon = 0 \\ u_t - \frac{\beta}{\epsilon} \ln[\mathbb{E}(\exp[-\epsilon V_{t+1}])] & \text{if } \epsilon \neq 0 \end{cases} \quad (1.1)$$

with u_t the instantaneous utility at time t , β a discount factor derived from pure time preference and ϵ the temporal risk aversion. We hereafter use the denomination of risk-sensitive preferences only for those stationary preferences for which the social planner is at least as risk averse ($\epsilon > 0$) as a standard planner with additive preferences. Cases where the social planner is temporally risk-seeking ($\epsilon < 0$) are not discussed because of potential nonconvexity issues (Bommier and Grand, 2019). A temporally risk-seeking planner would choose a max-max strategy and positive correlation between the social gambles. If $\epsilon = 0$, then the social planner is temporally risk-neutral, which comes down to the additive form.

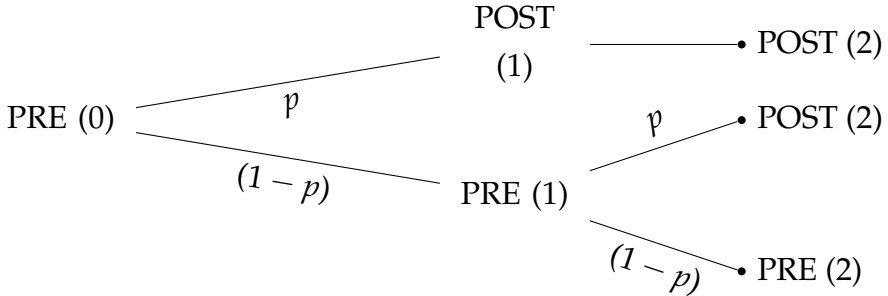
Firstly, we present our modelling approach (section 2) : a dynamic stochastic climate-economy integrated model with a stylized tipping risk, in which we compare two alternative social welfare functions. Then, we discuss analytically how temporal risk aversion affects optimal policy under a tipping risk (section 3). Finally, we quantify numerically the differences between the two social welfare functions under a tipping risk (section 4).

2 A dynamic climate-economy stochastic model

1 A simple illustration

Firstly, we illustrate the significance of temporal risk aversion in the analysis of climate tipping risks using a simplified scenario. Consider three consecutive time periods, representing distinct generations. Two climate regimes exist :

pre-tipping (PRE) and post-tipping (POST), each associated with different levels of economic damage. Each generation t can either be in a high (PRE) or a low (POST) welfare regime, described by the variable $u_i^t, i \in (pre, post), t \in 1, 2$. We assume that instantaneous welfare function in each potential situation is the same for both generations, i.e. $u_i^1 = u_i^2$.



We assume away time discounting and assume that the social planner has no preference on the order of the attributes and no preference for early resolution of uncertainty. Under the conditions listed above, a temporally risk-neutral social planner would be indifferent between the two following lotteries (Bommier, 2005) :

$$\left\{ \begin{array}{ll} (u_1^{post}, u_2^{post}) & \text{with probability } \frac{1}{3}, \\ (u_1^{pre}, u_2^{post}) & \text{with probability } \frac{1}{3}, \\ (u_1^{pre}, u_2^{pre}) & \text{with probability } \frac{1}{3}, \end{array} \right. \sim \left\{ \begin{array}{ll} (u_1^{post}, u_2^{post}) & \text{with probability } \frac{1}{2}, \\ (u_1^{pre}, u_2^{pre}) & \text{with probability } \frac{1}{2}. \end{array} \right. \quad (1.2)$$

A social planner under additive preferences would be indifferent between the two social lotteries A and B as the additive form assumes temporal risk-neutrality, while a temporally risk-averse social planner has a preference for lottery A. In other words, a temporally risk-averse social planner is willing to pay a temporal risk premium to hedge risks across generations and reduce the probability of complete failure across all generations.

In addition to positive intertemporal correlation aversion, temporal risk aversion bears preference for catastrophe avoidance¹ (Bommier et al., 2015), i.e. preference for a mean-preserving contraction in the distribution of catastrophic risks. The preference for catastrophe avoidance is highly debated in the literature for two main reasons. First, it is not clear that individual agents are catastrophe-averse (Rheinberger and Treich, 2017). Furthermore, preference for catastrophe avoidance may be seen as unethical as a catastrophe-averse planner prefers to

1. If the social planner is temporally risk-seeking ($\epsilon < 0$), she favors risk equity, i.e. equalizing and spreading the risk among generations.

concentrate risk on a single generation rather than spreading it evenly ([Fleurbaey, 2010](#)). Consequently, [Fleurbaey \(2018\)](#) highlights that catastrophe aversion might be appealing only if the catastrophe has a multiplier effect through externalities in society. The possible nonconvexities in the human-environment system, enhanced by ecological thresholds like climate tipping points, do have this multiplier property. Indeed, in the states of the world where the tipping point occurs, the regime change is *irreversible* and has an impact on all future generations.

We have described in a simple illustration the importance of temporal risk aversion in risky intertemporal settings. We now present a full-fledged stochastic climate-economy model to analyse and quantify the importance of temporal risk aversion for the definition of optimal climate policy under a tipping risk.

2 The model

A climate-economy integrated assessment model aims to study the interactions between the economy and the climate system. We introduce a simple growth model *à la Ramsey*, add a stylized representation of the climate dynamics and an endogenous stochastic tipping point in the climate system. We build on [Guivarch and Pottier \(2018\)](#) and [Taconet et al. \(2021\)](#), update the economic dynamics to match DICE-2016 ([Nordhaus, 2018](#)) and use an alternative social welfare function.

Economy In our global model, a single good is produced at each period t using two production factors, endogenous capital K_t and exogenous labour L_t , through a Cobb-Douglas production function $F(K_t, L_t) = A_t K_t^\alpha L_t^{1-\alpha}$ with exogenous Hicks-neutral technological change. The gross output $F(K_t, L_t)$ is affected by a damage factor $\Omega_t(T_t)$ that increases with global average temperature T_t . Net output Y_t is derived from the gross output net of damage : $Y_t = \Omega_t(T_t)F(K_t, L_t)$. Capital dynamics is determined by δ , the per-period capital depreciation, and s_t , the savings rate. It writes : $K_{t+1} - K_t = -\delta K_t + s_t Y_t$. Gross output induces emissions, which can be mitigated at a certain cost. The social planner trades off consumption C_t , mitigation costs (which represent a share Λ_t of Y_t), and investment : $C_t = Y_t(1 - \Lambda_t - s_t)$. The mitigation cost Λ_t depends on the abatement rate μ_t and on the cost of the abatement technology that decreases due to exogenous technical progress. The cost of the abatement technology is calibrated on [Nordhaus \(2018\)](#) as other parameters of the economic module.

Climate We use a simple representation for the climate system with a linear formula linking temperature change to the stock of carbon emissions (Dietz and Venmans, 2019). This approach avoids overestimating the delay between emissions and temperature rise. Indeed, the link between cumulative emissions and temperature has been shown to be almost independent of time and emissions pathways except for very high emission pathways (Leduc et al., 2015) such as the RCP 8.5 : it should thus hold for any reasonable optimal policy scenario. Emissions are derived from output : $E_t = \sigma_t Y_t (1 - \mu_t)$, where σ_t is the carbon content of production that decreases exogenously over time. Emissions increase carbon concentration in the atmosphere and there is no decay. Equation for temperature change is : $T_t = \psi (CE_0 + \sum_{s=0}^t E_s) = \psi S_t$ where T_t is the global temperature increase (in comparison with the pre-industrial era) at time t , CE_0 is cumulated emissions up to the first period of the model, E_s the emissions at time s , S_t the carbon stock in the atmosphere at time t and ψ the transient climate response to cumulative carbon emissions (TCRE, $\psi = 1.65^\circ\text{C}$ per TtC, according to Masson-Delmotte et al. (2021)).

Tipping risk We model one stylized endogenous tipping point that may decrease the output via an increase in the damage factor affecting the productivity. The tipping point is endogenous as its probability of occurrence is a function of global average surface temperature. If the tipping point is crossed, the damage factor Ω faces an irreversible $J\%$ increase. The pre-tipping damage function writes : $\Omega_1(T) = 1 - \pi T^2$. Once the tipping point is crossed, the damage increase by $J\%$ and the new damage function writes : $\Omega_2(T) = (1 - J)(1 - \pi T^2)$. The damage occurs with no delay. The probability of tipping is modeled with a uniform distribution between initial temperature increase with respect to pre-industrial era and an upper temperature threshold² to make as few assumptions as possible about the precise temperature at which a tipping event may occur. Along the path, this specification allows learnings from the bayesian policymaker as she updates her beliefs on the location of the threshold in the state space and on the probability of tipping at each period. The key assumption from this specification of the potential tipping event is that there is no tipping risk if the temperature is stabilized (Lemoine and Traeger, 2014). At each period t , the tip-

2. The lower bound is the 2015 current excess temperature in comparison with the preindustrial era (0.87°C in 2015). The upper bound is set to 5.7°C according to the upper bound of the temperature increase reached in 2100 in RCP 8.5 (Arias et al., 2021). See 1 for a sensitivity analysis.

ping point is crossed with probability h_t :

$$h_t(T_t, T_{t-1}) = \begin{cases} \frac{T_t - T_{t-1}}{T_{max} - T_{t-1}} & \text{if } T_t < T_{max}, \\ 1 & \text{if } T_t \geq T_{max}. \end{cases} \quad (1.3)$$

We have presented above a stochastic model with a stylized tipping point. A second step is to use a social welfare function that allows the study of temporal risk aversion. We present this function in more depth below. To allow comparison with previous literature, we compare how two forms of social preferences behave in a risky intertemporal social setting. The first form is the additive one. The second form is the one of risk-sensitive preferences with positive temporal risk aversion.

3 Social preferences

In our model, we write two Bellman equations for the two possible situations, pre- and post-tipping, under the additive and the risk-sensitive social welfare functions, as welfare is affected by a J% increase in the damage factor once the tipping point is crossed. If the tipping point is crossed, the Bellman equation writes the same way for the two programs. The two social welfare functions yield the same policy in the risk-free post-tipping situation : temporal risk aversion plays no role in these risk-free situations, whatever its level. Once the tipping is crossed, all risk is solved : the tipping risk is the sole risk we study here. The state variables of our optimization program are $x_t = (S_t, K_t)$ respectively the cumulative emissions stock and the capital stock at time t. The control variables are $y_t = (\mu_t, s_t)$, respectively the abatement rate and the savings rate at time t. The instantaneous utility function writes : $u_t(x_t, y_t) = C_t^{1-\eta} / (1 - \eta)$ with η the elasticity of marginal utility.

Additive preferences Under additive preferences, once the tipping point is crossed, we have : $U_t^{post}(x_t, y_t) = \max_{y_t} [u_t(x_t, y_t) + \beta U_{t+1}^{post}(x_{t+1})]$ under the constraints : $x_{t+1} = G(x_t, y_{t+1})$ and $y_t \in \Gamma(x_t)$, with Γ the space of possible (positive) values for the control variables and G a transfer function. If the tipping point has not been crossed yet at time t, then it may be crossed at time t+1 with probability h_{t+1} or the world can stay in a pre-tipping situation with a probability $(1 - h_{t+1})$. The pre-tipping Bellman equation under additive preferences and under the same

constraints as above writes :

$$U_t^{pre}(x_t, y_t) = \max_{y_t} \left[u_t(x_t, y_t) + \beta[(1 - h_{t+1})U_{t+1}^{pre}(x_{t+1}) + h_{t+1}U_{t+1}^{post}(x_{t+1})] \right] \quad (1.4)$$

Risk-sensitive preferences Once the tipping point is crossed, the program under risk-sensitive preferences reduces to the additive one. If $\epsilon = 0$, the program under risk-sensitive preferences reduces to the additive one. Finally, it should be noted that $V^{post} = U^{post}$. The Bellman equation under the same constraints in the pre-tipping situation writes :

$$V_t^{pre}(x_t, y_t) = \max_{y_t} \left(u_t(x_t, y_t) - \frac{\beta}{\epsilon} \ln \left[(1 - h_{t+1}) \exp(-\epsilon V_{t+1}^{pre}(x_{t+1})) + h_{t+1} \exp(-\epsilon V_{t+1}^{post}(x_{t+1})) \right] \right) \quad (1.5)$$

4 Comparison with alternative social preferences

We compare the additive expected utility model to risk-sensitive preferences in order to study temporal risk aversion. Two main other frameworks have been used to study risk aversion under endogenous catastrophic climate change : the Epstein-Zin-Weil framework (hereafter, EZW) and the multiplicative preferences.

1 Epstein-Zin-Weil preferences

EZW preferences have been widely used in risky intertemporal settings to discuss optimal policy, e.g. in [Cai and Lontzek \(2019\)](#), because of their flexibility, which allows to disentangle preference over time and preference over states of the world. We depart from it for two main reasons.

The first reason is that these preferences are monotone with respect to first-order stochastic dominance³ ([Bommier et al., 2017](#)) only in the limit cases where relative risk aversion equals the inverse of the elasticity of intertemporal substitution (they reduce to the standard additive model) or when the elasticity of intertemporal substitution equals one (EZW preferences are then risk-sensitive). If EZW preferences are well ordered in terms of risk aversion ‘in the large’ (willingness to pay to eliminate all risks), those preferences are not well ordered in terms of risk aversion ‘in the small’ (willingness to pay for marginal risk reductions). Thus, a social planner under EZW preferences might choose dominated strate-

3. A social planner has preferences that respect first-order dominance if, for two lotteries A and B with A dominating B, she prefers A to B regardless of her utility function, as long as it is weakly increasing. The lottery A dominates B if it gives more wealth than B realization by realization.

gies in social settings where it is not possible or optimal to eliminate all risk which may precisely be the case with climate change. In particular, it has been shown in the theoretical and applied literature that this non-monotonicity can lead to two types of counter-intuitive behaviours. On the one hand, the EZW agent can make more precautionary choices than necessary, choosing to build up more precautionary savings in a risky situation than the savings chosen in the worst state of the world that could occur under this risk if it happened deterministically (Bommier et al., 2017). This leads to a more extreme behavior than a max-min approach. On the other hand, the role of risk aversion could be non-monotone, meaning that for a higher relative risk aversion and the same risk, the planner can be less precautionous (Kimball and Weil, 2009; Bommier and Grand, 2019). The fact that such dominated strategies can be chosen, even if not always, makes this criterion less appealing for the definition of the optimal policy. Unlike the EZW framework, risk-sensitive preferences are monotone with respect to first-order stochastic dominance, which means that dominated strategies are never chosen. In particular, in our setting, we show in annex 3 that the risk premium is always positive and increasing in the temporal risk aversion ϵ . When relative risk aversion is lower than the inverse of the elasticity of intertemporal substitution, EZW preferences show preference for late resolution of uncertainty and a negative risk premium, while risk-sensitive preferences exhibit preference for early resolution of uncertainty whenever $\epsilon > 0$. Risk-sensitive preferences thus allow a more rational social choice while preserving the flexibility and recursivity properties of the Kreps and Porteus (1978) framework.

The second reason why we use risk-sensitive preferences rather than EZW preferences is that the coefficient of relative risk aversion studied in EZW preferences does not directly compare with the absolute risk aversion with respect to intertemporal utility studied under risk-sensitive preferences⁴, as a reduction in relative risk does not always come with a reduction in aggregate risk (Bommier et al., 2012). A relative risk averse agent prefers to have non-extreme payoffs

4. Risk-sensitive preferences use a constant *absolute* risk aversion certainty equivalent, whereas EZW preferences use a constant *relative* risk aversion certainty equivalent (Bommier et al., 2015). When comparing temporal lotteries of consumption, constant absolute risk aversion has been seen as unrealistic because risk aversion is the same for all levels of wealth under this assumption. Here, the constant absolute risk aversion certainty equivalent is applied to distributions of utility levels rather than consumption levels. This assumption is made under risk-sensitive preferences as monotonicity implies that risk aversion is considered with respect to aggregate utility. Thus, in order to preserve history independence, constant absolute risk aversion with respect to aggregate intertemporal risk ensures that the utility of the first periods does not impact social choice afterwards (Bommier et al., 2017).

across states of the world within periods, while a temporally risk-averse planner prefers to have non-extreme payoffs across states of the world over the whole time horizon considered.

2 Multiplicative preferences

The second form are the multiplicative preferences (Bommier et al., 2015) that rule out pure time preference so that different generations are not given different utility weights because they were born at different dates. Instead, we use an intermediate form of risk-sensitive preferences that does not assume away time discounting for three reasons. Firstly, we do not include an extinction risk, so that without pure time preference, our undiscounted dynamic program would be too sensitive to the arbitrary terminal value and limit the comparability between the two programs. The second reason is that we want to analyze the sole role of temporal risk aversion on social choice rather than intertwining this questioning with the debate between discounted and undiscounted utilitarianism (Stern, 2006; Nordhaus, 2008). The third reason is the comparability between additive and risk-sensitive preferences. Indeed, additive and risk-sensitive social planners have the same rankings over deterministic consumption paths regardless of the value of the temporal risk aversion ϵ . We can therefore simply vary ϵ within a reasonable value range and make comparisons between the two social choice criteria under risk for different values of ϵ .

We have characterized the additive and the risk-sensitive social welfare functions and explained how temporal risk aversion can be an important determinant of climate policy. We now assess analytically the impact of temporal risk aversion on optimal climate policy under a tipping risk.

3 How does temporal risk aversion affect optimal policy under a tipping risk?

Firstly, we derive analytically the impact of temporal risk aversion on the optimal policy under a tipping risk. We decompose the pre-tipping value functions (1.4) and (2.9) which incorporate the risk of tipping and analyze the case where a single state variable determines the chance of crossing the threshold. We focus solely on S_t , the cumulated stock of emissions at time t . As we are considering optimal climate policy, we focus on the abatement rate μ_t and derive the first-order condition of our policy programs. Our analytical decomposition is a two-step

procedure. First, we decompose the immediate short-term effect on next-period welfare of a marginal variation in abatement rate departing from the optimum, following Lemoine and Traeger (2014). Then, we derive the complete long-term effect of a marginal variation in the cumulative emissions stock on all future probabilities of tipping. The decomposition is done for the additive and risk-sensitive preferences : thus, we can derive how the channels through which a tipping risk affects optimal policy under additive preferences adjust to temporal risk aversion, in both the short and long term.

From the first-order condition of our policy programs, we show that the tipping risk affects optimal policy through three short-term channels. The first channel, the marginal hazard effect mhe , measures the impact of the control variable on the immediate probability of tipping. The second channel, the differential welfare impact dwi , measures the differential impact of the control variable on welfare depending on the situation, i.e. pre- or post-tipping, and if the tipping point is crossed. The last channel, the marginal impact pre-tipping mpe , defines the decrease in next-period's welfare resulting from an increase in the abatement policy if the tipping point has not been crossed yet : possible future tipping points are included in this last channel. Removing all arguments that are independent of μ_t in equation (3), the value of the optimal policy program in the pre-tipping situation under additive preferences writes :

$$u_t[\mu_t^*] + \beta \underbrace{\left[h_{t+1}(\mu_t^*) U_{t+1}^{post}(\mu_t^*) + (1 - h_{t+1}(\mu_t^*)) U_{t+1}^{pre}(\mu_t^*) \right]}_{U_{t+1}^{eff}} \quad (1.6)$$

The first term of equation (1.8) corresponds to the level of instantaneous utility at time t for an optimal choice of the control variable μ_t^* . The second term gives the expected welfare at time $t+1$ when there is a probability of tipping point under temporal risk neutrality and for an optimal choice of the control variable, scaled by the discount factor β . Varying μ_t gives us the immediate decomposition under additive preferences characterizing optimal policy : $u'_t = \beta(dwi_{t+1}^{add} + mhe_{t+1}^{add} + mpe_{t+1}^{add})$, with the following channels :

$$\begin{cases} mhe_{t+1}^{add} = \frac{\partial h_{t+1}}{\partial S_{t+1}} \frac{\partial S_{t+1}}{\partial \mu_t} (U_{t+1}^{pre} - U_{t+1}^{post}) \\ dwi_{t+1}^{add} = h_{t+1} \frac{\partial S_{t+1}}{\partial \mu_t} \left(\frac{\partial U_{t+1}^{pre}}{\partial S_{t+1}} - \frac{\partial U_{t+1}^{post}}{\partial S_{t+1}} \right) \\ mpe_{t+1}^{add} = -\frac{\partial U_{t+1}^{pre}}{\partial S_{t+1}} \frac{\partial S_{t+1}}{\partial \mu_t} \end{cases} \quad (1.7)$$

The risk-sensitive social planner maximizes at time t a utility function V_t which is linked to the random continuation utility V_{t+1} through the following recursion : $V_t = u_t + \beta\phi^{-1}(\mathbb{E}[\phi(V_{t+1})])$. The function ϕ writes $\phi(V) = (1 - \exp(-\epsilon V))/\epsilon$. It is increasing and strictly concave for any $\epsilon > 0$. The value of the optimal policy program in the pre-tipping situation under risk-sensitive preferences is :

$$u_t[\mu_t^*] + \underbrace{\beta\phi^{-1}\left[h_{t+1}(\mu_t^*)\phi(V_{t+1}^{post}(\mu_t^*)) + (1 - h_{t+1}(\mu_t^*))\phi(V_{t+1}^{pre}(\mu_t^*))\right]}_{V_{t+1}^{eff}} \quad (1.8)$$

The immediate decomposition under risk-sensitive preferences writes : $u'_t = \beta(dw_{t+1}^{rs} + mhe_{t+1}^{rs} + mpre_{t+1}^{rs})$, with the following channels :

$$\left\{ \begin{array}{l} mhe_{t+1}^{rs} = \frac{B_{t+1}}{\epsilon} \left(\frac{\partial h_{t+1}}{\partial S_{t+1}} \frac{\partial S_{t+1}}{\partial \mu_t} \left[\exp(-\epsilon V_{t+1}^{post}) - \exp(-\epsilon V_{t+1}^{pre}) \right] \right), \\ dw_{t+1}^{rs} = B_{t+1} \left(h_{t+1} \frac{\partial S_{t+1}}{\partial \mu_t} \left[\frac{\partial V_{t+1}^{pre}}{\partial S_{t+1}} \exp(-\epsilon V_{t+1}^{pre}) - \frac{\partial V_{t+1}^{post}}{\partial S_{t+1}} \exp(-\epsilon V_{t+1}^{post}) \right] \right), \\ mpre_{t+1}^{rs} = -B_{t+1} \left(\frac{\partial V_{t+1}^{pre}}{\partial S_{t+1}} \frac{\partial S_{t+1}}{\partial \mu_t} \exp(-\epsilon V_{t+1}^{pre}) \right), \\ \text{with } B_{t+1} = \left((1 - h_{t+1}) \exp(-\epsilon V_{t+1}^{pre}) + h_{t+1} \exp(-\epsilon V_{t+1}^{post}) \right)^{-1} \end{array} \right. \quad (1.9)$$

We highlight how temporal risk aversion implies an adjustment on these channels in comparison with additive temporally risk-neutral preferences. We extend the reasoning of [Lemoine and Traeger \(2016\)](#) under uncertainty and ambiguity aversion to a related setting with risk and risk-sensitive preferences⁵ and use their general approximations for the adjustments on the channels implied by a concave transformation of the additive social welfare function under a tipping risk. The complete procedure is depicted in 1. The measure of absolute temporal risk aversion $\left. \frac{-\phi''}{\phi'} \right|_{V^{eff}} = \epsilon$ is equal to ϵ . We adjust the temporally risk-neutral marginal hazard effect channel mhe^{add} obtained from additive preferences to find the risk-sensitive marginal hazard effect mhe^{rs} :

$$mhe^{rs} \approx mhe^{add} \left[1 + \epsilon \left(V^{eff} - \frac{V^{pre} + V^{post}}{2} \right) \right] \quad (1.10a)$$

5. They use an isoelastic function for the transformation with uncertainty aversion in a setting with an ambiguous tipping point. The equivalent of risk-sensitive preferences in an uncertain setting would be the multiplier criterion ([Bommier et al., 2017](#)).

where V^{post} is the continuation value if the tipping point has already been crossed, V^{pre} the continuation value if the tipping point has not been crossed yet and V^{eff} the random continuation value for an optimal choice of the policy variable. The amplitude and the sign of the adjustment can not be derived analytically. Indeed, an increase in temporal risk aversion ϵ is counter-balanced by its negative impact on V^{eff} as V^{eff} is decreasing in ϵ . In comparison with the arithmetic mean $(V^{pre} + V^{post})/2$, the two possible regimes in V^{eff} are weighted by the probability of (not) tipping, lower (higher) than one half in any optimal policy paths considered here. We thus expect the marginal hazard effect to be increasing with ϵ in our setting. The marginal hazard effect, depicting the marginal impact of a marginal increase in abatement on the immediate probability of tipping, relates to the social value of catastrophic risk reduction (Bommier et al., 2015) and the VSL-like parameter of Weitzman (2009). This channel is associated with self-protection in Lemoine and Traeger (2014).

We then adjust⁶ the temporally risk-neutral differential welfare impact dwi^{add} to obtain the risk-sensitive differential welfare impact dwi^{rs} . This channel is depicted as self-insurance in Lemoine and Traeger (2014). The adjustment writes :

$$dwi^{rs} \approx dwi^{add} + \epsilon h \left[(V^{eff} - V^{pre}) \left(\frac{\partial V^{pre}}{\partial \mu} \right) - (V^{eff} - V^{post}) \left(\frac{\partial V^{post}}{\partial \mu} \right) \right] \quad (1.10b)$$

Similarly, the sign of the adjustment of temporal risk aversion on the risk-neutral DWI cannot be determined analytically. An increase in the temporal risk aversion ϵ decreases V^{eff} and both terms in the bracket, so that the overall sign depends on the relative level of the marginal welfare impact of the change in policy variable in the pre-threshold and the post-threshold worlds as in the temporally risk-neutral case. The adjustment decreases with the probability of tipping. We expect this channel and the adjustment to be negligible. Indeed, they depend on the value and the trajectory of the tipping probability with respect to ϵ . But the larger ϵ is, the lower the probability of tipping, because optimal policy under large temporal risk aversion is expected to be stricter. In our specification as in Lemoine and Traeger (2014, 2016), the dwi might be completely overwhelmed by the mhe .

One can finally adjust the last channel : the direct impact of the change in

6. Taken from Lemoine and Traeger (2016), the approximation holds for a low shock.

policy variable on the welfare if one stays in a pre-tipping situation in the next period :

$$mpre^{rs} = mpre^{add} \frac{\phi'(V^{pre})}{\phi'(V_{eff})} \quad (1.10c)$$

The adjustment implied by temporal risk aversion is the relative slope of the transformed continuation value if we stay in a pre-tipping situation on the slope of the transformed random continuation value. The size of the adjustment depends on the concavity of ϕ , i.e., the strength of temporal risk aversion ϵ . This term is equal to one when there is no tipping risk, i.e. if the temperature is stabilized, and goes to 0 if the probability of tipping h increases. The adjustment implied by temporal risk aversion decreases $mpre$ unambiguously as $V_{pre} > V_{eff}$.

We have focused on the immediate impact of a marginal variation of the policy variable around the optimum and identified the channels through which the tipping risk affect next-period welfare under additive and risk-sensitive preferences. So far, we have only analyzed the immediate channels (mhe and dwi) and left all future impacts of a marginal change in the policy variable in the pre-tipping continuation value included in $mpre$ as in [Lemoine and Traeger \(2016\)](#). Indeed, today's emissions also affect all future probabilities of triggering the tipping point. In order to recover the full impact of temporal risk aversion on the optimal policy under a tipping risk, we need to decompose further this $mpre$ channel. We do not focus on the marginal impact of an increase in a control variable (i.e. the abatement rate), but on the marginal impact on the pre-tipping value function of a marginal increase in a state variable (the concentration stock S). As we assume that there is no decay, a marginal increase in the concentration stock can be analyzed as a marginal increase in carbon emissions. As in [Jensen and Traeger \(2014\)](#), we assume that the dynamic system is well-defined so that the shadow value of the carbon concentration increase $\partial V^{pre} / \partial S$ grows sufficiently slowly along the optimal path to make the limit approach zero over our large time horizon. We can advance the derivative of our pre-tipping value function with respect to emissions by one period and reinsert it in itself :

$$\frac{\partial V_t^{pre}}{\partial S_t} = u'_t - \beta \left(mhe_{t+1}^{rs} + dwi_{t+1}^{rs} - B_{t+1} \exp(-\epsilon V_{t+1}^{pre}) \left[u'_{t+1} - \beta(mhe_{t+2}^{rs} + dwi_{t+2}^{rs} - B_{t+2} \exp[-\epsilon V_{t+2}^{pre}] \frac{\partial V_{t+2}^{pre}}{\partial S_{t+2}}) \right] \right) \quad (1.11)$$

Iterating the procedure eventually yields a general expression of the marginal impact of a marginal increase in carbon emissions on all present and future

periods. The complete decomposition under risk-sensitive preferences writes :

$$\frac{\partial V_t^{pre}}{\partial S_t} = u'_t - \beta[mhe_{t+1}^{rs} + dwi_{t+1}^{rs}] + \sum_{i=t+1}^{\infty} \beta^{i-t} \left(\prod_{k=t+1}^i \underbrace{\frac{\phi'(V_k^{pre})}{\phi'(V_k^{eff})}}_{adjustment(mpre)} \right) (u'_i - \beta[mhe_{i+1}^{rs} + dwi_{i+1}^{rs}]) \quad (1.12)$$

The *mpre* channel of the immediate decomposition disappears. To differentiate them from the immediate decomposition terms, the full decomposition terms are in capital letters. The complete decomposition $\partial V_t^{pre} / \partial S_t = U'_t - MHE_t^{rs} - DWI_t^{rs}$ now includes all present and future effects :

$$\begin{cases} U'_t = u'_t + \sum_{i=t+1}^{\infty} \beta^{i-t} \left(\prod_{k=t+1}^i \frac{\phi'(V_k^{pre})}{\phi'(V_k^{eff})} \right) u'_i, \\ MHE_t^{rs} = \beta mhe_{t+1}^{rs} + \sum_{i=t+1}^{\infty} \beta^{i-t+1} \left(\prod_{k=t+1}^i \frac{\phi'(V_k^{pre})}{\phi'(V_k^{eff})} \right) mhe_{i+1}^{rs}, \\ DWI_t^{rs} = \beta dwi_{t+1}^{rs} + \sum_{i=t+1}^{\infty} \beta^{i-t+1} \left(\prod_{k=t+1}^i \frac{\phi'(V_k^{pre})}{\phi'(V_k^{eff})} \right) dwi_{i+1}^{rs} \end{cases} \quad (1.13)$$

The complete MHE^{rs} and DWI^{rs} depend on the sign and amplitude of all the present and future immediate mhe^{rs} and dwi^{rs} , and all future effects are scaled by the discount factor and the positive adjustment implied by temporal risk aversion. We have described analytically how temporal risk aversion changes the various channels through which a tipping risk affects a decision-maker, both short and long term. We assess numerically the impact of temporal risk aversion in a dynamic climate-economy stochastic model under a tipping risk and quantify the different channels depicted.

4 A numerical investigation

1 Calibration

We use the same specifications for the macroeconomic model as [Nordhaus \(2018\)](#). We use typical ranges of possible values for the key parameters. The pure

rate of time preference ρ is 1.5% (Nordhaus, 2018). The marginal utility parameter η is set to 1.5 with a sensitivity analysis from 0.5 to 2.5. We explore a large range for the shock J , ranging from 0 to 10% as explored in van der Ploeg and de Zeeuw (2018), Cai and Lontzek (2019) and van der Ploeg and de Zeeuw (2019).

Social planners under additive and risk-sensitive preferences have the same ordering over deterministic consumption paths⁷. Thus, we can make comparisons between the two social choice criteria under risk for different values of ϵ . We look for a range of plausible values for this parameter and a benchmark value within it to set a default value and perform a sensitivity analysis. The range of values used in the literature is large. Anderson (2005) uses 0.1, 1 and 2 to study the dynamics of optimal Pareto allocations of risk-sensitive agents. When studying precautionary savings, Bommier et al. (2017) explore large values ranging from 0 to 4, and Bommier and Grand (2019) explore very large values, up to 100. In order to reduce the plausible range, we use the fact that, when the elasticity of intertemporal substitution is set to one, the EZW preferences are risk-sensitive preferences (Tallarini Jr, 2000). Indeed, risk-sensitive and EZW preferences are special cases of the more general family of recursive Kreps and Porteus (1978) preferences. An analytical relation between the temporal risk aversion on the one hand and pure time preference ρ and relative risk aversion χ of EZW preferences on the other hand can thus be formulated in this precise case : $\epsilon = -(1 - \beta)(1 - \chi)$ with χ the coefficient of relative risk aversion with respect to atemporal wealth gambles, and β the discount rate. Following the IAM literature calibration for χ (Ackerman et al., 2013; Cai and Lontzek, 2019), we use $\chi = 10$ as a benchmark and run a sensitivity analysis around this value. In our benchmark case, with $\chi = 10$ and $\rho = 1.5\%$ yearly, we have $\epsilon = 0.133$. A low $\chi = 1.1$ would yield $\epsilon = 0.0015$ while a large $\chi = 20$ would yield $\epsilon = 0.3$. The lower the pure time preference, the lower the difference between additive and risk-sensitive preferences (Bommier et al., 2015). Our benchmark measure may not be adapted to social settings : a welfare-maximizing social planner might be more temporally risk averse than individuals when a catastrophic and irreversible risk bears on all future generations. In an empirical elicitation of the aversion towards correlated risks in the context of donations to risky aid projects, Gangadharan et al. (2019) find that individuals are more averse to correlated risks when they donate other people's money. This is

7. On the contrary, this is not the case for all values of ϵ under multiplicative preferences that are undiscounted ($\rho = 0$). Thus, Bommier et al. (2015) have to rely on a specific calibration of ϵ so that additive and multiplicative preferences yield the same discount rate and are comparable. The calibration of ϵ under multiplicative preferences depends on the form of the instantaneous utility, the level of pure time preference and the post-tipping exogenous consumption.

an interesting line of thought for climate change, where the contemporary social planner has to choose an appropriate level of temporal risk aversion for other generations than the one he belongs to. Thus, our benchmark value for the temporal risk aversion is conservative and in the lower bound of those estimates.

2 A comparison of the two social welfare functions under risk

We derive the optimal climate policy under the two social welfare functions in a risky intertemporal social setting using dynamic programming. Details of the resolution are in 2. A key instrument to compare optimal policy along the trajectory is the social cost of carbon (SCC) at initial time. For both specifications, it writes : $-\beta(\partial_S \mathbb{E}[W_1]|_{y_1} / \partial_C W_0|_{x_0, y_0^*})$ with y_0^* the optimal abatement and investment of the program at initial time given x_0 and β the discount rate derived from pure time preference. W , the value function, can be U (additive) or V (risk-sensitive). Figure 1 gives the absolute value of the SCC (\$/tC) under additive and risk-sensitive preferences at initial time for a range of irreversible increase in the damage factor J and the ratio of the SCC under risk-sensitive preferences to the SCC under additive preferences for various ϵ and J.

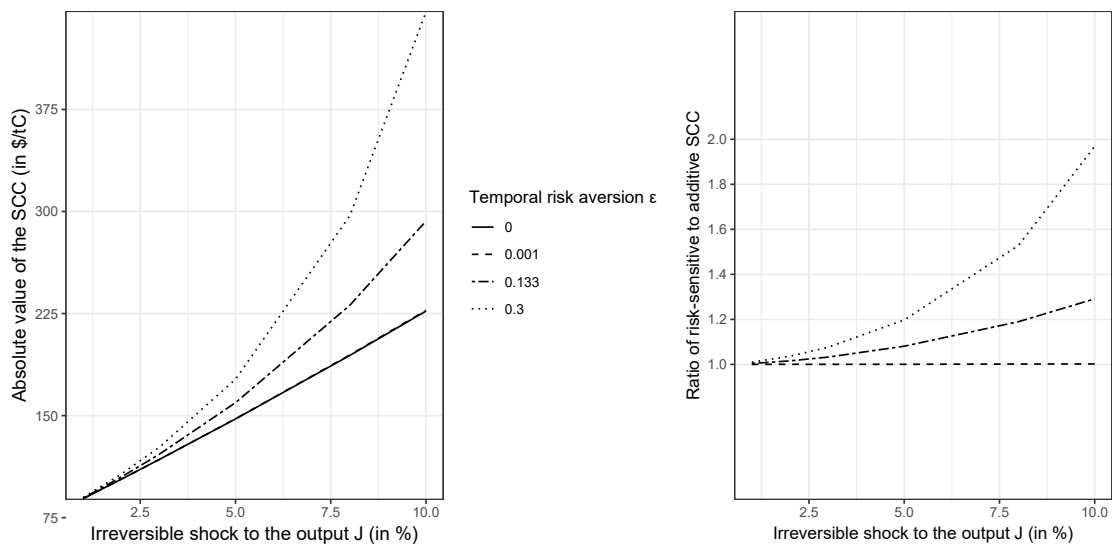


FIGURE 1.1 – Absolute values of the additive and risk-sensitive SCC (in \$ per tC) at initial time (left) and ratio of the risk-sensitive SCC to the additive SCC (right).

Graph for various J and ϵ under our benchmark calibration ($\eta = 1.5$, $\rho = 1.5\%$). The curves overlap for the two smallest values of ϵ in the left-hand graph. Same graphs with a wider range for J are given in 1.

We can draw three conclusions from the graphs above. First, optimal climate policy under risk-sensitive preferences is more stringent for any value of ϵ and J

than under additive preferences. An increase in temporal risk aversion unambiguously leads to an increase in the social cost of carbon due to the monotonicity of risk-sensitive preferences. The second conclusion is that switching from additive to risk-sensitive preferences under a tipping risk induces a large change in optimal policy : the form of the social welfare function matters, as already highlighted in [Bommier et al. \(2015\)](#) for more catastrophic collapses. For a tipping point inducing a 10% irreversible increase in the damage factor, the SCC under risk-sensitive preferences is 30% higher than under additive preferences under our benchmark $\epsilon = 0.133$: it goes from 227\$ per tC to 293\$ per tC. This difference is increasing with the size of the possible shock J : the larger the tipping risk, the larger the difference between the optimal policies. Finally, temporal risk aversion plays a key role : under risk-sensitive preferences, for the largest $\epsilon = 0.3$, the SCC at initial time is 2-times higher than under additive preferences for a 10% shock. The slope of the ratio of the risk-sensitive SCC to the additive SCC is also increasing with ϵ . Increasing temporal risk aversion increases unambiguously the weights attributed to the catastrophic states of the world where numerous generations are badly off with a low intertemporal utility level. We run a sensitivity analysis in 3 to check if our result is not affected by the calibration of the inequality aversion parameter η . The ratio of the risk-sensitive to the additive SCC is increasing in the value of the inequality aversion η . The SCC under risk-sensitive preferences is larger than under additive preferences for any value of η explored here.

To illustrate the magnitude of the change in optimal climate policy arising from temporal risk aversion, we show how switching from additive to risk-sensitive preferences compares with changes in the value of some parameters under additive preferences. We focus on two parameters that have been subject to debates in the literature. On the one hand, we consider the rate of pure time preference ρ ([Stern, 2006](#); [Nordhaus, 2008](#)). On the other hand, we focus on the value of the economic damage generated by climate change ([Piontek et al., 2021](#)), and more specifically by a climate tipping point. First, Figure 2 (left) shows how a change from additive to risk-sensitive preferences compares to a change in ρ under additive preferences. Switching from additive to risk-sensitive preferences under a 10% tipping risk and for our benchmark calibration of the temporal risk aversion ($\epsilon = 0.133$) is equivalent to a 50% decrease in the value of ρ under additive preferences. In other words, the optimal policy derived from risk-sensitive preferences for our benchmark calibration ($\epsilon = 0.133$, $\eta = 1.5$, $\rho = 1.5\%$) and under a 10% tipping risk is obtained under additive preferences when $\rho = 1\%$ other

things being equal. Figure 2 (right) shows that it takes a 14% shock for the additive preferences to give the same SCC as for a 10% irreversible increase in the damage factor under risk-sensitive preferences. The difference between the two approaches becomes more pronounced as the level of risk intensifies.

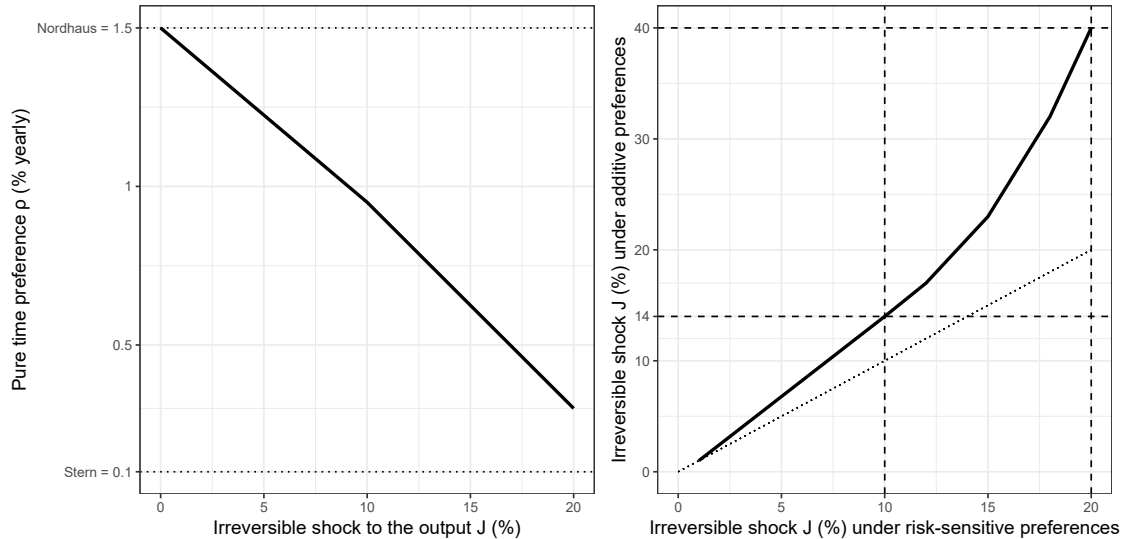


FIGURE 1.2 – Equivalence in ρ (left) and J (right) needed to obtain the same SCC at initial time under additive and risk-sensitive preferences under our benchmark calibration

On the left, we represent the pure time preference (ρ) that is needed under additive preference (all else being equal) to match the risk-sensitive SCC for various J . On the right, we represent the irreversible shock J that is needed under additive preference (all else being equal) to match the risk-sensitive SCC for various J . The dotted line from the right-hand graph is the identity function.

The numerical estimation of the channels analytically depicted in section (3) provides an understanding of the channels through which a tipping risk affects a temporally risk-averse planner. In our analytical decomposition, we firstly derived the channels through which a marginal increase in the policy variable departing from the optimum affects welfare in the next period under a tipping risk and for a risk-sensitive planner. Thus, we have left aside all future impacts on subsequent periods in this immediate decomposition, in particular the impact of a change in the policy variable on future probabilities of crossing the threshold. Then, we have performed a full decomposition to take into account the impact of this change in policy on welfare in all future periods : this is the complete decomposition. We have shown that there are two channels through which tipping risk can influence optimal policy : the marginal hazard effect (immediate and complete) and the differential welfare impact (immediate and complete). We now run a numerical estimation of these channels to understand how temporal risk aversion may affect the channels through which the tipping risk affects the planner.

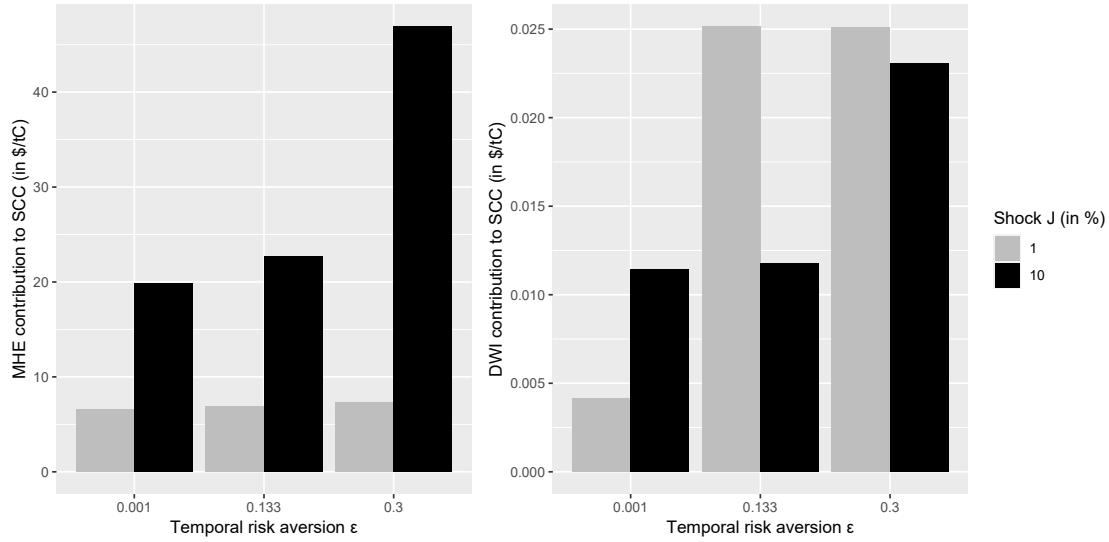


FIGURE 1.3 – Marginal contributions to the SCC at initial time (in \$) of the complete *MHE* (left) and the complete *DWI* (right) under risk-sensitive preferences for various J and ϵ .

The scales for the two graphs are different because the two channels are several orders of magnitude apart. We give the same graphs for the immediate decomposition in 4.

We can draw two conclusions from Figure 3. First, we see from our numerical estimation that the main channel is the marginal hazard effect. Indeed, the planner is ready to give up welfare in order to reduce all present (immediate) and future (complete) probabilities of crossing the threshold. This is partly due to the setting generally chosen in the literature to represent tipping points, as we do not model adaptation as an endogenous choice, which could for example decrease the level of damage J . Whether some form of adaptation can decrease the damage of such regime shifts remains uncertain, thus justifying its exclusion from our framework. The second conclusion from the numerical estimation is that the marginal hazard effect channel is increasing in the possible shock and in temporal risk aversion. A higher temporal risk aversion increases the stringency of the optimal policy, as highlighted above, and decreases even further the relative weight of the differential welfare impact in comparison with the marginal hazard effect.

5 Discussion

We study in an integrated model with a stochastic tipping risk the role of absolute risk aversion with respect to intertemporal utility, i.e. temporal risk aversion. We compare the optimal climate policy arising from the expected discoun-

ted utility model to a risk-sensitive social welfare function exhibiting temporal risk aversion. A temporally risk-averse social planner maximising the welfare of successive generations prefers to lower the possibility of an irreversible damage bearing on all subsequent generations. In this sense, she adopts a social risk diversification strategy to hedge against potential environmental regime shifts.

First, while the two social welfare functions yield the same optimal climate policy in a risk-free setting, they differ once a tipping risk is introduced. Assumptions regarding the structure of the social welfare function appear as least as important as the debated value of some parameters in the expected utility model, such as the damage from a tipping point or the value of pure time preference. It should be emphasized that the assumption of temporal risk neutrality embedded in expected utility, while justifiable in risk-free models with smooth climate change, may not adequately capture possible non-linearities and abrupt regime changes in the climate system, which have been extensively documented in climate science (Arias et al., 2021). Ignoring temporal risk aversion may lead to underestimating the severity of climate risks and result in more lenient climate policies. Therefore, considering temporal risk aversion becomes crucial when studying correlated intertemporal social risks.

Second, optimal policy under temporal risk aversion is more stringent than under temporal risk neutrality. The difference between the two social welfare functions increases more than proportionally to the increase in the shock J or the temporal risk aversion ϵ . For a 10% irreversible increase in the damage factor, the SCC under temporal risk aversion is 30% higher than the SCC under risk neutrality under our benchmark calibration. Our key take-away is that if one believes that major catastrophes bearing large multiplier effects such as irreversible regime shifts are possible, the social planner's aversion towards those risks bearing on intertemporal utility should be accounted for. On the other hand, if there is no such risk or if the possible damage is low, then we should stick to the additive model as it does not come with the ethical drawbacks catastrophe aversion bears.

The last conclusion is that optimal climate policy in our setting is mainly driven by the marginal hazard effect. The tipping risk affects optimal policy as the social planner wants to reduce all present and future probabilities of crossing the tipping point. This channel is increasing in the possible shock J and increasing in the temporal risk aversion. The risk-sensitive planner is willing to give up more wealth to avoid the catastrophic event.

Our analysis suffers three main limitations. Firstly, our model, although in-

cluding a stochastic risk, suffers from the limitations often pointed out in integrated climate-economy models : the specification of the damage function, the exogenous technological change dynamics and the assumptions regarding future growth are for example uncertain. Secondly, our representation of tipping points is limited, as we focus on a single tipping point and do not consider various characteristics, such as their probability of occurrence, reversibility, abruptness, and time horizons. Additionally, our tipping probability is solely a function of global temperature, while other drivers, such as deforestation, can also contribute to tipping points. These limitations leave room for further research to provide a more comprehensive and precise representation of climate tipping points and damages. Lastly, our model assumes known probabilities for the tipping risk. Under ambiguity about the tipping points, a temporally risk averse planner might not prefer higher diversification ([Berger and Eeckhoudt, 2021](#)).

Finally, we do not take any stance on what the *right* social welfare function is. This question remains open to scientific and public debates. In particular, the risk-sensitive social planner is not an expected utility maximizer. This may be defensible as one may ‘accept the sure-thing principle for individual choice but not for social choice, since it seems reasonable for the individual to be concerned solely with final states while society is also interested in the process of choice’ ([Diamond, 1967](#)). Temporal risk aversion helps us understand the specificity of the social choice issue climate change raises when it is considered not as a linear and smooth phenomenon, but as a phenomenon that can give rise to non-linearities and abrupt regime changes. A future research avenue could be to elicit the value that individuals would give to this parameter in the context of normative intergenerational social choice.

If our analysis is applied to a stylized climatic tipping risk, we believe that risk-sensitive preferences and temporal risk aversion might be used for the study of more standard smooth risks, as long as they are endogenous and correlated. Indeed, as risk-sensitive preferences exhibit preference for catastrophe avoidance when the social planner has temporal risk aversion, they comply with a weaker pareto axiom in comparison with additive preferences ([Bommier and Zuber, 2008](#)) : this axiom states that there is no difference between the social planner’s and the individuals’ preferences as long as uncorrelated risks are considered, but that some divergence may occur when correlated risks are at play. This intertemporal social choice criterion might thus bear critical implications for the management of correlated risks, for instance the large aggregate social risks due to potential ecological thresholds (e.g. biodiversity collapse).

6 Annex

1 Analytical decomposition details

We follow Lemoine and Traeger (2016) to find an analytic approximation of how the risk-neutral channels adjust under temporal risk aversion. In addition, we disentangle mpre from dwi. Starting from expression of mhe^{add} and mhe^{rs} in equation (1.7) and (1.9), we write :

$$mhe_{t+1}^{rs} = \frac{\partial h_{t+1}}{\partial S_{t+1}} \frac{\partial S_{t+1}}{\partial \mu_t} \left(\frac{\phi(V_{t+1}^{pre}) - \phi(V_{t+1}^{post})}{\phi'(V_{t+1}^{eff})} \right) \quad (1.14)$$

Thus :

$$mhe_{rs} = mhe_{add} \underbrace{\frac{\phi(V^{pre}) - \phi(V^{post})}{\phi'(V^{eff})(V^{pre} - V^{post})}}_{adj_{mhe}} \quad (1.15)$$

and recall that $\phi(V) = (1 - \exp(-\epsilon V))/\epsilon$. A second order Taylor expansion for $\phi(V^i)$ around $\phi(V^{eff})$ gives : $\phi(V^i) \approx \phi(V^{eff}) + \phi'(V^{eff})[V^i - V^{eff}] + \frac{1}{2}\phi''(V^{eff})[V^i - V^{eff}]^2 + O([V^i - V^{eff}]^3)$. We have :

$$\phi(V^{pre}) - \phi(V^{post}) \approx \phi'(V^{eff})[\phi(V^{pre}) - \phi(V^{post})] + \frac{1}{2}\phi''(V^{eff})[(V^{pre})^2 - (V^{post})^2 + 2V^{eff}(V^{post} - V^{pre})] \quad (1.16)$$

And :

$$adj_{mhe} \approx 1 + \left(\frac{-\phi''}{\phi'} \Big|_{V^{eff}} \left[V^{eff} - \frac{V^{pre} + V^{post}}{2} \right] \right) \quad (1.17)$$

This yields our final expression for the adjustment implied by temporal risk aversion on mhe^{rs} . Expression for dwi^{add} is in equation (1.7). For dwi^{rs} in equation (1.9), we use a more restricted expression than Lemoine and Traeger (2016). Indeed, we exclude mpre from dwi and consider only the differential impact of a marginal increase in the pre and post tipping if the tipping point is actually crossed (with probability h). The expression writes :

$$dwi_{t+1}^{rs} = h_{t+1} \frac{\partial S_{t+1}}{\partial \mu_t} \left(\frac{\phi'(V^{pre})}{\phi'(V^{eff})} \frac{\partial V_{t+1}^{pre}}{\partial S_{t+1}} - \frac{\phi'(V^{post})}{\phi'(V^{eff})} \frac{\partial V_{t+1}^{post}}{\partial S_{t+1}} \right) \quad (1.18)$$

Then, we can write :

$$dwi_{t+1}^{rs} = dwi_{t+1}^{add} + h_{t+1} \frac{\partial S_{t+1}}{\partial \mu_t} \left(\left[\frac{\phi'(V^{pre})}{\phi'(V^{eff})} - 1 \right] \frac{\partial V_{t+1}^{pre}}{\partial S_{t+1}} - \left[\frac{\phi'(V^{post})}{\phi'(V^{eff})} - 1 \right] \frac{\partial V_{t+1}^{post}}{\partial S_{t+1}} \right) \quad (1.19)$$

We do a first-order approximation of $\phi'(V^i)$ for $i \in \{pre, post\}$ as Lemoine and Traeger (2016), assuming that the tipping point does not cause too large a welfare loss, to obtain $\frac{\phi'(V^i)}{\phi'(V^{eff})} - 1 \approx \frac{\phi'(V^{eff}) + \phi''(V^{eff})(V^i - V^{eff})}{\phi'(V^{eff})} - 1 \approx -\epsilon(V^i - V^{eff})$. This approximation, together with equation (1.19), yields equation (1.10b). Finally, equation (1.10c) is derived from equations (1.7) and (1.9).

2 Numerical resolution

We solve our recursive programs using dynamic programming. For each social welfare function, we approximate the value function in the post-tipping world and then in the pre-tipping world using the solution from the post-threshold problem. We interpolate recursively starting from the last period and approximate the unknown value functions with Chebyshev polynomials. We choose a 10^{-3} tolerance for the solver : our result is not affected by stricter tolerance. In each regime (pre- and post-tipping), the value functions are expected to be smooth as the tipping risk is the only risk we consider. We use a four-degree complete Chebyshev approximation in the two-dimensional state space. Additional degrees do not affect the results. The state variables are the carbon stock in the atmosphere S_t and the stock of capital K_t at time t . The time-dependent approximation space is defined around a deterministic growth path derived from the Ramsey formula. Once we have interpolated recursively at each time step, we simulate the optimal path for each control and state variable starting from the first period. In the stochastic case with a tipping point, we run 1,000 simulations. An increase in the number of simulations does not significantly affect the median path. A key element is the definition of a terminal value in the program. The calculation is done on a finite horizon ($T = 600$ years) as an approximation of the infinite program. The terminal value is defined as the sum of all the period utilities from time T to infinity. The assumption made is that consumption will grow for a constant capital per efficient capita and total abatement, with a deterministic path for the capital derived from Ramsey. The terminal constraint uses a modified discount factor (Barr and Manne, 1967). The choice of the terminal value does not affect the program : a 10% increase in the terminal value does not significantly affect the optimal path. It writes :

$$TVF = \frac{\Delta L u(\bar{c})}{(1 - \beta(1 + GA))^{\delta \left(\frac{1-\eta}{1-\alpha} \right)}}$$

with \bar{c} the consumption for constant capital per efficient capita and total abatement, β the discount rate, δ the time step, η the marginal utility parameter, α the capital elasticity in the production function, and GA the annual growth rate of productivity from the last period.

3 Risk-sensitive preferences and the risk premium

We show that the risk premium is positive for all ϵ under risk-sensitive preferences. We provide the share of the risk-sensitive SCC under expected damages in the risk-sensitive stochastic SCC for various values of ϵ and J , and for our benchmark $\eta = 1.5$, following [Taconet et al. \(2021\)](#). In particular, we numerically demonstrate on the graph on the left below that the risk premium is positive for all values of $\epsilon \in \mathbb{R}^+$ under risk-sensitive preferences, unlike for EZW preferences. Since some pure risk is already priced under additive preferences with η , we also aim to highlight how much the risk premium is increased by temporal risk aversion under our benchmark calibration : we plot on the graph on the right, for different values of ϵ and under a benchmark of $J = 10\%$ and $\eta = 1.5$, the share of the additive risk premium in the risk-sensitive risk premium :

$$100 \times \frac{SCC_{stoch}^{add} - SCC_{ed}^{add}}{SCC_{stoch}^{rs} - SCC_{ed}^{rs}}. \quad (1.20)$$

The additive risk premium is always lower than the risk-sensitive risk premium for all $\epsilon \in \mathbb{R}^+$, i.e., when the social planner has temporal risk aversion.

On the graph on the left, we see that the share of expected damages in the stochastic SCC is 50% for $\epsilon = 0.3$. In the remaining 50% of the stochastic SCC that are due to pure risk for $\epsilon = 0.3$, we see on the graph on the right that the pure risk already priced under additive preferences represents around 2% of the risk-sensitive risk premium. Most of the risk premium under risk-sensitive preferences stems from temporal risk aversion.

4 Time paths

We provide some time paths for our key variables.

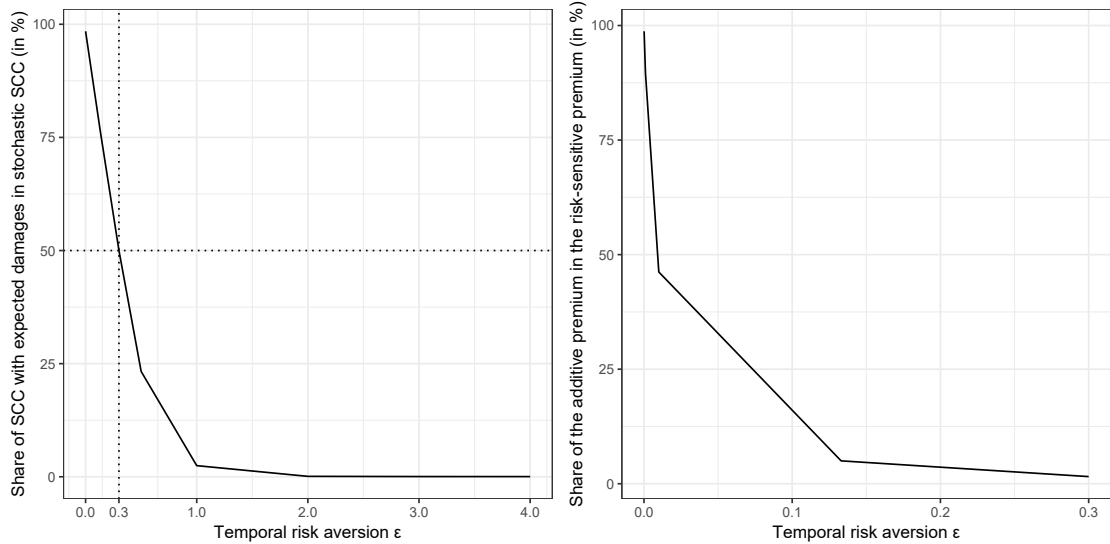


FIGURE 1.4 – Share of the stochastic SCC that is explained by expected damages (in %) (Left) Share of the risk-sensitive risk premium that is already priced under additive preferences (Right).

The lowest value explored for ϵ is 0.0001 and the share would converge to 100 for $\epsilon \rightarrow 0$ (Left). The lowest value explored for ϵ is 0.0001 and the share would converge to 100 for $\epsilon \rightarrow 0$ (Right). Both graphs are given for various ϵ and a benchmark $J=10\%$ and $\eta = 1.5$. The two graphs do not have the same scale for ϵ as the share goes quickly to 0 for values above $\epsilon > 0.3$ for the graph on the right

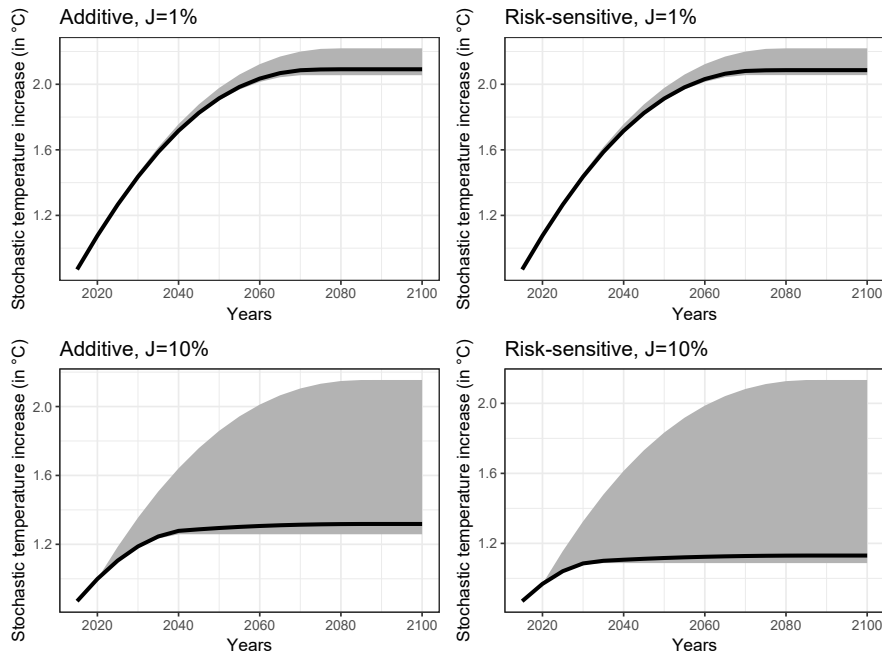


FIGURE 1.5 – Time paths of the mean temperature increase until 2100 under additive (left) and risk-sensitive (right) preferences.

Values are for $J=1\%$ (up) and a $J=10\%$ (down), for $\epsilon = 0.133$. We give the mean (solid line) and [5% : 95%] confidence interval (shaded area) over 1.000 stochastic runs.

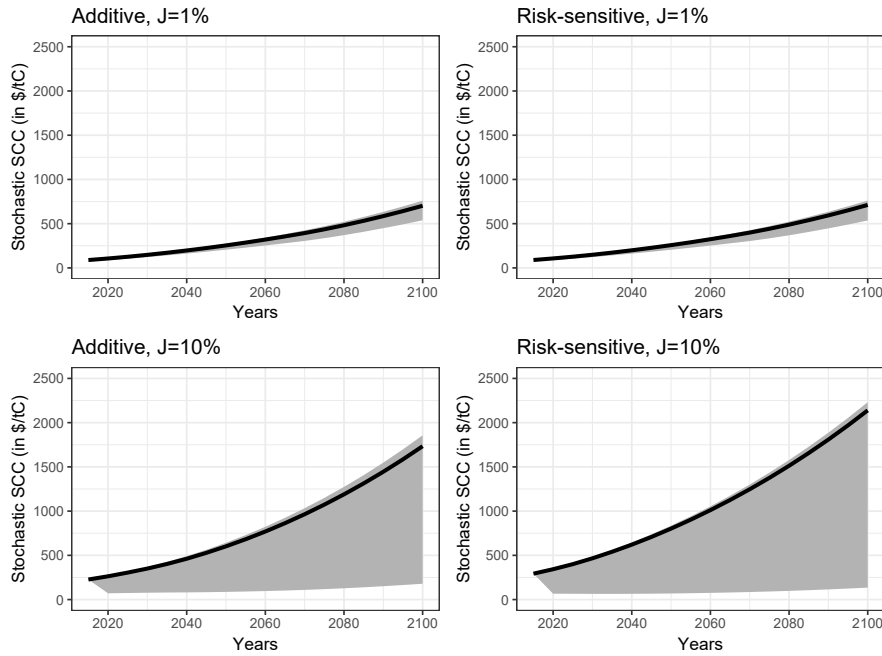


FIGURE 1.6 – Time paths of the SCC until 2100 under additive (left) and risk-sensitive (right) preferences.

Values are for $J=1\%$ (up) and a $J=10\%$ (down), for $\epsilon = 0.133$. We give the mean (solid line) and [5% : 95%] confidence interval (shaded area) over 1.000 stochastic runs.

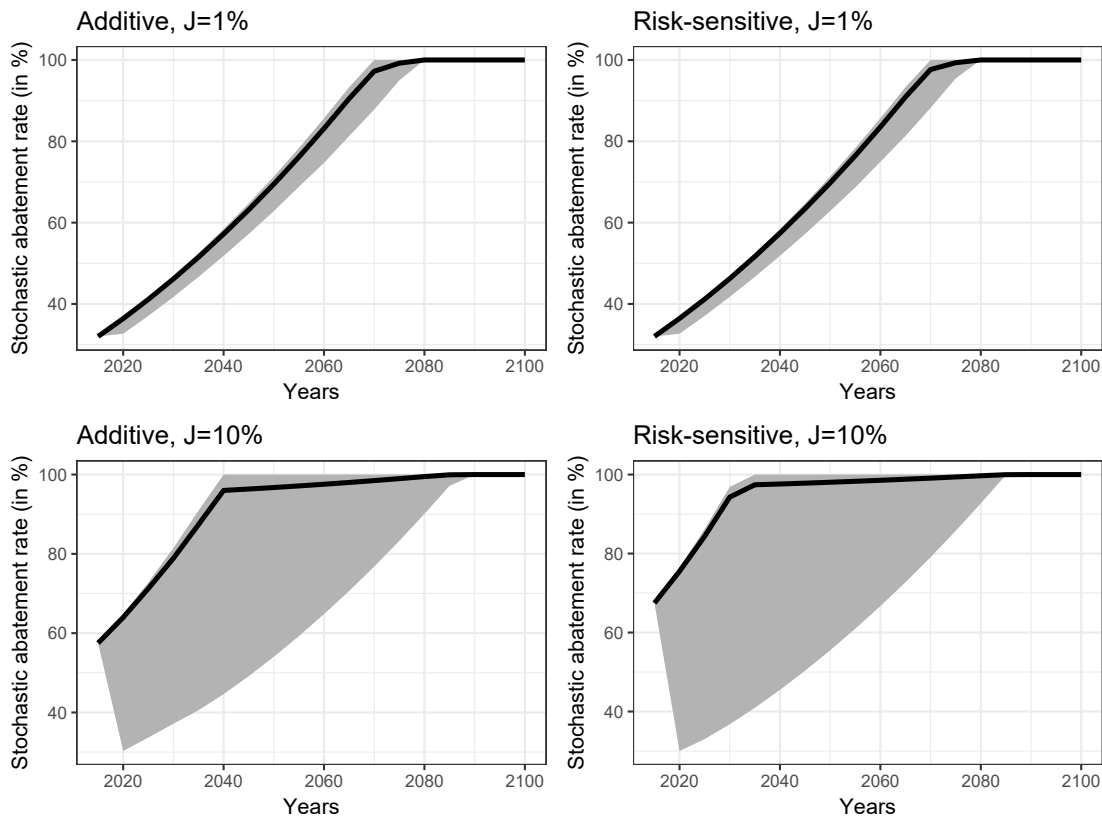


FIGURE 1.7 – Time paths of the abatement rate until 2100 under additive (left) and risk-sensitive (right) preferences.

Values are for $J=1\%$ (up) and a $J=10\%$ (down), for $\epsilon = 0.133$. We give the mean (solid line) and $[5\% : 95\%]$ confidence interval (shaded area) over 1.000 stochastic runs.

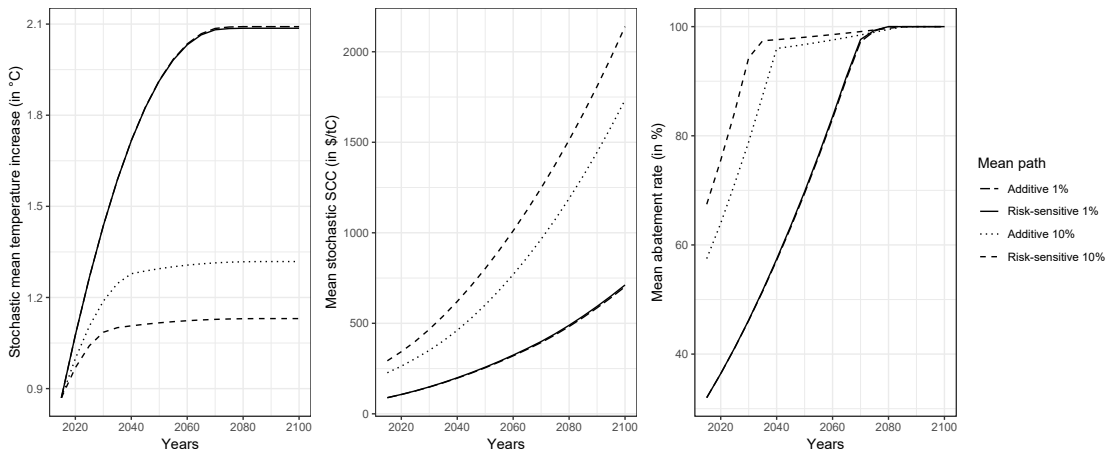


FIGURE 1.8 – Mean time paths of the temperature increase in °C with respect to pre-industrial era (left), the SCC (middle) and the abatement rate (in %) (right) until 2100.

In the risk-sensitive case and for $J=10\%$ ($J=1\%$), the tipping point is crossed 4.4% (22.8%) of the 1000 runs over the whole time horizon considered. In the additive case and for $J=10\%$ ($J=1\%$), it is 7.4% (26.9%).

5 Sensitivities

1 Upper temperature threshold

A lower probability of tipping decreases the difference between the two criteria.

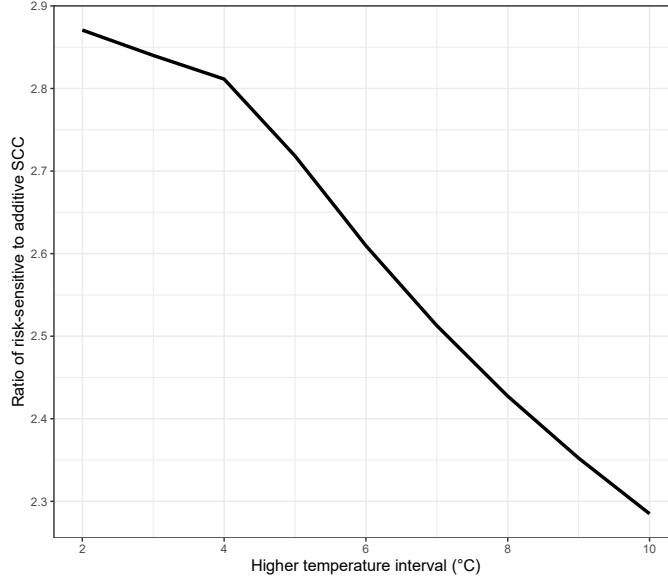


FIGURE 1.9 – Ratio of risk-sensitive to additive SCC for a benchmark $\epsilon = 0.133$, $J = 20\%$ and various upper temperature threshold.

2 Higher tipping damage J

We give the same graph as in the main text but for a larger range of J .

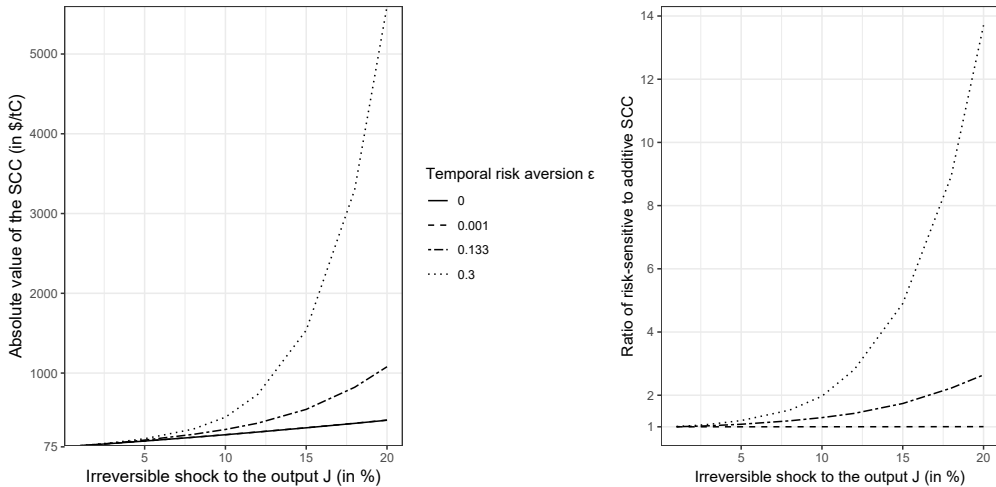


FIGURE 1.10 – Ratio of risk-sensitive to additive SCC at initial time for a benchmark $\epsilon = 0.133$ and various J .

3 Inequality aversion

The log ratio of the SCC under risk-sensitive preferences to the SCC under additive preferences increases with the elasticity of marginal utility.

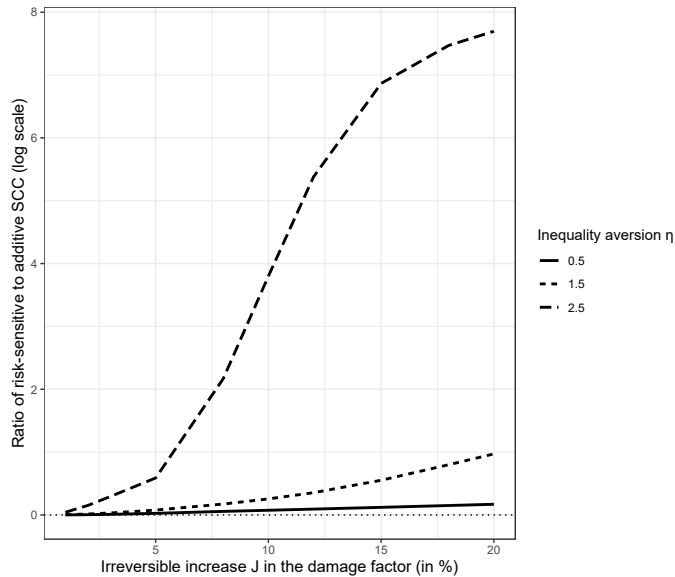


FIGURE 1.11 – Ratio of the SCC at initial time under risk-sensitive preferences on the additive SCC. The graph is for benchmark calibration and for different J and η

4 Sensitivity - immediate decomposition

Immediate channels under risk-sensitive preferences for various J and ϵ .

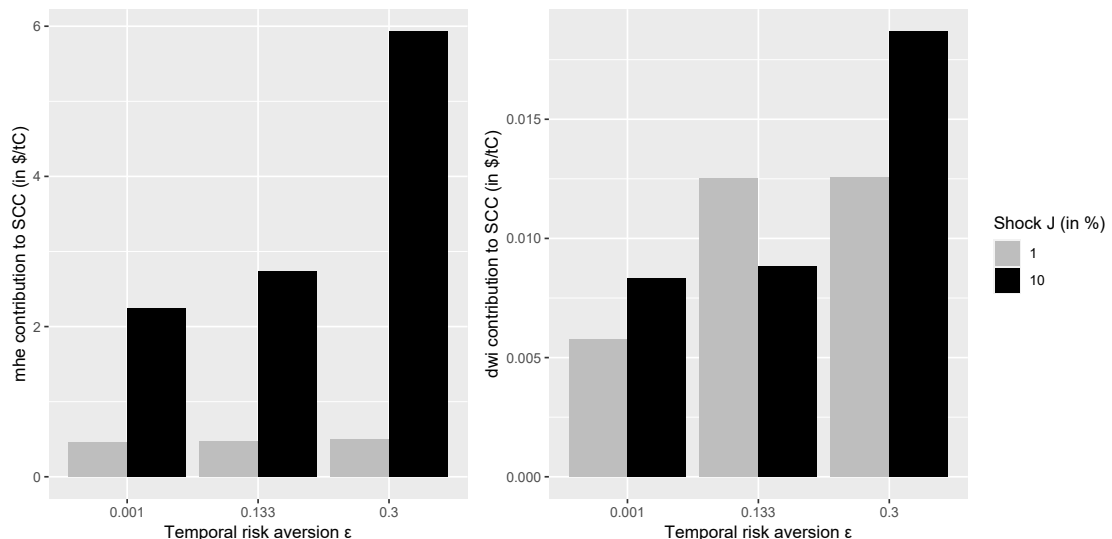


FIGURE 1.12 – Marginal contribution to the SCC at initial time (in \$) of the immediate *mhe* (left) and the immediate *dwi* (right) under risk-sensitive preferences. Graph is for various J and ϵ . Results based on 1000 stochastic runs.

Bibliographie

- F. Ackerman, E. A. Stanton, and R. Bueno. Epstein-zin utility in dice : Is risk aversion irrelevant to climate policy? *Environmental and Resource Economics*, 56(1) :73–84, 2013.
- C. M. Ahn. The effect of temporal risk aversion on optimal consumption, the equity premium, and the equilibrium interest rate. *The Journal of Finance*, 44(5) :1411–1420, 1989.
- S. Andersen, G. W. Harrison, M. I. Lau, and E. E. Rutström. Multiattribute utility theory, intertemporal utility, and correlation aversion. *International Economic Review*, 59(2) :537–555, 2018.
- E. W. Anderson. The dynamics of risk-sensitive allocations. *Journal of Economic theory*, 125(2) :93–150, 2005.
- P. Arias, N. Bellouin, E. Coppola, R. Jones, G. Krinner, J. Marotzke, V. Naik, M. Palmer, G.-K. Plattner, J. Rogelj, et al. Climate change 2021 : The physical science basis. contribution of working group14 i to the sixth assessment report of the intergovernmental panel on climate change; technical summary. 2021.
- K. J. Arrow. The theory of risk aversion chapter 3 in essays in the theory of risk bearing. *New ork : american Elsevier*, 1971.
- J. L. Barr and A. S. Manne. Numerical experiments with a finite horizon planning model. *Indian Economic Review*, 2(1) :1–31, 1967.
- M. Belaia, M. Funke, and N. Glanemann. Global warming and a potential tipping point in the atlantic thermohaline circulation : the role of risk aversion. *Environmental and Resource Economics*, 67(1) :93–125, 2017.
- L. Berger and L. Eeckhoudt. Risk, ambiguity, and the value of diversification. *Management Science*, 67(3) :1639–1647, 2021.
- A. Bommier. Risk aversion, intertemporal elasticity of substitution and correlation aversion. Technical report, ETH Zurich, 2005.
- A. Bommier. Life-cycle preferences revisited. *Journal of the European Economic Association*, 11(6) :1290–1319, 2013.
- A. Bommier and F. L. Grand. Risk aversion and precautionary savings in dynamic settings. *Management Science*, 65(3) :1386–1397, 2019.
- A. Bommier and S. Zuber. Can preferences for catastrophe avoidance reconcile social discounting with intergenerational equity ? *Social Choice and Welfare*, 31(3) :415–434, 2008.
- A. Bommier, A. Chassagnon, and F. Le Grand. Comparative risk aversion : A formal approach with applications to saving behavior. *Journal of Economic Theory*, 147(4) :1614–1641, 2012.
- A. Bommier, B. Lanz, and S. Zuber. Models-as-usual for unusual risks ? on the value of catastrophic climate change. *Journal of Environmental Economics and Management*, 74 :1–22, 2015.

- A. Bommier, A. Kochov, and F. Le Grand. On monotone recursive preferences. *Econometrica*, 85(5) :1433–1466, 2017.
- L. Bretschger and A. Vinogradova. Best policy response to environmental shocks : Applying a stochastic framework. *Journal of Environmental Economics and Management*, 97 :23–41, 2019.
- J. Bullard and A. Singh. Learning and the great moderation. *International Economic Review*, 53(2) :375–397, 2012.
- Y. Cai and T. S. Lontzek. The social cost of carbon with economic and climate risks. *Journal of Political Economy*, 127(6) :2684–2734, 2019.
- H. R. Clarke and W. J. Reed. Consumption/pollution tradeoffs in an environment vulnerable to pollution-related catastrophic collapse. *Journal of Economic Dynamics and Control*, 18(5) :991–1010, 1994.
- B. Crost and C. P. Traeger. Optimal climate policy : uncertainty versus monte carlo. *Economics Letters*, 120(3) :552–558, 2013.
- P. A. Diamond. Cardinal welfare, individualistic ethics, and interpersonal comparison of utility : Comment. *Journal of political economy*, 75(5) :765–766, 1967.
- S. Dietz and F. Venmans. Cumulative carbon emissions and economic policy : in search of general principles. *Journal of Environmental Economics and Management*, 96 :108–129, 2019.
- S. Ebert and G. van de Kuilen. Measuring multivariate risk preferences. Available at SSRN 2637964, 2015.
- M. Fleurbaey. Assessing risky social situations. *Journal of Political Economy*, 118(4) :649–680, 2010.
- M. Fleurbaey. Welfare economics, risk and uncertainty. *Canadian Journal of Economics/Revue canadienne d'économique*, 51(1) :5–40, 2018.
- L. Gangadharan, G. W. Harrison, and A. D. Leroux. Are risks over multiple attributes traded off? a case study of aid. *Journal of Economic Behavior & Organization*, 164 :166–198, 2019.
- C. Guiavarch and A. Pottier. Climate damage on production or on growth : what impact on the social cost of carbon? *Environmental Modeling & Assessment*, 23(2) :117–130, 2018.
- L. P. Hansen and T. J. Sargent. Discounted linear exponential quadratic gaussian control. *IEEE Transactions on Automatic control*, 40(5) :968–971, 1995.
- S. Jensen and C. P. Traeger. Optimal climate change mitigation under long-term growth uncertainty : Stochastic integrated assessment and analytic findings. *European Economic Review*, 69 :104–125, 2014.
- R. E. Kihlstrom and L. J. Mirman. Risk aversion with many commodities. *Journal of Economic Theory*, 8(3) :361–388, 1974.
- M. Kimball and P. Weil. Precautionary saving and consumption smoothing across time and possibilities. *Journal of Money, Credit and Banking*, 41(2-3) :245–284, 2009.

- D. M. Kreps and E. L. Porteus. Temporal resolution of uncertainty and dynamic choice theory. *Econometrica : journal of the Econometric Society*, pages 185–200, 1978.
- J. Lanier, B. Miao, J. K.-H. Quah, and S. Zhong. Intertemporal consumption with risk : A revealed preference analysis. *Review of Economics and Statistics*, 106(5) :1319–1333, 2024.
- M. Leduc, H. D. Matthews, and R. de Elía. Quantifying the limits of a linear temperature response to cumulative co2 emissions. *Journal of Climate*, 28(24) :9955–9968, 2015.
- D. Lemoine and C. Traeger. Watch your step : optimal policy in a tipping climate. *American Economic Journal : Economic Policy*, 6(1) :137–66, 2014.
- D. Lemoine and C. P. Traeger. Ambiguous tipping points. *Journal of Economic Behavior & Organization*, 132 :5–18, 2016.
- V. Masson-Delmotte, P. Zhai, A. Pirani, S. L. Connors, C. Péan, S. Berger, N. Caud, Y. Chen, L. Goldfarb, M. Gomis, et al. Climate change 2021 : the physical science basis. *Contribution of working group I to the sixth assessment report of the intergovernmental panel on climate change*, 2, 2021.
- W. Nordhaus. *A question of balance : Weighing the options on global warming policies*. Yale University Press, 2008.
- W. Nordhaus. Evolution of modeling of the economics of global warming : changes in the dice model, 1992–2017. *Climatic change*, 148(4) :623–640, 2018.
- F. Piontek, L. Drouet, J. Emmerling, T. Kompas, A. Méjean, C. Otto, J. Rising, B. Soergel, N. Taconet, and M. Tavoni. Integrated perspective on translating biophysical to economic impacts of climate change. *Nature Climate Change*, pages 1–10, 2021.
- J. W. Pratt. Risk aversion in the large and in the small. *Econometrica*, 32(1-2) :122–136, 1964.
- C. M. Rheinberger and N. Treich. Attitudes toward catastrophe. *Environmental and Resource Economics*, 67(3) :609–636, 2017.
- S. F. Richard. Multivariate risk aversion, utility independence and separable utility functions. *Management Science*, 22(1) :12–21, 1975.
- K. I. Rohde and X. Yu. Intertemporal correlation aversion-a model-free measurement. *Available at SSRN 4079812*, 2022.
- I. Rudik. Optimal climate policy when damages are unknown. *American Economic Journal : Economic Policy*, 12(2) :340–73, 2020.
- N. Stern. Stern review : The economics of climate change. 2006.
- N. Taconet, C. Guivarch, and A. Pottier. Social cost of carbon under stochastic tipping points. *Environmental and Resource Economics*, 78(4) :709–737, 2021.
- T. D. Tallarini Jr. Risk-sensitive real business cycles. *Journal of monetary Economics*, 45(3) :507–532, 2000.

- Y. Tsur and A. Zemel. Accounting for global warming risks : Resource management under event uncertainty. *Journal of Economic Dynamics and Control*, 20(6-7) :1289–1305, 1996.
- F. van der Ploeg and A. de Zeeuw. Climate tipping and economic growth : precautionary capital and the price of carbon. *Journal of the European Economic Association*, 16(5) :1577–1617, 2018.
- F. van der Ploeg and A. de Zeeuw. Pricing carbon and adjusting capital to fend off climate catastrophes. *Environmental and Resource Economics*, 72(1) :29–50, 2019.
- M. L. Weitzman. On modeling and interpreting the economics of catastrophic climate change. *The review of economics and statistics*, 91(1) :1–19, 2009.

Chapitre 2

The need for regulation of climate subsystems

This article^a is a joint work with Céline Guivarch (École des Ponts, CIRED).

Understanding stochastic interactions between climate change, the macroeconomy and Earth subsystems with non-linear, self-sustaining and debated dynamics is a major challenge with implications both for global climate policy and regional subsystem's management. We study Earth subsystems with three properties : their dynamics have an impact on climate change, climate change has an impact on their dynamics and their dynamics are not entirely determined by climate change. We analytically derive the three channels through which interactions between subsystem's idiosyncratic risk and aggregate climate risk over intertemporal welfare affect optimal climate policy. First, subsystems have direct scaling effect through their expected feedback on global climate. Second, perturbations in the subsystem caused by carbon emissions reduce its long-term survival and therefore affect intertemporal welfare because of future feedbacks on global climate. Third, subsystems have various insurance values. We also highlight how an explicit reduced-form subsystems's geophysical dynamics improves their management, taking into account the changing ability of the subsystems to self-perpetuate over time : we introduce the social cost of the dynamic subsystem (SCDS). We apply our framework in a calibrated stochastic quantitative model of the Amazon rainforest whose fate is fiercely debated. In our benchmark quantitative specification, an endogenous and explicit modeling of the Amazon rainforest implies a 15% risk premium on the social cost of carbon (SCC) at the global scale and a SCDS that is worth 16% of the standard stochastic SCC. These results imply that a 24% increase in the marginal value of a tCO₂ stored in the rainforest should be applied in local cost-benefit analysis.

Keywords : dynamic stochastic climate-economy model, robust environmental policy, Amazon rainforest, climate tipping elements, scientific uncertainty, risk, climate beta.

JEL classification : D61, D63, D71, D81, Q54, Q58.

^a. Computations were performed on the IPSL ESPRI mesocenter. Special thanks to Philippe Ciais and Thomas Gasser for their invaluable help in advising us on the quantified part on the Amazon rainforest : this paper owes them a great deal. We also thank Adrien Bilal, Delphine Clara-Zemp, Johannes Emmerling, Célia Escribe, Eli Fenichel, Emmanuel Gobet, Allan Hsiao, Simon Jean, Vincent Martinet, Aurélie Méjean, and Stéphane Zuber for fruitful discussions or comments on earlier versions of this work. Corresponding author : Romain Fillon.

1 Introduction

The Earth and human societies are complex systems with non-linear stochastic dynamics, entangled through time and space. Our knowledge of the climate system and the interactions of its components has made significant progress, even if it remains subject to scientific debate. Meanwhile, economic models usually rely on a stylized representation of climate change where feedbacks between global climate change and subsystems such as tropical rainforests are either omitted, deterministic or modeled as a generic catastrophe with no geophysical representation, even in reduced form. Yet, impacts of climate change on these subsystems are stochastic : for instance, the law that describes how more frequent occurrence of droughts under changing climate might affect tree losses in the Amazon rainforest is not deterministic ([Anderson et al., 2018](#)). Furthermore, the possible collapse of these subsystems is more complex than a probability defined *ex ante* : because of vegetation-rainfall feedbacks ([Zemp et al., 2017a](#)), a decrease in forest cover could for instance yield an abrupt partial dieback that is not a linear function of an additional CO₂ emission or an additional hectare of deforestation. In this paper, we analyze and quantify how moving beyond these simplifications yields fruitful insights for decision-making regarding adaptation and mitigation under a changing climate endogenous to our economic activities.

We focus on climate subsystems that have three properties. First, global climate change has an impact on their dynamics, e.g. through changes in the drought regime under a changing climate for the Amazon rainforest. Second, our subsystems have an impact on global climate change : indeed, rainforests can for instance store and release carbon. Both impacts can be positive or negative. Third, subsystem's dynamics cannot be simply deduced from climate change, because of inertia, self-sustaining dynamics or feedback effects : for instance, the Amazon rainforest recycles part of its precipitation to feed its own growth through evapotranspiration. Examples of Earth subsystems are for instance climate tipping elements ([Armstrong McKay et al., 2022](#)). Examples of Earth subsystems of relevance to this study also include other subsystems that do not have tipping behavior, such as the South-Eastern Asian rainforest and its feedback on the global carbon cycle or El Niño La Niña and its impact on intra- and inter-annual natural climate variability.

We build a dynamic climate-economy model, extending a well-established literature studying optimal policy under climate risks ([Golosov et al., 2014](#); [Cai](#)

and Lontzek, 2019; Folini et al., 2024). In comparison with previous work, we explicitly include a stylized climate subsystem with its own dynamics as a state variable of our program, e.g. the current forest cover of the Amazon, and model its stochastic interactions with climate change. Introducing a stylized subsystem has important implications both for optimal climate policy and regional subsystem management.

First, a key question for optimal climate policy is to know if and to what extent subsystem's idiosyncratic risk affects aggregate climate risk bearing over intertemporal welfare. Indeed, the feedbacks brought by these subsystems on global climate might not have the same social value for different states of the world where they might occur, which depend on their own dynamics, its interaction with climate change with possible thresholds and the timescales over which transitions to different states occur for the subsystem. Furthermore, while some subsystems are expected to decrease global and regional temperatures if global temperature increases, e.g. southern boreal forest dieback or Labrador-Irminger seas/Subpolar Gyre oceanic convection collapse, some others are expected to increase temperatures under warming climate, e.g. abrupt permafrost thawing or Arctic winter sea ice collapse (Armstrong McKay et al., 2022) : the subsystems have different insurance value with respect to intertemporal utility. Without loss of generality, we analytically derive the channels through which our subsystem changes optimal policy using value function decomposition. As in the climate economics literature inspired from asset pricing (Dietz et al., 2018; Lemoine, 2021; Van den Bremer and Van der Ploeg, 2021), we depict how the social cost of carbon (SCC) is affected by different components when accounting for climate risks, thinking of the subsystem as a climate asset that can increase or decrease aggregate risk of the wider climate portfolio.

We show that an Earth subsystem affects climate policy through three channels. First, it scales multiplicatively the standard certainty equivalent and precautionary channels driving SCC depending on how and how much its feedback affects global climate change. Second, a marginal change in the subsystem's state brought by a marginal emission today yields an additive change in optimal policy because of the marginal impact of this change in the future dynamics of the subsystem on the continuation value. Third, an insurance channel, i.e. a 'subsystem beta', increases the SCC if the subsystem has a larger feedback effect on global climate change in the states of the world where a marginal emission has the largest impact on intertemporal welfare.

Second, an important question for optimal subsystem management is to ana-

lyse and quantify how a marginal variation in the state of the subsystem affects intertemporal welfare. Indeed, a marginal change in the subsystem's state has a first-order impact on optimal policy as it changes global temperatures, for instance because of carbon releases from the Amazon rainforest. But a marginal change in the subsystem's state also has a second-order impact on optimal policy as it affects the growth of the subsystem in all future periods. We introduce the social cost of the dynamic system (SCDS) : it measures in present monetary terms the intertemporal social cost of a marginal decrease in the subsystem's state today, which captures the extent to which the future subsystem's ability to self-perpetuate changes with a marginal change in its current state. The decrease in the subsystem's ability to self-perpetuate increases aggregate risk bearing over intertemporal welfare through future feedbacks of the subsystem on global climate.

We apply our framework to the debated fate of the Amazon rainforest in a stochastic quantitative model. We focus solely on its value as a carbon stock. This subsystem has a major regulating function for the Earth. At the global scale, it acts as a carbon sink of $\sim 123 \pm 23$ GtC biomass ([Malhi et al., 2006](#)). This represents a significant 39% ($\pm 7\%$) of the remaining budget to keep two chances out of three of limiting global warming to 2°C according to IPCC ([Masson-Delmotte et al., 2021](#)). The Amazon rainforest is therefore very valuable. But the Amazon rainforest is in danger as a result of human actions. A combination of forest degradation, deforestation, climate change and feedback effects may cause a partial dieback of the rainforest ([Lovejoy and Nobre, 2019](#)). The direct human impact, through deforestation and degradation, is attracting a lot of attention among economists ([Balboni et al., 2023](#)), and for good reasons. But human activities also affect the rainforest indirectly through climate change. Anthropogenic climate change is expected to change precipitation patterns, especially make extreme droughts which generate tree mortality and carbon losses ([Phillips et al., 2009](#); [Yao et al., 2022](#)) more frequent. A ton of carbon emitted in Europe or Asia thus has an impact on the rainforest. In turn, the forest increases the damage of future climate change in Europe and Asia, as it might release carbon under changing climate. In particular, the rainforest feedback might be the largest in states of the world where cumulative emissions have the largest impact on aggregate welfare, thus increasing aggregate risk bearing over intertemporal welfare. Finally, vegetation-rainfall feedback effects limiting the recycling of water by the forest, i.e. forest's own dynamics, may magnify these human-induced perturbations ([Zemp et al., 2017b](#)). This self-sustained dynamics arising from temporal

autocorrelation, in which decisions in some part of the forest affect other parts because of spatial autocorrelation, is usually neglected in local cost-benefit analysis or in dynamic discrete choice approaches (Souza-Rodrigues, 2019; Araujo et al., 2020; Hsiao, 2021). Finally, the fate of the Amazon rainforest is not only risky, it is also uncertain. Aside from standard risk scenarios, where future state probabilities are known, uncertain situations are situations in which there is no unanimous probability assignment due to insufficient information or competing datasets, models, or expert opinions. Indeed, projections of rainfall patterns under climate change differ depending on the climate model used (Kent et al., 2015). Furthermore, there are debates about whether feedback effects might yield a tipping point in the Amazon rainforest (Flores et al., 2024). We calibrate the perturbations to the dynamics of the rainforest with three components : exogenous deforestation and degradation scenarii (Aguiar et al., 2016; Matricardi et al., 2020), bias-corrected downscaled output on monthly precipitation from hydrological model MATSIRO for four ISIMIP earth system models (IPSL-CM5A-LR, HadGEM2-ES, GFDL-ESM2M, MIROC5) forced with future emissions from three different Shared Socioeconomic Pathways (SSPs) and historical observations of the impact of droughts on tree losses (Phillips et al., 2009; Yao et al., 2022). Given these calibrations, we jointly calibrate the remaining parameters of the Lotka-Volterra equation describing tipping behavior of tropical forests in Ritchie et al. (2021) to match the central estimate of the core expert probability assessment of Kriegler et al. (2009). Finally, we use both discounted expected utility and a more flexible smooth ambiguity criterion (Berger et al., 2017; Barnett et al., 2020) as a sensitivity check to measure how our collective attitudes towards risks and scientific uncertainties might affect optimal policy estimates.

Our approach yields two key methodological insights for the Amazon rainforest. First, the social cost of carbon (SCC) should include the impact that a marginal increase in cumulative emissions at the global scale has on the dynamics of the rainforest. This includes a scaling of current policy by the carbon releases from the Amazon rainforest under changing climate, an additive risk premium in the SCC from the perturbation on the present and future dynamics of the rainforest and an insurance channel, the positive ‘amazon beta’, because the carbon releases occur in states of the world where carbon emissions have the largest marginal impact on intertemporal welfare. Second, the social value of the Amazon rainforest as a carbon stock cannot be reduced to the amount of carbon it contains : the social cost of the dynamic system (SCDS) matters too, i.e. the cost of a marginal decrease in subsystem’s state because of its reduced ability to self-perpetuate.

These methodological results yield two key policy insights. First, decision-makers should augment the social cost of carbon (SCC) from the impact of a marginal emission on the Amazon rainforest, that further releases carbon. Emitters around the world should pay for the welfare impact of their emissions : the wedge between standard SCC and SCC with endogenous amazon feedback could be leveraged to finance payment for ecosystem services for the preservation of the rainforest. In our benchmark specification, we show that this wedge represents 15% of the standard SCC under aggregate climate risk. Second, the social value given to a hectare of rainforest should not be only the standard social cost of carbon SCC, but the sum of the amazon-augmented social cost of carbon and the social cost of the dynamic system SCDS. Indeed, a marginal decrease in the forest cover has a first-order welfare impact, as it releases carbon, but also a second-order impact on the future dynamics of the subsystem as a whole. Under our benchmark specification, SCDS represents 16% of the standard stochastic SCC. Our theoretical work can therefore be operationalized in local cost-benefit analysis of deforestation and be used in complement to the significant progress in the quantification of carbon stored at the finest scale via satellite observation. Indeed, we show that the valuation of one tCO₂ of carbon stored in the forest should be increased by 24% in local cost-benefit analysis to reflect the true risk premium on intertemporal utility that this marginal change in its state and corresponding carbon releases represent. This scaling factor corresponds to the sum of the increase in the SCC due to the endogenous modelling of the rainforest dynamics and its interaction with global climate risk, and the share of the SCDS that corresponds to the marginal impact on intertemporal utility of a marginal change in subsystem's state. We believe that our framework could be extended to other climate subsystems to inform policy decisions at the global and regional scales.

To our knowledge, we provide the first analytical study of the stochastic interactions between the macroeconomy, climate change and a climate subsystem and the first quantitative study of the Amazon rainforest in a global perspective in a dynamic stochastic climate-economy model with an explicit geophysical representation of its uncertain dynamics. We contribute to different strands of literature. First, we bridge the gap between a literature using stochastic climate-economy models with stylized climate risks, e.g. [Cai and Lontzek \(2019\)](#), and a literature using deterministic models with explicit geophysical dynamics, e.g. [Nordhaus \(2019\)](#); [Dietz et al. \(2021a\)](#). Thus, we contribute, along with others e.g. [Dietz et al. \(2021b\)](#), to a better understanding of the impact of climate dynamics

on economic decisions. Second, we bring together complex numerical stochastic climate-economy models with analytical decompositions that allow to identify the precise channels through which climate risks affect optimal policy (Lemoine, 2021). In comparison with a prolific literature using more stylized approach where the tipping risk is a probability to switch from one qualitative state to another one (Lemoine and Traeger, 2014; Fillon et al., 2023), we have a more complex dynamics as the subsystem is a state in our dynamic program. Our decomposition also relates to the debates on the ‘climate beta’ (Dietz et al., 2018) and on how climate mitigation affects aggregate risk bearing on intertemporal welfare. Third, we contribute to the literature on the modeling of complex non-linear socio-ecological systems (Levin et al., 2013). Indeed, we model the catastrophic outcome as an emerging property of the dynamic system with an explicit reduced-form geophysical representation, in line with bifurcation theory (Ritchie et al., 2021). We depart from perturbation approaches considering small risks (Van den Bremer and Van der Ploeg, 2021), *ad hoc* probability assignments (Cai and Lontzek, 2019) or macroeconomics literature on disasters considering reversible extreme events that occur as one-off catastrophes along a smoothly evolving climate regime with fluctuations, traditionally modeled with Poisson and Wiener processes (Hong et al., 2023). Indeed, our framework allows a possible abrupt dieback of the rainforest, which raises numerical challenges : following insights from Cai (2019), we use simplicial Chebyshev polynomials and break one level of ‘curse-of-dimensionality’ related to approximation nodes with parallel CPU computing. Fourth, we contribute to the literature on the Amazon rainforest : in comparison with most approaches focusing on deforestation (Balboni et al., 2023), we consider the impact of climate change on the rainforest and model the dynamics of the subsystem as a whole. We take a welfarist approach at the global scale to provide estimates of the marginal value of an hectare of rainforest taking into account the impact that a marginal change has on all other parts of the forest. Finally, we contribute to the literature on robust social choice criteria for social decision-making under climate risks and uncertainties (Berger et al., 2017; Barnett et al., 2020, 2022). Beyond stochastic risk in climate and economic models, i.e. the distribution of a stochastic variable of interest within a given model, there are large scientific controversies between models, for instance on climate tipping points, their mechanisms, thresholds, timescales, for which authors provide confidence assessments (Armstrong McKay et al., 2022). The disagreements on the right modelling approaches to climate tipping elements yield debates on their possible economic consequences (Keen et al., 2022). These scientific dis-

gements and heterogeneous confidence in assessments on climate dynamics should be taken into account when making social choice, at least as a robustness check on our best policy estimates. Alongside a more in-depth modeling of climate risks, a key issue for public and scientific debate is indeed to provide greater flexibility in the attitudes towards these risks. Our approach allows for a clear distinction, using a two-step approach, between the purpose of the risk and our attitudes towards it.

In the first analytical part, we study through value function decomposition how our modelling approach of climate subsystems affects both global climate policy and regional subsystem's management. In the second numerical part, we apply this general framework and calibrate a dynamic stochastic climate-economy model with an explicit modelling of the Amazon rainforest.

2 Modeling approach

We build a dynamic climate-economy model, extending a common framework used in the economics literature to study optimal climate policy ([Cai and Lontzek, 2019](#); [Dietz et al., 2021a](#)). We augment the model with a stylized representation of a subsystem of the Earth system whose uncertain dynamics interacts with global climate change. We study optimal policy under two distinct social choice criteria. The first criterion is the expected utility criterion : the social planner chooses between prospects by comparing their expected utilities. The second criterion ([Klibanoff et al., 2005](#); [Hayashi and Miao, 2011](#)) allows to disentangle preference over time, over states of the world and over scientific models of the world. We highlight analytically how the subsystem might affect optimal global climate policy and suggest a measure for optimal regional management of this subsystem.

1 A dynamic climate-economy model

Our model has three ingredients : the macroeconomy, climate change, and an earth subsystem. This study focuses on their dynamic interactions. The three corresponding variables are net output Y , global surface temperature T , and the current state of the dynamic subsystem relative to its initial state A . The individual dynamics of these systems might be stochastic, for example due to other economic risks such as uncertain future technological change, but we focus on

stochasticity in the interactions between these dynamic systems. We do not model the interactions between the macroeconomy and the subsystem : we focus on the additional feedback the subsystem brings on global climate change. Other impacts are for instance regional health effects or loss of use and non-use values from the subsystem, but we focus on the first-order market impacts on global welfare through global climate change. Furthermore, while some subsystems have an impact via other channels, for instance rainfall changes under Atlantic Meridional Overturning Circulation (AMOC) collapse, our climate variable is global annual mean temperature. Alternative climate indicators could be used depending on the specific risk of each subsystem while keeping the same framework. Our framework also makes it possible to consider extensions, for example if several subsystems interact (Cai et al., 2016). Finally, we do not model impacts of the subsystems on regional temperature separately from global impacts, because they are of different magnitude but of the same sign. The framework could be extended to integrate this additional mechanism.

This set of assumptions leaves us with four key interaction channels between the macroeconomy, aggregate climate change and the stylized earth subsystem. First, climate change affects economic output ($\partial Y / \partial T$) through a global damage function. Second, economic output affects global climate change ($\partial T / \partial Y$) through emissions that can be abated at a given cost and add up to a cumulative emissions stock. Average surface temperature is a linear function of this cumulative emission stock through transient climate response to cumulative emissions. Third, subsystem's dynamics affects global climate change ($\partial T / \partial A$). Finally, climate change affects the subsystem's state ($\partial A / \partial T$) through various mechanisms which can be presented in a reduced-form approach with credible geophysical dynamics and an explicit calibration. These four channels are four components through which stochastic risk affects optimal policy. The two first channels, i.e. damage uncertainty and uncertainty in the transient climate response to cumulative emissions, are already well studied in the climate-economics literature and not specific to the study of subsystems. Instead, the question of the interaction of aggregate climate risk on intertemporal welfare with idiosyncratic subsystem risk is of interest to us. The two last channels, especially the fourth and most important one which determines whether or not there will be feedbacks between global climate change and the subsystem, are usually modeled (Nordhaus, 2019; Dietz et al., 2021a) as deterministic or with *ad hoc* probabilities. Furthermore, the dynamics of the subsystem itself is in general not represented, even though there are important debates and scientific uncertainty about its shape that matter for optimal

social choice. We model a dynamic subsystem whose dynamics is risky, uncertain, self-sustaining (e.g. a decrease in the subsystem's state reduces its ability to self-perpetuate) and interacts with global climate risk. We focus on two sources of stochastic risk and their interaction : standard aggregate risk on the transient response of global temperature to cumulative emissions ($\partial T / \partial Y$) and idiosyncratic subsystem risk on the impact of global climate change on the subsystem ($\partial A / \partial T$).

Consider a system A whose dynamics is a function of its state and of climate change. Let us assume that ϵ summarizes the impact of climate on the subsystem through temperature. We have that : $dA/dt = f(\epsilon(T), A)$. Examples of such stylized dynamics for slow-onset (AMOC collapse) or fast-onset (forest dieback) tipping elements are given in [Ritchie et al. \(2021\)](#). Let us assume that this subsystem's dynamics has an impact on welfare : it can affect global climate change and economic damages. But the system has a risky dynamics, as climate impacts on the system are stochastic : $dA/dt = f(\tilde{\epsilon}(T), A)$. Furthermore, there are scientific uncertainties, for instance on the transition law f of the dynamic system or on the distribution of stochastic $\tilde{\epsilon}(T)$ linking climate change to changes in A. Different models i and different models j give different transition functions and different distributions respectively, so that : $dA_{ij}/dt = f_i(\tilde{\epsilon}_j(T), A_{ij})$. To make optimal decisions, the planner takes into account the entire stochastic distribution of each ϵ_j within each possible function f_i and weights over the alternative models with a given aggregation rule g , so that : $dA/dt = g[dA_{ij}/dt] = g [f_i(\tilde{\epsilon}_j(T), A_{ij})]$. There are m alternative models, i.e. m alternative combinations of i and j .

2 Social choice criteria

Social planner maximizes intertemporal welfare under endogenous climate damages and subsystem's dynamics. The state space is \mathcal{S} . The state variables are $x = (A, T, Y)$. $\Gamma(x)$ is the control set. Control is μ , the abatement rate. Following [Golosov et al. \(2014\)](#), we assume a fixed savings rate. At time t , decision maker's information consists of history $\omega_t = \{\omega_0, \omega_1, \dots, \omega_t\}$ with ω_0 given. The uncertainty is described by the random m in the set M : a discrete indicator of alternative models for the subsystem. The decision maker has a prior χ_0 over m . Each m gives a probability distribution π_m over the state space. The posterior χ_t and conditional likelihood $\pi_{m,t}$ are obtained by Bayes' rule.

Discounted expected utility Under expected utility, the reduction of compound lotteries axiom states that χ_t and $\pi_{m,t}$ can be reduced to a single distribution, i.e. the social planner is uncertainty neutral. The social planner's welfare

at time t writes recursively :

$$U_t(x_t, \epsilon_t) = \max_{y_t} [u(x_t, y_t) + \delta \mathbb{E}_{\chi_t, \pi_{m,t}}(\tilde{U}_{t+1}(x_{t+1}, \tilde{\epsilon}_{t+1}))] \quad (2.1)$$

$$s.t \ x_{t+1} = G(x_t, y_{t+1}) \text{ and } \mu_t \in \Gamma(x_t) \quad (2.2)$$

with G the transfer function, \tilde{U}_{t+1} the random continuation value, $\tilde{\epsilon}$ the stochastic component, δ the discount factor and u the instantaneous utility, assumed to be of the constant-relative risk aversion form with η the elasticity of marginal utility : $u(x) = \frac{x^{1-\eta}}{1-\eta}$.

This expected utility approach has two drawbacks. On the one hand, preference over time and states of the world are entangled in η . On the other hand, the social planner is uncertainty neutral : that may not be the most natural approach to decision-making under uncertainty (Ellsberg, 1961). Recent empirical evidences suggest that policy-makers are uncertainty-averse (Berger and Bosetti, 2020). For robustness, we test how much our estimates for optimal global climate policy and optimal regional subsystem management derived under expected utility depend on our collective attitude towards risk and uncertainty. Thus, our second recursive criterion is a specific form of smooth ambiguity criterion that allows to introduce uncertainty aversion from the social planner and to disentangle intertemporal elasticity of substitution and relative risk aversion. Among other social choice criteria used to study risk and uncertainty, we use a form of recursive smooth ambiguity model for three reasons. First, these preferences are an extension of the expected utility model which makes the comparison with this framework more readable : as in this model, the flaw is that we have to define subjective probabilities for the different models. We assume that each model has an equal probability of being the ‘right’ one. The second reason is that this criterion allows a separation between the object (risk and uncertainty) from our attitude towards it (risk and uncertainty aversions). Thus, comparative statics with varying (risk) uncertainty aversion and constant (risk) uncertainty levels can be undertaken, whereas it is entangled in the penalty parameter in robust control (Hansen and Sargent, 2001). It is useful as our setting includes both risk and uncertainty. The third reason is that, in comparison with robust control, this model does not assume that the decision-maker has an approximate model and that the ‘real’ model is near this approximation.

Smooth-ambiguity With this criterion, χ_t and $\pi_{m,t}$ cannot be reduced to a single distribution (Hayashi and Miao, 2011; Berger et al., 2017). This is the case

here when the concave transformation $h \circ v^{-1}$ introduced below is non-linear, yielding uncertainty aversion. Social planner's welfare at time t writes :

$$V_t(x_t, \epsilon_t) = W(u_t, u(R_t(\tilde{V}_{t+1}(x_{t+1}, \tilde{\epsilon}_{t+1})))) \quad (2.3)$$

$$W(u, y) = u^{-1}[(1 - \delta)u + \delta y] \quad (2.4)$$

$$R_t(V_{t+1}(x_{t+1}, \epsilon_{t+1})) = h^{-1} \left[\mathbb{E}_{\chi_t} \left(h \circ v^{-1} \mathbb{E}_{\pi_{m,t}} [v(\tilde{V}_{t+1}(x_{t+1}, \tilde{\epsilon}_{t+1}))] \right) \right] \quad (2.5)$$

under the same constraints. $W : \mathbb{R}^2 \rightarrow \mathbb{R}$ is a time aggregator and R is an uncertainty aggregator that maps an ω_{t+1} -measurable random variable $\tilde{\epsilon}_{t+1}$ to an ω_t -measurable random variable. \mathbb{E}_{χ_t} is the expectation operator taken at time t over models, and $\mathbb{E}_{\pi_{m,t}}$ is the expectation operator taken at time t over future welfare, conditional on the model m . The three functions u , v and w are isoelastic, with θ , γ and μ the inverse of the elasticity of intertemporal substitution, the relative risk aversion and the relative uncertainty aversion. The two expectations highlight the two-step bayesian approach. In the first stage, the social planner evaluates the expected reward of a policy under each risky model and express it in monetary terms through a certainty equivalent that depends on her attitude towards risk. In the second stage, the policy maker evaluates an overall expected reward across the various certainty equivalents depending on her attitude towards uncertainty. The policy maker addresses risk within models, then uncertainty over models.

3 Analytical definitions

1 Global scale - optimal climate policy (SCC & SCCDS)

In the remainder of this work, SCC (SCC^{SA}) is the social cost of carbon under expected utility (smooth ambiguity), SCCDS (SCC) is the social cost of carbon when the dynamic subsystem is (not) included in the model. Without loss of generality, consider the optimal SCC and SCCDS for a policymaker under expected utility. For exposition, we focus on expected utility to highlight the various channels through which the subsystem affects optimal policy : same elements are derived under smooth ambiguity in annex. We simplify the notation for the expectation taken over stochastic risk and over models, reduced by compound lotteries under expected utility. The shadow cost of emissions is the negative partial derivative of the right-hand side of equation (2.1) with respect to time t emissions, S_t . It is brought from intertemporal utility to present monetary terms when scaled by

the marginal utility of consumption $u'_c(c_t)$ and a discount factor δ . We assume no decay, so that $\frac{\partial S_{t+1}}{\partial S_t} = \frac{\partial T_{t+1}}{\partial T_t} = 1$. In our setting, we have stochastic aggregate risk over transient response to cumulative emissions, $\partial T / \partial S$, and idiosyncratic risk over the subsystem's dynamics, $\partial A / \partial T$. We assume that the impact of the subsystem on global temperatures goes through carbon releases rather than other mechanisms as in our quantitative application. SCC and SCCDS write :

$$SCC_t = \frac{\delta}{u'_c(c_t)} \mathbb{E}_t \left(\frac{\partial U_{t+1}}{\partial T_{t+1}} \frac{\partial T_{t+1}}{\partial S_{t+1}} \right) \quad (2.6)$$

$$\left\{ \begin{array}{l} SCCDS_t = \frac{\delta}{u'_c(c_t)} \left[\underbrace{\mathbb{E}_t \left[\frac{\partial U_{t+1}}{\partial T_{t+1}} \frac{\partial T_{t+1}}{\partial S_{t+1}} \left(1 + \frac{\partial S_{t+1}}{\partial A_{t+1}} \frac{\partial A_{t+1}}{\partial S_t} \right) \right]}_{V_{1,t} : temperature\ channel} + \underbrace{\mathbb{E}_t \left[\frac{\partial U_{t+1}}{\partial A_{t+1}} \frac{\partial A_{t+1}}{\partial S_t} \right]}_{V_{2,t} : subsystem\ channel} \right] \\ V_{1,t} = \underbrace{\mathbb{E}_t \left(\frac{\partial U_{t+1}}{\partial T_{t+1}} \frac{\partial T_{t+1}}{\partial S_{t+1}} \right)}_{V_{1,t}^a : standard} \underbrace{\mathbb{E}_t \left(1 + \frac{\partial S_{t+1}}{\partial A_{t+1}} \frac{\partial A_{t+1}}{\partial S_t} \right)}_{V_{1,t}^b : subsystem\ scaling} + \underbrace{cov \left(\frac{\partial U_{t+1}}{\partial T_{t+1}} \frac{\partial T_{t+1}}{\partial S_{t+1}}; 1 + \frac{\partial S_{t+1}}{\partial A_{t+1}} \frac{\partial A_{t+1}}{\partial S_t} \right)}_{V_{1,t}^c : insurance} \\ V_{2,t} = \mathbb{E}_t \left[\frac{\partial U_{t+1}}{\partial A_{t+1}} \frac{\partial A_{t+1}}{\partial S_t} \right] \end{array} \right. \quad (2.7)$$

Modeling an endogenous subsystem in a global climate-economy model and its interaction with climate change implies a risk premium that can be decomposed in two immediate channels : a subsystem channel and a temperature channel. First, marginal changes in the subsystem's state, affected by current marginal carbon emissions, have an impact on the continuation value : it is the subsystem channel. Second, a marginal increase in carbon emissions affect next period temperatures and future welfare, both through the global carbon cycle and with the additional feedback on temperature from the subsystem : it is the temperature channel. The temperature channel has three components : a change in the continuation value of the standard channel driving optimal policy, a scaling factor of this same standard channel and an insurance component, the 'subsystem beta'.

The standard channel driving optimal climate policy, $\frac{\partial U_{t+1}}{\partial T_{t+1}} \frac{\partial T_{t+1}}{\partial S_{t+1}}$, is modified when we account for the subsystem's dynamics. In particular, $\partial U_{t+1} / \partial T_{t+1}$ can be decomposed in two components through a second-order taylor expansion depicted in annex : the certainty equivalent (CE) and the precautionary channel (PC), following [Lemoine and Rudik \(2017\)](#) and [Lemoine \(2021\)](#). Most of the future impacts on intertemporal welfare of a marginal carbon emission are included in the continuation value U_{t+1} . We decompose these impacts further for all future periods. Detailed in annex, the decomposition yields an expression for SCC and

SCCDS :

$$SCC_t = \frac{\delta}{u'_c(c_t)} \overbrace{\sum_{i=t}^{\infty} \delta^{i-t} \mathbb{E}_t [u'_S(c_{i+1})]}^{Complete\ standard} \quad (2.8)$$

$$SCCDS_t = \frac{\delta}{u'_c(c_t)} \left[\underbrace{\sum_{i=t}^{\infty} \delta^{i-t} \mathbb{E}_i (u'_S(c_{i+1})) \Pi_{l=t}^i V_{1,l}^b + V_{1,t}^c}_{Complete\ standard\ channel\ scaled} + \underbrace{\sum_{j=t}^{\infty} \delta^{j-t+1} V_{1,j+1}^c \Pi_{m=t}^j V_{1,m}^b + V_{2,t}}_{Complete\ insurance\ channel} + \underbrace{\sum_{k=t}^{\infty} \delta^{k-t+1} V_{2,k+1} \Pi_{n=t}^k V_{1,n}^b}_{Complete\ subsystem\ channel} \right] \quad (2.9)$$

Modeling an endogenous subsystem in a global climate-economy model and its interaction with climate change implies a risk premium that can be decomposed in three complete channels, accounting for present and future impacts. The first term of equation (2.9) is the sum of all future marginal impact of an increase in the carbon stock on instantaneous utility. The second term is the complete insurance channel. The last term is the subsystem channel at all future periods. I describe the three scaled channels in detail below. The three channels driving optimal policy are scaled by all present and future $V_{1,i}^b$ when the subsystem's dynamics is explicitly accounted for. $V_{1,i}^b$ measures the sign and magnitude of the additional present and future feedbacks the subsystem brings to climate change. It increases (decreases) the SCCDS if $(\partial S_{i+1}/\partial A_{i+1}) \cdot (\partial A_{i+1}/\partial S_i)$ is positive (negative), i.e. if the subsystem releases (absorbs) carbon when carbon concentration increases.

Complete standard channel scaled The first term in the bracket in equation (2.9) is the complete standard channel scaled. Introducing a climate subsystem in a dynamic climate-economy model scales the standard channel driving optimal climate policy by the present and future expected feedbacks this subsystem brings on climate change, and thus on intertemporal welfare through climate damages. The standard channel driving optimal climate policy is the sum on all present and future period of the marginal derivative of instantaneous utility with respect to a marginal increase in carbon concentration.

Complete insurance channel The second term in the the bracket in equation (2.9) is the complete insurance channel. This insurance channel measures how the additional feedback on climate change brought by the impact of climate change on the subsystem's dynamics covaries with the marginal impact of carbon emissions from economic activity on intertemporal welfare at all present and future period. This term V_1^c is familiar from the consumption-based capital asset pricing approach (Lucas Jr, 1978) and the climate-economics literature (e.g. Dietz et al.

(2018), Lemoine (2021), Van den Bremer and Van der Ploeg (2021)) : agents require a greater expected return on assets which increase aggregate risk bearing on future consumption¹. The left-hand side of this channel is the marginal effect of a change in cumulative emissions on intertemporal welfare : it is negative. The right-hand side of the covariance can be either positive if the marginal impact of a change in carbon concentration² on subsystem's state has the same sign as the marginal impact of a change in subsystem's state on carbon concentration, or negative if they have opposite signs. All these states of the world are possible within the same model and for the same dynamic subsystem. In the first case, the feedback of the subsystem on climate change is positive : a marginal increase in carbon concentration brings an even larger temperature change because of the change in subsystem's dynamics. The causal mechanism stems either from a growth effect (an increase in carbon concentration increases the subsystem's state which increases the temperature) or a degrowth effect (an increase in carbon concentration decreases the subsystem's state which decreases temperature). Examples of subsystem that have these cyclical properties are for instance cryosphere climate tipping elements (Armstrong McKay et al., 2022), such as the boreal permafrost, and the Greenland, West and East Antarctic ice sheets. In the second case, the feedback of the subsystem on climate change is negative : the effect of a marginal increase in temperature on temperature is mitigated by the decrease in temperature from the subsystem. Two causal mechanisms are possible : either a growth effect (an increase in carbon concentration increases the state of the subsystem which decreases the temperature) or a degrowth effect (an increase in temperature decreases the subsystem which increases the temperature). Examples of subsystem that have these countercyclical properties are for instance ocean-atmosphere climate tipping elements, such as Labrador-Irminger Seas, Subpolar Gyre (SPG) oceanic Convection and Altantic Meridional Overturning Circulation (AMOC). If the feedback brought by the subsystem covariates positively (negatively) with the impact of emissions on intertemporal welfare, then optimal policy is relatively more (less) stringent when this 'subsystem beta' is accounted for. The magnitude of the covariance depends on relative variations : for a positive

1. A parallel beta could be computed for scientific uncertainty, measuring how scientific uncertainty about this subsystem's dynamics and its interaction with climate change affects aggregate scientific uncertainty about climate change. A positive beta-risk, i.e. when the subsystem increases aggregate risk, should be decreased (increased) if the subsystem's uncertainty decreases (increases) aggregate scientific uncertainty, i.e. depending on subsystem beta-uncertainty (Izhaki, 2020).

2. In our analytical decomposition, we focus on temperature impacts through the carbon cycle, but the demonstration would apply to other mechanisms.

covariance, if the states of the world where the marginal effect of an additional emission on welfare is relatively greater (smaller) are also the states of the world where the right-hand side of the covariance is relatively greater (smaller), i.e. situation where the feedback of the subsystem on climate change is relatively more positive (more negative), then the insurance channel increases the social cost of carbon SCCDS more (less). This depends on subsystem dynamics, global climate damage, global temperatures, etc.

Complete subsystem channel The third term in the bracket in equation (2.9) is the complete subsystem channel, i.e. the sum of all present and future immediate subsystem channels $V_{2,t}$ scaled by the feedback of the climate subsystem on global climate change. The complete subsystem channel measures how a marginal change in the subsystem's state due to a marginal carbon emission affects intertemporal welfare. A contemporary increase in carbon concentration and in temperature has a stochastic impact on the subsystem. This impact can be sometimes positive, for instance if an increase in carbon concentration increases vegetation growth rates for rainforests because of fertilization effects. But the impact of a marginal emission is mostly negative, as increases in carbon concentration disrupts most climate subsystems (Armstrong McKay et al., 2022), such as the Barents Sea Ice. This impact can also be alternatively positive or negative for a given subsystem depending on its own dynamics or the current state of the climate system. A same marginal increase in carbon concentration does not have the same impact along a given concentration pathway. For instance, a marginal increase in carbon concentration at low concentration levels might increase the vegetation growth rate for the Amazon rainforest through fertilization effects, while an increase in carbon concentration at high concentration levels might put the rainforest in great danger through changes in El Niño, a collapse in the Atlantic meridional overturning circulation or temperature limits for the photosynthesis (Doughty et al., 2023). A same marginal increase in carbon concentration does not have the same impact depending on the state of the subsystem. For instance, while the Amazon rainforest might be resilient when not too disturbed, because of plant trait diversity (Sakschewski et al., 2016) or evapotranspiration by which the rainforest recycles the rainfall that will feed its future growth, these characteristics that enhance resilience of the subsystem might weaken when the subsystem's state decreases in extent. All these characteristics of the impacts a climate subsystem might have on intertemporal welfare are disregarded when the subsystem is not explicitly a state variable of our program and its collapse

represented as an *ad hoc* probability depending on carbon concentration.

Including a subsystem in a global climate-economy model and its interaction with global climate change implies a risk premium that can be decomposed in three components : a scaling of standard optimal policy measure, an insurance component, and a subsystem component. Each of these channels is scaled by the additional feedback the subsystem brings on global climate change in all present and future periods.

2 Regional scale - optimal subsystem's management (SCDS)

The social cost of the dynamic subsystem, SCDS, is the marginal impact on intertemporal welfare of a marginal change in subsystem's state, brought into present monetary terms. In other words, a marginal change in the current state of the subsystem has an impact on the future dynamics of the subsystem, which matters because this future dynamics has an impact on future climate damages. The subsystem has its own dynamics, which is not completely controlled by the policy-maker. Our representation of the dynamics of the subsystem allows to highlight and compute the SCDS. Without loss of generality, we derive the SCDS under expected utility. The same formula is given in annex for smooth ambiguity.

Starting from the optimal policy program, we seek for the derivative of our continuation value with respect to the subsystem's state. In comparison with SCCDS, we focus on the marginal derivative of the next-period continuation value with respect to next-period subsystem's state. Indeed, the subsystem might have short-term oscillatory behavior : thus, $\partial A_{t+1}/\partial A_t$ might have unstable varying signs. Under moderate conditions, for instance along the optimal path, reducing the subsystem's stock could increase its short-term growth by for instance reducing competition between patches of a forest, while still reducing its aggregate long-term survival that is of interest to public policy. A short-term oscillation $\partial A_{t+1}/\partial A_t < 0$ might thus bias the sign of the SCDS while we are interested in the long-term behavior of our system, i.e. its marginal impact on aggregate intertemporal welfare. \mathcal{L} is the initial value of the carbon stored in the subsystem in our application ; this rescaling allows to translate marginal changes in the subsys-

tem's state to a standard carbon unit. The SCDS has two different components :

$$SCDS_t = \frac{1}{\mathcal{L}} \frac{\delta}{u'_c(c_t)} \left[\underbrace{\mathbb{E}_t \left(\frac{\partial U_{t+1}}{\partial T_{t+1}} \frac{\partial T_{t+1}}{\partial S_{t+1}} \frac{\partial S_{t+1}}{\partial A_{t+1}} \right)}_{W_{1,t} : \text{temperature channel}} + \underbrace{\mathbb{E}_t \left(\frac{\partial U_{t+1}}{\partial A_{t+1}} \right)}_{W_{2,t} : \text{subsystem channel}} \right] \quad (2.10)$$

The temperature channel measures the feedback of the subsystem on aggregate climate change, i.e. how much a marginal change in the subsystem's state affects intertemporal welfare through its marginal impact on temperatures. The subsystem channel measures how a marginal change in the subsystem's state affects intertemporal welfare : it includes all future risk on the dynamics of the subsystem brought by a marginal perturbation in its current state, and thus all future potential increases in aggregate temperatures and climate damages, including the most disastrous.

We have highlighted the channels through which our modelling approach affects global climate policy and regional subsystem management. For illustration, we apply our framework to the debated fate of the Amazon rainforest. We quantify the impact of this specific subsystem on optimal climate policy in a dynamic stochastic climate-economy model. We measure the impact of the interactions between aggregate climate risk and amazon idiosyncratic risk and its explicit geophysical dynamics on optimal rainforest management. We compute the share of each of the channels depicted analytically.

3 A quantitative application : the Amazon rainforest

We use a macroeconomic growth model *à la Ramsey* and add climate dynamics (Guivarch and Pottier, 2018; Taconet et al., 2021; Fillon et al., 2023). We augment the model with a stylized representation of the Amazon rainforest whose uncertain dynamics interacts with climate change. We focus on two sources of stochasticity³ that are of particular interest : standard aggregate climate risk regarding transient climate response to cumulative emissions on the one hand, i.e. how much emissions from economic activity translates to climate change, idiosyncratic stochastic impact of global climate change on forest dynamics on the

3. More stochasticity and states would be difficult to handle with global solution methods without message passing interface on large computing clusters and would not provide more information on the mechanisms we want to highlight.

other hand, i.e. how much climate change affects the carbon stored in the rainforest. In other words, we price the Amazon rainforest climate asset within a broader risky climate portfolio. In addition to this stochasticity, we add an explicit geophysical representation of forest dynamics. The dynamics of the rainforest is self-sustaining, with possible feedback effects : a decrease in the forest cover decreases forest growth. This non-linear dynamics can generate some curvature in our value function in one dimension of our program. We include scientific uncertainty over both the functional form of this dynamics and on the impact of climate change on the rainforest, i.e. alternative scientific models embedded in our social choice. We identify key mechanisms and channels through which risks and uncertainties about the impact of global climate change on the rainforest affect optimal climate policy at the global scale and optimal rainforest management at the regional scale. We solve our recursive programs using dynamic programming : we interpolate recursively starting from the last period terminal value function and approximate our value functions with simplicial Chebyshev polynomials and adaptive approximation domains for our state variables ([Cai, 2019](#)). We employ simplicial Chebyshev polynomials, as they enable varying degrees of approximation across different dimensions of our dynamic problem : less precision is required for approximating the smooth dynamics of capital accumulation compared to the more complex dynamics of the Amazon rainforest. We break one level of ‘curse-of-dimensionality’ related to approximation nodes with parallel CPU computing for value function interpolation. Once we have interpolated recursively at each time step, we simulate 100 stochastic paths for each specification and use the mean path for each variable of interest.

1 Model specification

Economic model One global region produces at each period t a single good using capital K and exogenous labour L through a production function $F(K, L)$, with exogenous Hicks-neutral technological change from [Nordhaus \(2018\)](#). Capital dynamics is determined by the per-period capital depreciation δ and savings rate s : $K_{t+1} - K_t = -\delta K_t + Y_t s_t$. We assume a fixed savings rate $s_t = \alpha \delta$, where α is the share of capital in the Cobb-Douglas production function and δ the discount factor. Net output Y is derived from gross output net of damage : $Y = \Omega(T)F(K, L)$. The damage factor is increasing in temperature. Net output induces emissions, which can be mitigated at a certain cost : $E = \sigma Y(1 - \mu)$ with μ the abatement rate and σ the carbon content of production that decreases exogenously over time ([Nordhaus, 2018](#)). The emissions adds up to a global cumu-

lative emissions stock S and we assume no decay. The social planner trades off consumption and mitigation to maximize intertemporal welfare.

Climate model We use a simple representation for the climate system, with a linear formula linking global temperature T to the stock of global carbon emissions S through transient climate response to cumulative carbon emissions ψ , i.e. $\partial T / \partial S = \psi$, as in [Dietz and Venmans \(2019\)](#). Following [Barnett et al. \(2020\)](#), we assume a truncated normal distribution for ψ on the support $[0 : 3.5]$ with a best estimate of $\bar{\psi}=1.73^{\circ}\text{C}$ per 1000PgC and a standard deviation of 0.493. Quadratic climate damage to economic output Ω are derived from temperature changes.

Amazon rainforest The variable A used to represent rainforest's dynamics is the ratio of current carbon stored in the forest in comparison with the total possible carbon losses $\mathcal{L} = 75\text{GtC}$ ([Armstrong McKay et al., 2022](#)). We use a stylized vegetation dynamics ([Ritchie et al., 2021](#)), where the dynamics of A is a function of the current state A and of regional temperature T_{reg} interacted with the stochastic impact of climate on tree mortality via droughts $\tilde{\epsilon}$. T_{reg} is deduced from global cumulative emissions stock via linear and time-invariant regional transient climate response to global cumulative emissions ([Leduc et al., 2016](#)). There are two possible functional forms for the dynamics of the system : either without (f_1) or with (f_2) a feedback effect. There are four distributions for $\tilde{\epsilon}_j$ because four different climate models j are used to estimate how more frequent and intense droughts are under changing climate. This yields a total of eight models : we give each model m the same probability of being the 'true' one. The Lotka Volterra equation writes :

$$\frac{dA_{ij}}{dt} = \begin{cases} f_i(\tilde{\epsilon}_j \cdot T_{reg}, A_{ij}) \text{ with } i \in \{1, 2\}, j \in [1 : 4] \text{ if } t \leq 2200 \\ 0 \text{ if } t > 2200 \end{cases} \quad (2.11)$$

$$\text{with } \begin{cases} f_1(x) = g_0 \left[1 - \left(\frac{T_{reg}(0) + T_{reg}}{\beta_0} \right)^2 \right] x(1-x) - \tilde{\epsilon}_j T_{reg} x - \kappa x \\ f_2(x) = g_0 \left[1 - \left(\frac{Y[1-x] + T_{reg}(0) + T_{reg}}{\beta_0} \right)^2 \right] x(1-x) - \tilde{\epsilon}_j T_{reg} x - \kappa x \end{cases} \quad (2.12)$$

where g_0 is the forest growth rate under normal conditions, κ exogenous deforestation and degradation rates, $T_{reg}(0)$ regional temperature increase with respect to preindustrial at initial time, T_{reg} regional temperature increase with respect to initial time, β_0 half-width of the growth versus temperature curve, and Y the

temperature difference between bare soil and forest, driving the feedback. We assume that regional transient climate response to global cumulative emissions, from which T_{reg} is deduced, does not depend on A, which should hold for any optimal policy path where the rainforest is not too depleted.

2 Calibration

We use a standard calibration for the climate and macroeconomic modules : a complete description is in annex. We use exogenous deforestation and degradation scenarios. Our calibration is a two-step procedure. We first calibrate the maximum impact of climate on the rainforest via droughts using climate model projections and historical observations. Then, given these parameters, we jointly calibrate the remaining parameters internally so that the probability of forest die-back under a tipping risk (i.e. with functional form f_2 that includes a feedback effect in the dynamics) matches the central estimate of the core expert probability assessment of [Kriegler et al. \(2009\)](#) for each of their temperature corridors. In particular, we calibrate the shape of the distribution of $\tilde{\epsilon}$ between 0 and its estimated upper bound. We then assume that the parameters and the distribution for $\tilde{\epsilon}$ remains constant for the other specification f_1 where there is no tipping risk.

Exogenous deforestation and degradation κ At each t, a share κ_t of the forest cover is deforested or degraded. We use the mean of three deforestation scenarii ([Aguiar et al., 2016](#)). We assume that deforestation stops after 2050 as this is the maximum horizon for most scenarios. We multiply the area deforested by two to take into account forest degradation, including human-induced fires, based on the historical relationship observed between deforestation and degradation ([Mastricardi et al., 2020](#)). Scenarii are for the brazilian Amazon which covers 60% of the extent of the rainforest : we scale the scenario and assume that they hold for the whole rainforest. We convert the deforestation rate expressed in km^2 in a share of initial carbon storage, assuming homogeneity of the carbon stored over the forest.

External calibration - Endogenous climate change effects $\tilde{\epsilon}_j$ via droughts We model this link through four $\tilde{\epsilon}_j$ based on the climate model j used to predict the change in rainfall patterns. We assume that each $\tilde{\epsilon}_j$ follows a Beta distribution on a support whose upper limit $\bar{\epsilon}_j$ is estimated below. For the estimation of these upper bounds, we exploit in each climate model the variation in local climate conditions to measure how much carbon losses from tree mortality in the Amazon increases with local temperatures. We build a balanced panel dataset until

2100 along three representative concentration pathways (RCP 2.6, 6.0, 8.5) and use 60 arc-minutes resolution gridded data from the Inter-Sectoral Impact Model Intercomparison Project (ISIMIP) on monthly precipitation. We use precipitation projections taken from the hydrological model MATSIRO for all possible climate forcing models j : IPSL-CM5A-LR, HadGEM2-ES, GFDL-ESM2M, MIROC5. We compute an index of precipitation stress, the yearly maximum cumulative water deficit (MCWD) anomaly with respect to an historical baseline (1985-2004). We match this precipitation data with bias-adjusted and downscaled gridded surface temperature data specific to each climate forcing model. Data from historical observations ([Phillips et al., 2009](#); [Yao et al., 2022](#)) established a link between MCWD anomaly and carbon losses from tree mortality in the Amazon rainforest. We scale these yearly carbon losses obtained for each climate forcing model by the spatial heterogeneity observed in the carbon storage at initial time, taking data from EarthData (NASA). Our preferred specification is a fixed-effect approach with year and regional fixed effects and [Driscoll and Kraay \(1998\)](#) standard errors to account for heteroskedascity and serial correlation. We control for sub-regional diversity with [Silva-Souza and Souza \(2020\)](#) woody plant regionalization into 13 subregions. The dependent variable is the yearly carbon loss from tree mortality (in tC/ha/y) at the cell level for each climate model, and the independent variable is the local temperature observed over the same period (in °C). We estimate the following equation :

$$C_{i,r,t}^j = \beta_{carbon}^j X_{i,r,t}^j + \alpha_i^j + \delta_t^j + \zeta_r^j + u_{i,r,t}^j \quad (2.13)$$

with u the pixel-specific error term, i the geo-coded entity (e.g. a pixel of our grid whose resolution depends on the climate model j used), t the time period, r the [Silva-Souza and Souza \(2020\)](#) subregions. β_{carbon}^j is our coefficient of interest, α a vector of N-1 location-specific fixed effect and the constant, δ a vector of time fixed effects and ζ our vector of region-specific fixed effects to account for clusters in our data. We obtain our coefficient of interest $\hat{\beta}_{carbon}^j$ for four climate models. We multiply $\hat{\beta}_{carbon}^j$ by the size of the rainforest, ≈ 700 million ha ([Silva-Souza and Souza, 2020](#)), to obtain the yearly loss of carbon per additional degree of local temperature for each model j . We express this coefficient as a share of the total initial carbon stored that could be released under total dieback (75 GtC) in the forest and multiply by the number of years per period to obtain the maximum share of carbon stored in the rainforest that is lost per period because of droughts for a one degree increase in local temperature for each model j , $\bar{\epsilon}_j \in \{0.0376, 0.0661, 0.0774, 0.1447\}$. Our dynamic model relies on regional tem-

perature that depends linearly on the cumulative global emission stock (Leduc et al., 2016) : we make the assumption that the link between carbon losses and local temperatures holds for regional temperatures.

Internal calibration Information on how to evaluate the probability of a tipping point for the Amazon is scarce. We use expert's elicitations of a possible Amazon tipping point depending on temperature corridors expressed in Kriegler et al. (2009). $\tilde{\epsilon}$ is the coefficient and its probability distribution is a mixture of the four ϵ_j . $\tilde{\epsilon}$ follows a Beta law with parameter α_s and β_s over the support $[0 : \bar{\epsilon}]$ where $\bar{\epsilon}$ is the mean of the maximum $\bar{\epsilon}_j$. We jointly calibrate Y , g_0 , α_s , β_s so that the probability of tipping in our dynamic system, dependent on the distribution of $\tilde{\epsilon}$, follows approximately the imprecise central probability of the expert probability assessments. We have that $g_0 = 0.49$, $Y = 6$ and $\tilde{\epsilon} \sim \mathcal{B}(0.36, 0.32)$ with support $[0 : \bar{\epsilon}]$. For illustration, we simulate the cumulative carbon losses for all SSP under our model⁴. A partial or total dieback of the forest occurs by 2200 for a temperature increase with respect to pre-industrial era above 4°C, which is well above temperature levels obtained under optimized policy decisions. Thus, while our calibration is stylized, the forest dynamics is in line with the literature and not artificially more catastrophic to inflate policy estimates.

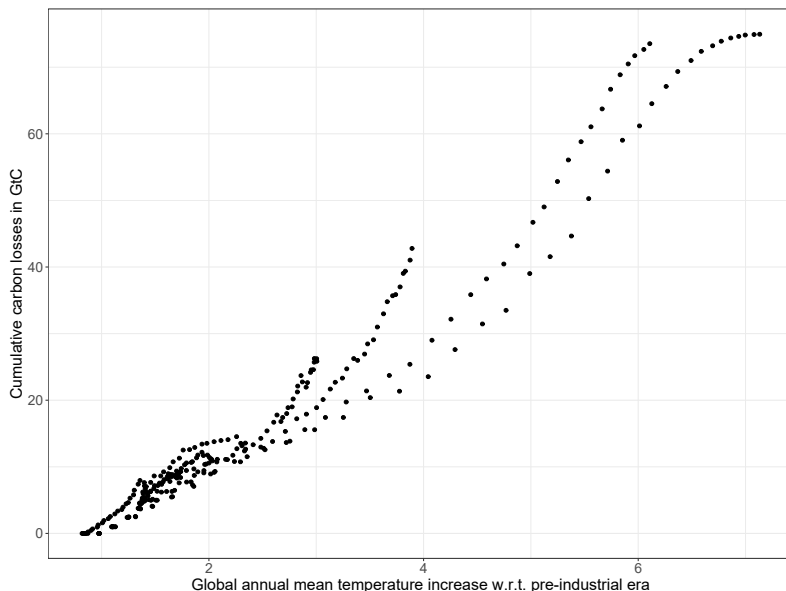


FIGURE 2.13 – Mean net cumulative carbon losses (in GtC) from the Amazon rainforest along mean temperature increases with respect to preindustrial era from various extended concentration pathways (SSP1-1.9, SSP1-2.6, SSP4-3.4, SSP5-3.4, SSP2-4.5, SSP4-6.0, SSP3-7.0, SSP5-8.5), from 2000 to 2200, under our calibration.

4. In appendix, we plot phase diagrams of the stochastic dynamic system in Figures (2.20) and (2.21) for the whole distribution of ϵ and different temperature pathways over time.

3 Results

We assess numerically the optimal climate policy in a stochastic model with an explicit modelling of the Amazon's dynamics under risk and uncertainty. We first measure how much the social cost of carbon at the global scale is affected by the Amazon rainforest under expected utility. In other words, we study the gap between SCC and SCCDS. We quantify how the various channels depicted above shape optimal global climate policy. Second, we quantify the social cost of the dynamic subsystem SCDS as a share of the standard social cost of carbon SCC under expected utility. Finally, for robustness, we price the risks and scientific uncertainties in the Amazon dynamics and its interaction with global climate change and the macroeconomy under smooth ambiguity : we quantify SCC^{SA} and $SCCDS^{SA}$ under various specifications. In annex, we present intertemporal stochastic paths for our control variable and for two state variables of interest : global average temperature and amazon rainforest's state with respect to its initial state.

1 Optimal global climate policy - SCC and SCCDS

We first compute SCCDS under expected utility. We compare SCCDS to the standard SCC that would be obtained under stochastic aggregate climate risk but without an explicit endogenous modeling of the Amazon rainforest. On Figure (2.14), we plot the increase (in %) from SCC to SCCDS for two specifications. The left bar shows the increase the Amazon rainforest brings to the SCC at the global scale when there is climate risk on the transient climate response to cumulative emissions but no idiosyncratic risk over the rainforest dynamics. The right bar shows the increase from SCC to SCCDS when we include both idiosyncratic stochastic risk in the dynamics of the rainforest and aggregate climate risk. For each measure, we compute the share that each of the various channels identified in the complete analytical decomposition from equation (2.7) contributes to the increase from SCC to SCCDS : the scaling of the standard channel through which carbon emissions affect intertemporal welfare, the insurance 'amazon beta' component, and the subsystem channel by which a marginal change in the amazon's state affects intertemporal welfare through the continuation value.

Figure (2.14) yields two main results. First, including the endogenous dynamics of the Amazon rainforest in a dynamic stochastic climate-economy model increases the SCC. Under aggregate climate risk over the transient climate response to cumulative emissions, the SCCDS that includes the dynamics of the Amazon rainforest is around 11% larger than the standard SCC. When additio-

nal idiosyncratic risk on the dynamics of the rainforest is added, i.e. stochastic risk on the impact of stochastic droughts from climate change on the rainforest, the SCCDS is around 15% larger than the SCC. In their meta-analysis based on Cai et al. (2016), Dietz et al. (2021a) highlight that the possible dieback of the Amazon rainforest leads to a 0.1% increase in the expected SCC when considering its value as a carbon stock. Our analysis suggests these estimates may be significantly understated for two reasons. First, we account for the rainforest's dynamics across all possible future states, rather than focusing on a stylized, catastrophic risk of partial dieback. Second, we incorporate the marginal impact of the rainforest subsystem on the continuation value—a mechanism described as the subsystem channel in equation (2.7). This channel is not explicitly captured in standard climate-economy models, which often rely on *ad hoc* probabilities for subsystem dieback without integrating an explicit state variable to represent the subsystem's dynamics.

Our second result from the right histogram on Figure (2.14) shows indeed that the largest share of the increase from SCC to SCCDS stems from the subsystem channel. Under climate risk, the subsystem channel represents around 74.3% of this increase, the scaling of the standard SCC by the additional feedback from carbon releases of the Amazon rainforest represents 25.3%, and the insurance channel represents 0.4%. Under both aggregate climate risk and idiosyncratic amazon risk, the subsystem channel accounts for 68%, the standard scaling represents 31.4%, and the insurance channel 0.6%. In other words, most of the increase between SCC and SCCDS stems from the subsystem channel under both specifications. The insurance channel, on the other hand, is rather weak, which can be explained by two factors. First, the risk specification in our model : the insurance relates to the interaction between the aggregate climate risk (transient climate response to cumulative emissions) and the idiosyncratic risk (of changing carbon concentration on forest dynamics). In reality, there are other sources of risk between the two systems, such as the risk on the forest impact on the climate system, i.e. stochasticity in possible carbon releases that might for instance arise due to heterogeneity over the rainforest in the carbon storage. This risk could increase the insurance component, i.e. the subsystem's contribution to the aggregate risk. Second, we study one subsystem in isolation, whereas there are several subsystems that interact with each other and could increase the overall aggregate risk, for example El Niño or AMOC and their feedbacks with the Amazon rainforest via precipitation cycles.

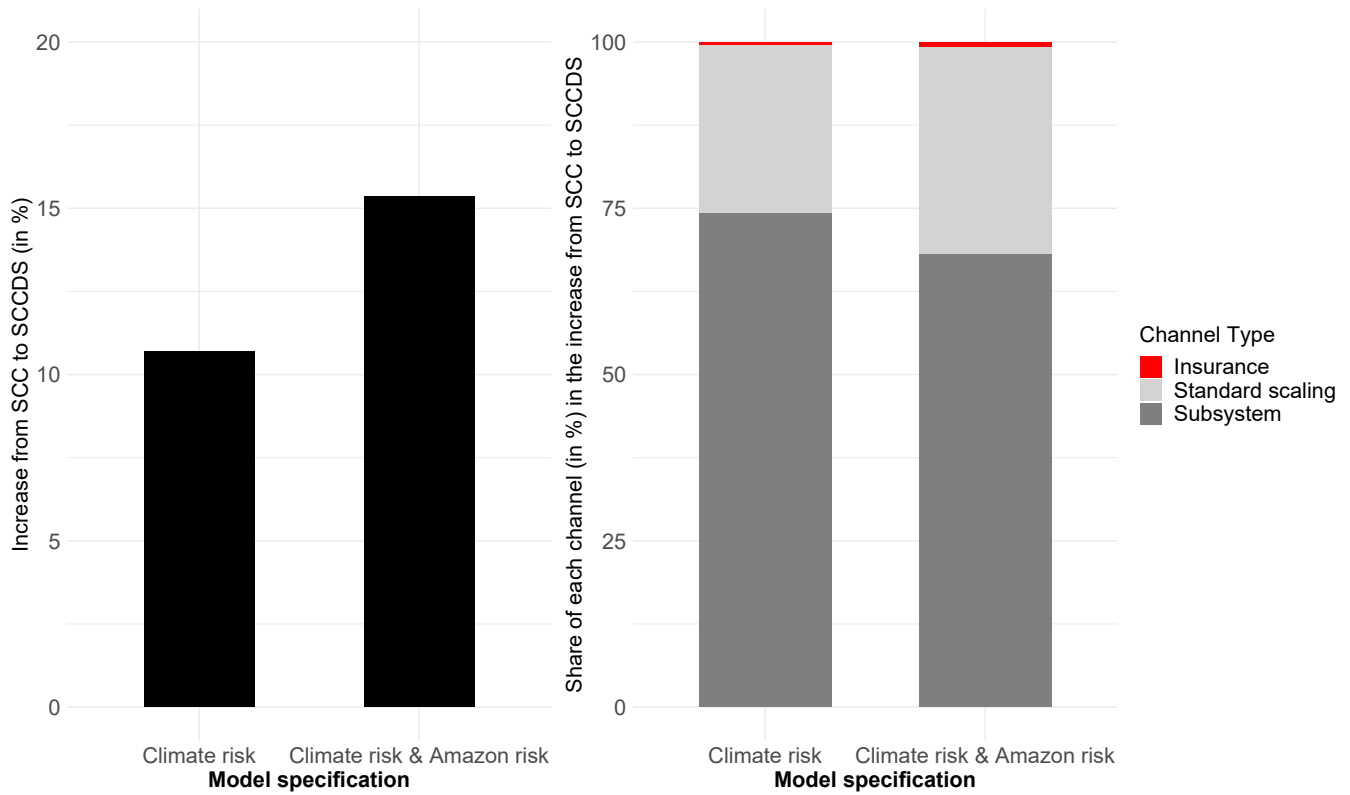


FIGURE 2.14 – Left Increase (in %) from SCC to SCCDS when the Amazon rainforest is added to the dynamics system, under stochastic aggregate climate risk (left), under both stochastic aggregate climate risk and idiosyncratic amazon risk (right). **Right** Share (in %) of each channel in this increase (scaling, insurance & subsystem channels) under aggregate climate risk (left) and both aggregate climate and idiosyncratic amazon risks (right).

A back of the envelope calculation helps to understand the magnitude these percentages might represent. Using a 2% discount rate, U.S. Environmental Protection Agency recently suggested to use a \$190 per tCO₂ social cost of carbon ([Agency, 2022](#)). Global CO₂ emissions in 2022 are estimated at 36.4Gt CO₂ ([Friedlingstein et al., 2023](#)). This means that if the increase from SCC to SCCDS under both stochastic risks represents 15% of the standard SCC, applying this increase to the universe of CO₂ emissions would raise around 1.0374 trillion dollars for 2022 only. Even the insurance channel, which represents only 0.6% of these 15% increase, accounts for nearly 6 billions dollar yearly, i.e. five time the \$1.2 billion pledges from Lula da Silva for the Amazon Fund in January 2023. The wedge between SCC and SCCDS could be leveraged at the global scale to finance co-Asian mechanisms at the regional scale to prevent deforestation and forest degradation. This regional management could indeed decrease the subsystem channel and reduce risk over the future dynamics of the Amazon rainforest. This global

redistribution would have a double dividend property : it would reduce both the negative externality of carbon emissions at the global scale and the global and regional risk over the dynamics of the rainforest.

Explicitly introducing the dynamics of a climate subsystem such as the Amazon rainforest into stochastic climate-economy modelling has an impact on optimal global climate policy. To assess the value of a hectare of Amazonian forest focusing only on its use value as a carbon stock, we first need to quantify the amount of carbon stored in that hectare Σ . Once this quantity is known, it must be multiplied by the standard social cost of carbon. Then, it should be multiplied by the increase implied by the stochastic modeling of the dynamic of the subsystem estimated above, i.e. $\Sigma * SCC * 1.15 = \Sigma * SCDS$. But that is not all. Explicitly introducing the dynamics of a climate subsystem such as the Amazon rainforest into stochastic climate-economy modelling also has an impact on the optimal management of the subsystem's resilience over time.

2 Optimal regional rainforest management - SCDS

We compute the social value of the dynamics system (SCDS) under expected utility as a share of standard social cost of carbon SCC under aggregate climate risk but without the amazon rainforest included in the dynamics, i.e. the standard measure of the SCC in the literature. On Figure (2.15), we plot the share for two specifications. On the left, we plot this share under standard aggregate climate risk. On the right, we plot the share under both standard aggregate climate risk and idiosyncratic amazon risk. For each specification, we report the share of the two channels analytically depicted in equation (2.10) in the SCDS.

Figure (2.15) yields two key results. First, SCDS represents a significant share of the SCC. Under aggregate climate risk, the SCDS represents 15.77% of the SCC. Under both aggregate climate risk and idiosyncratic risk over the dynamics of the rainforest, this share increases to 15.95%, a 1.1% increase with respect to the specification with aggregate climate risk only. Second, what matters most in the SCDS is the subsystem channel, i.e. the impact of a marginal change in the subsystem's state on the continuation value of our program, which includes all future risks over the dynamics of the forest and the welfare impacts of future possible carbon releases. Under aggregate climate risk, the subsystem channel represents 58.2% of the SCDS. Under both aggregate climate risk and idiosyncratic subsystem risk, the subsystem channel represents 57.6% of the SCDS.

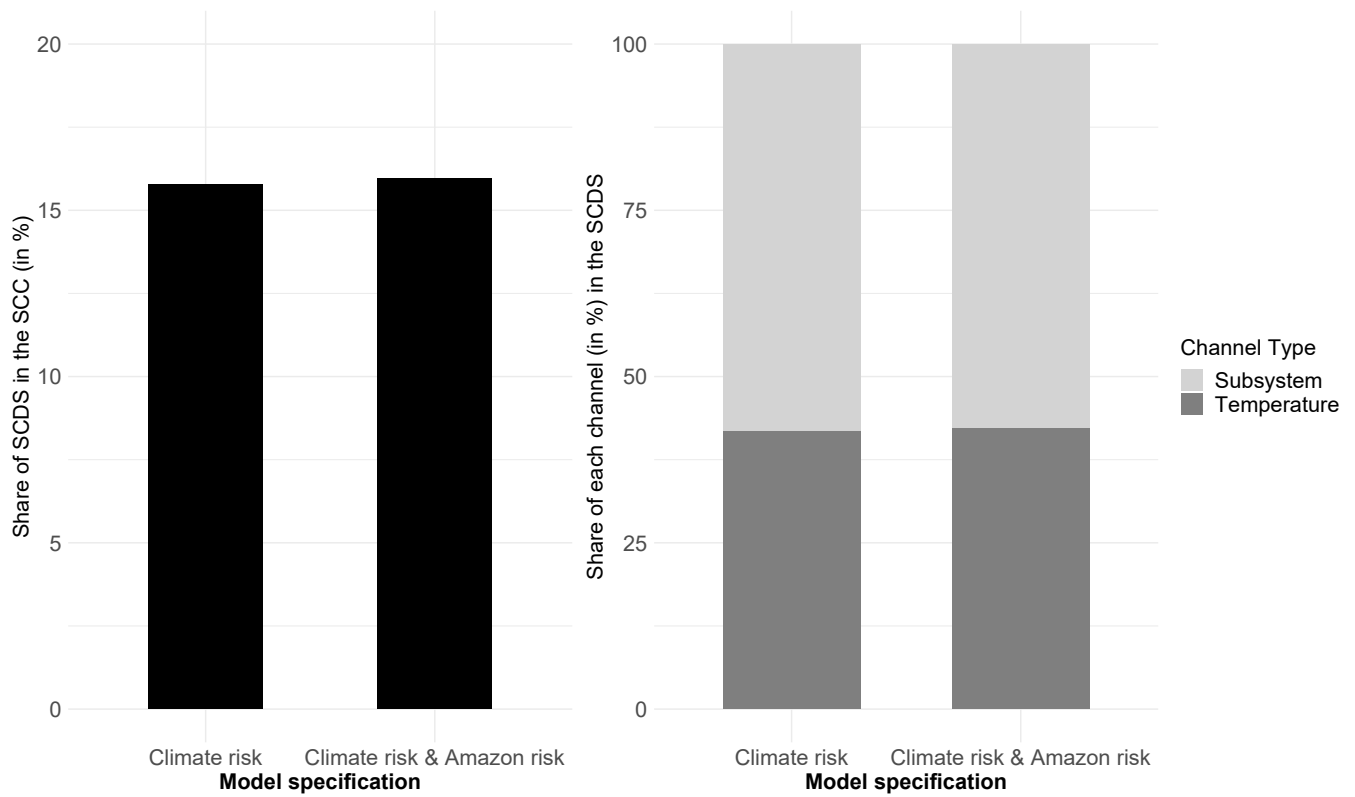


FIGURE 2.15 – Left Share (in %) of SCDS in the SCC under expected utility with stochastic climate risk under deterministic and stochastic specifications for the rainforest, i.e. without (left) and with (right) idiosyncratic amazon risk. **Right** Share (in %) of each channel in the SCDS (temperature and subsystem channels) under aggregate climate risk (left) and both aggregate climate risk and idiosyncratic amazon risk (right).

This has large implications for regional forest management. Indeed, when evaluating the value of a marginal hectare of rainforest in regional cost-benefit analysis, for instance for infrastructure projects, SCDS should be accounted for. In addition to the direct value of the carbon contained in this hectare of forest, which should be valued at the SCCDS level as argued above, we need to take into account the marginal value of the dynamic system on the continuation value, i.e. the sub-system channel of the SCDS. Indeed, choosing to deforest in one place releases carbon, but also has an impact on the forest's future carbon release dynamics and the probability of its dieback. Explicitly introducing the dynamics of a climate subsystem such as the Amazon rainforest into stochastic climate-economy modelling has an impact on optimal regional subsystem management via the valuation of an hectare of rainforest. To assess the value of a hectare of Amazonian forest focusing only on its use value as a carbon stock, we first need to quantify the amount of carbon stored in that hectare. Once this quantity Σ is known, it must be multiplied by the standard social cost of carbon. Then, it should

be multiplied by the increase implied by the stochastic modeling of the dynamic of the subsystem estimated above, i.e. $\Sigma * SCC * 1.15$. Finally, it should be scaled by the impact of a marginal change in the subsystem's state on the future of the rainforest, i.e. $\Sigma * SCC * (1.15 + (0.1595 * 0.576)) = \Sigma * SCC * 1.24$, which means a 24% increase in the valuation of this hectare of rainforest with respect to a standard valuation using the stochastic SCC under standard aggregate climate risk without the explicit modelling of the rainforest.

Revolution in satellite data has allowed a quick development in dynamic discrete choice methods that are useful tools to evaluate counterfactual policies ([Araujo et al., 2020](#)). While this granularity in satellite data is very complementary to our approach and important from a descriptive point of view in order to compute carbon stocks at the finest resolution or to monitor human disturbances on the forest in real time, it does not allow for prospective modelling of the system's dynamics. Although some early warning signals of critical transitions such as tipping points have been identified ([Scheffer et al., 2009](#)), they are not yet sufficiently developed for real-time monitoring. Furthermore, it is not certain that it is not too late once these signals are readable as the tipping point might already have been triggered irreversibly : [Biggs et al. \(2009\)](#) suggest that research should focus on defining critical indicator levels rather than detecting change in the indicators. We are in line with this robust approach to possible ecological regime shifts and SCDS might be operationalized to work in this direction within a global welfarist framework.

3 Robust social choice

Finally, for robustness, we look at the extent to which our attitude towards the large risks and uncertainties over the future dynamics of the rainforest can change the amplitude of our results on the SCCDS and SCDS under expected utility. We disentangle preference over time, risk and uncertainty (θ , γ and μ) under perturbations to the rainforest. Various parameter values are used in the literature either with positive or normative approaches ([Ju and Miao, 2012](#); [Cai and Lontzek, 2019](#)). Our approach is close to [Berger et al. \(2017\)](#) : we assume as a benchmark⁵ a setting with low-aversion $\theta = 1.5$, $\gamma = 2$, $\mu = 2$. The sensitivity is done on a high-aversion scenario with $\gamma = 10$, $\mu = 10$ while holding preference for intertemporal substitution constant. Under robust control, switching attitudes

5. We cannot directly compare robust social choice policy programs to expected utility under risk as they do not yield the same deterministic paths.

from low to high aversions yields an increase of about 40% for the SCCDSS^A and 60% for the SCDS^A .

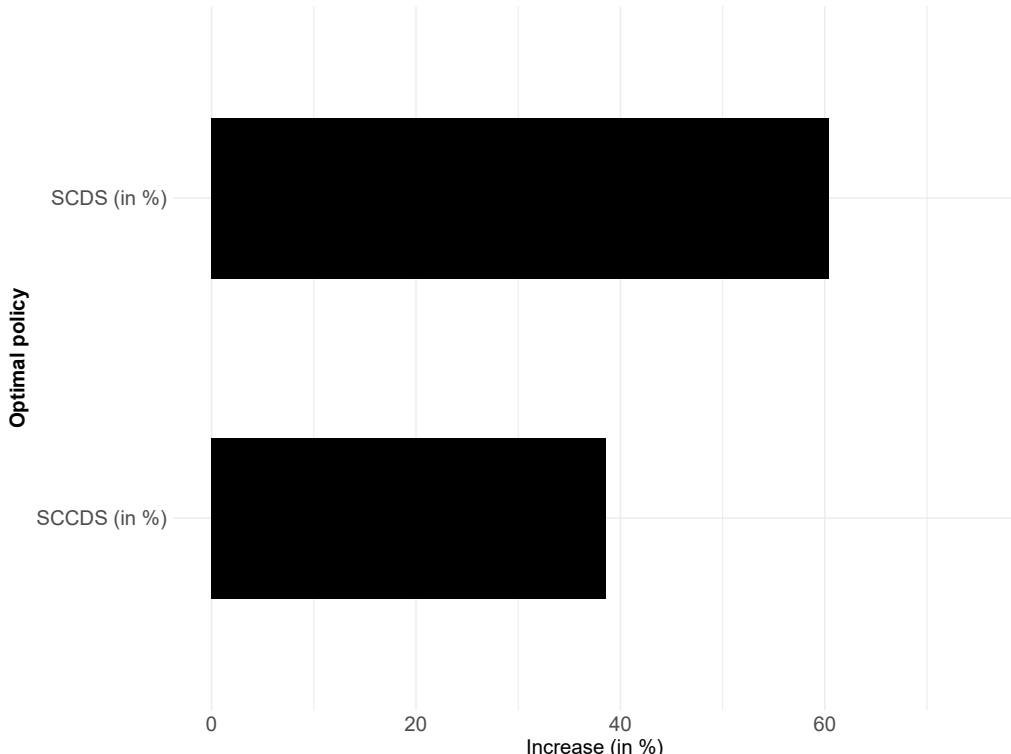


FIGURE 2.16 – Increase (in %) from low to high risk aversion parameter values under smooth ambiguity when the amazon rainforest is accounted for (Top) SCDS^A (Down) SCCDSS^A .

In our robust criterion, we abstract from learning as in [Millner et al. \(2013\)](#) and [Berger et al. \(2017\)](#). A dynamic learning model under uncertainty would require updating the weights given to each model. Even if it is not clear how and in which direction scientific progress will allow to reduce uncertainty, our estimates under uncertainty aversion should be considered as upper bounds of the possible increases in the SCCDSS brought by uncertainty. Meanwhile, a careful study of learning under a tipping risk ([Rudik, 2020](#)) shows that learning can backfire and reduce welfare by erroneously ruling out pending catastrophe. Our upper bound ruling out learning could be more in line with a robust approach to decision-making under uncertainty.

4 Conclusion

Modeling stochastic and debated interactions between climate change, the macroeconomy and Earth subsystems with a reduced-form geophysical repres-

tation of the dynamic subsystem is insightful for decision-makers, both at the global scale for climate policy and at the regional scale for management of the subsystem. Using value function decomposition, we show that the social cost of carbon is increased from SCC to SCCDS by the endogenous subsystem through three main channels : a scaling of the standard channel driving optimal policy by the sign and magnitude of the feedback the subsystem brings to climate change, an insurance channel that measures how subsystem idiosyncratic risk affects aggregate climate risk on intertemporal welfare, and the impact a marginal carbon emissions has on intertemporal welfare through its effect on the future dynamics of the subsystem. Thus, the subsystem has an impact on optimal climate policy that cannot be reduced to the expected value of the feedback it has on climate change. At the regional scale, the explicit reduced-form geophysical representation of subsystem's own dynamics which is nonlinear and partly beyond direct control of the decision-maker allows to study the social cost of the dynamic system SCDS, i.e. the cost of a marginal decrease in subsystem's state because of its reduced ability to self-perpetuate. Our methodological approach could be operationalized for public decision-making regarding other climate subsystems whose fate is debated.

For illustration, we apply our general framework to the fierce debates over the fate of the Amazon rainforest. We use a stochastic climate-economy model with aggregate climate risk over transient climate response to cumulative emissions and add a stylized reduced-form geophysical dynamics of the rainforest with idiosyncratic stochastic risk over the dynamics of the forest. We move away from the modeling of a generic catastrophe to represent it as an emergent property of the dynamic system. We calibrate the dynamics explicitly and take into account both stochastic risk within climate models and scientific uncertainty over various climate models in our decision criterion. Our approach yields three key results. First, the social cost of carbon should include the impact that a marginal increase in cumulative emissions at the global scale has on the dynamics of the rainforest. This includes both a scaling of current policy by the carbon releases from the Amazon rainforest under changing climate and an insurance channel because the carbon releases have not the same social value depending on the states of the world where they occur. This also includes the marginal value of a carbon emission on intertemporal welfare through its impact on future subsystem's dynamics. Second, the social value of the Amazon rainforest as a carbon stock cannot be reduced to the amount of carbon it contains : the SCDS matters too, as it repre-

sents a significant share of the SCC under expected utility and standard aggregate climate risk. Third, risk and scientific uncertainties are key components of these subsystems : decision-making should account for them in the decision process rather than averaging over deterministic realizations. This means first and foremost taking risk seriously in our modeling approach, with global solution methods and multiple sources of risk interacting. Finally, it means offering the general public decision-making tools that are flexible in terms of attitudes to scientific risk and uncertainty, such as the smooth ambiguity criterion. Both SCCDS and SCDS increase sharply with these preference parameters under our robust social choice criterion.

Our results yield three key policy insights at the global scale, from global to regional scales and at the regional scale respectively. First, decision-makers should use SCCDS instead of SCC, i.e. augment the SCC from the impact of a marginal emissions on the Amazon rainforest, that further releases carbon. Emitters around the world should pay around 15% per tCO₂ for the welfare impact of their emissions on the rainforest. Second, the wedge between SCCDS and SCC, i.e. between the SCC without endogenous Amazon rainforest and the SCCDS with this additional feedback, could be leveraged around the world and used to finance payment for ecosystem services for the preservation of the rainforest in a double dividend fashion. These mechanisms are the cornerstone of the UN-sponsored REDD+ strategy. The wedge could address the challenge of financing these coasian subsidies for not deforesting by clearly identifying who is responsible for what in this subsystem's dynamics whose fate is not entirely under the control of the governments of the territory in which they are located. Indeed, when multiplied by the universe of carbon emissions, a 15% increase in the SCC at the global scale represent an amount far larger than any other source of funding proposed so far. Third, the social value given to an hectare of rainforest should include not only the standard social cost of carbon SCC, but the sum of the amazon-augmented social cost of carbon SCCDS and the subsystem channel of the social cost of the dynamic system SCDS. This subsystem channel of the SCDS represents around 9% of the standard SCC obtained under aggregate climate risk. Indeed, a marginal decrease in the forest cover has a first-order welfare impact, as it releases carbon, but also a second-order impact on the future dynamics of the subsystem as a whole. Our theoretical work can therefore be operationalized in local cost-benefit analysis of deforestation and be used in complement to the significant progress in the quantification of carbon stored at the finest scale via satellite ob-

servation. We show that, considering only its value as a carbon stock, the value of a hectare of rainforest is 24% higher than the value currently used in cost-benefit analysis. This SCDS is also interesting to differentiate between different subsystems and understand how these differences bring differences in terms of optimal policy at the global and the regional scales. The dynamics of the Amazon rainforest, which includes a feedback effect, is different from other tropical rainforests (Staal et al., 2020) : feedback dynamics are weaker for Congo rainforest and southeast Asian rainforests are not vulnerable to forest-rainfall feedbacks because of their maritime climate zones. Incorporating an explicit geophysical dynamics of the subsystem also matters for risk ranking among various climate subsystems.

Our work has limitations. Some limitations are standard in this literature, for instance the simple representation of the macroeconomy. Two key limitations are related to our specific modeling choices regarding the rainforest : on its dynamics and on its valuation. First, there are more uncertainties at stake with the future of the Amazon rainforest than the one we consider. Here, we have tried to grasp some of this deep uncertainty to show how it influences our results. Second, the main limitation and way forward would be to include other values to the subsystems. For the Amazon rainforest, we focus on the use value of the rainforest as a global carbon stock and abstract from other values : direct use values e.g. timber products, indirect use value e.g. water and nutrient recycling, option and existence value, rights of the indigenous people, intrinsic value. Doing so, we could study how subsystem's idiosyncratic risk interacts with standard macroeconomic risk at the continental scale, for instance when the rainforest has other externalities such as health impacts that may affect economic growth at the continental scale. Integrating all these values is left for future research.

5 Appendix

1 Analytical decomposition - SCC

Expected utility A second-order Taylor expansion around $z := (\mathbb{E}_t(A_{t+1}), \mathbb{E}_t(T_{t+1}))$ writes :

$$\left\{ \begin{array}{l} \mathbb{E}_t \left(\frac{\partial U_{t+1}}{\partial T_{t+1}} \right) \approx \left. \frac{\partial U_{t+1}}{\partial T_{t+1}} \right|_z \text{ (zeroth-order)} \\ + \left. \frac{\partial^2 U_{t+1}}{\partial^2 T_{t+1}} \right|_z \mathbb{E}_t (T_{t+1} - \mathbb{E}_t(T_{t+1})) \text{ (first-order)} \\ + \left. \frac{\partial^2 U_{t+1}}{\partial T_{t+1} \partial A_{t+1}} \right|_z \mathbb{E}_t (A_{t+1} - \mathbb{E}_t(A_{t+1})) \text{ (first-order)} \\ + \frac{1}{2} \left. \frac{\partial^3 U_{t+1}}{\partial^2 T_{t+1} \partial A_{t+1}} \right|_z \mathbb{E}_t [(A_{t+1} - \mathbb{E}_t(A_{t+1})) (T_{t+1} - \mathbb{E}_t(T_{t+1}))] \text{ (second-order)} \\ + \frac{1}{2} \left. \frac{\partial^3 U_{t+1}}{\partial^2 T_{t+1} \partial A_{t+1}} \right|_z \mathbb{E}_t [(T_{t+1} - \mathbb{E}_t(T_{t+1})) (A_{t+1} - \mathbb{E}_t(A_{t+1}))] \text{ (second-order)} \\ + \frac{1}{2} \left. \frac{\partial^3 U_{t+1}}{\partial T_{t+1} \partial^2 A_{t+1}} \right|_z \mathbb{E}_t [(A_{t+1} - \mathbb{E}_t(A_{t+1})) (A_{t+1} - \mathbb{E}_t(A_{t+1}))] \text{ (second-order)} \\ + \frac{1}{2} \left. \frac{\partial^2 U_{t+1}}{\partial^3 T_{t+1}} \right|_z \mathbb{E}_t [(T_{t+1} - \mathbb{E}_t(T_{t+1})) (T_{t+1} - \mathbb{E}_t(T_{t+1}))] \text{ (second-order)} \end{array} \right. \quad (2.14)$$

The first-order terms are all zero. Indeed, the expectation passes through because the first part of each first-order term is not random as well as the zeroth-order term. The last second-order term is zero for the same reason. The second part of the first and the second second-order term correspond to $cov(T_{t+1}, A_{t+1})$. The second part of the third second-order term is $var(A_{t+1})$. That yields :

$$\mathbb{E}_t \left(\frac{\partial U_{t+1}}{\partial T_{t+1}} \frac{\partial T_{t+1}}{\partial S_{t+1}} \right) = \mathbb{E}_t \left(\frac{\partial U_{t+1}}{\partial T_{t+1}} \right) \mathbb{E}_t \left(\frac{\partial T_{t+1}}{\partial S_{t+1}} \right) + cov \left(\frac{\partial U_{t+1}}{\partial T_{t+1}}, \frac{\partial T_{t+1}}{\partial S_{t+1}} \right) \quad (2.15)$$

$$\mathbb{E}_t \left(\frac{\partial U_{t+1}}{\partial T_{t+1}} \right) \approx \left[\underbrace{\left. \frac{\partial U_{t+1}}{\partial T_{t+1}} \right|_z}_{CE} + \underbrace{\left. \frac{\partial^3 U_{t+1}}{\partial^2 T_{t+1} \partial A_{t+1}} \right|_z cov(T_{t+1}, A_{t+1}) + \frac{1}{2} \left. \frac{\partial^3 U_{t+1}}{\partial T_{t+1} \partial^2 A_{t+1}} \right|_z var(A_{t+1})}_{PC} \right] \quad (2.16)$$

We want to decompose all future components of SCCDS. Starting from equation (2.1) that defines optimal policy under expected utility. We assume that we are at the optimum and simplify notations for the expectations. There is no decay,

so that we have :

$$V_{1,t}^a = \mathbb{E}_t \left(\frac{\partial U_{t+1}}{\partial T_{t+1}} \frac{\partial T_{t+1}}{\partial S_{t+1}} \right) = \mathbb{E}_t (u'_S[c_{t+1}]) + \delta V_{1,t+1}^a V_{1,t+1}^b + \delta V_{1,t+1}^c + \delta V_{2,t+1} \quad (2.17)$$

$$V_{1,t}^a = \mathbb{E}_t (u'_S[c_{t+1}]) + \delta V_{1,t+1}^c + \delta V_{2,t+1} + \delta V_{1,t+1}^a V_{1,t+1}^b \quad (2.18)$$

Eventually advancing this equation and inserting it in itself yields :

$$V_{1,t}^a = \mathbb{E}_t (u'_S[c_{t+1}]) + \delta V_{1,t+1}^c + \delta V_{2,t+1} + \delta V_{1,t+1}^b \left(\mathbb{E}_t (u'_S[c_{t+2}]) + \delta V_{1,t+2}^c + \delta V_{2,t+2} + \delta V_{1,t+2}^a V_{1,t+2}^b \right) \quad (2.19)$$

Assuming that the shadow value of carbon concentration increase $\partial U / \partial S$ converges to 0 over our large time horizon and along an optimal path, we repeatedly advance and insert this equation in itself. Then, inserting this in equation (2.7), and repeating the operation, yields equation (2.9) that includes all future components.

Smooth ambiguity One can extend the conclusion made here under expected utility to our smooth ambiguity criterion. The SCC^{SA} and $SCCDS^{SA}$ write :

$$SCC_t^{SA} = \frac{\delta}{u'_c(c_t)} \frac{\partial V_{t+1}}{\partial T_{t+1}} \frac{\partial T_{t+1}}{\partial S_{t+1}} \quad (2.20)$$

$$SCCDS_t^{SA} = \frac{\delta}{u'_c(c_t)} a_t \mathbb{E}_{\chi_t} \left(b_t \mathbb{E}_{\pi_t} \left[d_t \left(\begin{array}{l} \text{Channels from main text} \\ \left[\frac{\partial V_{t+1}}{\partial T_{t+1}} \frac{\partial T_{t+1}}{\partial S_{t+1}} \left(1 + \frac{\partial S_{t+1}}{\partial A_{t+1}} \frac{\partial A_{t+1}}{\partial S_t} \right) \right] + \left[\frac{\partial V_{t+1}}{\partial A_{t+1}} \frac{\partial A_{t+1}}{\partial T_t} \frac{\partial T_t}{\partial S_t} \right] \end{array} \right) \right] \right) \quad (2.21)$$

where

$$a_t(x) = (u \circ h^{-1})' \mathbb{E}_{\chi_t} [(h \circ v^{-1}) \mathbb{E}_{\pi_t} (v \circ u^{-1})(x)] \quad (2.22)$$

$$b_t(x) = ((h \circ v^{-1})' \mathbb{E}_{\pi_t} (v \circ u^{-1})(x)) \quad (2.23)$$

$$d_t(x) = (v \circ u^{-1})'(x) \quad (2.24)$$

We use standard operations on expectations :

$$\left\{ \begin{array}{l} SCCDS_t^{SA} = \frac{\delta}{u'_c(c_t)} \underbrace{a_t [\mathbb{E}_{\chi_t}(b_t \mathbb{E}_{\pi_t}(d_t))] \mathbb{E}_{\chi_t, \pi_t} \left(\frac{\partial V_{t+1}}{\partial T_{t+1}} \frac{\partial T_{t+1}}{\partial S_{t+1}} \left(1 + \frac{\partial S_{t+1}}{\partial A_{t+1}} \frac{\partial A_{t+1}}{\partial S_t} \right) + \left[\frac{\partial V_{t+1}}{\partial A_{t+1}} \frac{\partial A_{t+1}}{\partial T_t} \frac{\partial T_t}{\partial S_t} \right] \right)}_{Scaling} \\ + \frac{\delta}{u'_c(c_t)} a_t cov \left[b_t \mathbb{E}_{\pi_t}(d_t); \mathbb{E}_{\pi_t} \left(\frac{\partial V_{t+1}}{\partial T_{t+1}} \frac{\partial T_{t+1}}{\partial S_{t+1}} \left(1 + \frac{\partial S_{t+1}}{\partial A_{t+1}} \frac{\partial A_{t+1}}{\partial S_t} \right) + \left[\frac{\partial V_{t+1}}{\partial A_{t+1}} \frac{\partial A_{t+1}}{\partial T_t} \frac{\partial T_t}{\partial S_t} \right] \right) \right] \\ \qquad \qquad \qquad \text{Temporal resolution of uncertainty (TRU}_t\text{)} \\ + \frac{\delta}{u'_c(c_t)} a_t \mathbb{E}_{\chi_t} \underbrace{\left[b_t cov \left(d_t; \frac{\partial V_{t+1}}{\partial T_{t+1}} \frac{\partial T_{t+1}}{\partial S_{t+1}} \left(1 + \frac{\partial S_{t+1}}{\partial A_{t+1}} \frac{\partial A_{t+1}}{\partial S_t} \right) + \left[\frac{\partial V_{t+1}}{\partial A_{t+1}} \frac{\partial A_{t+1}}{\partial T_t} \frac{\partial T_t}{\partial S_t} \right] \right) \right]}_{Temporal resolution of risk (TRR}_t\text{)} \end{array} \right. \quad (2.25)$$

In other words, the channel derived under expected utility is scaled with :

$$a_t \mathbb{E}_{\chi_t} (b_t \mathbb{E}_{\pi_t}(d_t)) = \underbrace{\left(\mathbb{E}_{\chi_t} \left[\mathbb{E}_{\pi_t} ((1 - \theta) V_{t+1})^{\frac{1-\gamma}{1-\theta}} \right]^{\frac{1-\mu}{1-\gamma}} \right)^{\frac{\mu-\theta}{1-\mu}}}_{a_t} \mathbb{E}_{\chi_t} \left[\underbrace{\left(\mathbb{E}_{\pi_t} [(1 - \theta) V_{t+1}]^{\frac{1-\gamma}{1-\theta}} \right)^{\frac{\gamma-\mu}{1-\gamma}}}_{b_t} \underbrace{\mathbb{E}_{\pi_t} ([1 - \theta] V_{t+1})^{\frac{\theta-\gamma}{1-\theta}}}_{d_t} \right] \quad (2.26)$$

The scaling does not affect the relative magnitude of the channels derived in equation (2.9) but the concave transformation increases the SCCDS. Thus, the conclusion made under expected utility on the relative magnitude of insurance in optimal policy applies under the smooth ambiguity criterion. Note that the scaling equals one when $\mu = \eta = \gamma$, which yields expected utility. It is well known that the dynamic models of ambiguity aversion yield timing nonindifference (Strzalecki, 2013), i.e. preference for the timing of resolution of risk and preference for the timing of resolution of uncertainty. The second line of equation (2.25) is the preference for temporal resolution of uncertainty and writes :

$$TRU_t = \left(\mathbb{E}_{\chi_t} \left[\mathbb{E}_{\pi_t} ((1 - \theta) V_{t+1})^{\frac{1-\gamma}{1-\theta}} \right]^{\frac{1-\mu}{1-\gamma}} \right)^{\frac{\mu-\theta}{1-\mu}} cov \left((\mathbb{E}_{\pi_t} [(1 - \theta) V_{t+1}]^{\frac{1-\gamma}{1-\theta}})^{\frac{\gamma-\mu}{1-\gamma}} \mathbb{E}_{\pi_t} ([1 - \theta] V_{t+1})^{\frac{\theta-\gamma}{1-\theta}}; \frac{\partial V_{t+1}}{\partial T_{t+1}} \frac{\partial T_{t+1}}{\partial S_{t+1}} \left(1 + \frac{\partial S_{t+1}}{\partial A_{t+1}} \frac{\partial A_{t+1}}{\partial S_t} \right) + \left[\frac{\partial V_{t+1}}{\partial A_{t+1}} \frac{\partial A_{t+1}}{\partial T_t} \frac{\partial T_t}{\partial S_t} \right] \right) \quad (2.27)$$

This channel increases (decreases) the SCC^{SA} and $SCCDS^{SA}$ when $\mu \geq (\leq) \theta$, i.e. when the planner has preference for early (late) resolution of uncertainty, which is the case for all values of μ and θ explored. The third line of equation (2.25), already depicted in Lemoine and Rudik (2017) under Epstein-Zin-Weil preferences, is preference for temporal resolution of risk (see also Lemoine (2021)) and writes :

$$TRR_t = \left(\mathbb{E}_{\chi_t} \left[\mathbb{E}_{\pi_t} ((1 - \theta) V_{t+1})^{\frac{1-\gamma}{1-\theta}} \right]^{\frac{1-\mu}{1-\gamma}} \right)^{\frac{\mu-\theta}{1-\mu}} \cdot \mathbb{E}_{\chi_t} \left[\left(\mathbb{E}_{\pi_t} [(1 - \theta) V_{t+1}]^{\frac{1-\gamma}{1-\theta}} \right)^{\frac{\gamma-\mu}{1-\gamma}} \cdot cov \left(([1 - \theta] V_{t+1})^{\frac{\theta-\gamma}{1-\theta}}, \frac{\partial V_{t+1}}{\partial T_{t+1}} \frac{\partial T_{t+1}}{\partial S_{t+1}} \left(1 + \frac{\partial S_{t+1}}{\partial A_{t+1}} \frac{\partial A_{t+1}}{\partial S_t} \right) + \left[\frac{\partial V_{t+1}}{\partial A_{t+1}} \frac{\partial A_{t+1}}{\partial T_t} \frac{\partial T_t}{\partial S_t} \right] \right) \right] \quad (2.28)$$

This channel increases (decreases) the SCC^{SA} and $SCCDS^{SA}$ when $\gamma \geq (\leq) \theta$, i.e. when the planner has preference for early (late) resolution of risk, which is the

case for all values of γ and θ explored here.

2 Analytical decomposition - SCDS

Smooth ambiguity Under this social choice criterion, the $SCDS_t^{SA}$ writes :

$$SCDS_t^{SA} = \frac{\delta}{u'_c(c_t)} a_t \mathbb{E}_{\chi_t} \left(b_t \mathbb{E}_{\pi_t} \left[d_t \left(\underbrace{\left(\frac{\partial V_{t+1}}{\partial T_{t+1}} \frac{\partial T_{t+1}}{\partial S_{t+1}} \frac{\partial S_{t+1}}{\partial A_{t+1}} \right)}_{\text{Channels from main text}} + \mathbb{E}_t \left(\frac{\partial V_{t+1}}{\partial A_{t+1}} \right) \right] \right) \right] \quad (2.29)$$

The same interpretation as equation (2.25) above applies to the $SCDS_t^{SA}$.

3 Resolution of the model

Simplicial Chebyshev Approximation. We use a simplicial complete Chebyshev approximation in the three-dimensional state space. Denote a d -dimensional hyperrectangle state space $[\mathbf{x}_{min}, \mathbf{x}_{max}]$ as $\{\mathbf{x} = (x_1, \dots, x_d) : x_{min,j} \leq x_j \leq x_{max,j}, j = 1, \dots, d\}$ with $d = 3$ and where $\mathbf{x}_{min,j}$ and $\mathbf{x}_{max,j}$ are lower and upper bounds of state variable x_j . The state variables are A, T and K (from which Y can be deduced). The time-dependent approximation space is defined around a deterministic growth path derived from Ramsey formula. This adaptive grid allows to use fewer collocation points than on a standard hyperrectangle grid. We do not use a complete Chebyshev approximation as it assumes symmetric approximation in each dimension. In our multidimensional problem, the value functions have higher curvature in the forest and temperature dimensions because of the feedback effect, while savings rate is fixed and capital dynamics smooth : we use degree-3, degree-4, degree-6 interpolation for capital, temperature and Amazon respectively. We do not have a proper kink so we do not use adaptive sparse grids ([Brumm and Scheidegger, 2017](#)) and stick to a tensor product grid that can handle our curvature. The approximation writes :

$$\hat{V}(\mathbf{x}, \mathbf{b}) = \sum_{\alpha \geq 0, \sum_{j=1}^d \alpha_j / n_j \leq 1} b_\alpha \Phi_\alpha(\mathbf{x}) \quad (2.30)$$

where n_j is the maximal degree in dimension j and Φ the product of one-dimensional Chebyshev basis functions $\tau_{\alpha_i}(Z_i(x_i)) = \cos(\alpha_i \cos^{-1}(Z_i(x_i)))$ where we have that

$Z_j(x_j) = \frac{2x_j - x_{max,j} - x_{min,j}}{x_{max,j} - x_{min,j}}$ for $j = 1, \dots, d$. Φ writes :

$$\Phi_\alpha(\mathbf{x}) = \prod_{i=1}^d \tau_{\alpha_i}(Z_i(x_i)) \quad (2.31)$$

Chebyshev nodes To get a not-overfitted approximation, the number of nodes, m , should not be less than the number of unknown coefficients, b_α . Choosing tensor-grids may lead to another level of curse of dimensionality. We chose Chebyshev nodes and let $m_j = n_j + 1$, so that the number of grids in dimension j is equal to one plus the maximal degree of Chebyshev approximation in dimension j . For our d -dimensional problem in the state space $[x_{min}, x_{max}]$, there are $m_1 * m_2 * \dots * m_d$ approximation nodes with the tensor grid and the values of Chebyshev nodes in dimension j are :

$$x_{i,j} = (z_{i,j} + 1)(x_{max,j} - x_{min,j})/2 + x_{min,j} \quad (2.32)$$

with $z_{i,j} = -\cos((2i - 1)\pi/(2m_j))$ for $i = 1, \dots, m_j$. Furthermore, we break the ‘curse-of-dimensionality’ on tensor grids using CPU parallel computing as the interpolation can be done independently between the different approximation nodes.

Terminal value The calculation is done on a finite horizon ($T = 500$ years) as an approximation of the infinite program. The terminal value is defined as the sum of all the period utilities from time T to infinity. The assumption made is that the consumption will grow for a constant capital per efficient capita and total abatement, with a deterministic path for the capital derived from Ramsey. The terminal constraint uses a modified discount factor ([Barr and Manne, 1967](#)). The choice of the terminal value does not affect the program : a 10% increase in the terminal value does not significantly affect the optimal path. It writes :

$$TVF = \left(\frac{1 - t_{step}}{1 - \delta(1 + g)^\theta} \right)^{\frac{1}{\theta}} u(\bar{c}) \quad (2.33)$$

with \bar{c} the consumption for constant capital per efficient capita and total abatement, δ the discount rate, g the growth rate of labour productivity from the last period, t_{step} the time step, θ the marginal utility parameter. Under uncertainty aversion, we assume that all uncertainty is solved at the end of our time horizon.

Bellman functions Starting from the social choice criterion from [Berger et al.](#)

(2017), we define Bellman functions to solve this dynamic program, $V_t = u(U_t)$:

$$V_t(x_t, \epsilon_t) = \max_{y_t} (1 - \delta)u(x_t, y_t) + \delta f[V_{t+1}(x_{t+1}, \tilde{\epsilon}_{t+1})] \quad (2.34)$$

where f accounts for the decision maker's attitude towards intertemporal substitution, uncertainty, and risk : $f(V_{t+1}) = u \circ h^{-1} [\mathbb{E}_{\chi_t} (h \circ v^{-1} \mathbb{E}_{\pi_{z,t}} [v \circ u^{-1}(V_{t+1})])]$, i.e. :

$$f(V_{t+1}) = \left[\mathbb{E}_{\chi_t} \left(\mathbb{E}_{\pi_{z,t}} [V_{t+1}]^{\frac{1-\gamma}{1-\eta}} \right)^{\frac{1-\mu}{1-\gamma}} \right]^{\frac{1-\eta}{1-\mu}} \quad (2.35)$$

4 Procedure for the calibration

We use deforestation rates from [Aguiar et al. \(2016\)](#) : ($\text{km}^2 / \text{year}$) decreasing to 3900 (2020) then to 1000 (2025) and stabilizing until 2050 (scenario A), decreasing to 3900 (2020) and stabilizing until 2050 (scenario B), increasing to 15000 (2020) and stabilizing until 2050 (scenario C). The calibration of our dynamics is a two-step procedure. First, we calibrate externally the maximum impact of local temperature changes on tree carbon losses through droughts $\bar{\epsilon}$. We use projections from climate models at a fine spatial resolution to derive a relationship between changes in local temperatures and changes in a drought index over the Amazon basin, the maximum cumulative water deficit (MCWD) anomaly with respect to an historical baseline. We use past observations to derive a link between MCWD and carbon losses. Then, we calibrate the whole distribution of $\bar{\epsilon}$ within the support $[0; \bar{\epsilon}]$ internally so that the dynamics of our system matches the expert assessments from [Kriegler et al. \(2009\)](#) on a possible tipping point. A taste of the uncertainty between models appear on the graph below :

5 Calibration

1 External calibration

Step 1 - Prepare and match datasets We use an Amazon shapefile ([Silva-Souza and Souza, 2020](#)) at a $0.5^\circ \times 0.5^\circ$ spatial resolution and calculate for each cell the MCWD anomaly observed along three representative concentration pathways (RCPs 2.6, 6.0, 8.5) in comparison with the historical baseline (1984-2004 as in [Phillips et al. \(2009\)](#)). We use projections from climate models taken from the Inter-Sectoral Impact Model Intercomparison (ISIMIP) for local precipitations and temperatures. For each RCP, we use fixed year-2005 land use, nitrogen depo-

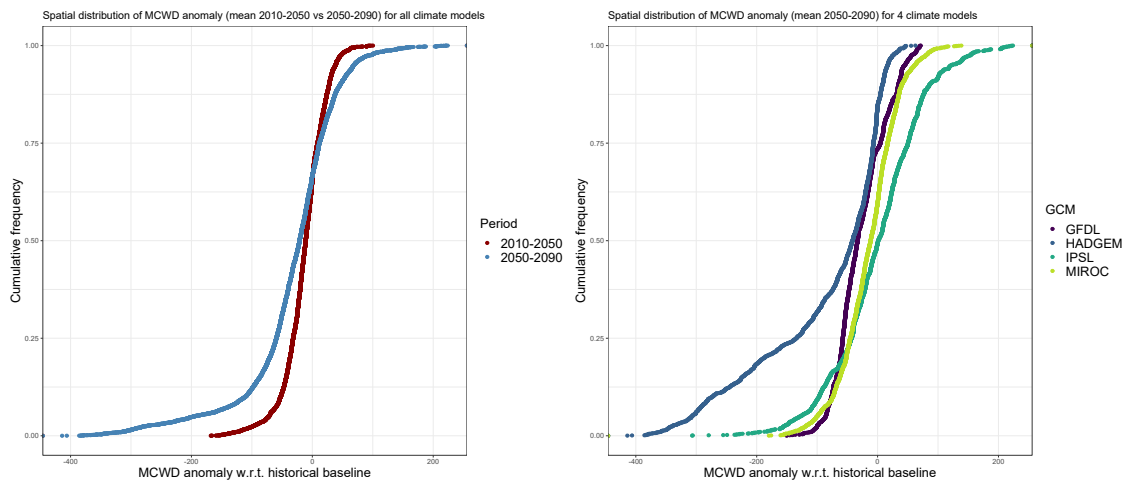


FIGURE 2.17 – Spatial cumulative distribution at 0.5° resolution of maximum cumulative water deficit anomaly with respect to historical baseline for RCP 8.5 over the Amazon rainforest. **Left** shows that over all climate models, the average MCWD anomaly shifts to more extreme and frequent droughts from 2010-2050 to 2050-2090. **Right** shows how the distribution of average MCWD anomaly over 2050-2090 depends on the climate model used

sition and fertilizer input to avoid double counting of human direct influences on the forest, as we already take into account deforestation and degradation. We use the estimates taken from one type of model : the hydrological model MATSIRO. We use all climate impact models available as the main climate uncertainty on future droughts stems from the differences between these models : GFDL-ESM2M, HadGEM2-ES, IPSL-CM5A-LR, MIROC5. Two other types of models could be used : dynamic global vegetation models and land surface models. But we do not have RCP trajectories for the dynamic global vegetation model and we do not have historical baseline for CLM45 : we would have to use fixed-2005 socioeconomic scenarios for the historical baseline. Furthermore, land-surface models are not appropriate for the study of the impact of droughts on the rainforest and the vegetation models assume fixed tree mortality while we want to use historical data (Phillips et al., 2009) to describe the link between droughts and carbon losses.

We transform precipitation data from $\text{kg/m}^{-2}/\text{s}^{-1}$ to mm^2/month . With P the precipitation level in mm^2/month , the cumulative water deficit (CWD) writes⁶ (Papastefanou et al., 2020), with m the months, k the grid cells ($m = 1, \dots, 12$) and i

6. A fixed value for evapotranspiration (ET) of 100 mm per month is used. When monthly rainfall is below 100 mm, the forest is under water deficit.

the climate model used :

$$CWD_{k,m,i} = CWD_{k,m-1,i,RCP} + P_{k,m,i} - 100 \text{ if } P_{k,m,i,RCP} < 100 \quad (2.36)$$

$$CWD_{k,m,i} = 0 \text{ if } P_{k,m,i} > 100 \text{ and } CWD_{k,0,i} = 0 \quad (2.37)$$

We calculate MCWD for each year (y) from october n to september n+1 for each cell k. We have : $MCWD_{k,y,RCP,i} = \min(CWD_{k,m,RCP,i})$, $m = 1, \dots, 12$. We obtain the MCWD anomaly, in comparison with the mean values taken from the baseline calculated at the cell level : $MCWD_{k,y,RCP,i}^{anomaly} = MCWD_{k,y,RCP,i} - MCWD_{k,RCP,i}^{baseline}$. We use local surface temperature data from all climate impact models along the three RCP and match it to the data on MCWD anomaly at the pixel level. We calculate the mean average local surface temperature from october n to september n+1. We translate the MCWD anomaly to carbon losses. We take observations from previous literature ([Phillips et al., 2009](#)) to derive a simple link c ($c \approx 0.05$ tC/ha/y/mm² MCWD anomaly) between yearly MCWD anomaly (in mm²) and the carbon losses observed (in tC / ha / year). The carbon losses observed depend on the size of the pixel, but the difference in size is minor (< 3%) and we focus on the difference in carbon stored. We take data from EarthData (NASA) for the carbon storage spatial heterogeneity ([Baccini et al., 2012](#)). We scale each C_i by the ratio of the carbon stock of this pixel i to the mean of the carbon stock in every pixel to take into account heterogeneity in the distribution of carbon stored.

Step 2 - Econometrics model selection and tests We have a balanced panel dataset with yearly projections of carbon losses and local temperatures from october 2006 to september 2099 ($T=93$) for each location (N depends on the climate impact model used but overall, $N \gg T$). The basic OLS regression model does not consider heterogeneity across locations or across years. We use fixed effects models as the Durbin-Wu-Hausman test is rejected for each model : while the fixed effect specification has a cost in terms of degrees of freedom, using random effects modelling would come with the too heavy assumption that the unobserved heterogeneity of the model is not correlated with the regressors. We check if time fixed effects are needed with Lagrange multiplier tests and F test : we reject the null hypothesis and add $T-1$ (to avoid perfect multicollinearity) time fixed effects to our fixed effects panel specification. Our specification limits the probability of coefficients being driven by omitted variables. We do not differentiate the data as stationarity is not a problem in our panel dataset with time fixed effects and $N \gg T$. We are not preoccupied by simultaneity as local tempe-

ratures are mainly driven by global cumulative emissions stock as long as the vegetation cover is not fully depleted. We test homoskedasticity and serial correlation with Breusch-Pagan and Breusch-Godfrey lagrange multipliers tests. We reject the null hypothesis and find evidence of heteroskedasticity and serial correlation : we might use robust covariance matrix estimators à la White for our standard errors but first need to test for cross-sectional dependence with Pesaran's and Breusch-Pagan's tests. As expected (spatial data), we reject the null hypothesis that residuals are not correlated so that there is cross-sectional dependence in each model, which might bias our coefficients. Furthermore, we use [Driscoll and Kraay \(1998\)](#) standard errors to account for this dependence structure. We also add regional fixed effects to account for heterogeneity in the vegetation. We use [Silva-Souza and Souza \(2020\)](#) woody plant regionalization into 13 subregions based on k-means partitioning. Let C be the carbon losses (in tC / ha / y), X the local temperature at the pixel level, u the error term, i the notation for our geo-coded entity, t the notation for time, r the [Silva-Souza and Souza \(2020\)](#) subregions. β is our coefficient of interest, α , δ and ζ vectors of location, time and region fixed effects respectively. We estimate the following :

$$C_{i,r,t}^j = \beta^j X_{i,r,t}^j + \alpha_i^j + \delta_t^j + \zeta_r^j + u_{i,r,t}^j \quad (2.38)$$

We have our coefficients of interest $\hat{\beta}^j$ for each model j that gives how a 1°C increase in local temperature translates into a change in carbon stored (in tC / ha / year).

Specification	Climate model	Coefficient	Standard Errors [robust]	t-value [robust]
FE	HADGEM	-1.1271	0.0031 [0.0226]	-365.806 [-49.8816]
	GFDL	-2.7006	0.0056 [0.025]	-484.8025 [-108.1676]
	IPSL	-0.4885	0.0043 [0.0133]	-114.0374 [-36.7257]
	MIROC	-1.1996	0.0036 [0.0225]	-332.0498 [-53.2061]
FE & year FE	HADGEM	-1.4039	0.0048 [0.0288]	-293.4842 [-48.7659]
	GFDL	-3.0708	0.0067 [0.0262]	-454.942 [-117.3824]
	IPSL	-0.7977	0.007 [0.0204]	-113.5831 [-39.1795]
	MIROC	-1.6436	0.0049 [0.0311]	-335.25 [-52.9338]
FE & regional FE	HADGEM	-1.1271	0.0031 [0.0563]	-365.806 [-20.0358]
	GFDL	-2.7006	0.0056 [0.1559]	-484.8025 [-17.3256]
	IPSL	-0.4885	0.0043 [0.1107]	-114.0374 [-4.4126]
	MIROC	-1.1996	0.0036 [0.0892]	-332.0498 [-13.45]
FE, year & regional FE	HADGEM	-1.4039	0.0048 [0.0048]	-293.4842 [-293.4842]
	GFDL	-3.0708	0.0067 [0.0067]	-454.942 [-454.942]
	IPSL	-0.7977	0.007 [0.007]	-113.5831 [-113.5831]
	MIROC	-1.6436	0.0049 [0.0049]	-335.25 [-335.25]

We multiply this coefficient by the size (≈ 705 million ha) of the forest ([Souza-Rodrigues, 2019](#)) and by the number of years per period (5 years) and express it as a share of the carbon stored in the forest at initial time that can be lost (75GtC ([Armstrong McKay et al., 2022](#))). This coefficient gives the upper bound of the

mean additional share of carbon stored in the rainforest that is released per period because of droughts for a one degree increase in local temperature in climate model j . Our coefficients ϵ_j are taken from observations of the 2005 drought (Phillips et al., 2009), one of the most severe droughts observed over the Amazon so far. Thus, we assume that $\bar{\epsilon}_j$ are higher estimates of the possible impact of droughts. We assume that on a given period, the impact of droughts on the carbon storage follows a beta distribution of unknown parameters α_s and β_s with support $[0 : \bar{\epsilon}_j]$.

2 Internal calibration

Data processing We use expert assessments from Kriegler et al. (2009) to calibrate our global dynamics : we calibrate the growth rate g_0 , the feedback effect Y and the parameters α_s and β_s of the beta distribution of stochastic droughts $\tilde{\epsilon}$ to recover the same probabilities of tipping along three RCP. We want to make sure that our dynamic system is approximately in line with these expert elicitations. In the low temperature corridor, the central weighted estimate from core experts in Kriegler et al. (2009) is a probability of 24% of tipping. In the medium temperature corridor, their central estimate is a probability of 49% of tipping. In the high temperature corridor, the central estimate is a probability of 67%. The temperature corridors used by Kriegler et al. (2009) are wide, and we assume fair approximations for their ‘low’, ‘medium’ and ‘high’ temperature corridors are the Shared Socioeconomic Pathways SSP4-3.4, SSP4-6.0, SSP5-8.5. These SSP are available in IPCC AR6 (Smith et al., 2021) : more specifically, we use extended SSP as we need data until 2200. The data is available as effective radiative forcing (in $\text{W} \cdot \text{m}^{-2}$) time series. We use a simple two-layers box model described in IPCC AR6 (Smith et al., 2021) to translate this data to global average surface temperature :

$$C \frac{d}{dt} \Delta T = \Delta F(t) + \alpha \Delta T - \epsilon \gamma (\Delta T - \Delta T_d) \quad (2.39)$$

$$C_d \frac{d}{dt} \Delta T_d = \gamma (\Delta T - \Delta T_d) \quad (2.40)$$

where ΔT ($^{\circ}\text{C}$) is the temperature change of the surface components of the climate system, ΔT_d ($^{\circ}\text{C}$) is the temperature change in the deep ocean layer, C and C_d are the effective heat capacities for the surface and deep layers, ϵ is the efficacy of the deep ocean heat uptake and γ is the heat transfer coefficient between the surface and deep layer. We use the central estimates from IPCC for the key parameters

and abstract from uncertainty on these parameters⁷. We use Leduc et al. (2016) regional transient climate response to cumulative emissions (2.0°C per TtC over the Amazon basin) and the IPCC (Masson-Delmotte et al., 2021) best estimate for global transient climate response to cumulative emissions (1.65°C per TtC) to have a simple mapping from global to regional temperature.

Jointly calibrate the parameters and distribution of ϵ Reasonable ranges for Y , the temperature difference between bare soil and forest, range from 3.98 (forest-to-pasture) to 7.06 (forest-to-cropland) in Silvério et al. (2015). Ritchie et al. (2021) use 5. The Beta distribution is chosen so that the expected value of the mean yearly drought impact over a period is between one half and one fifth of the value of the impact calibrated from the 2005 extreme drought in Phillips et al. (2009). Furthermore, we assume α_s and β_s below 1 to model situations where observations are either close to the upper bound or the lower bound and intermediate values are less likely. This seems reasonable as these extreme droughts seem to occur every five years as observed in the past twenty years, either associated with positive sea surface temperature anomalies in the tropical Atlantic (2005, 2010) or with strong El Niño events (1997/98, 2015/16). Ritchie et al. (2021) use a perturbation rate of 0.2 and a growth rate of 2 so we keep the ratio constant with our perturbation rate ϵ to seek values for which the dynamics fits with experts views. Using the inverse of the cumulative distribution function of our beta distribution of unknown shape α_s and β_s , we give the values of ϵ_{low} , ϵ_{medium} and ϵ_{high} that corresponds to the expert probabilities. Then, along the three SSP4-3.4, 4-6.0, 5-8.5, we calibrate g_0 , Y , α_s , and β_s , so that in 2200, the dynamic system experiences a dieback for $\epsilon_{low} + \delta$ (same for ϵ_{medium} and ϵ_{high}) but no dieback for $\epsilon_{low} - \delta$ (same for ϵ_{medium} and ϵ_{high}), with $\delta \pm 1\%$. There is a large, potentially infinite number of solutions. Arbitrarily, coefficients are taken to one decimal only and find the ensemble of combinations for which the criteria for convergence are respected. We pick one of the combinations. Our central estimate is : $g_0 = 0.49$, $\alpha_s = 0.36$, $\beta_s = 0.32$, $Y = 6$. The distribution for ϵ is given in Figure 2.18 :

7. $C = 8.1 \pm 1 \text{ W.yr.m}^{-2} \text{ }^{\circ}\text{C}^{-1}$, $C_d = 110 \pm 63 \text{ W.m}^{-2} \text{ }^{\circ}\text{C}^{-1}$, $\gamma = 0.62 \pm 0.13 \text{ W.m}^{-2} \text{ }^{\circ}\text{C}^{-1}$, $\epsilon = 1.34 \pm 0.41$, $\alpha = -1.33 \pm 0.5$. We calculate the cumulated sum starting from 1750.

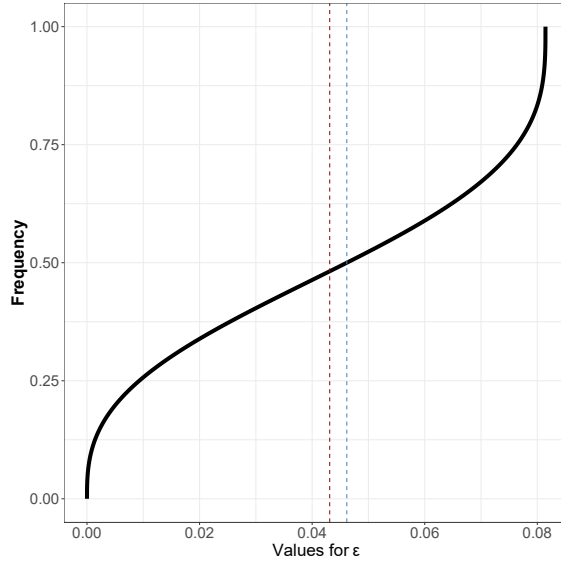


FIGURE 2.18 – Cumulative distribution function of $\tilde{\epsilon}$ with red mean $\mathbb{E}(\epsilon) \approx 0.0431$ and blue median $\mathbb{P}(\epsilon > 0.0462) = 50\%$.

6 Consistency of the coefficients

We run a simulation (1000 paths) of our dynamics for the carbon stored in the rainforest, including all the perturbations, along various extended concentration pathways in Figure (2.19). We give the mean total carbon net losses (in GtC) for different temperature increases (in $^{\circ}\text{C}$), with (left) and without (middle) the tipping risk. Finally, we give the same path but under the assumption made in our model that, as there is scientific uncertainty, there is a 50% chance of tipping risk (right). After 2200, we assume that the carbon stored in the forest remains constant : the carbon losses are permanent. In our model, there is no SSP (even the most extreme one) for which there is a dieback of the rainforest before 2100 under deforestation and degradation scenarii.

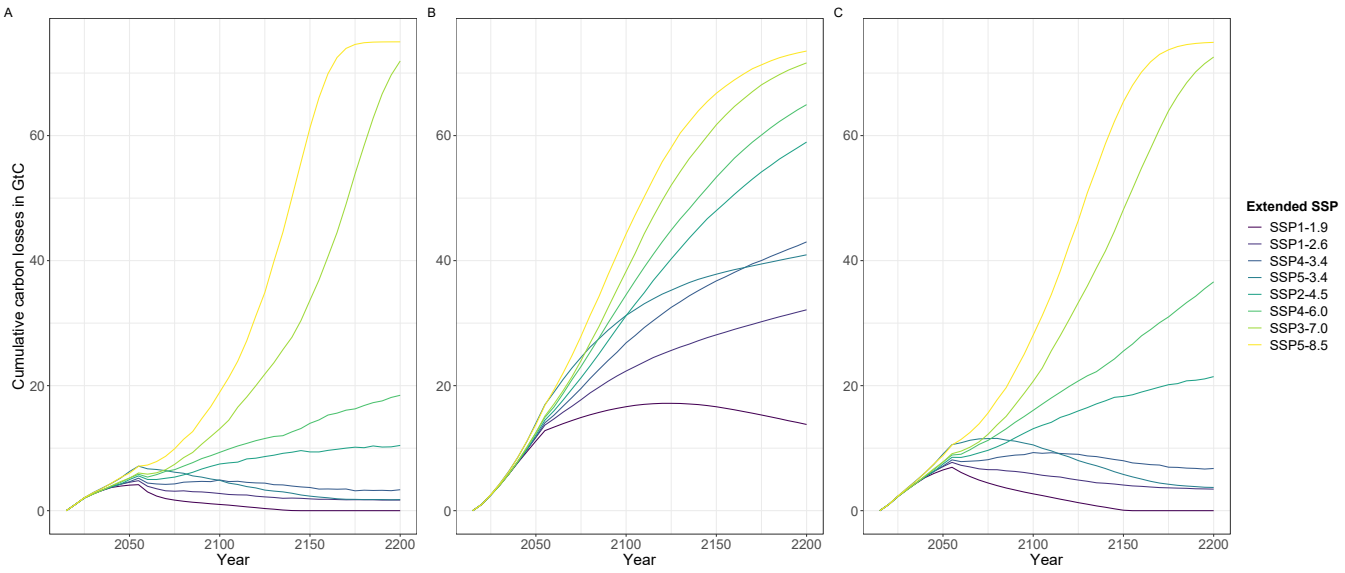


FIGURE 2.19 – Time horizon Mean cumulative carbon losses (in GtC) from the Amazon rainforest along various extended concentration pathways (in °C) from 2000 to 2200 under no tipping risk (A), a tipping risk (B), and in our model (C).

We give the phase diagrams of our dynamic system under no tipping risk and under a tipping risk. The diagrams give for various values of the stochastic impact of temperatures on the dynamics of the rainforest ϵ , over time, and for different scenarios, the change in forest cover with respect to initial period. A dieback of the forest occurs by 2200 only for carbon-intensive scenarios that are usually not optimal (so, these scenarios will not occur in our optimized framework), for a tipping risk, and for large values of the impact of global temperatures on the dynamics of the rainforest.

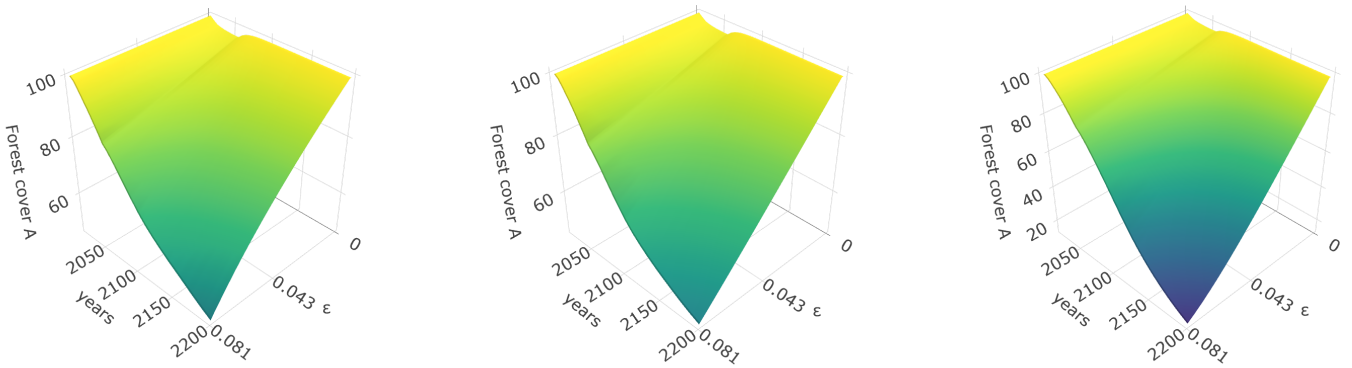


FIGURE 2.20 – Phase diagram. Dynamics of the forest under no tipping risk for various ϵ and for a low, medium and a high temperature corridor. $E(\epsilon) \approx 0.0431$ and $P(\epsilon > 0.0462) = 50\%$.

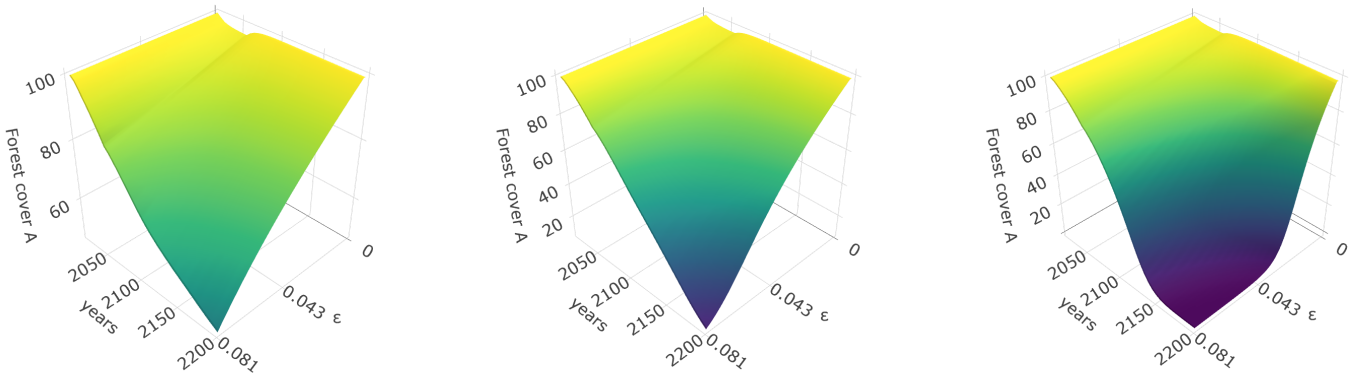


FIGURE 2.21 – Phase diagram. Dynamics of the forest under a tipping risk, i.e. $Y \neq 0$, for various $\tilde{\epsilon}$ and for a low, medium and a high temperature corridor. $E(\epsilon) \approx 0.0431$ and $P(\epsilon > 0.0462) = 50\%$.

7 Stochastic paths for some variables of interest

We plot the distribution of stochastic paths until 2100 for temperature increases, forest stock, abatement rate, from our optimized programs under expected utility. The bold line gives the mean of 100 stochastic paths (gray area are for 5% and 95% paths). Specification 1 is the benchmark, with aggregate climate risk over transient response to cumulative emissions, but no explicit representation of the amazon rainforest. Specification 2 is the first counterfactual, where there is aggregate climate risk and an explicit representation of the amazon rainforest. Specification 3 is the second counterfactual, where there is both aggregate climate risk and idiosyncratic risk over the dynamics of the rainforest.

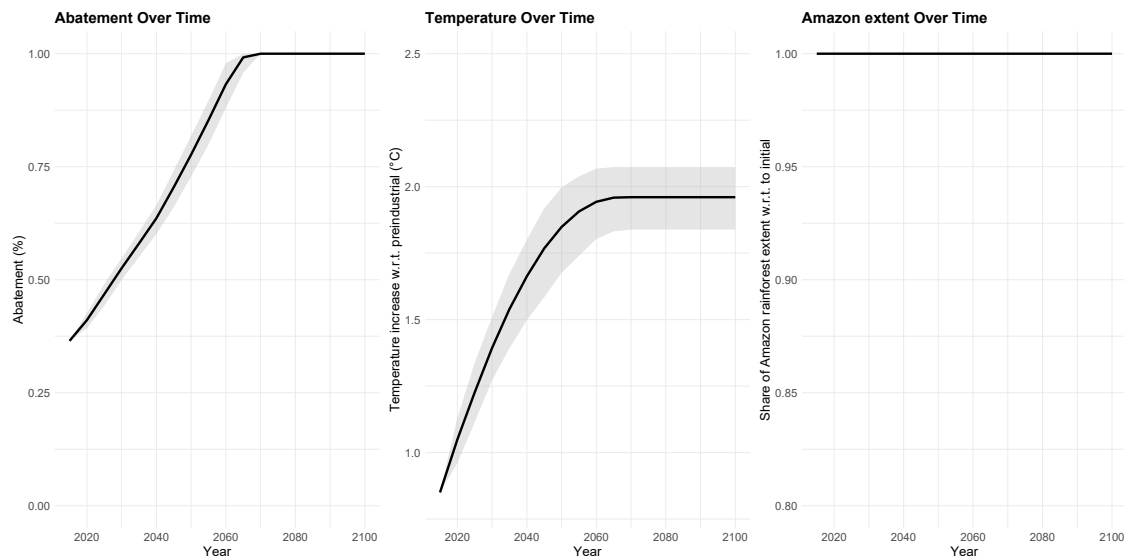


FIGURE 2.22 – Stochastic optimized paths under aggregate climate risk, without endogenous amazon dynamics.

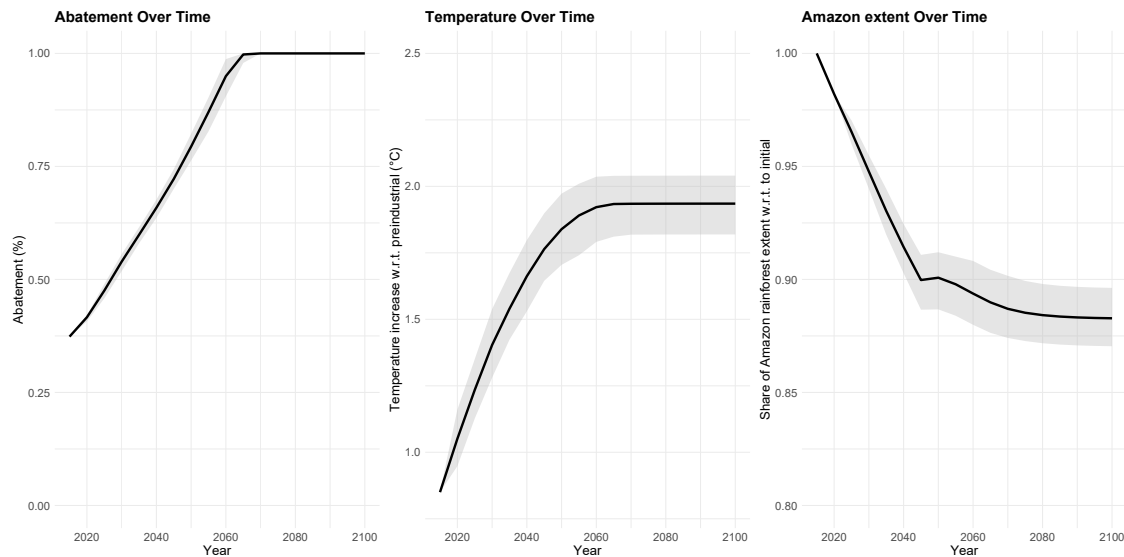


FIGURE 2.23 – Stochastic optimized paths under aggregate climate risk, with endogenous amazon dynamics, without amazon idiosyncratic risk.

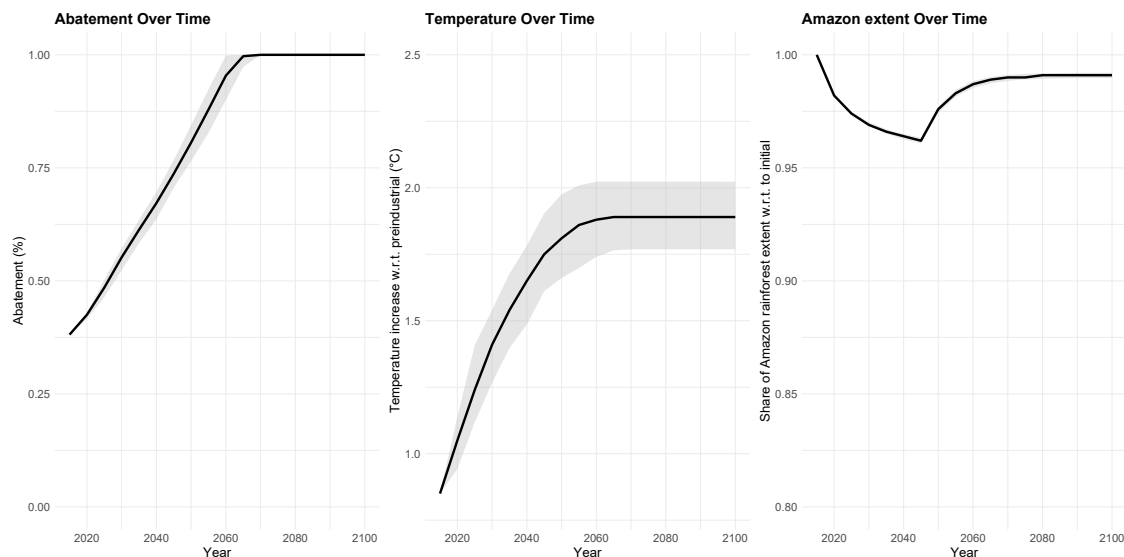


FIGURE 2.24 – Stochastic optimized paths under aggregate climate risk, with endogenous amazon dynamics, with amazon idiosyncratic risk.

Bibliographie

- E. P. Agency. Report on the social cost of greenhouse gases : Estimates incorporating recent scientific advances, 2022.
- A. P. D. Aguiar, I. C. G. Vieira, T. O. Assis, E. L. Dalla-Nora, P. M. Toledo, R. A. Oliveira Santos-Junior, M. Batistella, A. S. Coelho, E. K. Savaget, L. E. O. C. Aragão, et al. Land use change emission scenarios : anticipating a forest transition process in the brazilian amazon. *Global change biology*, 22(5) :1821–1840, 2016.
- L. O. Anderson, G. Ribeiro Neto, A. P. Cunha, M. G. Fonseca, Y. Mendes de Moura, R. Dalagnol, F. H. Wagner, and L. E. O. e. C. de Aragão. Vulnerability of amazonian forests to repeated droughts. *Philosophical Transactions of the Royal Society B : Biological Sciences*, 373(1760) :20170411, 2018.
- R. Araujo, F. Costa, and M. Sant'Anna. Efficient forestation in the brazilian amazon : Evidence from a dynamic model. 2020.
- D. I. Armstrong McKay, A. Staal, J. F. Abrams, R. Winkelmann, B. Sakschewski, S. Loriani, I. Fetzer, S. E. Cornell, J. Rockström, and T. M. Lenton. Exceeding 1.5 c global warming could trigger multiple climate tipping points. *Science*, 377(6611) :eabn7950, 2022.
- A. Baccini, S. Goetz, W. Walker, N. Laporte, M. Sun, D. Sulla-Menashe, J. Hackler, P. Beck, R. Du-bayah, M. Friedl, et al. Estimated carbon dioxide emissions from tropical deforestation improved by carbon-density maps. *Nature climate change*, 2(3) :182–185, 2012.
- C. Balboni, A. Berman, R. Burgess, and B. A. Olken. The economics of tropical deforestation. *Annual Review of Economics*, 15 :723–754, 2023.
- M. Barnett, W. Brock, and L. P. Hansen. Pricing uncertainty induced by climate change. *The Review of Financial Studies*, 33(3) :1024–1066, 2020.
- M. Barnett, W. Brock, and L. P. Hansen. Climate change uncertainty spillover in the macroeconomy. *NBER Macroeconomics Annual*, 36(1) :253–320, 2022.
- J. L. Barr and A. S. Manne. Numerical experiments with a finite horizon planning model. *Indian Economic Review*, 2(1) :1–31, 1967.
- L. Berger and V. Bosetti. Are policymakers ambiguity averse? *The Economic Journal*, 130(626) :331–355, 2020.
- L. Berger, J. Emmerling, and M. Tavoni. Managing catastrophic climate risks under model uncertainty aversion. *Management Science*, 63(3) :749–765, 2017.
- R. Biggs, S. R. Carpenter, and W. A. Brock. Turning back from the brink : detecting an impending regime shift in time to avert it. *Proceedings of the National academy of Sciences*, 106(3) :826–831, 2009.
- J. Brumm and S. Scheidegger. Using adaptive sparse grids to solve high-dimensional dynamic models. *Econometrica*, 85(5) :1575–1612, 2017.

- Y. Cai. Computational methods in environmental and resource economics. *Annual Review of Resource Economics*, 11(1) :59–82, 2019.
- Y. Cai and T. S. Lontzek. The social cost of carbon with economic and climate risks. *Journal of Political Economy*, 127(6) :2684–2734, 2019.
- Y. Cai, T. M. Lenton, and T. S. Lontzek. Risk of multiple interacting tipping points should encourage rapid co2 emission reduction. *Nature Climate Change*, 6(5) :520–525, 2016.
- S. Dietz and F. Venmans. Cumulative carbon emissions and economic policy : in search of general principles. *Journal of Environmental Economics and Management*, 96 :108–129, 2019.
- S. Dietz, C. Gollier, and L. Kessler. The climate beta. *Journal of Environmental Economics and Management*, 87 :258–274, 2018.
- S. Dietz, J. Rising, T. Stoerk, and G. Wagner. Economic impacts of tipping points in the climate system. *Proceedings of the National Academy of Sciences*, 118(34) :e2103081118, 2021a.
- S. Dietz, F. van der Ploeg, A. Rezai, and F. Venmans. Are economists getting climate dynamics right and does it matter? *Journal of the Association of Environmental and Resource Economists*, 8 (5) :895–921, 2021b.
- C. E. Doughty, J. M. Keany, B. C. Wiebe, C. Rey-Sanchez, K. R. Carter, K. B. Middleby, A. W. Cheesman, M. L. Goulden, H. R. da Rocha, S. D. Miller, et al. Tropical forests are approaching critical temperature thresholds. *Nature*, pages 1–7, 2023.
- J. C. Driscoll and A. C. Kraay. Consistent covariance matrix estimation with spatially dependent panel data. *Review of economics and statistics*, 80(4) :549–560, 1998.
- D. Ellsberg. Risk, ambiguity, and the savage axioms. *The quarterly journal of economics*, pages 643–669, 1961.
- R. Fillon, C. Guivarch, and N. Taconet. Optimal climate policy under tipping risk and temporal risk aversion. *Journal of Environmental Economics and Management*, 121 :102850, 2023.
- B. M. Flores, E. Montoya, B. Sakschewski, N. Nascimento, A. Staal, R. A. Betts, C. Levis, D. M. Lapola, A. Esquivel-Muelbert, C. Jakovac, et al. Critical transitions in the amazon forest system. *Nature*, 626(7999) :555–564, 2024.
- D. Folini, F. Kübler, A. Malova, and S. Scheidegger. The climate in climate economics. *Review of Economic Studies*, 2024.
- P. Friedlingstein, M. O’sullivan, M. W. Jones, R. M. Andrew, D. C. Bakker, J. Hauck, P. Landschützer, C. Le Quéré, I. T. Luijckx, G. P. Peters, et al. Global carbon budget 2023. *Earth System Science Data*, 15(12) :5301–5369, 2023.
- M. Golosov, J. Hassler, P. Krusell, and A. Tsivinski. Optimal taxes on fossil fuel in general equilibrium. *Econometrica*, 82(1) :41–88, 2014.
- C. Guivarch and A. Pottier. Climate damage on production or on growth : what impact on the social cost of carbon? *Environmental Modeling & Assessment*, 23(2) :117–130, 2018.

- L. Hansen and T. J. Sargent. Robust control and model uncertainty. *American Economic Review*, 91(2) :60–66, 2001.
- T. Hayashi and J. Miao. Intertemporal substitution and recursive smooth ambiguity preferences. *Theoretical Economics*, 6(3) :423–472, 2011.
- H. Hong, N. Wang, and J. Yang. Mitigating disaster risks in the age of climate change. *Econometrica*, 91(5) :1763–1802, 2023.
- A. Hsiao. Coordination and commitment in international climate action : evidence from palm oil. *Job market paper*, 2021.
- Y. Izhakian. A theoretical foundation of ambiguity measurement. *Journal of Economic Theory*, 187 :105001, 2020.
- N. Ju and J. Miao. Ambiguity, learning, and asset returns. *Econometrica*, 80(2) :559–591, 2012.
- S. Keen, T. M. Lenton, T. J. Garrett, J. W. Rae, B. P. Hanley, and M. Grasselli. Estimates of economic and environmental damages from tipping points cannot be reconciled with the scientific literature. *Proceedings of the National Academy of Sciences*, 119(21) :e2117308119, 2022.
- C. Kent, R. Chadwick, and D. P. Rowell. Understanding uncertainties in future projections of seasonal tropical precipitation. *Journal of Climate*, 28(11) :4390–4413, 2015.
- P. Klibanoff, M. Marinacci, and S. Mukerji. A smooth model of decision making under ambiguity. *Econometrica*, 73(6) :1849–1892, 2005.
- E. Kriegler, J. W. Hall, H. Held, R. Dawson, and H. J. Schellnhuber. Imprecise probability assessment of tipping points in the climate system. *Proceedings of the national Academy of Sciences*, 106(13) :5041–5046, 2009.
- M. Leduc, H. D. Matthews, and R. de Elía. Regional estimates of the transient climate response to cumulative co₂ emissions. *Nature Climate Change*, 6(5) :474–478, 2016.
- D. Lemoine. The climate risk premium : how uncertainty affects the social cost of carbon. *Journal of the Association of Environmental and Resource Economists*, 8(1) :27–57, 2021.
- D. Lemoine and I. Rudik. Managing climate change under uncertainty : Recursive integrated assessment at an inflection point. *Annual Review of Resource Economics*, 9(1) :117–142, 2017.
- D. Lemoine and C. Traeger. Watch your step : optimal policy in a tipping climate. *American Economic Journal : Economic Policy*, 6(1) :137–66, 2014.
- S. Levin, T. Xepapadeas, A.-S. Crépin, J. Norberg, A. De Zeeuw, C. Folke, T. Hughes, K. Arrow, S. Barrett, G. Daily, et al. Social-ecological systems as complex adaptive systems : modeling and policy implications. *Environment and development economics*, 18(2) :111–132, 2013.
- T. E. Lovejoy and C. Nobre. Amazon tipping point : Last chance for action, 2019.
- R. E. Lucas Jr. Asset prices in an exchange economy. *Econometrica : journal of the Econometric Society*, pages 1429–1445, 1978.

- Y. Malhi, D. Wood, T. R. Baker, J. Wright, O. L. Phillips, T. Cochrane, P. Meir, J. Chave, S. Almeida, L. Arroyo, et al. The regional variation of aboveground live biomass in old-growth amazonian forests. *Global Change Biology*, 12(7) :1107–1138, 2006.
- V. Masson-Delmotte, P. Zhai, A. Pirani, S. L. Connors, C. Péan, S. Berger, N. Caud, Y. Chen, L. Goldfarb, M. Gomis, et al. Climate change 2021 : the physical science basis. *Contribution of working group I to the sixth assessment report of the intergovernmental panel on climate change*, 2, 2021.
- E. A. T. Matricardi, D. L. Skole, O. B. Costa, M. A. Pedlowski, J. H. Samek, and E. P. Miguel. Long-term forest degradation surpasses deforestation in the brazilian amazon. *Science*, 369(6509) : 1378–1382, 2020.
- A. Millner, S. Dietz, and G. Heal. Scientific ambiguity and climate policy. *Environmental and Resource Economics*, 55(1) :21–46, 2013.
- W. Nordhaus. Evolution of modeling of the economics of global warming : changes in the dice model, 1992–2017. *Climatic change*, 148(4) :623–640, 2018.
- W. Nordhaus. Economics of the disintegration of the greenland ice sheet. *Proceedings of the National Academy of Sciences*, 116(25) :12261–12269, 2019.
- P. Papastefanou, C. S. Zang, Z. Angelov, A. A. de Castro, J. C. Jimenez, L. F. C. De Rezende, R. Russica, B. Sakschewski, A. Sörensson, K. Thonicke, et al. Quantifying the spatial extent and intensity of recent extreme drought events in the amazon rainforest and their impacts on the carbon cycle. *Biogeosciences Discussions*, pages 1–37, 2020.
- O. L. Phillips, L. E. Aragão, S. L. Lewis, J. B. Fisher, J. Lloyd, G. López-González, Y. Malhi, A. Monteagudo, J. Peacock, C. A. Quesada, et al. Drought sensitivity of the amazon rainforest. *Science*, 323(5919) :1344–1347, 2009.
- P. D. Ritchie, J. J. Clarke, P. M. Cox, and C. Huntingford. Overshooting tipping point thresholds in a changing climate. *Nature*, 592(7855) :517–523, 2021.
- I. Rudik. Optimal climate policy when damages are unknown. *American Economic Journal : Economic Policy*, 12(2) :340–73, 2020.
- B. Sakschewski, W. Von Bloh, A. Boit, L. Poorter, M. Peña-Claros, J. Heinke, J. Joshi, and K. Thonicke. Resilience of amazon forests emerges from plant trait diversity. *Nature climate change*, 6 (11) :1032–1036, 2016.
- M. Scheffer, J. Bascompte, W. A. Brock, V. Brovkin, S. R. Carpenter, V. Dakos, H. Held, E. H. Van Nes, M. Rietkerk, and G. Sugihara. Early-warning signals for critical transitions. *Nature*, 461(7260) :53–59, 2009.
- K. J. Silva-Souza and A. F. Souza. Woody plant subregions of the amazon forest. *Journal of Ecology*, 108(6) :2321–2335, 2020.

- D. V. Silvério, P. M. Brando, M. N. Macedo, P. S. Beck, M. Bustamante, and M. T. Coe. Agricultural expansion dominates climate changes in southeastern amazonia : the overlooked non-ghg forcing. *Environmental Research Letters*, 10(10) :104015, 2015.
- C. Smith, Z. Nicholls, K. Armour, W. Collins, a. M. M. P. Forster, M. Palmer, and M. Watanabe. 2021 : The earth's energy budget, climate feedbacks, and climate sensitivity supplementary material. in climate change 2021 : The physical science basis. *Contribution of working group I to the sixth assessment report of the intergovernmental panel on climate change*, 2, 2021.
- E. Souza-Rodrigues. Deforestation in the amazon : A unified framework for estimation and policy analysis. *The Review of Economic Studies*, 86(6) :2713–2744, 2019.
- A. Staal, I. Fetzer, L. Wang-Erlandsson, J. H. Bosmans, S. C. Dekker, E. H. van Nes, J. Rockström, and O. A. Tuinenburg. Hysteresis of tropical forests in the 21st century. *Nature communications*, 11(1) :4978, 2020.
- T. Strzalecki. Temporal resolution of uncertainty and recursive models of ambiguity aversion. *Econometrica*, 81(3) :1039–1074, 2013.
- N. Taconet, C. Guivarch, and A. Pottier. Social cost of carbon under stochastic tipping points. *Environmental and Resource Economics*, 78(4) :709–737, 2021.
- T. S. Van den Bremer and F. Van der Ploeg. The risk-adjusted carbon price. *American Economic Review*, 111(9) :2782–2810, 2021.
- Y. Yao, P. Ciais, N. Viovy, E. Joetzjer, and J. Chave. How drought events during the last century have impacted biomass carbon in amazonian rainforests. *Global Change Biology*, 2022.
- D. Zemp, C.-F. Schleussner, H. Barbosa, and A. Rammig. Deforestation effects on amazon forest resilience. *Geophysical Research Letters*, 44(12) :6182–6190, 2017a.
- D. C. Zemp, C.-F. Schleussner, H. M. Barbosa, M. Hirota, V. Montade, G. Sampaio, A. Staal, L. Wang-Erlandsson, and A. Rammig. Self-amplified amazon forest loss due to vegetation-atmosphere feedbacks. *Nature communications*, 8(1) :1–10, 2017b.

Chapitre 3

Climate shift uncertainty and economic damages

This working paper^a is a joint work with Manuel Lisenmeier (Princeton University, HMEI) and Gernot Wagner (Columbia University, CBS).

Focusing on global annual averages of climatic variables, as in the standard damage function approach, can bias aggregate and distributional estimates of the economic impacts of climate change. Here we empirically estimate global and regional dose-response functions of GDP growth rates to daily mean temperature levels and combine them with regional climate projections of daily mean temperatures. We disentangle for various shared socio-economic pathways (SSPs) how much of the missing impacts are due to heterogeneous warming versus heterogeneous damage patterns over space and time. Global damages in 2050 are around 25% higher when accounting for the shift in the shape of the entire intra-annual distribution of daily mean temperatures at the regional scale.

Keywords : damage functions, climate risk, uncertainty, climate shift, temporal and spatial disaggregation, temperature downscaling.

JEL : Q54.

^a. Romain Fillon thanks the Fulbright Program (France) for funding his research stay at Columbia University. The authors thank François Bareille, Adrien Delahais, Célia Escribe, Radley Horton, Adam Sobel and especially Kevin Schwarzwald for fruitful comments on earlier versions of this work. Computations were performed on the Columbia University Research Grid. Corresponding author : Romain Fillon.

1 Introduction

Knowing how future climate damages might be distributed in time and space is a key research frontier and policy issue for climate scientists, economists, and decision-makers. Projections of endogenous climate damages in macroeconomic models ([Fernández-Villaverde et al., 2024](#)) typically rely on reduced-form relationships between climate change and the macroeconomy, which are generally based on *annual* climatic statistics—e.g. mean annual temperatures. Furthermore, models are generally aggregated for that climate variable to be *global*—mean annual global temperatures. In these integrated climate-economy models, carbon emissions are a by-product of regional economic activities. A reduced-form climate module then allows to capture how these carbon emissions turn into global annual mean temperature anomaly, from which regional annual mean temperature anomaly can be down-scaled through a simple linear and time-invariant factor; a process also called pattern scaling. The regional physical impacts are then interacted with dose-response functions estimated on global data to measure the economic impacts of endogenous climate change. These macroeconomic models are either global ([Nordhaus, 1994](#)), regional ([Nordhaus and Yang, 1996](#)) or gridded, as in the burgeoning spatial integrated assessment modelling (IAM) literature ([Desmet and Rossi-Hansberg, 2024](#)), e.g. [Krusell and Smith Jr \(2022\)](#) and [Cruz and Rossi-Hansberg \(2024\)](#).

The underlying assumption behind these approaches is that the shapes of the spatio-temporal distributions of mean temperatures do not matter. First, with regard to the temporal dimension, the intra-annual shape of the distribution of daily mean temperature is assumed to remain constant : temperature increases due to climate change are shape-preserving increases in annual mean. Second, regarding the spatial dimension, an average increase in temperature at global level is assumed to affect the regional annual distribution by a linear and time-invariant down-scaling factor such as the regional transient response to cumulative emissions ([Leduc et al., 2016](#)). The reality of future regional weather changes, however, seems more complex, for two main reasons. First, natural climate variability over time and space, both from external (e.g. solar cycles) and internal factors (e.g. El Niño-La Niña), might distort future temperature distributions beyond the annual mean ([Schwarzwald and Lenssen, 2022](#)). Second and more fundamentally, the process determining the shape of the weather distribution within a given year for a given regional mean temperature might not be stationary, so that time-invariant relations between annual averages and the intra-annual distribution of

weather only imperfectly reflect regional-specific shifts in warming patterns. In North-West Europe, for example, hottest summer days are warming twice as fast as mean summer days ([García-León et al., 2021](#); [Patterson, 2023](#)). That opens the question around the ‘right’ level of spatial and temporal aggregation for projecting future impacts. Aggregation has advantages, as it comes with statistical robustness, clear identification of causal relationships, and tractability in models where anomaly in climate results from endogenous anthropogenic emissions; it also has shortcomings, such as the risk of averaging contradictory effects between regions both in terms of damage and warming patterns.

In parallel to integrated assessment models with endogenous climate change stemming from anthropogenic carbon emissions, some integrated assessment models use exogenous global circulation model projections to infer the costs of climate change with adapting agents, e.g. spatial IAM such as [Bilal and Rossi-Hansberg \(2023\)](#) and [Rudik et al. \(2022\)](#). In these models, which incorporate credible climate projections, climate change remains exogenous to economic activities. As a result, the estimates from the two bodies of literature, i.e. endogenous and exogenous, evolve in parallel, yet the effects of this divergence on the aggregate and distributional estimates of climate impacts remain unclear. Our paper aims to shed light on this gap. Indeed, our paper tests the impact of two separate (but related) limitations of many existing studies : the effect of separately fitting models by region on the initial dose response function, and the effect of including regional climate change and projections that sample changes in the entire distribution on future projections using those dose response functions. To disentangle these effects, we here follow a two-step approach. First, we switch from annual average temperatures to the complete daily temperature distribution over a year and show how this affects the heterogeneous distribution of warming patterns between regions, compared to a setting where we assume a shape-preserving shift in mean annual temperatures under a synthetic changing climate. Second, we interact these regional-specific shifts in warming patterns with regional-specific damage patterns, in comparison with a setting where we assume homogeneous damage patterns at the global scale. Indeed, when disaggregating to regional levels, economists often use global damage functions, instead of using estimates from regional-specific damage patterns. Meanwhile, it seems intuitive that a hot day in a relatively warm country has a different impact than the same day in a cold country; [Heutel et al. \(2021\)](#) show this to be the case for U.S. counties. Alongside efforts to measure the non-linear effects of temperature on economic activity, for example with temperature bins ([Dell et al., 2014](#);

[Hsiang, 2016](#); [Auffhammer, 2018](#)), we measure regional dose response functions, to capture some of the regional idiosyncrasies in the climate-society relation. We focus on a physical idiosyncrasy and estimate regional dose-response functions for each aggregate Köppen-Geiger climatic zone : arid, continental, polar, temperate, tropical.

These debates over the spatio-temporal aggregation of climate projections might have important consequences, not only for establishing our best approximation of future damage and reconciling different approaches, but also in quantifying the uncertainty surrounding this best guess. Uncertainties in climate-economic modelling abound ([Rising et al., 2022](#); [Kotz et al., 2023](#)). The quantifiable variance of future projections of climate impacts is affected by scenario uncertainty (differences in Shared Socioeconomic Pathways - SSPs), model uncertainty (differences in Earth System Models - ESM - responses to the SSPs), internal variability (spatiotemporally, due to the chaotic nature of the climate and due to regional differences that may be hidden by regional aggregation), any choices made in post-processing or bias-correcting ESM output (including how finely to apply projected changes in climate distributions from ESMs), in addition to regression uncertainty from the dose-response functions, and differences between observational data products used to fit the dose-response function and act as a baseline to which future ESM output is compared. Historically, many studies use global annual average climate variables to estimate and project climate damages, thereby ignoring an important source of internal variability stemming from regional differences in climate states and from only extracting mean changes from ESM projections. Among all uncertainties, we focus on two uncertainties and their interaction : the sensitivity of economic impact projections to an improved sampling of internal variability (through capturing regional differences in impacts) and an improved treatment of ESM output (by capturing changes in the full shape of the temperature distribution instead of annual averages). We take part in uncovering some of the model uncertainties between ESM using the whole shape of warming patterns that is usually reduced by the aggregation procedure on a global and annual scale. We provide a framework based on temperature distributions that can be applied to other climate data, for instance precipitation or maximum temperatures, and a quantification to show how much the regional-specific shift in the shape of warming patterns interacting with regional-specific damage patterns matter empirically, both at the aggregate level and in the distribution of impacts, with the year 2050 as a case study.

Our work yields two main conclusions. First, switching from annual global

mean temperature to the regional annual distribution of daily mean temperatures affects the magnitude of the estimates of economic damages : in 2050, using regional damage patterns interacted with the shift in the whole shape of the distribution of daily temperatures yields climate damage at the global scale that are around 25% larger than the damage obtained under the assumption of homogeneous damage patterns over the world and a shape-preserving shift in annual mean daily temperature. Standard aggregation comes with underestimation of future climate damages. This result holds for a variety of more or less carbo-intensive SSPs : SSP1-2.6, SSP3-7.0 and SSP5-8.5. Second, we show that the distributional effect is not clear-cut. Uncertainty in the change in the shape of the temperature distributions affects all regions of the world in a heterogeneous way, but is particularly strong in continental areas. This result is important for standard climate change adaptation modelled in spatial integrated assessment models. Indeed, they project that adaptation through migration to some regions ([Cruz and Rossi-Hansberg, 2024](#)) or greater agricultural output in these regions through structural change ([Conte et al., 2021](#)) might reduce the aggregate welfare impacts of climate change and have large distributional implications, with many benefits shifting to the northern hemisphere. The benefits of adaptation to mitigate the aggregate welfare costs of climate change could therefore be overestimated if the regions to which people migrate and where more agricultural output is produced are continental climatic zones, which is the case.

2 Climate and economic data

1 Warming patterns

We compare the distribution of daily mean temperatures in actual climate projections to a counter-factual synthetic projection where the shape of the distribution remains the same while the mean annual temperature increases, a standard assumption in the literature. We build different climate landscapes, where ‘climate’ is defined as the underlying distribution, from which a specific regional temperature distribution over a year is drawn ([Waidelich et al., 2023](#)). We use CMIP6 bias-corrected and downscaled data at a resolution of 60 arc-minutes from five earth system models (ESM) stored in ISIMIP Protocol 3B ([Frieler et al., 2023](#)) : GFDL-ESM4, IPSL-CM6A-LR, MPI-ESM1-2-HR, MPI-ESM2-0, UKESM1-0-LL. ISIMIP subset of climate models and de-biasing techniques were designed to assess impacts of climate change and to span the larger ensemble of CMIP mo-

odels ([Warszawski et al., 2014](#)). Thus, our illustrative study underestimates inter-model uncertainty among the over 100 CMIP6 models. Data is available for three shared socioeconomic pathways (SSP 1-2.6, 3-7.0, 5-8.5). We construct four different climate landscapes for each SSP. The first is the climate landscape without climate change, the ‘control’ climate : it is the mean distribution of ‘picontrol’ time series experiments run over 2006 to 2100 with pre-industrial CO₂ concentration. The second is the landscape from actual climate projections which consists of bias-corrected, downscaled output from five ESMs forced with future emissions from three different SSPs, the ‘projection’ climate : we use the average of the 10-year distribution around a date to approximately capture the underlying distribution from which the specific weather realization from a specific year is drawn, i.e. 2045-2055 in our example¹. This landscape samples scenario uncertainty, inter-model uncertainty, and regionally specific changes in the shape of daily mean temperature distributions. The third climate landscape is a ‘synthetic-model’ landscape, where we add for each temperature observed in the ‘control’ climate of each of the five ESM the mean of the change in annual temperature in ‘projection’ climate in this specific ESM. This yields a ESM-specific shape-preserving mean-shifted climate. This landscape samples scenario uncertainty, inter-model uncertainty, and regional differences in mean changes, but keeps the shape of daily mean temperature distributions unchanged. The last climate landscape is a ‘synthetic-general’ landscape. The difference with the ‘synthetic-model’ approach is that we sum the mean ‘control’ climate over all ESM and the mean change in annual mean temperature across ESM. This yields a mean shape-preserving, mean-shifted climate, which aggregates heterogeneity between climate models. This landscape samples scenario uncertainty and regional differences in mean changes while aggregating across ESMs and keeping the shape of daily mean temperature distributions unchanged.

Rather than aggregating this data at the global scale, we construct regional climate landscapes. Indeed, using a global dataset means that locations in which a given temperature is relatively cold and places in which the same temperature is relatively warm in the two locations fall within the same bin of temperature, which distorts the picture of regional climate shifts, and biases the estimates used to convert these climate shifts into economic damage. We aggregate at the level

1. On the one hand, adding more years around 2050 would enable us to capture more of the internal variability which characterizes 2050 climate ([Schwarzwald and Lenssen, 2022](#)), for instance more El Niño cycles. On the other hand, it would come with a costly assumption of perfect symmetry around 2050 in climate change dynamics. By capturing less internal variability, we probably under-count the impact of including regional information.

of five major Köppen regions ([Beck et al., 2023](#)) : arid, continental, polar, temperate and tropical. It is reasonable to think that these climate classifications are both good ensembles in terms of warming patterns but also in terms of damage patterns to capture differences between relatively homogeneous regions. If the differences between damage patterns differ for many other reasons (e.g. cultural and political), we capture some of the regional heterogeneity due to climatic conditions. A finer disaggregation would reduce the statistical robustness of the estimates we obtain from our econometric specification below because of limited sample size and variation. When building these climate landscapes, we keep only locations for which we have economic data to estimate dose-response functions below and treat each of these economic region within each climatic Köppen region as a single unit.

2 Econometric estimates of climate damages

For the empirical analysis we combine [Wenz et al. \(2023\)](#)'s Database Of Sub-national Economic Output (DOSE v2) with [Hersbach et al. \(2020\)](#)'s climate reanalysis (ERA5). We process the climate reanalysis by first calculating degree-days at the grid-cell level and then aggregating to DOSE regions. We use the combined data to estimate global and regional dose-response functions of GDP growth to daily mean temperatures. We estimate the model :

$$g_{it} = \alpha_i + P_{it}\beta + \sum_{b=1}^B n_{bit}\gamma_b + \mu_t + \epsilon_{it}$$

with the growth rate of GDP per capita PPP in USD in administrative unit i in year t as g_{it} , with the number of days with daily mean temperature in the bin indexed b as n_{bit} , and with total annual precipitation P_{it} . Note that here, P_{it} is indeed only a control, focused on global annual values, rather than regionally disaggregated daily ones ([Kotz et al., 2022](#)). The model also includes region fixed effects α_i and year fixed effects μ_t . Errors ϵ_{it} are clustered at the level of countries to account for spatial and temporal autocorrelation. We estimate this model for all regions jointly and for each Köppen-Geiger climate zone k separately. Our main parameters of interest are the coefficients of temperature bins γ_b (for the global model) and γ_{bk} (for the regional models) which represent the non-linear association between daily temperature levels and economic growth. For the regional model, we use a gridded dataset on Köppen climate regions and assign to every administrative unit the share of each climatic zones it is included in based

on surface area. The 2°C temperature bins are winsorized at level 99% for econometric estimation to limit the influence of rare events for which we do not have sufficient observations. Furthermore, we follow [Cruz and Rossi-Hansberg \(2024\)](#) and smooth the behavior of the point estimates across temperature bins on the whole temperature distribution in 2050 with degree-two polynomials, assuming that temperature effect on growth changes remains constant above and below our upper and lower bins used for the estimation. We also weigh each point estimate by the inverse of their standard errors to provide a greater weight to the more accurate estimates.

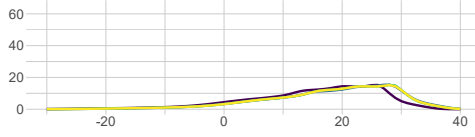
3 Descriptive statistics

We give summary statistics for the warming and damage patterns of each region in 2050 for SSP5-8.5. Graphs on the left plot the distribution of mean daily temperatures for all climate landscapes, taking the average of all five earth system models. The distributions have different shapes, both in terms of their dispersion and their mean. The shifts in the average temperature are also of different magnitude, which is consistent with the observation of spatially heterogeneous global warming. Shifts in shapes are also diverse, and not just because of the initial shape of each distribution as we show on the middle graphs. The middle graphs describe the difference between the ‘synthetic-model’ and the ‘projection’ landscapes for different earth system models : for each 1°C temperature bin, it gives the difference in frequency (in number of days) between two distributions. The first distribution is constructed by adding to each daily temperature for each climate model the mean of the annual anomaly observed in that model, thus obtaining a shape-preserving shift in mean, which is the assumption generally made in the literature. The second distribution is taken from climate model projections of daily mean temperatures. These difference can have opposite signs and various magnitude depending on the model considered. The graphs on the right present the minimum, central and maximum estimates of the two global and regional dose-response functions of GDP growth rate to an additional day in a given bin in comparison with a day in the $[20 : 22^{\circ}\text{C}]$ bin, estimated for each region. Our regional dose-response functions reveals different damage patterns than the global dose-response function. For instance, while the positive effect of colder temperatures on GDP growth in the global functions stills holds with regional estimates in the continental areas, the sign of this effect is reversed for polar and temperate areas. For warmer days, in relatively warmer areas, the effect of higher temperatures goes in both directions, i.e. positive effect for arid areas, negative effects

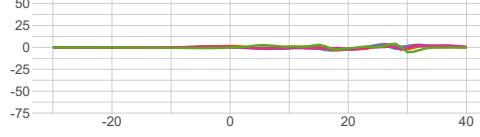
for tropical areas, while it is flat in our global estimate that conflates both climatic zones. Disentangling global and regional damage patterns matter for climate policy because it provides a more accurate picture of the spatial and temporal heterogeneity in future climate damage.

ARID

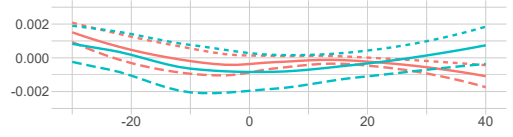
Distribution of daily mean temperatures



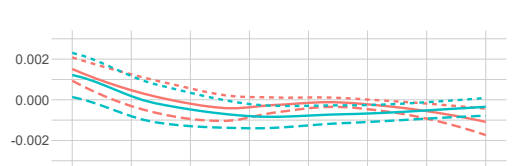
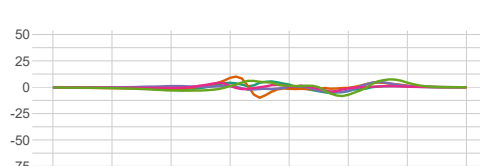
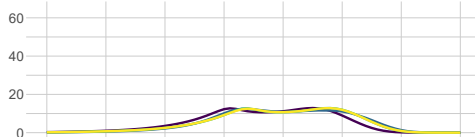
Difference in future change in distribution



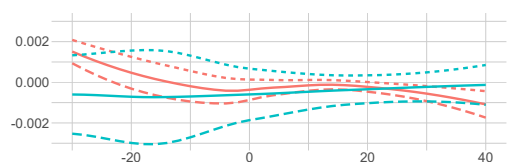
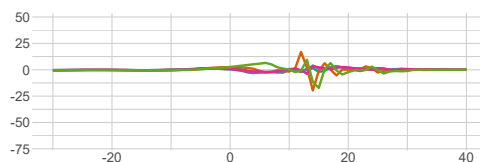
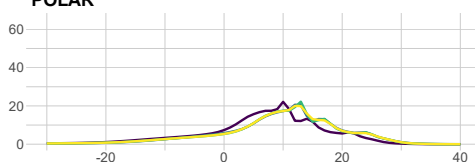
Change in growth rate relative to [20°C:22°C]



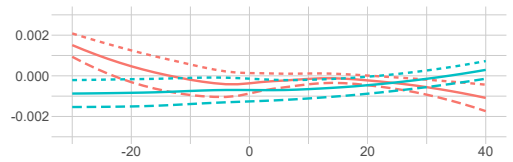
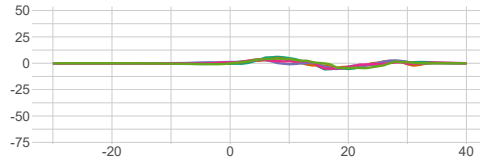
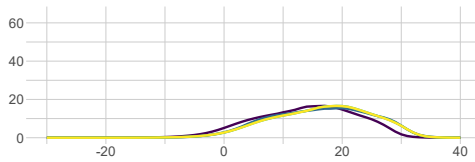
CONTINENTAL



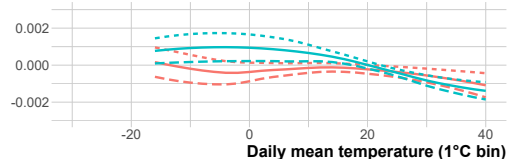
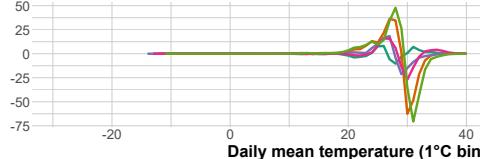
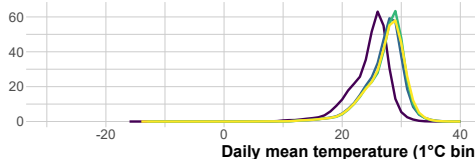
POLAR



TEMPERATE



TROPICAL



Landscape — Control — Proj. — Synth. General — Synth. Model

ESM — GFDL — IPSL — MPI — MRI — UK

Estimates — Central — Max — Min Scale — Global — Regional

FIGURE 3.1 – Left Distribution of daily mean temperatures for four climate landscapes. **Middle** Distribution of climate shift, i.e. difference in distribution of daily mean temperatures under projection vs. a synthetic-model climate. **Right** Change in growth rate from one day in this bin relative to one additional day in [20°C : 22°C].

Data are for all DOSE regions, SSP5-8.5, 2050.

3 Quantification

1 Missing shape-related growth effect of climate change

We express the GDP growth effect of daily temperatures in climate projections as a share of this effect in synthetic climate, i.e. in a setting where we assume that the shape of the distribution of daily temperatures remains the same when the mean increases. Indeed, we want to measure how much the change in the shape of the distribution of daily mean temperatures matter for the estimation of economic damages. To have a measure that approaches standard climate damages, growth effects in warming climates are expressed with respect to growth effects in control climate. Growth effect at each 1°C bin b is γ_b (γ_{bk}) if we use global (regional) dose-response functions, where k stands for a Köppen-Geiger climate zone. The global growth effect Ω for a given SSP and year in our climate landscape C for a given dose-response function in subadministrative region DOSE d in Köppen-Geiger climate zone k is :

$$\Omega_{ymd}^{glob,C} = \frac{\left(\sum_b \gamma_b t_{bymd}^C - \sum_b \gamma_b t_{bymd}^{control}\right)}{\sum_b \gamma_b t_{bymd}^{control}}, \quad \Omega_{ymdk}^{reg,C} = \frac{\left(\sum_b \gamma_{bk} t_{bymdk}^C - \sum_b \gamma_{bk} t_{bymdk}^{control}\right)}{\sum_b \gamma_{bk} t_{bymdk}^{control}}$$

Then, we apply a double difference procedure to find the change in growth effect between synthetic climate and projections. For damage function γ , and synthetic climate : $DD_{ymdk}^{\omega} = 100 * (\Omega_{ymdk}^{\omega,projection} - \Omega_{ymdk}^{\omega,synthetic}) / \Omega_{ymdk}^{\omega,synthetic}$, with $\omega \in \{\text{global}, \text{regional}\}$. This estimate expresses the share the missing shift in shape represents in the standard estimates of damages assumed from shape-preserving synthetic shift in mean. We summarize the values of this estimate for various specifications in Figure 3.2 below which disentangles various layers of uncertainty. On the top left graph, we plot the dispersion in our DD estimate for each Köppen climatic region and each SSP, for each ESM (in blue) and the average over ESM (in red). This graph captures how for each region the differences between SSP and between climate models drives the impact omitting the whole shape of warming pattern has on the assessment of damages. There is an important climate model uncertainty. Outside continental areas, depending on the climate model used, the sign of the difference between the standard assumption and the full shape of the distribution is either positive or negative. Part of this structural uncertainty between climate models is already captured when comparing climate models at the aggregate annual scale. Thus, on the top right graph, we plot the dispersion between two methods to build our synthetic climate : ei-

ther using the model-specific control climate and mean aggregate temperature increase to build the new synthetic benchmark, or using the average over different ESM. On the bottom left graph, we plot the difference in our estimates depending on the dose-response function of GDP growth to daily temperatures that is used : either the global dose-response function which combines potentially contradictory effects of changes in temperature distribution over space, or the regional estimates which might capture part of the spatial heterogeneity in damage patterns. On the bottom right graph, we plot our coefficient for the central, minimum and maximum estimates of the regional dose-response function to measure how much parametric uncertainty for a given damage function specification matters in comparison with structural uncertainty about the damage function, i.e. either global or regional. All four sources of uncertainty that are hidden under the assumption of a shape-preserving mean-shifted synthetic climate matter, especially in the continental areas.

2 Aggregate impacts

While we build regional climate landscapes that use the granularity given in climate datasets rather than too aggregated information to discuss climate policy, we seek for global indicators that can easily be applied to aggregate economic models. We compute for each DOSE region within each larger Köppen-Geiger zone the share of missing growth due to disaggregated warming and damage patterns. We use area-weighting to build DOSE-level estimates of missing growth from DOSE*Koppen estimates. We then aggregate the DOSE-level growth effect to the global scale based on the share of each zone in global GDP. We use the synthetic-model approach to build a synthetic climate, assuming that aggregate uncertainty between climate model is already taken into account in the literature studying aggregate annual mean temperatures. Indeed, our study focuses on one channel of uncertainty : the interactions between intra-annual warming patterns and damage patterns at the regional scale. On left graph in Figure 3.3, we plot our estimate of the share of missing growth effects for various ESM and the mean across ESM under regional damages. On the right graph, we plot global DD for two specifications of the dose-response function : either global or regional.

The assumption made in the literature of a shape-preserving shift in mean annual global temperature interacted with global damage patterns thus yields biased estimates of future economic damages of climate change. For all climate models and across various specifications of damage patterns and economic scenarios, this bias is an underestimation of future damages : accounting for the shift

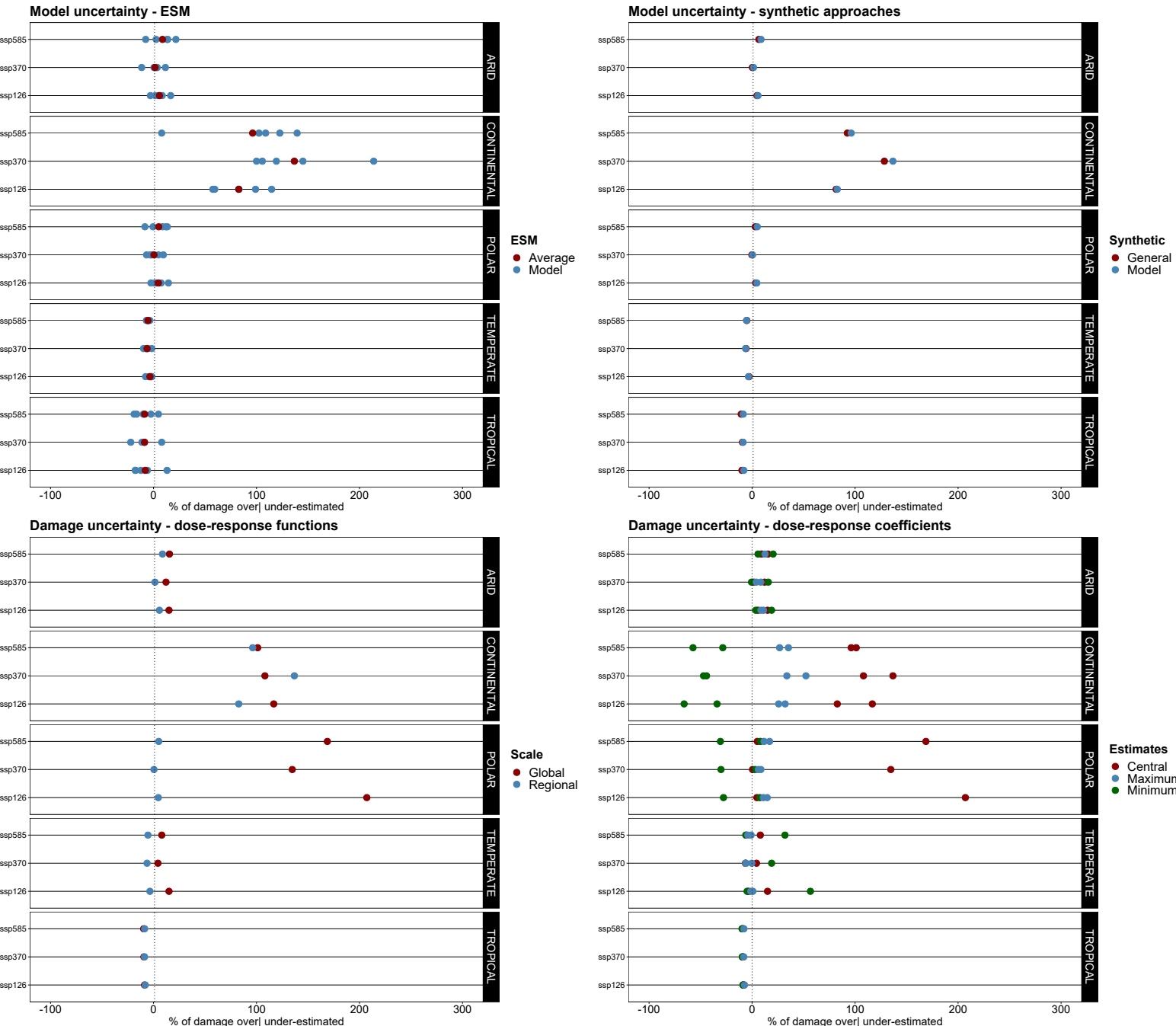


FIGURE 3.2 – Double difference DD estimates for year 2050, all SSP and climatic regions.
Left Top For each ESM vs. average, using synthetic-model and regional damage
Right Top For synthetic-model vs. synthetic-general, using regional damage, averaging over ESM
Left Bottom For global vs. regional damage, using synthetic-model, averaging over ESM
Right Bottom For central, minimum and maximum estimates of regional damage, using synthetic-model, averaging over ESM.

in regional shape would increase the actual damage by around 25% under all concentration pathways in 2050. The shift in shape matters also for less carbon-intensive pathways. Both uncertainty between climate models on the shape of

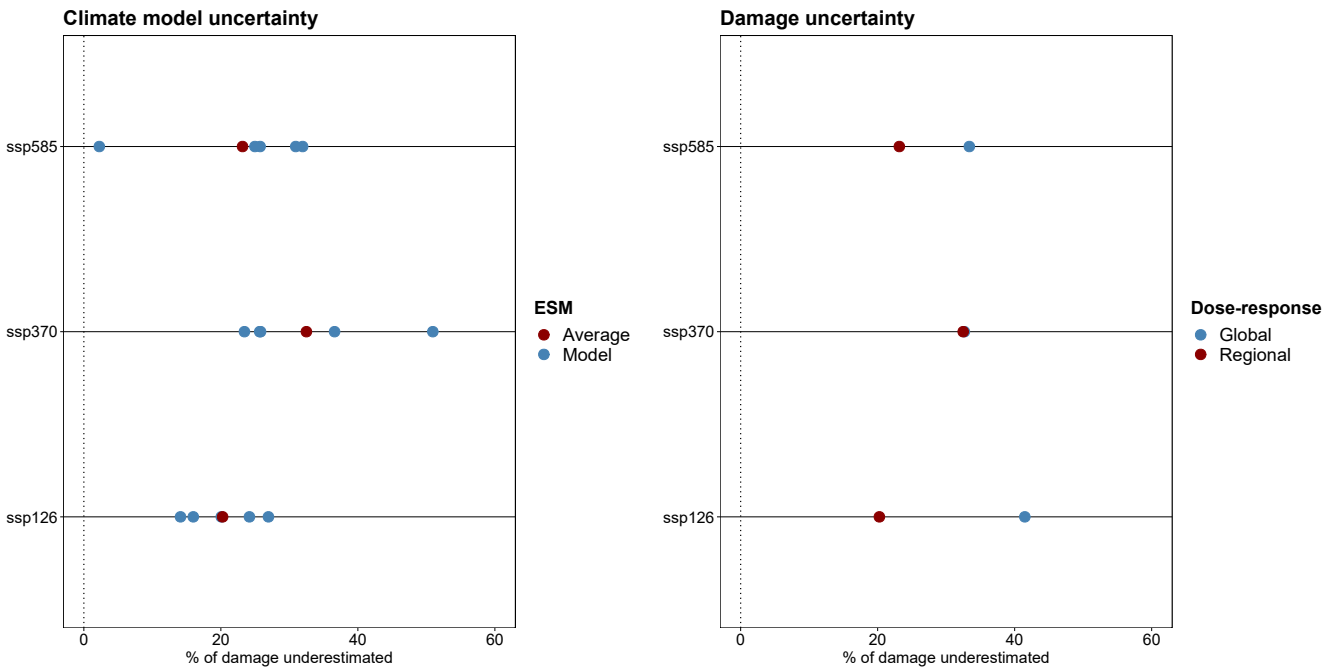


FIGURE 3.3 – **Left** Global DD under synthetic-model approach for each ESM and the average over ESM with regional dose-response function **Right** Global DD for each dose-response function, synthetic-model approach and average climate model with regional dose-response function.

regional warming patterns and uncertainty on the damage patterns matter. Their interaction is likely to significantly alter the temporal and spatial distribution of the economic damage caused by climate change. This change in the aggregate picture of climate impacts should encourage greater mitigation and adaptation. But what about the distributional effects?

3 Distributional impacts

We have focused on the aggregate impact of this omitted shift in regional daily temperature shape. Now, when we look in more detail at the distribution of damage, we see that there is no perfect correlation with income : the countries most affected by these shifts in the patterns of intra-annual weather distribution are not necessarily the poorest. In fact, the opposite is true, even if the data are widely scattered. In Figure (3.4) below, we show on the left that, for certain DOSE regions, climate impacts are in fact lower when using climate projections with intra-annual temperature distributions with regional response functions than in a synthetic approach using a mean-shifted shape-preserving climate. In particular, we show on the right graph that gives the distribution of omitted impacts for

each quantile of the 2015 distribution of DOSE regions in terms of USD GDP per capita that this applies to the poorest 20% of regions, even if the distribution is fairly skewed.

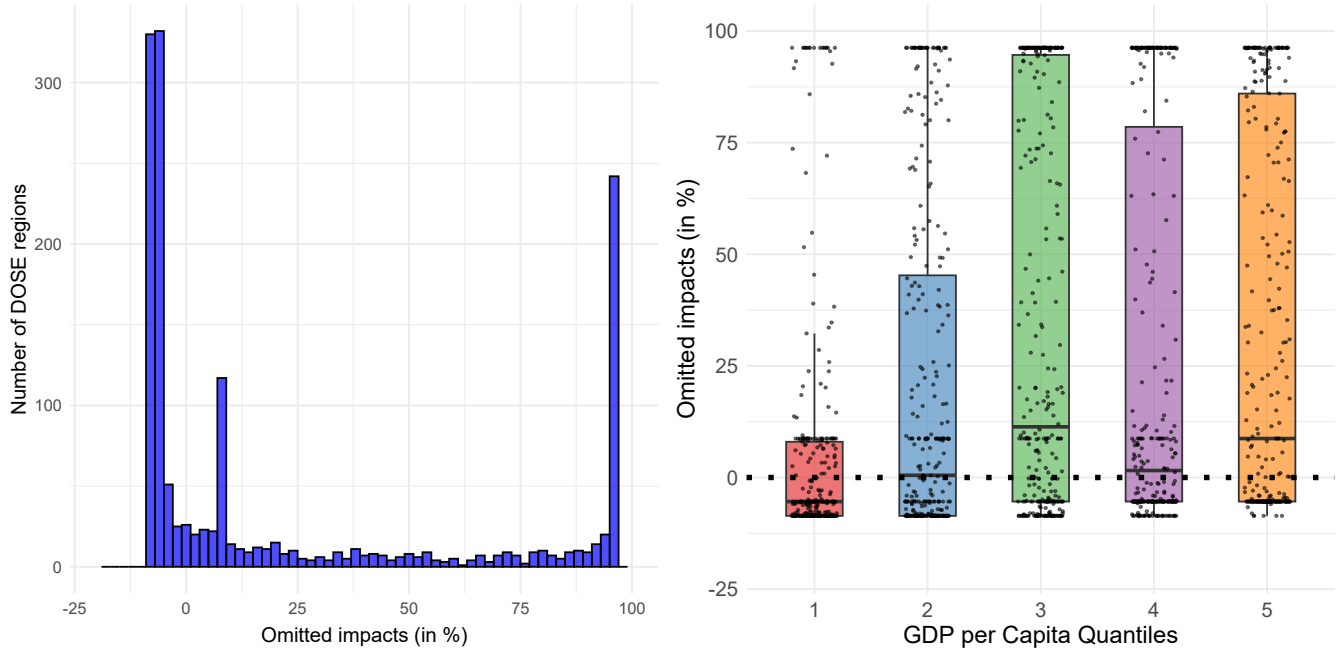


FIGURE 3.4 – Left Distribution of impacts (in % of current estimates) across DOSE regions
Right Distribution of impacts across and within 2015 USD GDP per capita quantiles of DOSE regions.

The colored bars span the interquartile range for each quantile. The black lines represent the mean for each quantile. Estimates are for year 2050, SSP5-8.5.

Uncertainty about changes in the shape of regional temperature distributions interacts with regional damage functions mainly concerning continental regions, as we show on Figure (3.5), in line with estimates from Figure (3.5). This is particularly important if less significant impacts are expected in these regions, notably on agricultural productivity, but also on regional amenities, which could justify adaptations that reduce the total cost of climate change. The welfare benefit of these adaptations would be particularly reduced if it turns out that these regions have very significant welfare changes : impacts on growth up to 100% higher than estimates based on global dose-responses interacted with shape-preserving projected climates.

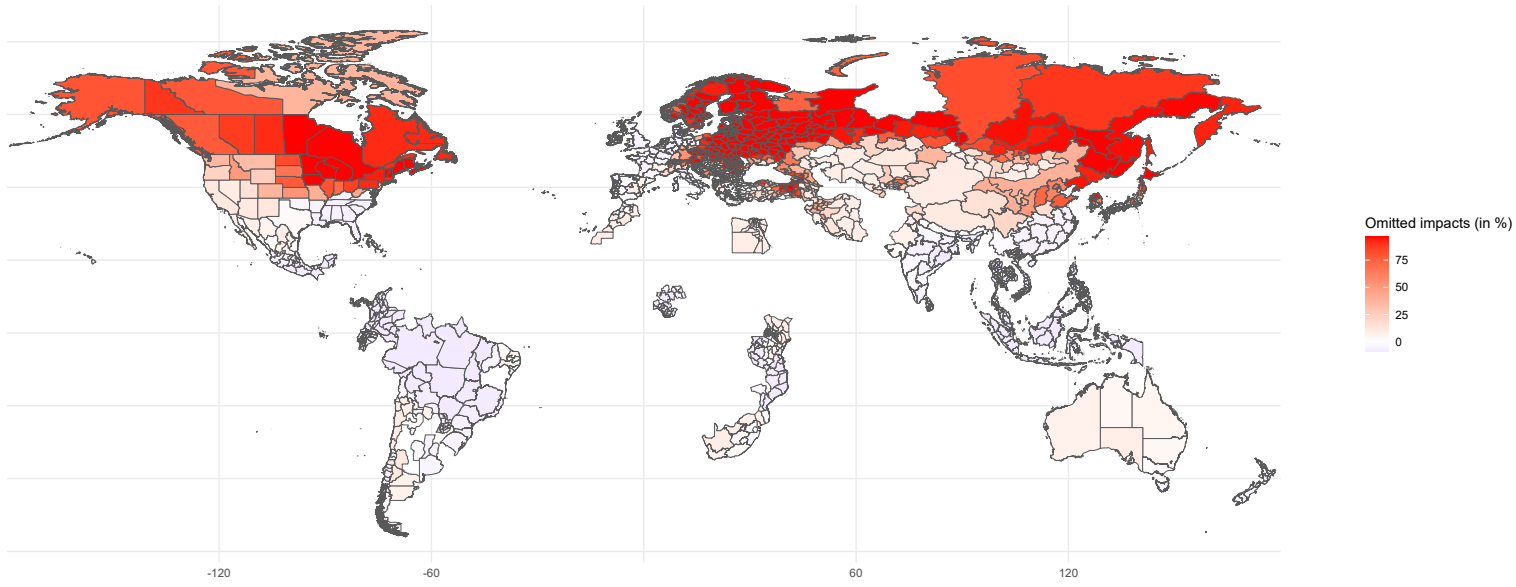


FIGURE 3.5 – Map of DOSE regions with their associated missing-shaped related climate impacts, as a share of 2050 estimated growth impacts along SSP5-8.5.

4 Conclusion

If climate-society relationships were linear, then aggregating would not make any difference. But since they are nonlinear, what happens at the regional and intra-annual levels matters. Indeed, switching from annual global mean temperature to a regional annual distribution of daily mean temperatures affects the magnitude of economic damages from climate change. This change comes from heterogeneity in both damage and warming patterns across regions. Spatio-temporal disaggregation, thus, reveals how uncertainty between climate models on the whole shape of the distribution of future weather realizations cascades down to regional damage estimates. This shape uncertainty affects risk rankings across models and increases the magnitude of uncertainty between models. Mo-

reover, accounting for daily temperatures rather than annual averages increases the estimation of economic damages, a finding consistent with previous studies (Rudik et al., 2022). In 2050, under SSP5-8.5, using regional damage patterns interacted with the shift in the entire shape of the distribution of daily temperatures, yields climate damages at the global scale that are 25% larger than the damage obtained under the assumption of homogeneous damage patterns over the world and shape-preserving shift in annual mean daily temperature. The shape uncertainty about shifts in daily temperature distributions and regional damage patterns should therefore be taken into consideration for decision-making.

To our knowledge, we provide the first comparison between various approaches to spatial and temporal aggregation regarding impacts of changes in mean surface temperatures on economic activity and quantify how much these often-overlooked aggregation procedures matter empirically. We believe that this procedure can be reasonably translated horizontally and vertically. Vertically, this framework can be applied to other economic damages stemming, for instance, from changes in maximum or minimum daily temperatures. Horizontally, the framework could be used to infer results in regions for which we do not have socioeconomic data to estimate damage functions. In this work, we have kept the DOSE regions for the sake of consistency. But using Köppen-Geiger climatic zones, i.e. widely available physical data, to build ensembles and generalize the results over these ensembles could be a useful detour at first, alongside a necessary deepening in the availability of socioeconomic data, particularly in Africa.

Our analysis also comes with limitations. In particular, our estimation of regional damage functions is based on the idea that differences in the economic damage caused by weather—and therefore by climate change—is intimately linked to climatic zones. However, there are many factors that go well beyond geographical determinism that we do not explore here. Furthermore, Earth System Models are imperfect, and some may not be able to capture well the shape (or changes in the shape) of the temperature distribution (Kornhuber et al., 2023). When it comes to estimating the future damage of climate change, other approaches use annual temperature (Bilal and Känzig, 2024) and thus avoid the problem of time-fixed effects, which erase a large proportion of the impacts. The question of aggregation is less of an issue in this case, as these approaches consider annual temperature to be a sufficient statistic for estimating impacts. Nevertheless, the question of the relevance of past natural variability as a proxy for global annual climate change based on complex processes and rising carbon concentration remains. This question is left for future research. Finally, while we studied

variations of warming patterns in space and time, and variation of damage patterns in space, we have left out the question of variation of damage patterns in time under a ‘swinging climate’ (Mérel et al., 2024)—i.e. adaptation to shifts in climate. How might a given daily temperature yield different damages in any particular region under a different climate, as the region moves away from its normal climatic zone? Lastly, that raises the question of how adaptation might interact with the entire distribution of climatic factors, a question left for further research.

5 Annex

1 Building climate landscapes

We scale the frequency of observations by the share of land area in each cell using GPW4 dataset. We compare changes in shapes of daily mean temperature distributions T_{mr} in five Köppen regions r and climate model m, i.e. the distribution of all T_{mr} daily mean temperatures in region r and model m, in four different climates C. Climate C are : a control climate, ISIMIP projections, the synthetic distribution with model average, the synthetic distribution with average over models. We bin the temperature distributions t at 1°C : $f(\cdot)$ is a function that bin the distributions. Our final landscapes for each year are :

- Control climate, without climate change $T_{mr}^{control} = f(t_{mr}^{control})$
- ISIMIP projections $T_{mr}^{proj} = f(t_{mr}^{proj})$
- Synthetic model with model average are built by adding the difference between binned projections and control climate

$$T_{mr}^{synth.model} = f\left(t_{mr}^{control} + T_{mr}^{proj} - T_{mr}^{control}\right)$$
- Synthetic model with total average are built by adding the difference between binned projections and control climate, averaged over all models m in ensemble M

$$T_{mr}^{synth.general} = f\left(t_{mr}^{control} + \text{mean}_M(T_{mr}^{proj} - T_{mr}^{control})\right)$$

Let us define a climate shift indices for a given year : $CSI_{mr} = T_{mr}^{proj} - T_{mr}^{synth.model}$, which gives for each bin the difference in the frequency of this temperature in the projections with respect to the synthetic shape-preserving mean-shifted climate for each ESM. The Köppen region of use are :

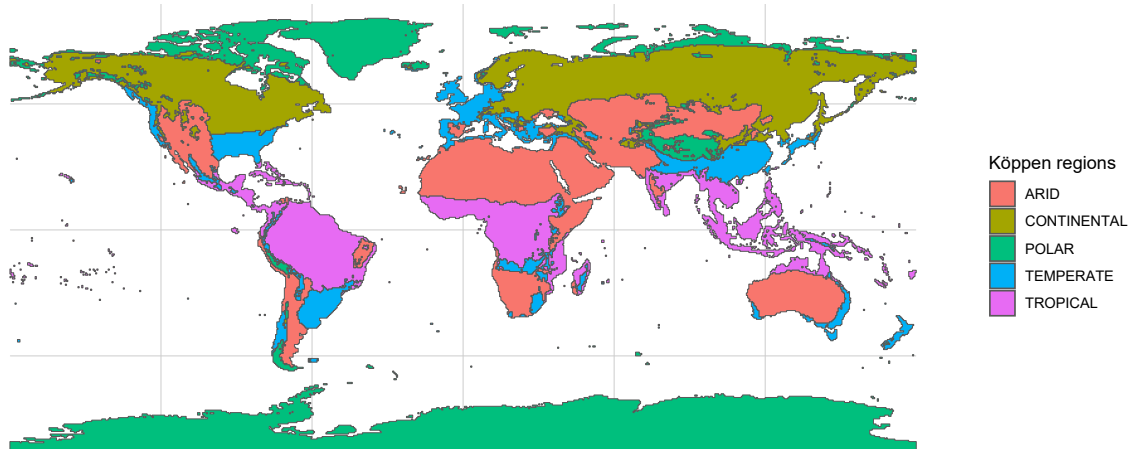


FIGURE 3.6 – Köppen climatic zones.

Bibliographie

- M. Auffhammer. Quantifying economic damages from climate change. *Journal of Economic Perspectives*, 32(4) :33–52, 2018.
- H. E. Beck, T. R. McVicar, N. Vergopolan, A. Berg, N. J. Lutsko, A. Dufour, Z. Zeng, X. Jiang, A. I. van Dijk, and D. G. Miralles. High-resolution (1 km) köppen-geiger maps for 1901–2099 based on constrained cmip6 projections. *Scientific data*, 10(1) :724, 2023.
- A. Bilal and D. R. Känzig. The macroeconomic impact of climate change : Global vs. local temperature. Technical report, National Bureau of Economic Research, 2024.
- A. Bilal and E. Rossi-Hansberg. Anticipating climate change across the united states. Technical report, National Bureau of Economic Research, 2023.
- B. Conte, K. Desmet, D. K. Nagy, and E. Rossi-Hansberg. Local sectoral specialization in a warming world. *Journal of Economic Geography*, 21(4) :493–530, 2021.
- J.-L. Cruz and E. Rossi-Hansberg. The economic geography of global warming. *Review of Economic Studies*, 91(2) :899–939, 2024.
- M. Dell, B. F. Jones, and B. A. Olken. What do we learn from the weather? the new climate-economy literature. *Journal of Economic literature*, 52(3) :740–798, 2014.
- K. Desmet and E. Rossi-Hansberg. Climate change economics over time and space. *Annual Review of Economics*, 16, 2024.
- J. Fernández-Villaverde, K. Gillingham, and S. Scheidegger. Climate change through the lens of macroeconomic modeling. 2024.
- K. Frieler, J. Volkholz, S. Lange, J. Schewe, M. Mengel, M. d. R. Rivas López, C. Otto, C. P. Reyer, D. N. Karger, J. T. Malle, et al. Scenario set-up and forcing data for impact model evaluation and impact attribution within the third round of the inter-sectoral model intercomparison project (isimip3a). *EGUsphere*, pages 1–83, 2023.
- D. García-León, A. Casanueva, G. Standardi, A. Burgstall, A. D. Flouris, and L. Nybo. Current and projected regional economic impacts of heatwaves in europe. *Nature communications*, 12 (1) :5807, 2021.
- H. Hersbach, B. Bell, P. Berrisford, S. Hirahara, A. Horányi, J. Muñoz-Sabater, J. Nicolas, C. Peubey, R. Radu, D. Schepers, A. Simmons, C. Soci, S. Abdalla, X. Abellán, G. Balsamo, P. Bechtold, G. Biavati, J. Bidlot, M. Bonavita, G. De Chiara, P. Dahlgren, D. Dee, M. Diamantakis, R. Dragani, J. Flemming, R. Forbes, M. Fuentes, A. Geer, L. Haimberger, S. Healy, R. J. Hogan, E. Hölm, M. Janisková, S. Keeley, P. Laloyaux, P. Lopez, C. Lupu, G. Radnoti, P. De Rosnay, I. Rozum, F. Vamborg, S. Villaume, and J.-N. Thépaut. The ERA5 global reanalysis. *Quarterly Journal of the Royal Meteorological Society*, 146(730) :1999–2049, July 2020. ISSN 0035-9009, 1477-870X. doi : 10.1002/qj.3803.

- G. Heutel, N. H. Miller, and D. Molitor. Adaptation and the mortality effects of temperature across us climate regions. *Review of Economics and Statistics*, 103(4) :740–753, 2021.
- S. Hsiang. Climate econometrics. *Annual Review of Resource Economics*, 8(1) :43–75, 2016.
- K. Kornhuber, C. Lesk, C. F. Schleussner, J. Jägermeyr, P. Pfleiderer, and R. M. Horton. Risks of synchronized low yields are underestimated in climate and crop model projections. *Nature Communications*, 14(1) :3528, 2023.
- M. Kotz, A. Levermann, and L. Wenz. The effect of rainfall changes on economic production. *Nature*, 601(7892) :223–227, 2022.
- M. Kotz, A. Levermann, and L. Wenz. The economic commitment of climate change. 2023.
- P. Krusell and A. A. Smith Jr. Climate change around the world. 2022.
- M. Leduc, H. D. Matthews, and R. de Elía. Regional estimates of the transient climate response to cumulative co₂ emissions. *Nature Climate Change*, 6(5) :474–478, 2016.
- P. Mérel, E. Paroissien, and M. Gammans. Sufficient statistics for climate change counterfactuals. *Journal of Environmental Economics and Management*, page 102940, 2024.
- W. D. Nordhaus. *Managing the global commons : the economics of climate change*, volume 31. MIT press Cambridge, MA, 1994.
- W. D. Nordhaus and Z. Yang. A regional dynamic general-equilibrium model of alternative climate-change strategies. *The American Economic Review*, pages 741–765, 1996.
- M. Patterson. North-west europe hottest days are warming twice as fast as mean summer days. *Geophysical Research Letters*, 50(10) :e2023GL102757, 2023.
- J. Rising, M. Tedesco, F. Piontek, and D. A. Stainforth. The missing risks of climate change. *Nature*, 610(7933) :643–651, 2022.
- I. Rudik, G. Lyn, W. Tan, and A. Ortiz-Bobea. The economic effects of climate change in dynamic spatial equilibrium. 2022.
- K. Schwarzwald and N. Lenssen. The importance of internal climate variability in climate impact projections. *Proceedings of the National Academy of Sciences*, 119(42) :e2208095119, 2022.
- P. Waideleich, F. Batibeniz, J. A. Rising, J. Kikstra, and S. Seneviratne. Climate damage projections beyond annual temperature. 2023.
- L. Warszawski, K. Frieler, V. Huber, F. Piontek, O. Serdeczny, and J. Schewe. The inter-sectoral impact model intercomparison project (isi-mip) : project framework. *Proceedings of the National Academy of Sciences*, 111(9) :3228–3232, 2014.
- L. Wenz, R. D. Carr, N. Kögel, M. Kotz, and M. Kalkuhl. Dose–global data set of reported sub-national economic output. *Scientific Data*, 10(1) :425, 2023.

Chapitre 4

The biophysical channels of climate impacts

To what extent does regional economic activity shape regional climate impacts ? Land use land cover (LULC) changes with regional economic activity through agricultural and urban land demands. At the regional scale, LULC changes affect climate impacts through changes in albedo, evapotranspiration and roughness length, i.e. biophysical channels. These spatially heterogeneous regional feedbacks have so far been neglected in the quantitative spatial literature assessing the economic consequences of climate change. Indeed, the literature focuses on the biogeochemical channel from global carbon concentration. Accounting for this additional biophysical feedback between regional economic activities and regional climate change yields important welfare implications for both adaptation and mitigation, as the biophysical feedbacks change temperature impacts and interact with regional adaptation decisions. I build a dynamic-spatial sectoral equilibrium model to understand the impact of this omitted nonlinear physical mechanism and take the model to the data at the global gridded 1° resolution to quantify its magnitude along ‘middle-of-the-road’ SSP2-4.5 with agents that adapt to climate impacts through migration and trade. I leverage recent advances in the climate adaptive response literature to estimate model-consistent dose-response functions of regional amenities and sectoral productivities to regional annual distributions of daily mean surface temperatures from the equilibrium conditions of the model. In my baseline SSP2-4.5 simulation, without biophysical impacts, almost all locations experience negative welfare changes from non-linear regional intra-annual warming patterns interacted with nonlinear binned damage patterns : there are no benefits to be expected from climate change in the Northern Hemisphere. Adding biophysical channels, i.e. a non-linear and time-varying downscaling from global to regional temperature distributions, accounts for 2.4% of the aggregate biogeochemical welfare impacts of climate change. Both biogeochemical and biophysical climate impacts are regressive, decreasing with 2015 income per capita levels.

Keywords : environmental policy, spatial integrated assessment models, endogenous adaptation, land use land cover, albedo, evapotranspiration, soil roughness, downscaling.

JEL Codes : Q50, R13, R14

1 Introduction

'Any local land changes that redistribute energy and water vapour between the land and the atmosphere influence regional climate (biophysical effects, high confidence)' (IPCC).

Uncertainties about changes in land conditions originating from anthropogenic land uses have become a major concern, as highlighted by IPCC in its 2019 special report on climate change and land (Masson-Delmotte et al., 2019). Changes in land conditions have for instance a major impact on biodiversity and contribute to global climate change through carbon releases or by reducing land carbon storage potential. But in this study, I focus on the *regional biophysical climate impacts* of changes in regional land conditions. These biophysical impacts are not driven by carbon emissions but by changes in albedo, evapotranspiration and soil roughness, which can reduce or accentuate regional warming (Georgescu et al., 2011; Alkama and Cescatti, 2016) depending on the location and season (Duveiller et al., 2018b).

To my knowledge, economists usually omit these mechanisms in their assessments of climate impacts : they focus on the biogeochemical channel of global carbon emissions. For instance, in the burgeoning field of spatial integrated assessment modelling (Desmet and Rossi-Hansberg, 2024), regional temperatures at location r and time t are inferred from global average temperatures through statistical downscaling, also called pattern scaling (Santer et al., 1990). As depicted in Fernández-Villalverde et al. (2024), pattern-scaling suggests a simple functional relation such as : $T_t(r) = f(T_t^A) + \eta_t(r)$, where local temperature $T_t(r)$ at grid cell r and time t is a response to global average temperature T_t^A indicated by $f(\cdot)$ and a stochastic local residual temperature variability term $\eta_t(r)$. The stochastic process that determines the distribution of local residual $\eta_t(r)$ is assumed to be *stationary* and *exogenous* to regional economic activities. In this work, I reconsider these two assumptions. As our understanding of the mechanisms through which human activities and climate impacts interact goes to finer spatial resolution, I investigate the heterogenous endogenous dynamic biophysical regional impacts and their interactions with adaptation and economic decisions. I quantify how much the regional biophysical channels driven by land use land cover (LULC) changes matter along 'middle-of-the-road' Shared Socioeconomic Pathways (SSP) 2-4.5.

Human-induced LULC changes affect regional climate through three key biophysical channels : change in albedo, change in evapotranspiration and change in surface roughness length. Albedo is the fraction of solar radiation reflected

by a surface. Evapotranspiration is the combined process of evaporation from the Earth's surface and transpiration from vegetation. Roughness length refers to the measure of a surface's roughness, which influences how air moves above that surface. Surfaces with less albedo, e.g. because of urbanization, absorb more solar radiation which leads to higher temperatures as more solar energy is converted to heat in these areas. Evapotranspiration decreases in a given location, e.g. because of deforestation, mean that less water is evaporated from surfaces, requiring less energy to change state from liquid to gas while this energy is usually drawn from the environment, cooling both the surface and the surrounding air. The decrease in evapotranspiration can thus bring regional temperature increases. Rough surfaces, such as forests or areas with rugged topography, can slow down air movement, thereby promoting the cooling of local temperatures. Smoother agricultural and urban areas, on the other hand, can reduce frictional drag on the air, allowing warmer air from surrounding regions to flow into these areas. These three biophysical mechanisms are affected by changes in physical land surface characteristics, especially human-driven land use land cover changes : there are regional feedbacks between human activity and these biophysical channels. The two key human drivers that I study here are changes in agricultural and urban land demands.

The biophysical channels matter for climate economics for two main reasons. First, there are heterogeneous LULC changes to be expected around the world depending on current LULC, future economic growth, structural change, demography and climate impacts. Second, these biophysical channels interact with adaptation decisions. For instance, population concentration in areas that are less affected by climate impacts drives urban land demand and changes in regional biophysical impacts that can reduce the aggregate benefits of migration and change the distributional impacts of the climate burden between regions. This might matter if climate change and population growth have their most damaging effects in similar places ([Henderson et al., 2024](#)). Heterogeneous climate impacts and economic dynamics in different regions of the world and in different sectors are driving changes in sectoral specializations, for example by shifting the optimal climate zones for agricultural activities or changing relative prices. These changes in sectoral specialization come with changes in agricultural land extent which have biophysical impacts. The biophysical channels might reduce or increase the benefits of regional adaptation expected from structural change.

There are large heterogeneities in the impacts of these biophysical feedbacks, both physical and socioeconomic. On the one hand, there are spatial and tem-

poral heterogeneities in the biophysical mechanisms. Indeed, observations show that biophysical channels do not have the same impact over different periods of the year (Duveiller et al., 2020). Furthermore, biophysical channels can vary in sign and magnitude depending on regional background climate (Duveiller et al., 2018b) : land use changes, for instance from forest to grassland, bring conflicting changes in albedo (increase) and evapotranspiration (decrease). These conflicting changes may lead to cooling or warming depending on which process dominates, which depends on local climate background. Huang et al. (2020) explore this spatial heterogeneity within Europe. On the other hand, there are large spatial and temporal heterogeneity in the socio-economic drivers of land use land cover changes bringing biophysical impacts, because there are various land use land covers today and future land use land cover changes. Different paths of urbanization are to be expected in different parts of the world, depending on demography, economic growth and climate impacts, among others drivers (UN World Urbanization Prospects). Different paths of agricultural land use land cover changes will also occur depending on structural change, food needs and heterogeneous impacts of climate change on agricultural yields, etc. (Future of Food and Agriculture, UN FAO). The interaction between these sources of spatial and temporal heterogeneity, both biophysical and socioeconomic, might even increase the divergence between different locations over the world.

In this paper, I estimate the aggregate and distributional welfare impacts of the biophysical channels of climate impacts along SSP2-4.5. First, I match LULC scenario from LUMIP MESSAGE-Globiom along SSP2-4.5 with Duveiller et al. (2018b) and Zhou et al. (2022) gridded estimates of the historical impact of LULC changes on daily mean daytime and nighttime land surface temperatures. More specifically, I compute the mean impact over thirteen Köppen-Geiger climate zones as the regional biophysical feedbacks depend on background climate. I then use a gridded linear relation between daytime and nighttime land surface temperatures and daily mean surface temperature (Hooker et al., 2018), a metric adapted to the measure of climate impacts on economic activities. This procedure allows me to build a reduced-form representation of the regional biophysical feedbacks that can be projected using anticipated gridded changes in Köppen-Geiger zones along SSP2-4.5 (Beck et al., 2023) and changes in LULC.

I build a two-sectors (agricultural sector and all other sectors), dynamic quantitative spatial equilibrium model (Eaton and Kortum, 2002; Redding and Rossi-Hansberg, 2017) where locations differ in regional annual distribution of mean

daily surface temperature, sectoral productivities, amenities, bilateral trade and migration costs. Productivities represent features that make different regions more or less attractive in terms of the costs of production, which may include natural advantages (such as proximity of natural resources) or induced advantages (such as infrastructure). Regional amenities capture characteristics of each location that make them more or less desirable places to live. Workers in each location have preference for regional amenities and consume a variety of horizontally differentiated goods. They experience idiosyncratic preference shocks. Workers are mobile across locations but face time-invariant migration costs. Their migration decisions are simplified *a la* Desmet et al. (2018b) to make the 1° gridded model tractable. I use Caliendo et al. (2019); Kleinman et al. (2023) dynamic exact hat algebra technique that avoids the shortcomings of regional fundamental amenities estimation. Finally, firms face monopolistic competition without intermediate inputs in the production as in Conte et al. (2021), with time-invariant and symmetric bilateral trade costs that are not sector-specific, and without trade imbalances. I solve the model under the assumption of a stationary equilibrium.

The simulations are done under exogenous biogeochemical climate change with projections of future distributions of daily mean temperatures taken from the average of bias-adjusted (Lange, 2019) and down-scaled SSP2-4.5 CMIP6 experiments of four Earth System models (ESM) (GFDL-ESM4, IPSL-CM6A-LR, MPI-ESM1-2-HR, MRI-ESM2-0) with the assumption of 2015 fixed land use. Biophysical impacts are added to these exogenous projections with the implicit assumption of a shape-preserving mean increase in the annual distribution of daily mean temperatures. I could compare these simulations to CMIP projections with exogenous land use change scenarios, but this would lump the two biophysical and biogeochemical effects of land use change together : a change in land use in an ESM leads to a biogeochemical impact via the global carbon cycle (e.g. carbon releases from deforestation), which is not disentangled from the biophysical impact. An important work is done by the LUMIP platform (Lawrence et al., 2016) to disentangle these future land use impacts, especially for deforestation, e.g. in Boysen et al. (2020). But these studies treat the various biophysical impacts in silo, or model them along exogenous scenarios of population, trade, sector specialization, without modeling the endogenous reaction of agents to climate impacts as in the recent quantitative spatial literature (Cruz and Rossi-Hansberg, 2024).

I follow Rudik et al. (2022) and use the equilibrium conditions of the theoretical model to compute model-consistent dose-response function of regional amenities and sectoral productivities to distortions in the annual regional distribution

of daily mean temperatures. The intuition behind this estimation approach is that changes in migration and trade flows allows *ceteris paribus* to identify changes in amenity and sectoral productivity levels. As the dose-response functions are estimated from the equilibrium conditions of the theoretical model, the simulation results reflect the actual welfare impacts of climate change given the model's assumptions regarding macroeconomic dynamics and adaptation decisions. I combine ERA-5 climate reanalysis ([Hersbach et al., 2020](#)) of the population-weighted country-level annual distribution of daily mean temperatures with BACI CEPII and [Abel and Cohen \(2019\)](#) datasets on trade and migration flows at the country level. Focusing on the whole shape of the intra-annual distribution of daily mean temperatures rather than an arbitrary moment such as the mean annual temperature ([Fillon et al., 2024](#)) allows to capture more complex changes in the high-dimensional temperature vector. The temperature bins allows to capture some of the non-linearity in the climate impacts ([Burke et al., 2015](#)).

To what extent does regional economic activity shape regional climate impacts? My quantitative estimation of the biophysical channels of climate change under SSP2-4.5 proceeds in two steps. First, I estimate the aggregate and distributional welfare impacts of the SSP2-4.5 scenario, considering only the carbon cycle—i.e., I ignore the impact of regional economic activity on regional climate change. Then, I assess the aggregate and distributional impacts of SSP2-4.5 with the addition of biophysical channels. Two key conclusions emerge from the first step, where I estimate the baseline impacts of biogeochemical climate change. First, climate change impacts are negative for most regions : by accounting for intra-annual warming patterns and non-linear damage patterns across temperature bins, I find no evidence of benefits from warming in the Northern Hemisphere. The aggregate welfare impact of SSP2-4.5 is, however, consistent with existing literature ; most impacts are driven by the non-linear effect of temperature distortions on sectoral productivities. Second, biogeochemical climate change is regressive : the magnitude of welfare changes under SSP2-4.5 is inversely related to initial income levels in 2015. In the second step, I estimate the impact of biophysical channels. From my simulations, two conclusions arise. First, regional economic activity does indeed influence regional climate impacts and the corresponding welfare changes. On average, this additional biophysical effect accounts for 2.5% of the biogeochemical impacts estimated in the first step. Second, the biophysical impacts vary across both time and space. This heterogeneity is, first, socioeconomic : it depends on scenarios of urban land-use change and the net

transitions of shrublands and forests into croplands. It is also climatic : the effect of biophysical channels depends on the climate zone in which a location is situated (e.g., arid, temperate, etc.), with these classifications shifting over time due to global climate change. For some biophysical channels, this heterogeneity is also seasonal, which further strengthens the case for considering the intra-annual distribution of temperatures in the study of climate impacts. In my simulations, I find that most locations experience a negative impact from biophysical channels on welfare under SSP2-4.5. Like the biogeochemical impacts, the biophysical effects are regressive relative to 2015 income levels.

I contribute to three main strands of economic literature. First, I contribute to the growing literature in climate economics using dynamic spatial quantitative equilibrium model to measure the impacts of climate change under endogenous and regional adaptation ([Krusell and Smith Jr, 2022](#); [Cruz and Rossi-Hansberg, 2024](#)). In comparison with these spatial integrated assessment models, I do not assume a time-invariant exogenous linear relation between global climate change and regional climate impacts. Indeed, downscaling from global to regional climate change cannot be considered as stable across time and space : it is not exogenous to our regional economic activities. Averaging over multiple deterministic draws taking the whole scientific information into account, e.g. similar to work of [Desmet et al. \(2018a\)](#) on sea level rise but in application to parametric uncertainty over regional transient climate response to global cumulative emissions, would not allow to capture these nonlinear biophysical mechanisms. Thus, in addition to non-linearities in climate impacts, largely documented since seminal work from [Schlenker and Roberts \(2009\)](#); [Burke et al. \(2015\)](#), i.e. non-linearity in the mapping from a given summary statistics of regional climate change to economic impacts on amenities and productivities, I add physical non-linearities in the mapping from global climate change to regional climate change via endogenous LULC changes. Another venue in this literature is to use actual climate projections ([Rudik et al., 2022](#); [Bilal and Rossi-Hansberg, 2023](#)) but this implies that LULC are either assumed time-invariant, or that the biophysical channels of LULC are entangled with their biogeochemical impacts.

Second, I contribute to the literature modelling adaptation which has developed in response to the Lucas critique addressed to the standard climate-economy models ([Nordhaus, 2008](#); [Barrage and Nordhaus, 2024](#)) : in comparison with previous approaches, I study how adaptation decisions might interact with climate impacts. Thus, I relate to the literature on structural transformation under a chan-

ging climate (Conte et al., 2021; Albert et al., 2021; Nath, 2022) and urbanization and their interaction with LULC changes (Michaels et al., 2012; Ahlfeldt et al., 2015; Coeurdacier et al., 2022; Eckert and Peters, 2022). I quantify the impact of these sectoral specialization and urbanization changes on regional climates via biophysical mechanisms.

Third, I contribute to the literature studying the interactions between economic activity, land uses and climate impacts. This literature usually focuses on forest covers (Grosset et al., 2023) and micro-scale impacts, for instance health impacts related to urban heat island (Manoli et al., 2019). I extend this literature in three directions : I consider various transitions in land uses (transition from forests to croplands, transition from shrublands to croplands, transition from non-impervious to impervious surfaces), at the global scale (around 13000 gridded locations) and with larger regional impacts at the 1° gridded resolution, in response to climate scientists' concerns that biophysical impacts are not solely local (Duveiller et al., 2018b; Chakraborty and Qian, 2024).

2 Motivation

1 Regional biophysical channels and their impacts

1 Impact of regional agricultural land demand on regional climate

Changes in agricultural LULC have heterogeneous impacts on regional climates and depending on the season. Duveiller et al. (2018a) provide gridded estimates of climate impacts stemming from regional transitions from and to croplands at 1° spatial resolution. While the authors also provide estimates for grasslands, they do not differentiate between rangelands grazed by domestic livestock and other uses. I thus focus on changes in croplands without considering pastures. I compute the mean temperature impact of these land transitions over Köppen-Geiger climate zones because biophysical impacts depend on regional climate backgrounds (Duveiller et al., 2020). In table (4.1), I give the distribution of change in mean daily surface temperature observed for two LULC transitions in all Köppen-Geiger climatic zones : transition from forests to croplands and transition from shrublands to croplands. I convert daytime and nighttime land surface temperatures to mean two-meters surface temperature using gridded linear relations uncovered in Hooker et al. (2018).

Koppen-Geiger climate zone	Forests to Croplands	Shrublands to Croplands
Arid, desert	- / -	0.0108/0.0169°C
Humid continental	0.0078/0.0015°C	-0.0102/0.0018°C
Humid subtropical	0.002/0.0017°C	0.0046/-0.0021°C
Mediterranean	0.0029/0.0003°C	- / -
Mediterranean continental	-0.0087/0.0007°C	-0.0007/-0.0025°C
Oceanic	-0.0013/-0.0038°C	0.0098 / - °C
Semi-Arid	-0.0015/0.0013°C	0.0043/0.009°C
Subarctic	-0.0037/0.0005°C	-0.0048/0.0028°C
Tropical, Monsoon	0.0022/0.0001°C	0.0032/-0.0033°C
Tropical, Rainforest	0.0017/0.003°C	0.0043/-0.0079°C
Tropical, Savannah	-0.0048/-0.0004°C	0.0026/0.0037°C
Tundra	0.0022/0.0104°C	0.0148/-0.0016°C

TABLE 4.1 – Change in monthly (January/July for illustration) mean daily surface temperature (in °C) for various Köppen-Geiger climatic zones for a 1% absolute change in land use for two net transitions of interest : from forests to croplands, from shrublands to croplands. 1% absolute change over 1° gridded regions represents around 123km² at Equator and 87km² on the French mainland. Data is missing for some combinations.

2 Impact of regional urban land demand on regional climate

Changes in urban LULC have an impact on regional climates ([Zhou et al., 2022](#)). To my knowledge, most studies focus on local urban heat islands effect in cities while I refer to all global artificial impervious surfaces as these areas have temperature impacts that go beyond local effects ([Chakraborty and Qian, 2024](#)). Past decades have seen large changes in global artificial impervious surfaces. [Zhou et al. \(2022\)](#) give gridded regional climate impacts of global artificial impervious surfaces extension at 50km x 50 km resolution. More specifically, the authors give the change in urbanization over 1985 to 2015 and the change in daytime and nighttime land surface temperature (LST) due to increase in urbanization over the same period. I convert daytime and nighttime LST to mean two-meters surface temperature using [Hooker et al. \(2018\)](#). I compute the mean impact over Köppen-Geiger climate zones because I expect the impact to depend on regional climate background as for urban heat islands ([Zhao et al., 2014](#)). In table (4.2), I give the distribution of annual mean daily temperature changes from a 1% increase in impervious surfaces.

Mean change	Koppen-Geiger climate zone
0.0077°C	Arid, desert
0.0096°C	Humid continental
0.0115°C	Humid subtropical
0.0103°C	Mediterranean
0.0083°C	Mediterranean continental
0.0106°C	Oceanic
0.0076°C	Semi-Arid
0.0068°C	Subarctic
0.0108°C	Tropical, Monsoon
0.0077°C	Tropical, Rainforest
0.0123°C	Tropical, Savannah
0.0114°C	Tundra

TABLE 4.2 – Change in mean daily temperature (in °C) for various Köppen-Geiger zones for a 1% absolute change in impervious surfaces over 1° regions.

In order to use these estimates for simulations using distributions of daily mean temperatures, I make two assumptions. First, I assume homogeneity in the shift in distribution of daily mean temperatures within each year (urban land) and each month (croplands). Second, I assume that the change computed for each Köppen-Geiger zone holds in the future for the same climatic zone.

3 Köppen-Geiger climates

I plot the 2015 distribution of Köppen-Geiger climate zones.

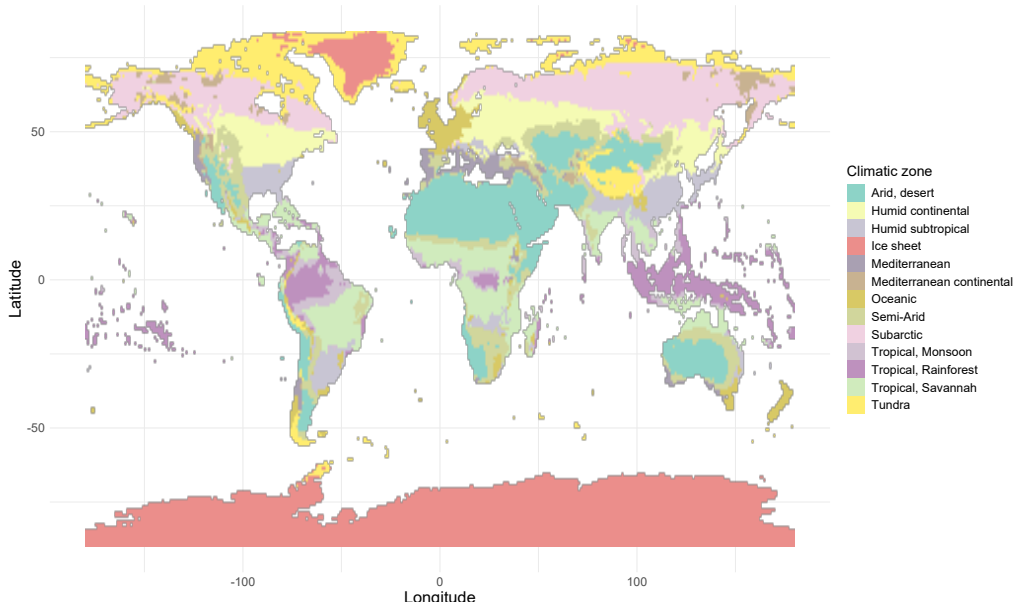


FIGURE 4.1 – 13 Köppen-Geiger climate reference regions in 2015.

According to [Beck et al. \(2023\)](#), 8% of current land surface will transition to another Koppen-Geiger region along SSP2-4.5. Thus, I can not use fixed current Koppen-Geiger zone while the sign and magnitude of the biophysical channel stemming from land use land cover changes depend on it. I use [Beck et al. \(2023\)](#) data to project in which Köppen-Geiger zone each 1° grid cell will be along SSP2-4.5. Regions that change affiliation between 2015 and 2100 are :

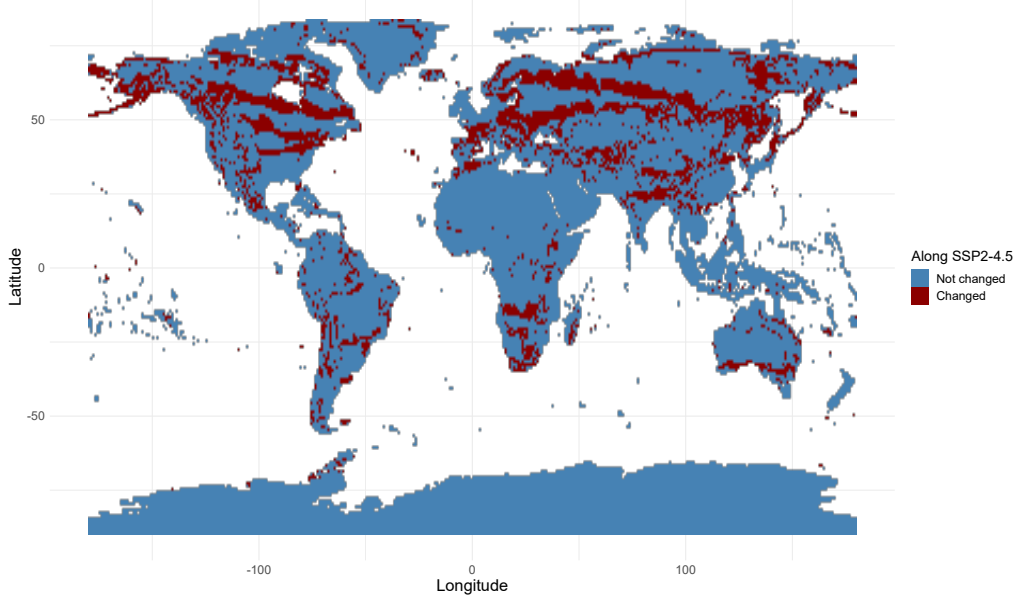


FIGURE 4.2 – 1° locations who change Köppen-Geiger classification between 2015 and 2100 under SSP2-4.5.

2 Impact of economic activities on LULC changes

Once I have retrieved these estimates linking LULC to biophysical impacts, I map changes in economic activities to LULC changes. In table (4.3), I give summary statistics for the distribution of cumulative net transitions from forests to croplands, from rangelands¹ to croplands, from non-impervious to impervious surfaces from 2015 to 2100 under SSP2-4.5 in MESSAGE-Globiom ([Hurtt et al., 2020](#)), stored on the LUMIP platform.

1. As a first approximation, I assume that biophysical channels estimated in [Duveller et al. \(2018b\)](#) for generic shrublands applies to the MESSAGE Globiom category of rangelands that does not include domestic pastured grasslands. I could disentangle further between savannas and shrublands.

Quantiles	Forests to croplands	Rangelands to croplands	Non-urban to urban
0%	-56.88	-27.19	-4.65
20%	-0.49	0.00	0.00
40%	0.19	0.01	0.03
60%	1.01	0.17	0.13
80%	3.60	0.83	0.51
100%	63.96	43.36	19.19

TABLE 4.3 – Cumulative net change (as a share of total cell extent, in %) between 2015 and 2100 in LUMIP MESSAGE-Globiom SSP2 4-5 for the 1° gridded locations used in the simulations, from forests to croplands (left), from rangelands to croplands (middle), from non-impervious to urban impervious surfaces (right).

Interacted with biophysical changes from tables (4.1) and (4.2), these LULC changes have a heterogeneous impact on the future annual distributions of daily mean temperatures around the world and over time. These dynamic biophysical impacts affect the future distribution of economic activities, populations and welfare throughout the world in a way that is omitted from estimates of climate change impacts of the quantitative spatial literature that uses time-invariant linear temperature down-scaling. Model that use projections from CMIP6 earth system models either assume fixed land use or use projections forced with direct human forcing such as land use changes which do not differentiate between the various channels by which land and other elements of the SSP affect climate, e.g. the specific biophysical channels that we study here.

I have retrieved estimates linking economic activity to heterogeneous biophysical impacts at the regional scale *via* changes in agricultural and urban land demands. I build a spatial sectoral equilibrium model to understand how these regional feedbacks interact with standard biogeochemical climate impacts and regional adaptation decisions. I quantify how these dynamic mechanisms shape the distribution of economic activity, population and climate impacts along SSP2-4.5.

3 Theoretical Model

1 Households

1 Preferences and migrations

Period utility of a worker j who resides in location r at t is multiplicative in four elements : the level of regional amenities $a_t(r)$ that captures how valuable living in a given location is other things being equal, the consumption of goods $C_t(r)$, an individual-specific idiosyncratic preference shock ϵ_t^j , drawn from a Fréchet distribution (i.i.d. across locations, individuals, and time) with a shape parameter that equals the elasticity of migration to real income, and the cost of migrating from location r in period $s - 1$ to a location r in period s .

$$U_t^j(r) = a_t(r)C_t(r)\epsilon_t^j(r)\prod_{s=1}^t m(r_{s-1}, r_s)^{-1} \quad (4.1)$$

Dynamic migration decisions are simplified to static decisions as in Desmet et al. (2018b), so that : $m(s, r) = m_1(s)m_2(r)$ and $m(r, r) = 1$, i.e. there is no cost to staying in the same place and the utility discount from migration is the product of origin and destination-specific discounts. This yields that $m_2(r) = 1/m_1(r)$, i.e. the cost of entering a location is fully compensated by the benefit from leaving. This symmetry assumption allows to reduce the dimension of my spatial dynamic migration problem with many locations and makes it tractable at the global 1° gridded scale with standard resolutions methods.

2 Consumption and income

I assume a Cobb-Douglas preference structure between goods and a Spence-Dixit-Stiglitz preference structure between horizontally differentiated varieties for each good, with $1/(1 - \rho)$ the elasticity of substitution between goods. I assume $\rho > 1$ in my setting, so that varieties are substitutes. χ_i is the fixed share of good i in the worker's expenditure. Consumption of goods at time t in location r writes :

$$C_t(r) = \prod_{k=1}^K \left[\int_0^1 c_t^{k\omega}(r)^\rho d\omega \right]^{\frac{\chi_i}{\rho}} \quad (4.2)$$

Workers in location r supplies one unit of labor inelastically and receive wage $w_t(r)$ in location r and sector k in which they live in period t so that total income is : $y_t(r) = L_t(r)w_t(r)/(\prod_{k \in K} P_t^k(r)^{\chi^k})$ where $\prod_{k \in K} P_t^k(r)^{\chi^k}$ is the ideal price index over K sectors. There is no money lending, so every period agents fully

consume their income and $C_t(r) = y_t(r)$. In each location, there is immobile and non-accumulating capital which I call regional sectoral structures H_t^k as in [Caliendo et al. \(2019\)](#). H_t^k is assumed to be fixed over time and generate a rent that is fully used to maintain these structures.

3 Regional amenities

Following [Desmet et al. \(2018b\)](#), idiosyncratic non-weather time-invariant fundamental regional amenities $\bar{a}_t(r)$ are affected by congestion, with $L_t(r)$ the population in location r at time t and λ the congestion elasticity of amenities to population density. Following [Rudik et al. \(2022\)](#), regional amenities $a_t(r)$ are multiplicatively separable in a weather component $\exp(f[T_t(r); \zeta_a])$, where $T_t(r)$ is a vector of weather variables that summarizes the high-dimensional climate, f an arbitrary function taken over this distribution (e.g. orthogonal polynomials, cubic splines) and ζ_a the set of parameters to be estimated that governs how the weather vector affects regional amenities non-linearly. In my benchmark estimation for ζ_a , I use third-degree orthogonal polynomials for smoothing across the annual distribution of daily mean temperatures with 1°C temperature bins. Regional temperature is a function of the biogeochemical cycle, taken from exogenous SSP projections, and the biophysical channel driven by endogenous LULC changes. Regional amenity writes : $a_t(r) = \bar{a}_{t-1}(r)L_t(r)^{-\lambda}\exp(f[T_t(r); \zeta_a])$. [Desmet et al. \(2018b\)](#) show that $u_t(r) = a_t(r)y_t(r)$ fully summarizes how individuals value the amenity and production characteristics of a location. But uncovering the initial distribution of non-weather time-invariant amenities $\bar{a}_t(r)$, i.e. what makes a location attractive irrespective of economic activity, is challenging². I use [Caliendo et al. \(2019\)](#)'s dynamic exact hat algebra approach to get around this issue.

4 Dynamic exact hat algebra and population dynamics

Following [Desmet et al. \(2018b\)](#), the share of the population in location r that moves to location s from $t-1$ to t among all possible locations N is :

$$\mu_t(rs) = \frac{u_t(s)^{1/\Omega}m_2(rs)^{-1/\Omega}}{\sum_{n \in N} u_t(n)^{1/\Omega}m_2(rn)^{-1/\Omega}} \quad (4.3)$$

2. Attempts include [Desmet et al. \(2018b\)](#), who use model inversion to recover these initial amenities with subjective well-being survey from the Gallup World Poll, and [Cruz and Rossi-Hansberg \(2024\)](#) with [Kummu et al. \(2018\)](#)'s gridded data on reconstructed human development index.

Following Caliendo et al. (2019) and Balboni (2019), I write the change in the bilateral matrix of migration flows in dynamic exact hat algebra :

$$\dot{\mu}_{t+1}(rs) = \frac{\mu_{t+1}(rs)}{\mu_t(rs)} = \frac{\dot{u}_{t+1}(s)^{1/\Omega}}{\sum_{n \in N} \mu_t(rn) \dot{u}_{t+1}(n)^{1/\Omega}} \quad (4.4)$$

And, as the idiosyncratic non-weather dependent part of regional amenities are constant in time : $\dot{u}_{t+1}(r) = \dot{y}_{t+1}(r) \dot{L}_{t+1}(r)^{-\lambda} \exp [f(T_{t+1}(r), \zeta_a) - f(T_t(r), \zeta_a)]$. Once I have migration flows, I build population dynamics for each location, accounting for exogenous birth and death rates from SSP projections without migrations. In comparison with Cruz (2021), I do not model endogenous fertility and death rates. Population dynamics, with $L_t(r) = \sum_{k \in K} L_t^k(r)$, writes :

$$L_{t+1}^k(r) = (b_{t+1}(r) - d_{t+1}(r))L_t^k(r) + \sum_{l=0, l \neq r}^N \sum_{k \in K} \mu_{t+1}(lr) L_t^k(l) - \sum_{l=0, l \neq r}^N \sum_{k \in K} \mu_{t+1}(rl) L_t^k(r) \quad (4.5)$$

Thus, to recover the full dynamics of population under changing climate, I need gridded projections for births and deaths rates along SSP2-4.5 without migration, a guess for the change in utility, observed initial bilateral matrix of migration flows $\mu_0(rs)$, initial distribution of sectoral population $L_0^k(r)$ and the gridded path of the future annual distributions of mean daily temperatures. Then, period by period, I can recover migration flows, without information on the initial distribution of non-weather time-invariant regional amenities.

2 Production

1 Profit maximization

I assume that each 1° economy produces a continuum of varieties ω in sector k with a Cobb-Douglas production technology. A firm produces $q_t^{k\omega}(r)$ units of good from sector k and variety ω in location r at t with technology

$$q_t^{k\omega}(r) = z_t^{k\omega}(r) L_t^{k\omega}(r)^{\mu^k} H_t^{k\omega}(r)^{1-\mu^k}$$

and constant returns to scale with two factors of production, regional sectoral structures and labour, $H_t^{k\omega}(r)$ and $L_t^{k\omega}(r)$. I assume away inter-sectoral intra-location trade, i.e. intermediate inputs in the production function. $z_t^{k\omega}(r)$ is a location-sector-variety random variable drawn independently for each triplet (r, k, ω)

from a Frechet distribution :

$$F_t^{k\omega}(r) = \exp \left[-Z_t^{k\omega}(r)(z)^{-\theta^k} \right].$$

Firms are perfectly competitive. Taking all prices as given, a firm producing variety ω of good in location r and sector k chooses inputs to maximize static profits :

$$\Pi_t^{k\omega}(r) = p_t^{k\omega}(r)q_t^{k\omega}(r) - w_t(r)L_t^{k\omega}(r) - R_t(r)H_t^{k\omega}(r),$$

where $p_t^{k\omega}(r)$ is the price of variety ω of good produced and sold in location r and sector k and input costs are not sector-specific. The unit price of an input bundle in location r , i.e. the marginal cost of production, with κ^k the sector-specific constants, writes :

$$x_t^k(r) = \kappa^k(w_t(r))^{\mu^k}(R_t(r))^{1-\mu^k}.$$

First-order conditions of the firm's profit maximization problem for sector k , time t and location r relate regional structure rents to wages and sectoral labour employment levels :

$$R_t^k(r)H_t^k(r) = w_t(r)\frac{1-\mu^k}{\mu^k}L_t^k(r).$$

2 Regional productivities

As for amenities, productivity Z in each location r is multiplicatively separable in a vector of weather variables, where \bar{Z} is non-weather base productivity : $Z_t^k(r) = \bar{Z}_t^k(r)\exp(g[T_t(r);\zeta_z])$. Non-weather productivity \bar{Z}_{rt}^k grows exogenously³ at a rate ϕ that is not sector-specific. In each location, the vector of temperatures T depend on both biogeochemical and biophysical channels. In hat algebra, productivity changes in location i , sector k and time t write $\dot{Z}_{t+1}^k(r) = \phi\exp(g[T_{t+1}(r);\zeta_z] - g[T_t(r);\zeta_z])$, where ζ_z is a set of parameters to be estimated that govern how productivity changes non-linearly across temperature bins and g an arbitrary function over the regional annual distribution of daily mean temperatures $T_t(r)$.

3 Trade, prices, market clearing

I use time-invariant iceberg trade costs τ_{rs} from location r to s among N locations. The trade costs are not specific to sectors. Following [Eaton and Kortum](#)

3. Spatial diffusion models might not reflect how innovation spreads ([Audretsch and Feldman, 1996](#)).

(2002), trade shares write :

$$\lambda_t^k(rs) = \frac{Z_t^k(s) (x_t^k(s) \tau_{rs}^k)^{-\theta^k}}{\sum_l^N Z_t^k(l) (x_t^k(l) \tau_{rl}^k)^{-\theta^k}} \quad (4.6)$$

where $\lambda_t^k(rs)$ is the share of expenditures from region s and sector k in region r total expenditures from sector k. The price index for industry k in region r is therefore, with Γ^k a constant and $1 + \theta^k > \sigma^k$:

$$P_t^k(r) = \Gamma^k \left(\sum_{l=1}^N Z_t^k(l) [x_t^k(l) \tau_{rl}^k]^{-\theta^k} \right)^{-1/\theta^k} \quad (4.7)$$

Finally, market clearing at t in r means that labor income in sector k equals the labor share of global expenditures from location r and sector k product : $w_t(r)L_t^k(r) = \chi^k \sum_l^N \lambda_t^k(lr) [w_t(l)L_t^k(l)]$, with χ^k the share of goods from sector k in location's expenditures. Combining this equation for both sectors yield a clearing equation from which guess on wage can be updated for the period equilibrium.

4 Production in exact hat algebra

In exact hat algebra, change in unit price of an input bundle is :

$$\dot{x}_{t+1}^k(r) = (\dot{w}_{t+1}(r))^{\mu^k} (\dot{R}_{t+1}^k(r))^{1-\mu^k} \quad (4.8)$$

and from equation on rents I have that : $\dot{R}_{t+1}^k(r) = \frac{\dot{w}_{t+1}(r)}{\dot{H}_{t+1}^k(r)} \dot{L}_{t+1}^k(r)$ and $\dot{H}_{t+1}^k(r) = 1$. Finally, in dynamic hat algebra, change in price index writes :

$$\dot{P}_{t+1}^k(r) = \left(\sum_{l=1}^N \lambda_t^k(lr) \dot{Z}_{t+1}^k(l) [\dot{x}_{t+1}^k(l)]^{-\theta^k} \right)^{-1/\theta^k} \quad (4.9)$$

Change in trade flows writes :

$$\lambda_{t+1}^k(rs) = \frac{\dot{Z}_{t+1}^k(s) (\dot{x}_{t+1}^k(s))^{-\theta^k}}{\sum_l^N \lambda_t^k(lr) \dot{Z}_{t+1}^k(l) (\dot{x}_{t+1}^k(l))^{-\theta^k}} = \dot{Z}_{t+1}^k(s) \left(\frac{\dot{x}_{t+1}^k(s)}{\dot{P}_{t+1}^k(r)} \right)^{-\Theta^k} \quad (4.10)$$

3 Estimation of dose-response functions

Climate impacts now come into play. They multiplicatively affect sectoral productivity and amenities, thereby distorting market clearing and the distribution of populations and economic activities over time. I follow the insights of [Eaton and Kortum \(2002\)](#) that trade flows contain information on productivity, and insights from [Rudik et al. \(2022\)](#) that migration flows contain information on amenity value. I use the equilibrium conditions of the model governing bilateral migration and trade flows to estimate impact of regional climates on regional amenities and productivities. I follow a procedure close to [Rudik et al. \(2022\)](#) with more countries, different datasets and relative levels of temperature distributions winsoring rather than absolute temperature bounds. This procedure guarantees internal validity of my estimates, i.e. model-consistent amenity and productivity dose-response functions. Indeed, I leverage the model's structure at equilibrium, so that the non-linear dose-response functions account for the dynamic and spatial interactions modelled in my framework. Finally, the estimates are more robust to spatial autocorrelation than standard panel fixed-effect approaches.

1 Regional amenities

The intuition behind this estimation is that an observed change in bilateral migration flows, controlling for changes in relative populations and outputs, migration costs and country and time fixed effects, as well as differences in annual distribution of daily mean temperatures between countries allows to identify non-linear impacts of an additional day in a temperature bin on amenity value. Indeed, the model at equilibrium yields :

$$\log \left(\frac{\mu_t(rs)}{\mu_t(rr)} \right) = \frac{1}{\Omega} \log \left(\frac{\bar{a}_{t-1}(s)}{\bar{a}_{t-1}(r)} \right) - \frac{\lambda}{\Omega} \log \left(\frac{L_t(s)}{L_t(r)} \right) + \frac{1}{\Omega} \log \frac{y_t(s)}{y_t(r)} + \frac{1}{\Omega} \log(m(r,s)) + \frac{1}{\Omega} (f(T_t(s), \zeta_a) - f(T_t(r), \zeta_a)) \quad (4.11)$$

The left hand side is the ratio of households who move to location s (r, s) versus stay in the original location r (r, r) from t-1 to t. The right side has five components. The first component is the ratio of non-weather time-invariant idiosyncratic amenities. The second and third components are the difference in population and output. The fourth component is the difference in time-invariant migration costs. Finally, I estimate the non-linear marginal impact of an additional day in a temperature bin on amenity values, ζ_a , from $f(T_t(s), \zeta_a) - f(T_t(r), \zeta_a)$. Arbitrarily, I use a third-degree orthogonal polynomial smoothing across daily 1°C binned mean temperatures for f. For the empirical estimation, I combine

[Abel and Cohen \(2019\)](#) data on international migrations flows from 1990 to 2019 with World Bank population and GDP per country estimates and [Hersbach et al. \(2020\)](#)'s climate reanalysis (ERA5) for daily mean surface temperatures. I process the climate reanalysis to aggregate it at the country level, weighting the 0.25° temperature observations by population levels. The estimation with Poisson Pseudo Maximum Likelihood and ψ_{rs} an origin-destination fixed effect, is :

$$\log \left(\frac{\mu_t(rs)}{\mu_t(rr)} \right) = -\frac{\lambda}{\Omega} \log \left(\frac{L_t(s)}{L_t(r)} \right) + \frac{1}{\Omega} \log \left(\frac{y_t(s)}{y_t(r)} \right) + \frac{1}{\Omega} (f(T_t(s), \zeta_a) - f(T_t(r), \zeta_a)) + \psi_{rs} + \delta_t + \epsilon_{rst} \quad (4.12)$$

with a congestion elasticity of regional amenities to population, $\lambda = 0.32$, taken from [Desmet et al. \(2018b\)](#). The regression is done on a temperature distribution that is winsorized at 95% so that the tails do not drive results.

Variable	Coefficient	p-value
First-Degree Orthogonal Polynomial	-2.21e-03	3.84e-03
Second-Degree Orthogonal Polynomial	-1.23e-03	3.26e-02
Third-Degree Orthogonal Polynomial	-9.26e-04	2.30e-02
Wald test, joint significance	1.81e+01	4.20e-04

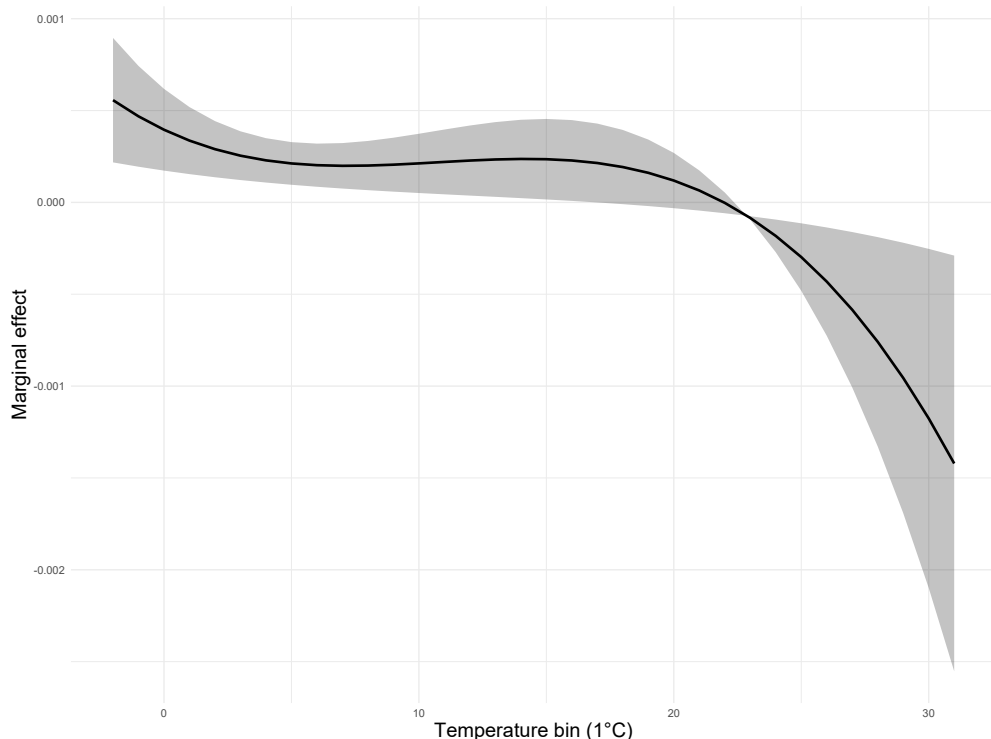


FIGURE 4.3 – Non-linear marginal effect (in %) of an additional day in the 1°C temperature bin on regional amenities. Estimates are computed with 95% confidence intervals. The regression is done with 95% winsorized bins [-2°C : 31°C] for 194.032 observations.

In this dose-response function, estimates are for myopic households as my global approach does not allow to solve a fully dynamic migration decisions for 12674 locations. This approach with myopic households might underestimate negative marginal effects of low temperatures on regional amenities as shown in [Rudik et al. \(2022\)](#), which might explain why the marginal effect of low temperature on regional amenity is positive. As suggested in [Albouy et al. \(2016\)](#) for US households, we find a positive effect of moderate temperatures (around 18°C) on amenity value and large and increasing negative value of excess heat on the amenity value, consistent with observations on US data that households will pay more on the margin to avoid excess heat than cold. Finally, as amenity values are inferred from migration flows, a drawback of this estimation approach is that standard migration costs which are commensurable with changes in amenity values cannot be distinguished from the impossibility of migrating, such as administrative barriers, which are not. But I do not think that there is a reason to believe that it specifically biases a temperature bin over another.

2 Regional productivities

I follow a close procedure for regional productivities. The intuition behind this estimation is that an observed change in bilateral trade flows at the product level, controlling for changes in relative input costs, trade costs, and country and time fixed effects, as well as differences in annual distribution of daily mean temperatures between countries allows to identify nonlinear impacts of an additional day in a temperature bin on productivity value for the specific product. At equilibrium, expenditures of region n on industry k goods from region i write :

$$X_t^k(rs) = \left(\Gamma^k\right)^{-\theta^k} \frac{Z_t^k(s)(x_t^k(s))^{-\Theta^k}(\tau_t^k(rs))^{-\Theta^k}}{(P_t^k(r))^{\Theta^k}} X_t^k(r) \quad (4.13)$$

Normalizing by importer's own expenditures X_{rr}^k in industry k, using the expression for Z_{it}^k and taking the logarithm on both sides of the equation yields :

$$\log\left(\frac{X_t^k(rs)}{X_t^k(rr)}\right) = [g(T_t(s); \zeta_Z^k) - g(T_t(r); \zeta_Z^k)] + \log\left(\frac{\bar{Z}_t^k(s)}{\bar{Z}_t^k(r)}\right) - \theta^k \log(\tau_t^k(rs)) - \theta^k \log\left(\frac{x_t^k(s)}{x_t^k(r)}\right) \quad (4.14)$$

The left hand side is the ratio of expenditures on products of sector k from another region i to expenditures on products of sector k produced domestically. In equilibrium, it is equal to four terms. The first term on the right is the marginal difference in productivity between i and n due to climate impacts. Arbitrarily, I use a third-degree orthogonal polynomial smoothing across the regional annual

distribution of daily 1°C binned mean temperatures. The second term is the difference in productivity due to non-weather fundamental differences. The third term are iceberg trade costs between i and n. The fourth term is the relative price of inputs. For the empirical estimation, I combine BACI CEPII dataset for yearly sectoral international trade from 1995 to 2019 with World Bank population and GDP per country and sectors and [Hersbach et al. \(2020\)](#)'s climate reanalysis (ERA5) for annual distributions of daily mean surface temperatures at the country level. I process the climate reanalysis to aggregate it at the country level, weighting the 0.25° daily mean temperature observations with GHSL-POP population weights. I include tariffs in the fixed effects as data on tariffs (preferential and most-favoured nation) and non-tariffs trade costs τ from WITS database is very incomplete. I estimate the following regression with PPML :

$$\log \left(\frac{X_t^k(rs)}{X_t^k(rr)} \right) = I_k * [g(T_t(s); \zeta_Z^k) - g(T_t(r); \zeta_Z^k)] + \zeta_X X_t^k + \rho_t^k + \phi_{ni}^k + \epsilon_{nit}^k \quad (4.15)$$

with ρ_t^k sector-year fixed effects and ϕ_{ni}^k importer-exporter-sector fixed effects. With X_t , I proxy for unobserved relative input costs with sectoral GDP per capita. Values for θ^k are taken from [Caliendo and Parro \(2015\)](#). Estimates are done at ISIC Rev.3 product level and the sector-specific response functions come from a regression where I interact the response function g with a set I_k of two sector dummy variables : agriculture and non-agriculture. The sector-specific regression is done on a distribution that is winsorized at 95%, so that the tails of the temperature distributions do not drive the results.

Variable	Coefficient	p-value
First-Degree Orthogonal Polynomial - Agriculture	1.57e-02	2.81e-08
First-Degree Orthogonal Polynomial - Non Agriculture	-2.02e-02	9.58e-02
Second-Degree Orthogonal Polynomial - Agriculture	-3.20e-02	0.00e+00
Second-Degree Orthogonal Polynomial - Non Agriculture	-2.22e-02	8.75e-04
Third-Degree Orthogonal Polynomial - Agriculture	-1.70e-02	0.00e+00
Third-Degree Orthogonal Polynomial - Non Agriculture	-2.07e-02	4.49e-03
Wald test, joint significance (Agriculture)	2.62e+02	0.00e+00
Wald test, joint significance (Non Agriculture)	3.01e+01	1.31e-06

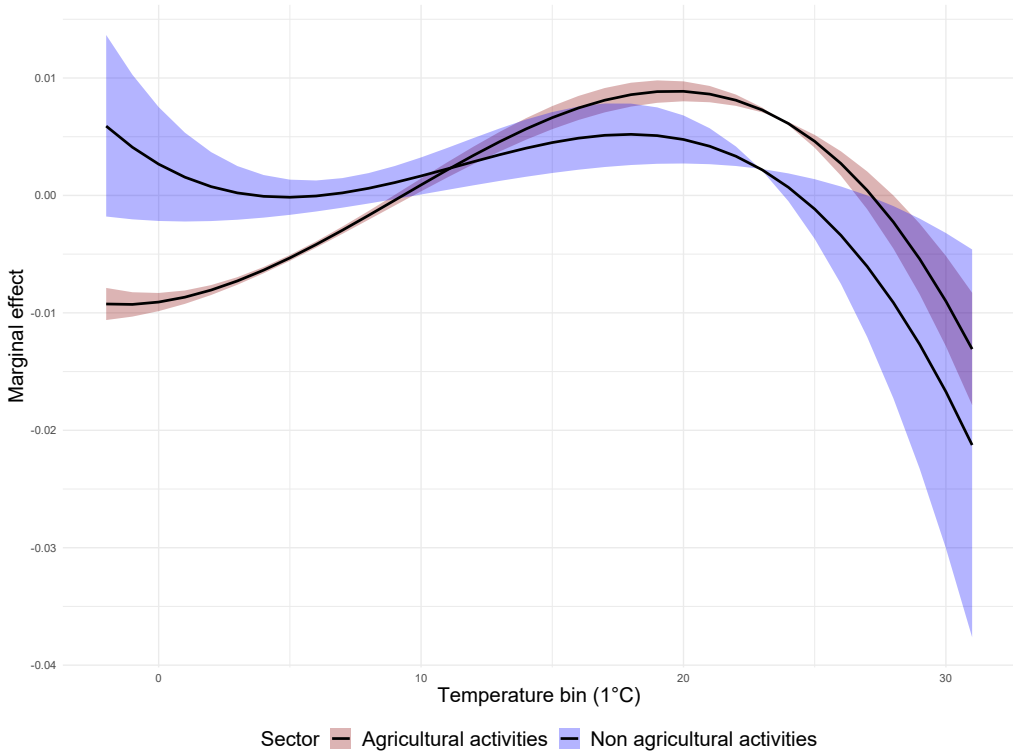


FIGURE 4.4 – Non-linear marginal effect of an additional day in the 1°C temperature bin on regional sectoral productivities

Estimates are computed from regression (4.12) with 95% confidence intervals and third-order orthogonal polynomials. The regression is done with 95% winsorized bins [-2°C : 31°C] for N=14.527.500 observations. For the simulations, I assume that below and above these thresholds, marginal effects remain constant.

As in [Rudik et al. \(2022\)](#), and consistent with previous literature ([Burke et al., 2015](#)), I find substantial evidence of negative impacts from elevated mean daily temperatures on sectoral productivity, affecting both agricultural and non-agricultural activities. Surprisingly, the marginal effects are more pronounced in non-agricultural sectors, even if confidence intervals are wider. Two factors may explain this finding. First, I employ a winsorizing technique at 31°C computed from the temperature distribution rather than an absolute threshold. This approach may wrongly reflect extreme temperature effects on agriculture, particularly at very high temperatures, due to a lack of sufficient observations. Second, since the analysis infers climate change impacts on sectoral productivity from trade flows, the estimates are on products and people that are engaging in international trade. This might distort the estimated damage since agricultural sectors involved in export may be more competitive and adaptable, potentially underestimating the full extent of climate impacts. Related to this interpretation, a limitation of my estimation approach is that it does not allow for the estimation of dose-response

functions for certain goods and services that are either untraded or non-tradable, such as transportation, education, healthcare, real estate, and local services like restaurants.

For agricultural sectors, I observe a bell-shaped relationship, with an optimal temperature for productivity around 20°C, consistent with results such as those of [Conte et al. \(2021\)](#). A key limitation in comparing my results to prior studies lies however in the use of daily average temperature bins rather than annual averages, which alters the form of temperature-productivity relationships. For non-agricultural sectors, I observe positive productivity effects for non-agricultural sectors on colder days (around and below 0°C). This result might be related to the differentiated effects identified by [Burke et al. \(2015\)](#), where wealthier countries—which might be disproportionately represented in trade data for non-agricultural products—demonstrate a greater capacity to adapt to lower temperatures. This distinction between rich and poor countries in their responses to temperature variations could explain the observed resilience of non-agricultural productivity to colder conditions.

4 Numerical results

1 Model resolution

Given the distribution of labor across markets $L_t \equiv \{L_t^k(r)\}_{r=1,k=0}^{N,K}$, location-industry fundamental productivities $Z_t \equiv \{Z_t^k(r)\}_{r=1,k=0}^{N,K}$, location-specific fundamental amenities $a_t \equiv \{a_t(r)\}_{r=1}^N$, I define a time-t momentary equilibrium as a vector of wages $w_t \equiv \{w_t(r)\}_{r=1}^N$ and aggregate price index $P_t \equiv \{P_t(r)\}_{r=1}^N$ satisfying equilibrium conditions of the static multi-regional and multi-industry trade model. Let $\dot{\mu}_t \equiv \{\dot{\mu}_t(rs)\}_{r=1,s=1,t=1}^{N,N,\infty}$, $\dot{a}_t \equiv \{\dot{a}_t\}_{t=1}^\infty$, $\dot{u}_t \equiv \{\dot{u}_t\}_{t=1}^\infty$ be migration shares, amenities, and lifetime utilities changes respectively. Given an initial allocation of labor L_0^k , initial migration flows, initial sectoral trade flows, initial time-invariant exogenous fundamentals (migration costs, non-weather fundamental productivities and amenities, local structures), and a path of time-varying exogenous fundamentals (amenities, productivities, land uses and climate change), I define a sequential competitive equilibrium as a sequence of $\{L_t, \mu_t, u_t, w_t\}_{t=0}^\infty$ that solves the temporary equilibrium at each time t. Finally, I define a stationary equilibrium as a sequential competitive equilibrium such that the sequence $\{L_t, \mu_t, u_t, w_t\}_{t=0}^\infty$ is constant for every t. The intuition behind this approach is that observed data (migration flows, wages) are a good proxy for unobserved

characteristics (migration costs, productivities) and that this observed data provides sufficient information to bypass the estimation of some fundamentals, for instance idiosyncratic non-weather regional amenities, to project future decisions by agents that include the distribution of this unobserved characteristics.

Some more datasets are needed at 1° gridded level for the simulations. I use 2015 GHSL-POP gridded population distribution and population-weighted country-level estimates of the share of employment in labour from World Bank. Exogenous productivity paths are taken from SSP database and downscaled to 1° zone for SSP2 based on 2015 population coverage. For productivity paths, I take the mean of two modelling approaches for SSP2 : OECD Env-Growth and IIASA. Population projections are taken from [KC et al. \(2024\)](#) SSP2 projections without migration. I use [Conte et al. \(2021\)](#) gridded sectoral initial bilateral sectoral trade flows. Agricultural and non-agricultural wages are computed using [Kummu et al. \(2018\)](#) gridded estimates of GDP per capita and population-weighted country-level estimates of the labour share of total income from ILOSTAT.

The initial bilateral migration flows are computed from [Kummu et al. \(2018\)](#) and [Abel and Cohen \(2019\)](#) : the gridded flows are constructed so that they match international migration flows, and internal migrations are built from within-country population-weighted net gridded migration stocks. There are two main issues with the modeling of migrations. First, when migration are fully dynamic, models cannot be solved at both global scale and fine resolution, while it would be useful to keep both characteristics. Applications with fully dynamic decisions ([Caliendo et al., 2019; Balboni, 2019; Rudik et al., 2022](#)) are for a subset of countries⁴. A second issue regarding migration dynamics is data availability at the right resolution : data is scarce, especially outside the USA. I keep a worldwide resolution ([Cruz and Rossi-Hansberg, 2024](#)) rather than restricting the analysis to the USA ([Caliendo et al., 2019; Bilal and Rossi-Hansberg, 2023](#)) or subset of countries for which rich migration data are available ([Rudik et al., 2022](#)). I reconstruct gridded migration flows from both international migration flows and gridded net migration stocks in a simplistic way that probably underestimate them but this first-order and fully explicit approximation relies on best-available gridded data products ([Kummu et al., 2018; Abel and Cohen, 2019](#)) and can be checked for robustness. Another avenue would be to invert the model to recover fundamentals such as migration costs, but it is also based on important modelling assumptions regarding the estimation of regional fundamental amenities.

4. Recent advances include using deep neural networks ([Azinovic et al., 2022](#)) or perturbation approaches ([Bilal and Rossi-Hansberg, 2023](#)) could allow to keep both fully dynamic decisions and global 1° gridded approach. I leave work on these methodologies for future research.

2 Counterfactual climates and policies

To evaluate the aggregate welfare consequences of global warming and the welfare consequences of the biophysical channels, I compare at the global scale the present discounted value of regional utilities that are not idiosyncratic, namely,

$$W_0 = \sum_{r \in N} \sum_{t=0}^{\infty} \beta^t u_{t+1}(r) = \sum_{r \in N} \sum_{t=0}^{\infty} \beta^t \dot{a}_{t+1}(r) \dot{y}_{t+1}(r) \quad (4.16)$$

In my approach, as in [Cruz and Rossi-Hansberg \(2024\)](#), I thus focus on changes in how individuals value the amenity and production characteristics of a location under changing climate. A drawback of this choice, discussed in [Desmet et al. \(2018a\)](#), is that the welfare cost computed does not include two components : the mobility costs incurred to get there and the idiosyncratic preferences of individuals who live there.

I simulate the model in three alternative settings.

Simulation 1 - without climate change In this benchmark simulation, I compute the distribution of future sectoral economic activities, population and trade flows that clear markets in each location at all future periods under the assumption that there is no climate change, i.e. no deviation in the annual distribution of daily mean temperatures in each location.

Simulation 2 - under biogeochemical SSP2-4.5 In the second simulation, I use bias-adjusted ([Lange, 2019](#)) and down-scaled projections from five CMIP6 Earth System Models forced with SSP2-RCP4.5 emissions under the assumption of fixed 2015 land use : GFDL-ESM4, IPSL-CM6A-LR, MPI-ESM1-2-HR, MRI-ESM2-0. More specifically, I construct a synthetic annual distribution of daily mean temperatures for each 1° location taking the average over five years. Thus, I can have a better proxy of the underlying climate distribution from which weather from a given year is drawn and capture some internal variability in climate, for instance due to El Niño. I compute the distribution of future sectoral economic activities, population and trade flows that clear markets in each location at all future periods under these nonlinear deformations in the annual distributions of daily mean temperatures in each location. The deviation between this simulation and the first one allows to compute the aggregate and distributional welfare impact of exogenous biogeochemical change along SSP2-4.5.

Simulation 3 - under both biogeochemical and biophysical SSP2-4.5 In the third simulation, I add the biophysical impacts driven by urban and agricultural

land demands to the exogenous biogeochemical projections, using the mapping between LULC changes and biophysical impacts that applies in this specific 1° Koppen Geiger climate zone at a given time period. The distribution of daily mean temperature in year t is the sum of exogeneous SSP2-4.5 scenarii and biophysical channels over each month within a year (net transitions to croplands) and over a year (transitions to urban areas). The comparison between this simulation and the second one allows to compute the aggregate and distributional welfare consequences of biophysical channels.

3 Benchmark biogeochemical climate impacts (SSP2-4.5)

First, I plot on the left graph of Figure (4.5) the 2100 future climate under SSP2-4.5 with respect to the 2015 distribution of temperatures, treating each location as a unit. The distortion of annual daily mean temperature distributions is less pronounced than in SSP5-8.5 or equivalent carbo-intensive pathways previously assessed ([Cruz, 2021](#); [Krusell and Smith Jr, 2022](#)). Indeed, annual average temperature increases only from 15°C in 2015 to 17.3°C in 2100, i.e. a 2.3°C increase in mean annual surface temperature over our gridded locations of interest. On the right graph on Figure (4.5), I compare two shifts in the global intra-annual distribution of daily mean temperatures between 2015 and 2100. In red, I plot the difference in the frequency of a given mean daily temperature in the annual distribution using actual climate projections, i.e. I show how more frequent a given temperature is on average at the annual scale and over all locations in 2100 climate in comparison with 2015 initial climate conditions. In green, I apply a shape-preserving shift in annual mean to the 2015 distribution in blue on the left graph : I add to each mean temperature bin in 2015 the mean global annual difference between 2015 and 2100 in climate projections. This shift is approximate and illustrative as I round this shift again to match it to climate projections. These graphs show that even when aggregated to the global level, there are large changes in the shape of the intra-annual distribution of daily mean temperatures that are not perfectly summarized by the annual mean deviation. This non-linearity is accounted for in our approach where we use the whole distribution of daily mean temperature to estimate climate impacts from the equilibrium conditions of the model and simulate their welfare consequences along our scenario.

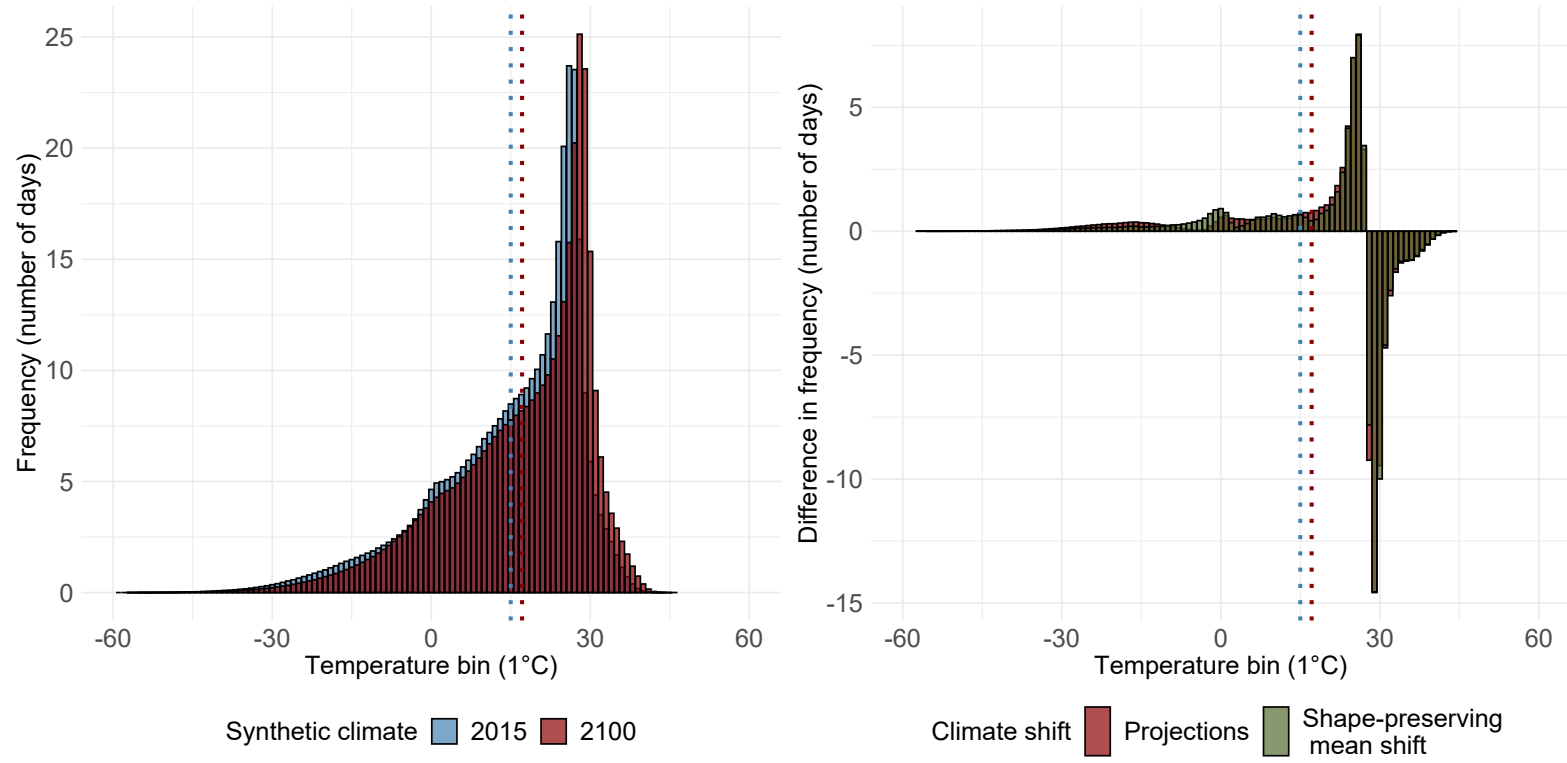


FIGURE 4.5 – **Left** Synthetic global annual distributions of daily mean temperatures in 2015 (in blue) and 2100 (in red), under SSP2-4.5, for all gridded locations studied in the paper. **Right** Shifts from 2015 to 2100 in the frequency of daily mean temperatures per temperature bin (in number of days) for climate projections (in red) and for a synthetic shape-preserving approximate annual mean shift.

In the approximate climate shift, the annual mean increase observed between the two distributions 2015 and 2100 is added to each bin of the 2015 distribution. Dotted lines represent average annual mean surface temperature. I treat each location as one unit.

I analyze both the aggregate and distributional welfare effects of climate change under the SSP2-4.5 scenario, focusing on locations where data is available (e.g. Libya is excluded due to missing data) and where population and economic activity were present in 2015. Thus, my analysis centers on the intensive margin of adaptation, considering only existing areas and not the extensive margin—such as migration to currently uninhabited regions or the emergence of economic activity in areas with none in 2015. As there is no data on population and economic flows to reliably calibrate such predictions for these areas, I believe projections on this extensive margin would require a level of external model validity that is hard to achieve. In Figure 4.7, I present the distribution of changes in amenities and sectoral productivities across 12,674 gridded locations, using estimated dose-response functions.

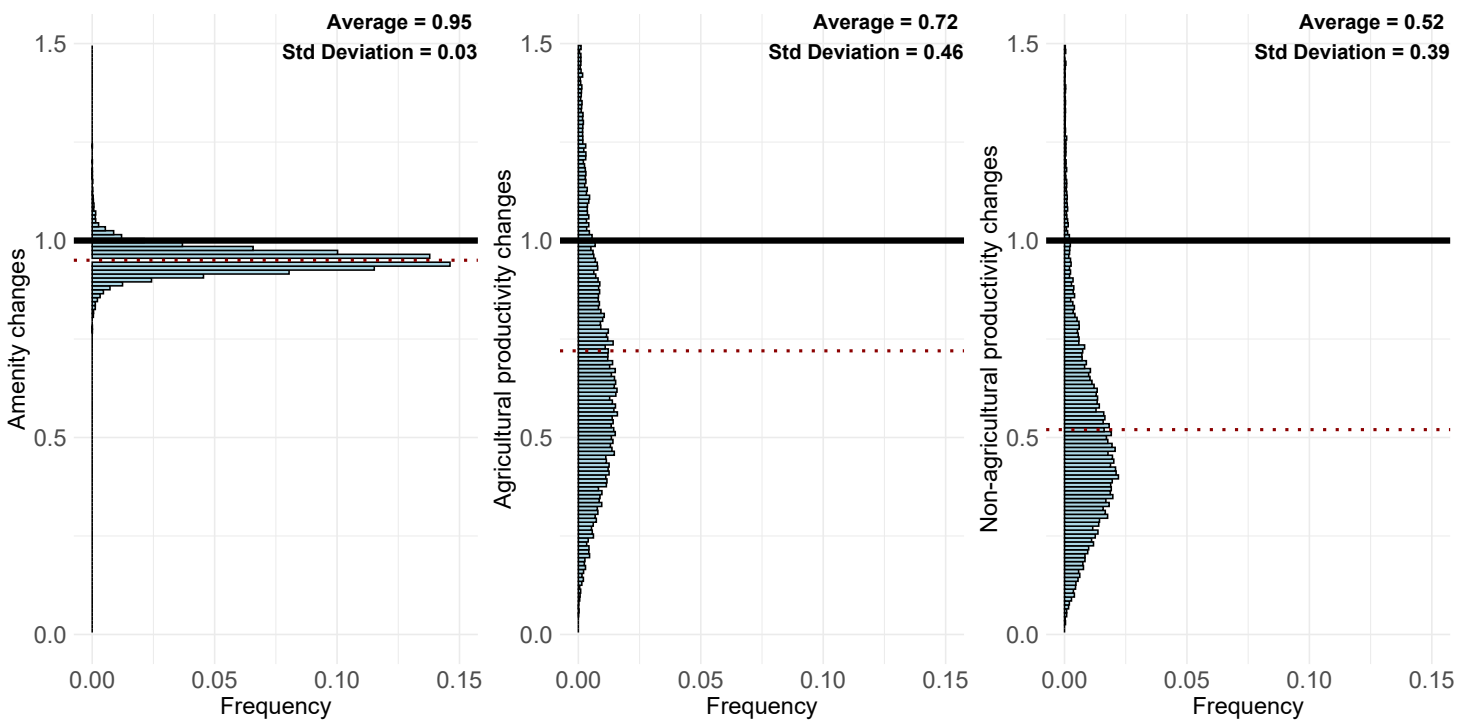


FIGURE 4.6 – Ratio of amenity (left), agricultural productivity (middle), non-agricultural productivity (right) changes between scenario 2 with SSP2-4.5 forced with biogeochemical anthropogenic impacts and scenario 1 without climate change.

For sectoral productivities, I winsorize the top of the distribution at 1.5 for illustration.

This graph yields three main conclusions. First, the average impact of climate change is negative for amenities and sectoral productivities. As in [Cruz \(2021\)](#) and as suggested by our dose-response functions, the marginal impact on amenity is one order of magnitude below the marginal nonlinear impact of temperatures on sectoral productivities. Indeed, mean amenity changes are 5% with respect to baseline, while mean sectoral productivity changes are as large as 28% and 48% for agricultural and non-agricultural productivities. Second, in comparison with previous estimates yielding benefits from climate change for amenities and sectoral productivities in many locations, the impacts of climate change are negative for almost all locations when the entire intra-annual temperature distribution is considered. Even if some moderate daily mean temperatures have positive impacts on these variables in our dose-response functions, the aggregate effect is negative. Third, the impacts for sectoral productivities are much more dispersed than the impacts of climate change on amenities : most of the spatial heterogeneity will therefore come from these channels. I then study how these changes in sectoral amenities and productivities translate into welfare impacts, once the adaptation of agents is taken into account. In Figure (4.7), I plot the dis-

tribution of changes in welfare in scenario 2 with biogeochemical climate change with respect to baseline scenario 1 without climate change.

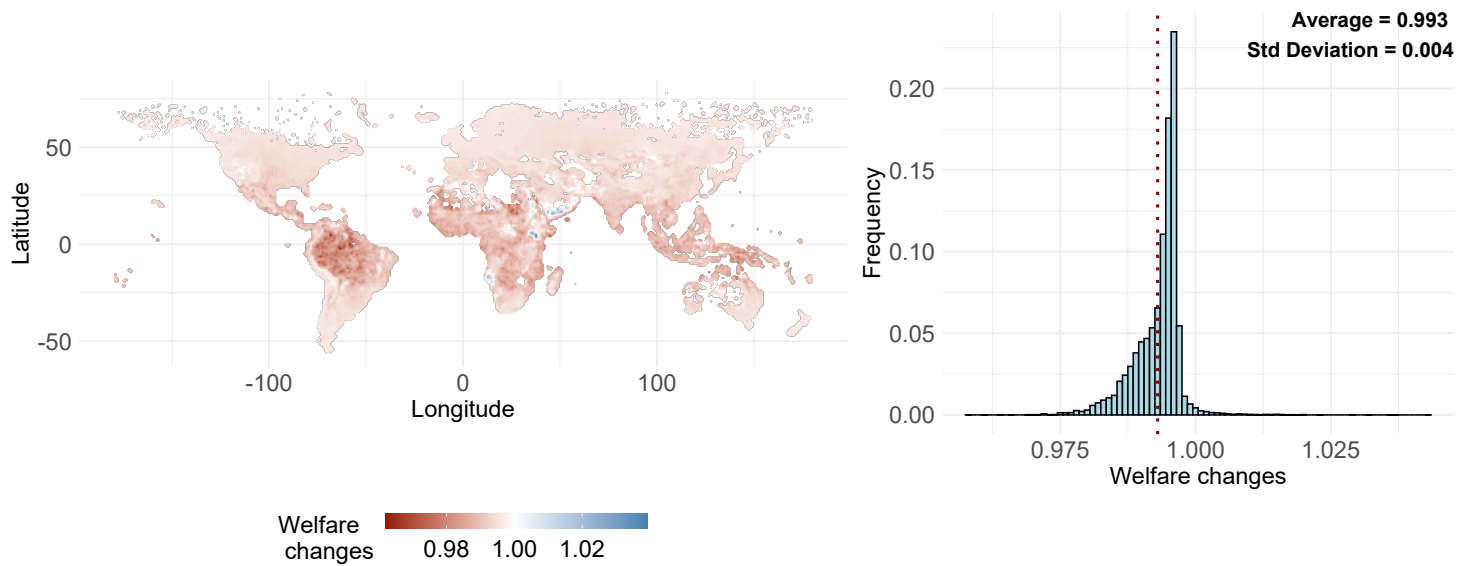


FIGURE 4.7 – Ratio of welfare changes between scenario 2 with SSP2-4.5 climate impacts and counterfactual scenario 1 without climate change, plotted on a map (left) and on an histogram (right).

On the map, transitions between gridded locations are smoothed. The dotted red line represents the avarage effect across locations.

Figure (4.7) highlights two key findings. First, the mean welfare change under the SSP2-4.5 scenario is negative, with a 0.7% decline in welfare, equivalent to the 0.7% decrease estimated by [Cruz \(2021\)](#) for RCP6.0, despite RCP6.0 being a more carbon-intensive pathway. Second, with few exceptions driven by specific regional climates, such as the southern Arabian Peninsula, the marginal impact of climate change under SSP2-4.5 is negative across most regions. Contrary to previous estimates, I find no evidence of marginal benefits from climate change in northern locations. Since my analysis incorporates the intra-annual distribution of daily mean temperatures interacted with non-linear dose-response functions based on these distributions, the resulting welfare changes do not follow a simple isomorphic relationship to annual time-invariant temperature scalers that mimic polar amplification. The changes in annual temperature distributions are more complex than a uniform shift in the mean. These non-linear warming patterns, when combined with the non-linear response of welfare to temperature variations within the year, result in non-linear welfare impacts.

4 Counterfactual exogenous biophysical impacts (SSP2-4.5)

Building on the baseline estimates that include the biogeochemical impacts of climate change, I now assess the relative contribution of biophysical channels through LULC changes—the effects of albedo, evapotranspiration, and surface roughness. Figure 4.8 illustrates the distribution of welfare changes in scenario 3, which incorporates biophysical channels, relative to scenario 2, where only climate change impacts from the carbon cycle are considered without biophysical effects. These welfare changes are expressed as a fraction of the total change between scenarios 2 and 1, reflecting the standard climate impact estimates under SSP2-4.5, excluding biophysical channels. Thus, the estimates give the share the biophysical impacts represent in the standard biogeochemical estimates of the welfare impacts of climate change along SSP2-4.5.

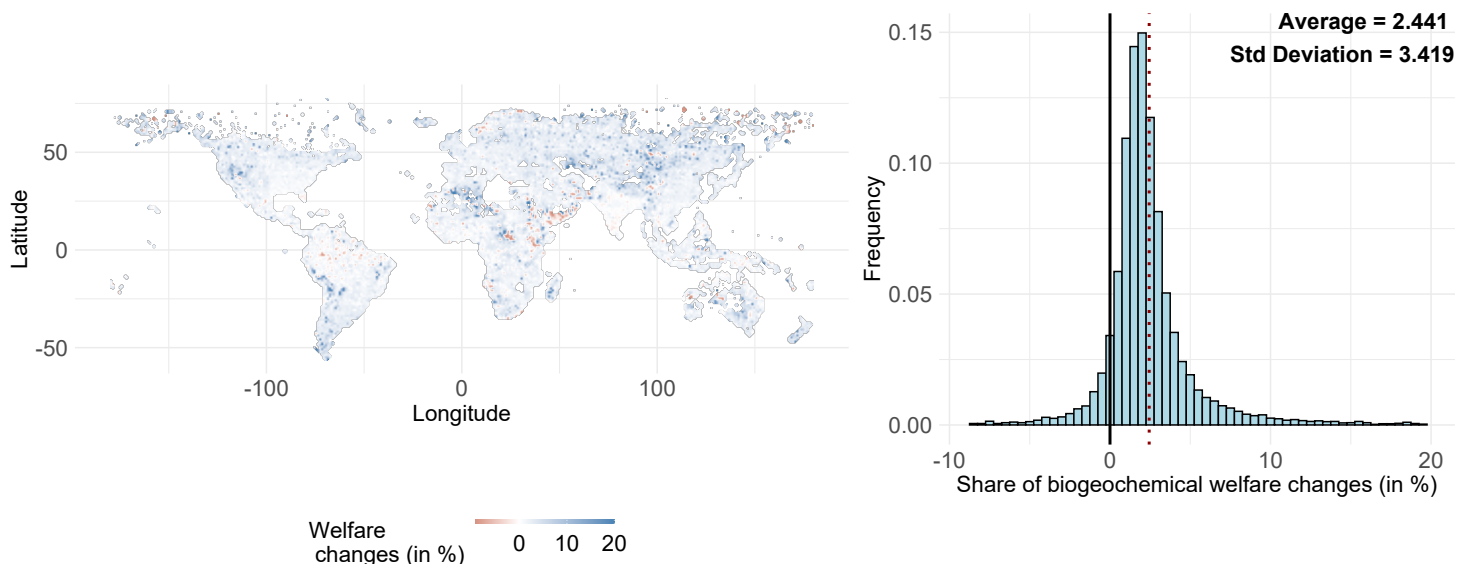


FIGURE 4.8 – Share of welfare changes (in %) between scenario 3 with both SSP2-4.5 biogeochemical and biophysical channels and counterfactual scenario 2 without biophysical channels in the change between scenario 1 and scenario 2, plotted on a map (left) and on an histogram (right).

On the map, transitions between gridded locations are smoothed. The distribution are 98% winsorized for illustration. The dotted red line represents the average welfare change.

Figure (4.8) provides two key insights. First, biophysical channels account for a non-negligible portion of the welfare impacts of climate change typically estimated from biogeochemical factors under SSP2-4.5, i.e. when temperature downscaling is assumed to be linear, time-invariant and exogenous to regional economic activities. Specifically, these regional biophysical processes, driven by LULC changes, contribute approximately 2.4% to the overall welfare impacts cur-

rently attributed to climate change. Regional economic activity does shape regional climate impacts. Second, the effects of these biophysical channels are predominantly negative across most regions.

Once I have retrieved the aggregate welfare impact of the biophysical channels, I estimate their distributional impacts with respect to standard biogeochemical climate impacts. In Figure (4.9), I plot the distribution of welfare impacts under biogeochemical impacts (left), under both biogeochemical and biophysical impacts (middle) , the distribution of the share of biophysical welfare impacts with respect to standard biogeochemical impacts (right) against the log of 2015 GDP per capita (ppp USD).

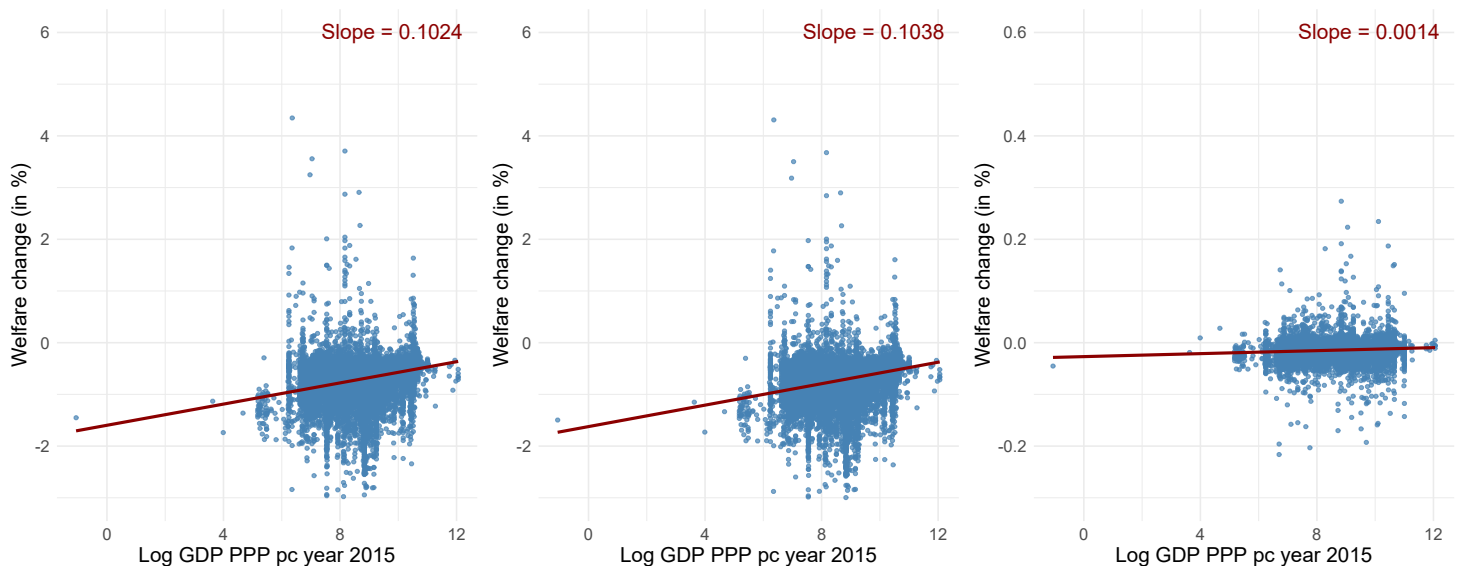


FIGURE 4.9 – Distributional impacts of biogeochemical and biophysical channels along SSP2-4.5 **Left** Biogeochemical only with respect to no climate change (scenario 2 and scenario 1) **Middle** Both biogeochemical and biophysical impacts with respect to no climate change (scenario 3 and scenario 1). **Right** Deviation between scenario 2 and scenario 3 (scenario 3 and scenario 2).

The red lines represent correlation, fitted using a linear regression model.

Figure (4.9) shows that the biogeochemical climate impacts are regressive, affecting more the poorest 2015 location. Indeed, a simple linear regression suggests that a 1% increase in GDP per capita yields a 0.1% decrease in welfare change with respect to the baseline simulation without climate impacts. Biophysical impacts further exacerbate the regressivity of biogeochemical impacts, by a 0.001% decrease in marginal welfare impacts for a 1% increase in 2015 GDP per capita. Thus, biophysical channels imply a 1% increase in the slope of the regressivity of standard biogeochemical climate impacts.

5 Discussion

As our understanding of the mechanisms through which human activities and climate impacts interact goes further, I investigate a mechanism qualitatively distinct from the traditional biogeochemical one : the biophysical channel by which LULC changes bring regional climate impacts because of changes in albedo, evapotranspiration and soil roughness. While this mechanism might be negligible at a global scale in the first-order computation of the impacts of climate change, it does have heterogeneous regional effects that should be scrutinized carefully because they can cascade into large aggregate welfare effects and distributional consequences. In this paper, I quantify how and how much the regional biophysical channel of climate impacts driven by land use land cover changes matter. I first build a reduced-form representation of the regional biophysical feedbacks. Then, I leverage a dynamic quantitative spatial economic model applied to climate change with an explicit modelling of adaptation through trade, migration and changes in sectoral specialization. Furthermore, I estimate model-consistent dose-response functions of regional amenities and sectoral productivities to changes in the annual distribution of daily mean temperatures. Finally, I take the theoretical setting to the data at 1° gridded global scale. I solve the model with dynamic exact hat algebra and compare a baseline with forward-looking agents under ‘middle-of-the-road’ SSP2-4.5 without regional biophysical feedback to the counterfactuals with regional LULC changes and biophysical feedbacks. I compute the distributional and aggregate welfare impact for benchmark model and under counterfactual climates regarding LULC.

In conclusion, my analysis demonstrates that regional economic activity plays a significant role in shaping regional climate impacts. By incorporating biophysical channels into the assessment of SSP2-4.5, I find that these channels account for an additional 2.5% of the biogeochemical impacts on welfare, on average. The effects are unevenly distributed, influenced by both socioeconomic factors—such as urban land-use changes and transitions from shrublands or forests to croplands—and by shifting climate zones. Notably, the impacts of biophysical channels are predominantly negative across regions and, like biogeochemical effects, are regressive, disproportionately affecting lower-income regions based on 2015 income levels. In both scenarii of future climate impacts, interacting intra-annual warming patterns with non-linear damage functions from temperature bins implies that nearly all regions will suffer from the impacts of climate change, with no significant benefits expected in the Northern Hemisphere.

A future direction, which is already underway for this paper, is to endogenize marginal deviations from SSP2-4.5 in land-use change. I use the exogenous MESSAGE-Globiom scenario SSP2-4.5 as a first approximation. But around this benchmark SSP2-4.5 from which I calibrate productivity and population exogenous paths, climate impacts and endogenous adaptation decisions (migration, sectoral specialization and trade) drive marginal changes in LULC changes in comparison with the standard MESSAGE-Globiom scenario. I could map marginal changes in the model input stemming from endogenous adaptation decisions in my quantitative spatial model to changes in model output around this scenario with a flexible statistical relationship, e.g. a surrogate model with gaussian processes (GP) to emulate the more complex land-use model. Alternative avenues could be taken, each with its limits. First, I could use reduced-form econometrics on historical data, but there is no exogenous variation to leverage, be it an instrument or a quasi-experimental setting. Panel fixed effect approaches ([Chen et al., 2020](#)) are affected by endogeneity and simultaneity as the authors have no control over the data-generating process. Second, I could build a complete dynamic model of land use changes including a market for crops, for land prices, etc., as well as assumptions about agricultural and urban policies. But the dynamic relation in the competition for land use would be computationally demanding and hard to calibrate at the global 1° gridded scale. This GP approach might be adapted for four main reasons. First, it allows me to map marginal deviations around an established exogenous scenario SSP2-4.5 building on robust land-use models. Second, I have control over the data-generating process, both exogenous scenario for drivers and mechanistic relations between variables of interest. Third, the GP is flexible : it is a non-parametric regression tool where I do not define a specific functional form to the input-output mapping ex-ante and I can handle non-linear relations. Fourth, GP allows uncertainty quantification as they are probability distribution over a function space.

There are other limits to my approach. First, I should include other impacts, as LULC changes have large impacts on other planetary limits, for instance biodiversity. Second, I could estimate counterfactual policies to reduce the welfare cost of these biophysical channels, for instance zero net land take or irrigation policies ([Braun and Schlenker, 2023](#)). Finally, I would like to explore further impacts, for instance precipitation ([Devaraju et al., 2015; Smith et al., 2023](#)) and its interaction with temperature changes (e.g. wet bulbs). Water cycle indeed raises concerns not only because of deforestation ([Grosset et al., 2023](#)), but also following urbanization ([Sui et al., 2024](#)). These investigations are left for further research.

6 Appendix

1 Migration in hat algebra

I write the change in bilateral migration flows in dynamic exact hat algebra. Starting from the initial equation for bilateral migration flows, I write the equation in time differences :

$$\dot{\mu}_{r,s,t+1} = \frac{\frac{u_{t+1}(s)^{1/\Omega} m(s)^{-1/\Omega}}{\sum_{n \in N} u_{t+1}(n)^{1/\Omega} m(n)^{-1/\Omega}} - \frac{u_t(s)^{1/\Omega} m(s)^{-1/\Omega}}{\sum_{n \in N} u_t(n)^{1/\Omega} m(n)^{-1/\Omega}}}{\frac{u_t(s)^{1/\Omega} m(s)^{-1/\Omega}}{\sum_{n \in N} u_t(n)^{1/\Omega} m(n)^{-1/\Omega}}} \quad (4.17)$$

Then, as migration costs are assumed to be time-invariant :

$$\dot{\mu}_{r,s,t+1} = \frac{\dot{u}_{t+1}(s)^{1/\Omega}}{\frac{\sum_{n \in N} u_{t+1}(n)^{1/\Omega} m(n)^{-1/\Omega}}{\sum_{n \in N} u_t(n)^{1/\Omega} m(n)^{-1/\Omega}}} \quad (4.18)$$

I have that :

$$\dot{\mu}_{r,s,t+1} = \frac{\dot{u}_{t+1}(s)^{1/\Omega}}{\frac{\sum_{n \in N} u_{t+1}(n)^{1/\Omega} m(n)^{-1/\Omega} \frac{u_t(n)^{1/\Omega} m(n)^{-1/\Omega}}{u_t(n)^{1/\Omega} m(n)^{-1/\Omega}}}{\sum_{n \in N} u_t(n)^{1/\Omega} m(n)^{-1/\Omega}}} \quad (4.19)$$

This yields the equation of interest.

2 Profit maximization

Profit in sector k (i.e. good i), location r, writes (symmetry between varieties ω) :

$$\Pi_t^k(r) = p_t^k(r) z_t^k(r) L_t^k(r)^{\mu^k} H_t^k(r)^{1-\mu^k} - w_t(r) L_t^k(r) - R_t^k(r) H_t^k(r) \quad (4.20)$$

First-order conditions of profit maximization problem write :

$$\frac{\partial \Pi_t^k(r)}{\partial L_t^k(r)} = 0 \quad (4.21)$$

$$\frac{\partial \Pi_t^k(r)}{\partial H_t^k(r)} = 0 \quad (4.22)$$

Thus :

$$\mu^k p_t^k(r) z_t^k(r) L_t^k(r)^{\mu^k-1} H_t^k(r)^{1-\mu^k} - w_t(r) = 0 \quad (4.23)$$

$$(1 - \mu^k) p_t^k(r) z_t^k(r) L_t^k(r)^{\mu^k} H_t^k(r)^{-\mu^k} - R_t^k(r) = 0 \quad (4.24)$$

Replacing $p_t^k(r)$ yields :

$$R_t^k(r) H_t^k = \frac{1 - \mu^k}{\mu^k} w_t(r) L_t^k \quad (4.25)$$

3 Prices and bilateral trade flows in exact hat algebra

Starting from the definition of prices (4.7), I write :

$$\dot{P}_{n,t+1}^k = \left(\sum_{l=1}^N \frac{Z_{l,t+1}^k [x_{l,t+1}^k \tau_{nl,t+1}^k]^{-\theta^k}}{\sum_{m=1}^N Z_{m,t}^k [x_{m,t}^k \tau_{nm,t}^k]^{-\theta^k}} \right)^{-1/\theta^k} \quad (4.26)$$

Multiplying and dividing each element in the summation just as what I have done for migration :

$$\dot{P}_{n,t+1}^k = \left(\sum_{l=1}^N \frac{Z_{l,t+1}^k [x_{l,t+1}^k \tau_{nl,t+1}^k]^{-\theta^k} \frac{Z_{l,t}^k [x_{l,t}^k \tau_{nl,t}^k]^{-\theta^k}}{Z_{l,t}^k [x_{l,t}^k \tau_{nl,t}^k]^{-\theta^k}}}{\sum_{m=1}^N Z_{m,t}^k [x_{m,t}^k \tau_{nm,t}^k]^{-\theta^k}} \right)^{-1/\theta^k} \quad (4.27)$$

Using trade flows from equation (4.10), I have the equation of interest (as trade costs are time invariant). Similarly for trade flows, I multiply and divide the numerator of (4.10) by $Z_{it}^k (x_{it}^k \tau_{nit}^k)^{-\Theta^k}$ and do the same for each element of the summation of the denominator :

$$\lambda_{nit+1}^k = \frac{Z_{it+1}^k (x_{it+1}^k \tau_{nit+1}^k)^{-\Theta^k} \frac{Z_{it}^k (x_{it}^k \tau_{nit}^k)^{-\Theta^k}}{Z_{it}^k (x_{it}^k \tau_{nit}^k)^{-\Theta^k}}}{\sum_l Z_{lt+1}^k (x_{lt+1}^k \tau_{nl,t+1}^k)^{-\Theta^k} \frac{Z_{lt}^k (x_{lt}^k \tau_{nl,t}^k)^{-\Theta^k}}{Z_{lt}^k (x_{lt}^k \tau_{nl,t}^k)^{-\Theta^k}}} \quad (4.28)$$

Which yields :

$$\lambda_{nit+1}^k = \frac{\dot{Z}_{it+1}^k (\dot{x}_{it+1}^k)^{-\Theta^k} Z_{it}^k (x_{it}^k \tau_{nit}^k)^{-\Theta^k}}{\sum_l \dot{Z}_{lt+1}^k (\dot{x}_{lt+1}^k)^{-\Theta^k} Z_{lt}^k (x_{lt}^k \tau_{nl,t}^k)^{-\Theta^k}} \quad (4.29)$$

Then, dividing by the sum :

$$\dot{\lambda}_{nit+1}^k = \frac{\dot{Z}_{it+1}^k (\dot{x}_{it+1}^k)^{-\Theta^k}}{\sum_l \lambda_{nlit}^k \dot{Z}_{lt+1}^k (\dot{x}_{lt+1}^k)^{-\Theta^k}} \quad (4.30)$$

4 Welfare

We study :

$$W_0 = \sum_{r \in N} \sum_{t=0}^{\infty} \beta^t i u_{t+1}(r) = \sum_{r \in N} \sum_{t=0}^{\infty} \beta^t \dot{a}_{t+1}(r) \dot{y}_{t+1}(r) \quad (4.31)$$

We have the equation for amenity changes. Changes in real income write :

$$\dot{y}_{t+1}(r) = \frac{\left(\sum_{k=1}^K (L_{t+1}^k(r)/L_{t+1}(r)) w_{t+1}^k(r) \right)}{\left(\prod_{k \in K} \dot{P}_t^k(r) \chi^k \right) \left(\sum_{k=1}^K (L_t^k(r)/L_t(r)) w_t^k(r) \right)} \quad (4.32)$$

5 Dose-response functions

At equilibrium :

$$\frac{\mu_{r,s,t}}{\mu_{r,r,t}} = \frac{u_t(s)^{1/\Omega} m(r,s)^{-1/\Omega}}{u_t(r)^{1/\Omega} m(r,r)^{-1/\Omega}} = \frac{(a_t(s) y_t(s))^{1/\Omega} m(r,s)^{-1/\Omega}}{(a_t(r) y_t(r))^{1/\Omega} m(r,r)^{-1/\Omega}} \quad (4.33)$$

Which yields :

$$\log \left(\frac{\mu_{r,s,t}}{\mu_{r,r,t}} \right) = -\frac{\lambda}{\Omega} \log \left(\frac{L_t(s)}{L_t(r)} \right) + \frac{1}{\Omega} \log \left(\frac{\bar{a}_{t-1}(s)}{\bar{a}_{t-1}(r)} \right) + \frac{1}{\Omega} \log(m(r,s)) + \frac{1}{\Omega} \log \frac{y_t(s)}{y_t(r)} + \frac{1}{\Omega} (f(T_{s,t}, \zeta_a) - f(T_{r,t}, \zeta_a)) \quad (4.34)$$

6 Migration data

The key gap in our simulations is the matrix of intersectoral bilateral migration flows. First of all, I do not have data on sectoral migration at this grid level and at the global scale : I thus focus on bilateral migration flows without sector-specific mobility. Then, I combine a dataset $M_{c1,c2}^{inter}$ of 5-years international bilateral migration flows between c_1 (out) and c_2 (in) for each pair of N countries from 2010 to 2015 ([Abel and Cohen, 2019](#)) with gridded data of net migration stocks from 2010 to 2015 M_z^{intra} for each 1° gridded zone z from [Kummu et al. \(2018\)](#). The procedure, detailed in annex, has two steps. First, I compute the probability of international inflows and outflows for each zone times country based on net

migration stocks and assign international migration flows based on these probabilities. Then, once international migration flows are deducted from net gridded migration stocks for each zone*country, I compute within-country migration flows between each region zone*country based on probability of intra-migration flows given gridded net migration stocks net of inter-country migration flows. I then aggregate the flow at 1° zone level. My procedure probably underestimates migration flows (i.e. overestimates migration costs) but I unfortunately do not have gridded births and deaths data to reconstruct migration flows à la [Abel and Cohen \(2019\)](#). For robustness, I run simulations with lower migration costs.

- Compute the share $s_{z,c,L2010}$ of each 1° zone z that is in country c based on 2010 population at level 0.1° . Compute the net migration stock $M_{z,c}^{intra} = s_{z,c,L2010} * M_z^{intra}$ of each pair (c,z) based on these population weights
- Normalize net migration stock at country c level for inflows
 $\bar{M}_{z,c}^{inflows} = M_{z,c}^{intra} + min_c(M_{z,c}^{intra})$
which yields a probability of international inflows for each (c,z)
 $P_{z,c}^{inflows} = \bar{M}_{z,c}^{inflows} / sum_c(\bar{M}_{z,c}^{inflows})$
- Normalize net migration stock at country c level for outflows, i.e. :

$$\bar{M}_{z,c}^{outflows} = - \left(M_{z,c}^{intra} - max_c(M_{z,c}^{intra}) \right) \quad (4.35)$$

, which yields a probability of international outflows for each (c,z) :

$$P_{z,c}^{outflows} = \bar{M}_{z,c}^{outflows} / sum_c(\bar{M}_{z,c}^{outflows}) \quad (4.36)$$

- Assign bilateral international migration flows (in and out) for each country c to each zone z based on these probabilities to obtain (1) $MB_{z1,z2}$ the 1° bilateral matrix of international migration flows and (2) $M_{z,c}^{intra-net}$, i.e. stock of migration flows at gridded-country level net of international migration flows.
- For each zone z1 in c :
 1. If stock in z1 is positive, compute the probability of receiving internal flows from all other z2. Normalize net migration stock at country c level for inflows for all z2, i.e. $\bar{M}_{z2,c}^{inflows,net} = M_{z2,c}^{intra,net} + min_c(M_{z2,c}^{intra,net})$, which yields a probability of internal inflows for each (c,z1,z2), $P_{z2,c}^{inflows,net} = \bar{M}_{z2,c}^{inflows,net} / sum_{c-z1}(\bar{M}_{z2,c}^{inflows,net})$
 2. If stock in z1 is negative, compute the probability of sending internal flows to all other z2. Normalize net migration stock at country c level for inflows for all z2, i.e. $\bar{M}_{z2,c}^{inflows,net} = -(M_{z2,c}^{intra,net} - max_c(M_{z2,c}^{intra,net}))$,

which yields a probability of internal inflows for each $(c, z1, z2)$, $P_{z2,c}^{outflows,net} = \bar{M}_{z2,c}^{outflows,net} / \sum_{c-z1} (\bar{M}_{z2,c}^{outflows,net})$

- Add these internal flows to our matrix $MB_{z1,z2}$.

7 Algorithm

Algorithm. Solve period by period the sequential competitive equilibrium given an initial allocation $(L_0^k, w_0^k, \mu_{i,n,0}, \lambda_{i,n,0})$ and an anticipated convergent sequence of changes in fundamentals, $\{\dot{\Theta}_t\}_{t=0}^\infty$ (regional productivities and amenities affected by exogenous biogeochemical climate impacts). without changes in LULC and biophysical channel. From this baseline scenario, I compute distributional and aggregate welfare impact of climate change along SSP2-4.5. The counterfactual [without climate change] is the same algorithm but with no climate impacts.

- Scenario 1 : without climate impacts. In this baseline scenario, I compute the distribution of people and activity without future climate impacts.
- Scenario 2 : with SSP2-4.5 climate impacts, without biophysical impacts. In this first counterfactual, I compute the distribution of people and activity and the aggregate and distributional welfare impacts of exogenous SSP2-4.5 without land use changes.
- Scenario 3 : with SSP2-4.5 climate impacts and exogenous biophysical impacts. In this second counterfactual, I compute the distribution of people and activity and the aggregate and distributional welfare impacts of exogenous SSP2-4.5 with exogenous land use changes from MESSAGE-Globiom model.

Algorithm 1 Resolution

Inner loop solves the static equilibrium at each time period t . Outer loop computes path for fundamental variables given market clearing at each time t in each location r .

- Make an initial convergent (to 1 when T large) guess for the path of expected lifetime utilities expressed in time differences $\{\dot{u}_{r,t}^0\}_{t=0,r=1}^{T,N}$, where the superscript (0) indicates a guess.;
 - While [outer loop] convergence criteria not met (tolerance, nb of loops)
 1. For all t , use $\{\dot{u}_{r,t}^{(0)}\}_{t=0,r=1}^{T,N}$ and $\{\mu_{r,n,0}\}_{r=1,n=1}^{N,N}$ to solve for the path of $\{\mu_{r,n,t}\}_{t=0,r=1,n=1}^{T,N,N}$.
 2. For all t , use equation for population dynamics, $\{\mu_{r,n,t}\}_{t=0,r=1,n=1}^{T,N,N}$, $\{L_{r,0}^k\}_{r=1,k=1}^{T,N,K}$ and SSP2 exogenous birth & death rates scenarii to get $\{L_{r,t}^k\}_{t=0,r=1,k=1}^{T,N,K}$
 3. Select climate scenario and recover the path of regional productivity and amenity changes in each r $\{\dot{Z}_t^k(r)\}_{t=0,r=1,k=1}^{T,N,K}$, $\{\dot{a}_t(r)\}_{t=0,r=1}^{T,N}$ from the scenario using estimated dose-response functions and exogenous productivity growth rates.
 4. For [inner loop] each period $t > 0$
 - Define a guess for wages $\{\dot{w}_{r,t+1}^{(0)}\}_{t=0,r=1}^{T,N}$
 - Obtain $\{\dot{x}_{r,t+1}^k\}_{r=1,k=1}^{N,K}$ using $\{L_t^k(r)\}_{r=1,k=1}^{N,K}$ and guess for $\{\dot{w}_{r,t+1}\}_{r=1}^N$.
 - Use $\{\dot{x}_{r,t+1}^k\}_{r=1,k=1}^{N,K}$, $\{\dot{Z}_t^k(r)\}_{r=1,k=1}^{N,K}$ and $\{\lambda_{rn,t}^k\}_{r=1,n=1,k=1}^{N,N,K}$ to obtain $\{\dot{P}_{r,t+1}^k\}_{r=1,k=1}^{N,K}$
 - Obtain $\{\lambda_{rn,t+1}^k\}_{r=1,n=1,k=1}^{N,N,K}$ from $\{\dot{P}_{r,t+1}^k\}_{r=1,k=1}^{N,K}$, $\{\dot{Z}_t^k(r)\}_{r=1,k=1}^{N,K}$, $\{\dot{x}_{r,t+1}^k\}_{r=1,k=1}^{N,K}$ and $\{\lambda_{rn,t}^k\}_{r=1,n=1,k=1}^{N,N,K}$
 - Compute $\{\dot{w}_{r,t+1}\}_{r=1}^N$ and check if market clears in each location
 - Update $\{\dot{w}_{r,t+1}^{(0)}\}_{r=1}^N$ if market does not clear
 - If market clears at t , compute aggregate price index $\{\dot{P}_{r,t+1}\}_{r=1}^N$ using fixed share of each good in worker's expenditure
 5. Repeat for each t to obtain at each period the momentary equilibrium and recover full paths of $\{\dot{w}_{n,t+1}\}_{t=0}^T$ and $\{\dot{P}_{r,t+1}\}_{t=0,r=1}^{T,N}$, which gives change in worker's real income.
 - For each t , compute $\{\dot{u}_{t+1}(r)\}_{t=0,r=1}^{T,N}$ and change in worker's real income using $\{\dot{w}_{r,t+1}\}_{t=0,r=1}^{T,N}$ and $\{\dot{P}_{r,t+1}\}_{t=0,r=1}^{T,N}$. Check if $\{\dot{u}_{t+1}(r)\}_{t=0,r=1}^{T,N} \approx \{\dot{u}_{t+1}^{(0)}(r)\}_{t=0,r=1}^{T,N}$ according to convergence criterion. If not, go back to first step and update initial outer guess.
-

Bibliographie

- G. J. Abel and J. E. Cohen. Bilateral international migration flow estimates for 200 countries. *Scientific data*, 6(1) :82, 2019.
- G. M. Ahlfeldt, S. J. Redding, D. M. Sturm, and N. Wolf. The economics of density : Evidence from the berlin wall. *Econometrica*, 83(6) :2127–2189, 2015.
- C. Albert, P. Bustos, and J. Ponticelli. The effects of climate change on labor and capital reallocation. Technical report, National Bureau of Economic Research, 2021.
- D. Albouy, W. Graf, R. Kellogg, and H. Wolff. Climate amenities, climate change, and american quality of life. *Journal of the Association of Environmental and Resource Economists*, 3(1) :205–246, 2016.
- R. Alkama and A. Cescatti. Biophysical climate impacts of recent changes in global forest cover. *Science*, 351(6273) :600–604, 2016.
- D. B. Audretsch and M. P. Feldman. R&d spillovers and the geography of innovation and production. *The American economic review*, 86(3) :630–640, 1996.
- M. Azinovic, L. Gaegauf, and S. Scheidegger. Deep equilibrium nets. *International Economic Review*, 63(4) :1471–1525, 2022.
- C. A. Balboni. *In harm's way? infrastructure investments and the persistence of coastal cities*. PhD thesis, London School of Economics and Political Science, 2019.
- L. Barrage and W. Nordhaus. Policies, projections, and the social cost of carbon : Results from the dice-2023 model. *Proceedings of the National Academy of Sciences*, 121(13) :e2312030121, 2024.
- H. E. Beck, T. R. McVicar, N. Vergopolan, A. Berg, N. J. Lutsko, A. Dufour, Z. Zeng, X. Jiang, A. I. van Dijk, and D. G. Miralles. High-resolution (1 km) köppen-geiger maps for 1901–2099 based on constrained cmip6 projections. *Scientific data*, 10(1) :724, 2023.
- A. Bilal and E. Rossi-Hansberg. Anticipating climate change across the united states. Technical report, National Bureau of Economic Research, 2023.
- L. R. Boysen, V. Brovkin, J. Pongratz, D. M. Lawrence, P. Lawrence, N. Vuichard, P. Peylin, S. Liddicoat, T. Hajima, Y. Zhang, et al. Global climate response to idealized deforestation in cmip6 models. *Biogeosciences*, 17(22) :5615–5638, 2020.
- T. Braun and W. Schlenker. Cooling externality of large-scale irrigation. Technical report, National Bureau of Economic Research, 2023.
- M. Burke, S. M. Hsiang, and E. Miguel. Global non-linear effect of temperature on economic production. *Nature*, 527(7577) :235–239, 2015.
- L. Caliendo and F. Parro. Estimates of the trade and welfare effects of nafta. *The Review of Economic Studies*, 82(1) :1–44, 2015.

- L. Caliendo, M. Dvorkin, and F. Parro. Trade and labor market dynamics : General equilibrium analysis of the china trade shock. *Econometrica*, 87(3) :741–835, 2019.
- T. Chakraborty and Y. Qian. Urbanization exacerbates continental-to regional-scale warming. *One Earth*, 2024.
- G. Chen, X. Li, X. Liu, Y. Chen, X. Liang, J. Leng, X. Xu, W. Liao, Y. Qiu, Q. Wu, et al. Global projections of future urban land expansion under shared socioeconomic pathways. *Nature communications*, 11(1) :537, 2020.
- N. Coeurdacier, F. Oswald, and M. Teignier. Structural change, land use and urban expansion. 2022.
- B. Conte, K. Desmet, D. K. Nagy, and E. Rossi-Hansberg. Local sectoral specialization in a warming world. *Journal of Economic Geography*, 21(4) :493–530, 2021.
- J.-L. Cruz. Global warming and labor market reallocation. *Unpublished Manuscript*, 2021.
- J.-L. Cruz and E. Rossi-Hansberg. The economic geography of global warming. *Review of Economic Studies*, 91(2) :899–939, 2024.
- K. Desmet and E. Rossi-Hansberg. Climate change economics over time and space. *Annual Review of Economics*, 16, 2024.
- K. Desmet, R. E. Kopp, S. A. Kulp, D. K. Nagy, M. Oppenheimer, E. Rossi-Hansberg, and B. H. Strauss. Evaluating the economic cost of coastal flooding. Technical report, National Bureau of Economic Research, 2018a.
- K. Desmet, D. K. Nagy, and E. Rossi-Hansberg. The geography of development. *Journal of Political Economy*, 126(3) :903–983, 2018b.
- N. Devaraju, G. Bala, and A. Modak. Effects of large-scale deforestation on precipitation in the monsoon regions : Remote versus local effects. *Proceedings of the National Academy of Sciences*, 112(11) :3257–3262, 2015.
- G. Duveiller, J. Hooker, and A. Cescatti. A dataset mapping the potential biophysical effects of vegetation cover change. *Scientific data*, 5(1) :1–15, 2018a.
- G. Duveiller, J. Hooker, and A. Cescatti. The mark of vegetation change on earth’s surface energy balance. *Nature communications*, 9(1) :679, 2018b.
- G. Duveiller, L. Caporaso, R. Abad-Viñas, L. Perugini, G. Grassi, A. Arneth, and A. Cescatti. Local biophysical effects of land use and land cover change : towards an assessment tool for policy makers. *Land Use Policy*, 91 :104382, 2020.
- J. Eaton and S. Kortum. Technology, geography, and trade. *Econometrica*, 70(5) :1741–1779, 2002.
- F. Eckert and M. Peters. Spatial structural change. Technical report, National Bureau of Economic Research, 2022.

- J. Fernández-Villalverde, K. T. Gillingham, and S. Scheidegger. Climate change through the lens of macroeconomic modeling. Technical report, National Bureau of Economic Research, 2024.
- R. Fillon, M. Linsenmeier, and G. Wagner. Climate shift uncertainty and economic damage. Technical report, working paper, 2024.
- M. Georgescu, D. B. Lobell, and C. B. Field. Direct climate effects of perennial bioenergy crops in the united states. *Proceedings of the National Academy of Sciences*, 108(11) :4307–4312, 2011.
- F. Grossset, A. Papp, and C. Taylor. Rain follows the forest : Land use policy, climate change, and adaptation. *Climate Change, and Adaptation (December 1, 2023)*, 2023.
- J. V. Henderson, B. Y. Jang, A. Storeygard, and D. N. Weil. Climate change, population growth, and population pressure. Technical report, National Bureau of Economic Research, 2024.
- H. Hersbach, B. Bell, P. Berrisford, S. Hirahara, A. Horányi, J. Muñoz-Sabater, J. Nicolas, C. Peubey, R. Radu, D. Schepers, et al. The era5 global reanalysis. *Quarterly Journal of the Royal Meteorological Society*, 146(730) :1999–2049, 2020.
- J. Hooker, G. Duveiller, and A. Cescatti. A global dataset of air temperature derived from satellite remote sensing and weather stations. *Scientific data*, 5(1) :1–11, 2018.
- B. Huang, X. Hu, G.-A. Fuglstad, X. Zhou, W. Zhao, and F. Cherubini. Predominant regional biophysical cooling from recent land cover changes in europe. *Nature communications*, 11(1) :1066, 2020.
- G. C. Hurtt, L. Chini, R. Sahajpal, S. Frolking, B. L. Bodirsky, K. Calvin, J. C. Doelman, J. Fisk, S. Fujimori, K. K. Goldewijk, et al. Harmonization of global land-use change and management for the period 850–2100 (luh2) for cmip6. *Geoscientific Model Development Discussions*, 2020 :1–65, 2020.
- S. KC, M. Dhakad, M. Potančoková, S. Adhikari, D. Yıldız, M. Mamolo, T. Sobotka, K. Zeman, G. Abel, W. Lutz, et al. Updating the shared socioeconomic pathways (ssps) global population and human capital projections. 2024.
- B. Kleinman, E. Liu, and S. J. Redding. Dynamic spatial general equilibrium. *Econometrica*, 91(2) :385–424, 2023.
- P. Krusell and A. A. Smith Jr. Climate change around the world. 2022.
- M. Kummu, M. Taka, and J. H. Guillaume. Gridded global datasets for gross domestic product and human development index over 1990–2015. *Scientific data*, 5(1) :1–15, 2018.
- S. Lange. Trend-preserving bias adjustment and statistical downscaling with isimip3bsd (v1. 0). *Geoscientific Model Development*, 12(7) :3055–3070, 2019.
- D. M. Lawrence, G. C. Hurtt, A. Arneth, V. Brovkin, K. V. Calvin, A. D. Jones, C. D. Jones, P. J. Lawrence, N. de Noblet-Ducoudré, J. Pongratz, et al. The land use model intercomparison project (lumip) contribution to cmip6 : rationale and experimental design. *Geoscientific Model Development*, 9(9) :2973–2998, 2016.

- G. Manoli, S. Fatichi, M. Schläpfer, K. Yu, T. W. Crowther, N. Meili, P. Burlando, G. G. Katul, and E. Bou-Zeid. Magnitude of urban heat islands largely explained by climate and population. *Nature*, 573(7772) :55–60, 2019.
- V. Masson-Delmotte, H. Pörtner, J. Skea, E. Buendía, P. Zhai, and D. Roberts. Climate change and land. *IPCC Report*, 2019.
- G. Michaels, F. Rauch, and S. J. Redding. Urbanization and structural transformation. *The Quarterly Journal of Economics*, 127(2) :535–586, 2012.
- I. Nath. Climate change, the food problem, and the challenge of adaptation through sectoral reallocation. 2022.
- W. Nordhaus. *A question of balance : Weighing the options on global warming policies*. Yale University Press, 2008.
- S. J. Redding and E. Rossi-Hansberg. Quantitative spatial economics. *Annual Review of Economics*, 9 :21–58, 2017.
- I. Rudik, G. Lyn, W. Tan, and A. Ortiz-Bobea. The economic effects of climate change in dynamic spatial equilibrium. 2022.
- B. D. Santer, T. M. Wigley, M. E. Schlesinger, and J. F. Mitchell. Developing climate scenarios from equilibrium gcm results. 1990.
- W. Schlenker and M. J. Roberts. Nonlinear temperature effects indicate severe damages to us crop yields under climate change. *Proceedings of the National Academy of sciences*, 106(37) :15594–15598, 2009.
- C. Smith, J. Baker, and D. Spracklen. Tropical deforestation causes large reductions in observed precipitation. *Nature*, 615(7951) :270–275, 2023.
- X. Sui, Z.-L. Yang, M. Shepherd, and D. Niyogi. Global scale assessment of urban precipitation anomalies. *Proceedings of the National Academy of Sciences*, 121(38) :e2311496121, 2024.
- L. Zhao, X. Lee, R. B. Smith, and K. Oleson. Strong contributions of local background climate to urban heat islands. *Nature*, 511(7508) :216–219, 2014.
- D. Zhou, J. Xiao, S. Frolking, L. Zhang, and G. Zhou. Urbanization contributes little to global warming but substantially intensifies local and regional land surface warming. *Earth's Future*, 10(5) :e2021EF002401, 2022.

Conclusion

An economic analysis of climate change operates at the intersection of four key dimensions central to the issue : time, space, stochastic risk, and scientific uncertainty. The interplay among these dimensions gives rise to two complementary questions, one normative and the other positive.

How do the uncertainties arising from these four dimensions affect optimal social choice at the Earth-Human interface ? These uncertainties, in my view, necessitate pursuing two interconnected but distinct agendas. First, we should improve the modelling of the spatio-temporal spectrum of possible futures given stochastic risk and scientific uncertainty about these possible futures. In other words, we should inform decisions with the best information available. Second, we should adopt social choice criteria that enable optimal judgments of these situations, ensuring citizens have flexible decision-making frameworks that accommodate diverse preference parameters across the four dimensions discussed. We can then separate our knowledge of possible futures from our attitude towards these various possible futures. Our understanding of potential futures should inform the development of appropriate social choice frameworks. When scientific uncertainty is the predominant issue, greater flexibility in decision-making in this dimension is necessary. When spatial heterogeneity is the key concern, inequality aversion may become more relevant. If the primary challenge lies in large aggregate risk from irreversible catastrophic events, social choice criteria should be adaptable enough to incorporate aversion to such risks.

In Chapter 1, we explore the validity conditions of expected utility in the presence of tipping point risk, where the aggregate risk on intertemporal utility is very high. This aggregate risk is high because of a particular characteristic of these catastrophic events compared to more standard extreme events such as natural disasters : their irreversible nature, at least on scales that are relevant for economic policy. Accordingly, we adjust our risk modeling approach, opting for a framework based on irreversible regime shift risk—characterized by transitions from one qualitative state to another—rather than volatility or reversible risks typically modeled along smooth macroeconomic trends. If the tipping threshold is crossed, the well-being of all future generations is low and positively correlated. In traditional expected utility models, planners exhibit neutrality toward aggregate risk. Hence, we explore alternative approaches that provide decision-makers

and the public with greater flexibility when confronting irreversible risks. Our conclusions, however, remain nuanced, as they depend on the estimated magnitude of the risk. As mentioned earlier, the process of modeling possible futures is inseparable from the task of collectively determining our stance toward them. If catastrophic risk is very important and has multiplier effects, then it may be wise to turn to a social choice criterion that places more weight on situations in the world where intertemporal welfare is low. Otherwise, it may be preferable to stick with expected utility, given the good normative properties of this functional form. Throughout this analysis, as well as in Chapter 2, we ensured the modeling of genuine stochastic risk. Our framework enables the social planner to explore the entire tree of possible outcomes and the full spectrum of potential futures. This has significant computational implications, as we employ global solution methods rather than relying on deterministic approaches or averaging deterministic outcomes.

In Chapter 2, we extend both approaches : offering a more comprehensive representation of possible futures and refining the social choice criterion to incorporate greater flexibility in addressing aversion to scientific uncertainty. Our aim was to depict tipping point risks more precisely, using calibrated dynamics in which potential catastrophes emerge as properties of the dynamic system, rather than as stylized phenomena with arbitrary probabilities defined *ex ante*. Analytically, we delve deeper into the interactions between various types of risks over time. Specifically, we examine the relationship between standard aggregate climate risks—such as the transient climate response to cumulative emissions, which involves uncertainty in how carbon emissions drive temperature changes and their subsequent economic impacts—and subsystem idiosyncratic risks, which affect the dynamics of the system itself. Additionally, we account for scientific uncertainty, a crucial factor that permeates the analysis of these subsystems, as highlighted by the IPCC's use of confidence and probability scales, and the ongoing debates within climate science over tipping risks. In particular, we model two distinct forms of uncertainty : uncertainty about the relationship between global climate change and the dynamics of the subsystem, and uncertainty regarding the functional form of these dynamic subsystem. More scientific uncertainty could be explored, particularly if they interact with uncertainty about the dynamics of the subsystems of interest.

How do the uncertainties stemming from the four dimensions outlined above—time, space, risk, and scientific uncertainty—influence our estimations

of future climate impacts at the Earth-human interface? Recent advances in climate economics have been less focused on time (e.g., refining our understanding of the dynamic economic impacts of climate change or extending analyses to long-term horizons like the millennium scale), risk (e.g., better comprehending the non-linear responses of societies to climate impacts), or scientific uncertainty (e.g., predicting its likely trajectory with a learning framework). The most significant developments have been in the spatial dimension. As the literature increasingly works at finer spatial scales, driven by the rapid growth in the availability of gridded data for decision-making, it is crucial to assess the implications for our existing methods and approximations, especially along two aspects. First, what holds true at the global scale may not apply at local or regional levels. Second, we must consider how advancements in one dimension impact our understanding of other dimensions in addressing climate challenges.

In Chapter 3, we demonstrate that due to the non-linear nature of climate-society relationships, regional dynamics play a critical role in climate impact projections : temporal and spatial aggregations alter the picture of welfare impacts and the risk ranking across climate models. These differences are driven by regional heterogeneity in both damage and warming patterns. Spatial disaggregation reveals how uncertainties in climate models regarding the full distribution of future weather outcomes cascade down to regional damage estimates. Furthermore, instead of extending the time horizon, we focus on how current annual temporal aggregation may distort climate impact projections. By using the full annual distribution of daily mean temperatures, we capture intra-annual variations in temperature patterns, avoiding reliance on arbitrary summary statistics of the high-dimensional climate vector, e.g. annual mean or number of days above a threshold. We could take this further by disaggregating the temporal dimension further, considering daytime and nighttime temperatures separately, to better capture phenomena like heatwave days.

In Chapter 4, I incorporate the regional biophysical impacts of land-use changes within a quantitative spatial model under the SSP2-4.5 scenario. These impacts arise from changes in albedo, evapotranspiration, and surface roughness, triggered by shifts from and to croplands and urbanization changes. Other biophysical impacts and land-use transitions could also be considered. I emphasize the importance of accounting for interactions between regional economic activities, global and regional physical changes, and their local impacts. These impacts also have spillover effects because people migrate, because of changes in relative prices,

sectoral specialization and trade patterns. It is crucial to address not only exogenous uncertainties when downscaling global climate change to local impacts, but also how local decisions influence these processes endogenously. Local land-use choices significantly shape future climate impacts and may undermine the expected benefits of adaptation measures. Many uncertainties beyond the primary effects of global emissions remain understudied. Although secondary in aggregate terms, these mechanisms can have important distributional consequences at the regional level and more precise qualitative effects on the models. Focusing solely on high-end scenarios like SSP5-8.5 restricts our ability to examine these more intricate dynamics.

This thesis enables me to offer some modest public policy recommendations.

First, not all climate risks are equal. Risks with multiplier effects and irreversible consequences should be addressed with greater urgency, warranting substantial emission reductions today. A similar conclusion could be drawn for repeated but reversible events that lead to irreversible damage over time. However, the potential non-linear interactions between human systems and repeated climate events remain underexplored — both in the damage function estimates within the econometrics literature and in theoretical models, where impacts are typically assumed to be additive.

Second, I propose policies for managing large climate subsystems, such as the Amazon rainforest. I recommend measuring the impact of carbon emissions on the dynamics of these subsystems to more equitably allocate responsibility for future changes in their behavior. This approach could also help raise funds to support Coasian incentive mechanisms for optimal management of these subsystems at the regional level. Moreover, considering the system's dynamics as a whole can enhance regional management, such as in cost-benefit analyses of deforestation in tropical forests, by factoring in the impact of marginal changes on the subsystem's long-term self-sustainability. While these mechanisms constitute a small part of the social cost of carbon, they represent significant amounts when applied to the global taxation of all GHG emissions.

Third, I advocate for regional decision-making that is more informed about climate uncertainty, particularly when downscaling global climate change to local impacts. Adaptation plans at finer scales, from national to local levels, should be designed to withstand the full distribution of possible futures, rather than focusing on an average scenario. The average scenario obscures significant uncertainties, which not only persist but often intensify at smaller scales. Crucially, it

also fails to account for the various sources of uncertainty. The quantifiable variance in regional climate impact projections is influenced by scenario uncertainty (differences in Shared Socioeconomic Pathways, SSPs), model uncertainty (variations in Earth System Models' responses to SSPs), internal variability (due to the chaotic nature of climate, varying across space and time), as well as decisions made in post-processing or bias-correction of ESM output. Additionally, regression uncertainty from impact models affects the estimation of damage functions. Differentiating and prioritizing these sources of uncertainty can provide clearer guidance for regional-scale decision-making.

Fourth, I call for adaptation policies that are robust to potential negative feedbacks on local climate impacts. Land-use changes have dramatic impacts on biodiversity and global climate change. They also affect regional climate impacts. In my work, I suggest carefully considering the feedback effects that our economic activities and adaptation actions to a given climate impact scenario may have on these regional impacts, as well as potential spillovers. These feedbacks are likely to reverse and reduce the welfare gains expected from adaptation along a warming scenario. Robust adaptation policies must account for these more complex interactions between economic activity, climate change and climate impacts at the regional scale to avoid maladaptation.

This research has several limitations. First, high-dimensional problems are often numerically intractable when integrating all dimensions simultaneously, necessitating a siloed approach to different dimensions. This segmentation means that the total welfare cost of these uncertainties is not fully considered. Often, it is assumed that the costs of each new uncertainty are additive, which is unlikely due to the dynamic interactions and interdependence among subsystems at the earth-human interface. Second, while physical knowledge has advanced significantly with gridded data, socio-economic data at a comparable scale and quality are generally lacking, especially outside OECD countries and China. Establishing a research center at Université Paris-Saclay to systematically develop harmonized datasets or implement harmonized downscaling practices for gridded socio-economic data globally could provide a substantial global public good and have a large research impact. Some researchers are already investigating these directions ([Mikou et al., 2024](#)).

These studies pave the way for numerous future research opportunities. Building on the four dimensions previously discussed, I aim to develop a more inte-

grated approach that bridges the positive and normative perspectives. My goal is to retain the detailed, evolving gridded spatial data from the positive approach, along with its insights into endogenous adaptation mechanisms. Simultaneously, I wish to preserve the optimal intertemporal ethical framework from the normative approach, which addresses economic risk, climate risk, and other critical issues such as biodiversity loss and planetary limits, including their complex interactions. To accomplish this, we need to model credible geophysical mechanisms and their interactions with economic activity. Additionally, advancing this approach will require improved modeling of system robustness, adaptability, and emergent properties that arise from complex interactions among system components—elements that cannot be predicted by analyzing components in isolation. Beyond space, time, risk, and scientific uncertainty, there are other intriguing aspects of the climate challenge and its policy implications to explore. These include system complexity (e.g., interactions, feedback loops), our attitude towards this complexity, and its interplay with conventional risk and scientific uncertainty levels and aversions ([Oprea, 2024](#)). Finally, further understanding is needed regarding preferences for managing unequal risk exposure, including both market and non-market impacts across various scales (such as health) and differing adaptive capacities. This exploration may lead to a focus on place-based *ex ante* environmental policies ([Gaubert et al., 2021](#); [Conte et al., 2022](#)), for instance in the more general framework of the European Union cohesion policy. I have already started diving into these intriguing waters!

Conclusion

L'analyse économique du changement climatique se situe à l'intersection de quatre dimensions essentielles : le temps, l'espace, le risque stochastique et l'incertitude scientifique. L'interaction entre ces dimensions donne lieu à deux questions complémentaires, l'une normative et l'autre positive.

Comment les incertitudes découlant de ces quatre dimensions affectent-elles le choix social optimal à l'interface des systèmes naturels et humains ? Selon moi, ces incertitudes nécessitent la poursuite de deux programmes connectés mais distincts. Premièrement, nous devrions améliorer la modélisation du spectre spatio-temporel des futurs possibles compte tenu du risque stochastique et de l'incertitude scientifique concernant ces futurs possibles. En d'autres termes, nous devrions fonder nos décisions sur les meilleures informations disponibles. Deuxièmement, nous devrions adopter des critères de choix social qui permettent de porter un jugement optimal sur ces situations, en veillant à ce que les citoyens disposent de cadres décisionnels flexibles qui tiennent compte des divers paramètres de préférence dans les quatre dimensions examinées. Nous pouvons alors séparer notre connaissance des futurs possibles de notre attitude à l'égard de ces divers futurs possibles. Notre compréhension des futurs possibles devrait nous permettre d'élaborer des cadres de choix sociaux appropriés. Lorsque l'incertitude scientifique est la question prédominante, une plus grande flexibilité dans la prise de décision dans cette dimension est nécessaire. Lorsque l'hétérogénéité spatiale est la principale préoccupation, l'aversion pour l'inégalité peut devenir plus pertinente. Si le principal défi réside dans le risque global important lié à des événements catastrophiques irréversibles, les critères de choix social doivent être suffisamment adaptables pour intégrer l'aversion à l'égard de ces risques.

Dans le premier chapitre, nous explorons les conditions de validité de l'utilité espérée en présence d'un risque de basculement, où le risque global sur l'utilité inter-temporelle est très élevé. Ce risque global est grand en raison d'une caractéristique particulière de ces événements catastrophiques par rapport à des événements extrêmes plus classiques tels que les catastrophes naturelles : leur nature irréversible, du moins à des échelles pertinentes pour la politique économique. En conséquence, nous adaptions notre approche de modélisation du risque, en optant pour un cadre basé sur le risque de changement de régime irréversible - caractérisé par des transitions d'un état qualitatif à un autre - plutôt que sur la volatilité ou les risques réversibles typiquement modélisés le long de tendances macroéconomiques lisses. Si le seuil de basculement est franchi, le bien-être de toutes les

générations futures est faible et positivement corrélé. Dans les modèles traditionnels additifs d'utilité espérée escomptée, les planificateurs font preuve de neutralité à l'égard du risque global. Nous explorons donc des approches alternatives qui offrent aux décideurs et au public une plus grande flexibilité lorsqu'ils sont confrontés à des risques irréversibles. Nos conclusions restent toutefois nuancées, car elles dépendent de l'ampleur estimée du risque. Comme nous l'avons déjà mentionné, le processus de modélisation des futurs possibles est indissociable de la tâche consistant à déterminer collectivement notre position à leur égard. Si le risque catastrophique est très important et a des effets multiplicateurs, il peut être judicieux de se tourner vers un critère de choix social qui accorde plus de poids aux situations dans le monde où le bien-être inter-temporel est faible. Dans le cas contraire, il peut être préférable de s'en tenir à l'utilité espérée, étant donné les bonnes propriétés normatives de cette forme fonctionnelle. Tout au long de cette analyse, ainsi que dans le chapitre 2, nous avons veillé à modéliser un véritable risque stochastique. Notre cadre permet au planificateur social d'explorer l'arbre complet des résultats possibles et le spectre complet des futurs potentiels. Cela a des implications importantes en termes de calcul, car nous utilisons des méthodes de résolution globales plutôt que de nous appuyer sur des approches déterministes ou de calculer la moyenne des résultats déterministes.

Dans le deuxième chapitre, nous étendons les deux approches : nous offrons une représentation plus complète des futurs possibles et nous affinons le critère de choix social afin d'intégrer une plus grande flexibilité dans la prise en compte de l'aversion pour l'incertitude scientifique. Notre objectif était de décrire plus précisément les risques liés au point de basculement, en utilisant une dynamique calibrée dans laquelle les catastrophes potentielles émergent comme des propriétés naturelles du système dynamique, plutôt que comme des phénomènes stylisés avec des probabilités arbitraires définies *ex ante*. D'un point de vue analytique, nous étudions les interactions entre les différents types de risques au fil du temps. Plus précisément, nous examinons la relation entre les risques climatiques globaux standard - tels que la réponse climatique transitoire aux émissions cumulées, qui implique une incertitude sur la manière dont les émissions de carbone entraînent des changements de température et leurs impacts économiques ultérieurs - et les risques idiosyncratiques du sous-système, qui affectent la dynamique du système lui-même. En outre, nous tenons compte de l'incertitude scientifique, un facteur crucial qui imprègne l'analyse de ces sous-systèmes, comme le montre l'utilisation par le GIEC d'échelles de confiance et de probabilité, ainsi que les débats en cours au sein de la science climatique sur les risques de

basculement, en particulier pour l'Amazonie. Nous modélisons deux formes distinctes d'incertitude : l'incertitude concernant la relation entre le changement climatique mondial et la dynamique du sous-système, et l'incertitude concernant la forme fonctionnelle de ce sous-système dynamique. D'autres incertitudes scientifiques pourraient être étudiées, en particulier si elles interagissent avec l'incertitude concernant la dynamique des sous-systèmes en question.

Comment les incertitudes découlant des quatre dimensions décrites ci-dessus - le temps, l'espace, le risque et l'incertitude scientifique - influencent-elles nos estimations des impacts climatiques futurs à l'interface des systèmes naturels et humains ? Les progrès récents de l'économie du climat ont été moins axés sur le temps (par exemple, affiner notre compréhension des impacts économiques dynamiques du changement climatique ou étendre les analyses à des horizons à long terme comme l'échelle du millénaire), le risque (par exemple, mieux comprendre les réponses non linéaires des sociétés aux impacts climatiques) ou l'incertitude scientifique (par exemple, prédire sa trajectoire probable avec un cadre d'apprentissage). Les développements les plus significatifs ont eu lieu dans la dimension spatiale. Comme la littérature travaille de plus en plus à des échelles spatiales plus fines, sous l'impulsion de la croissance rapide de la disponibilité des données en grille pour la prise de décision, il est crucial d'évaluer les implications pour nos méthodes et approximations existantes de ces évolutions, en particulier en ce qui concerne deux aspects. Premièrement, ce qui est vrai à l'échelle mondiale peut ne pas s'appliquer aux niveaux local ou régional. Deuxièmement, nous devons tenir compte de l'impact des progrès réalisés dans une dimension sur notre compréhension des autres dimensions pour relever les défis climatiques.

Dans le troisième chapitre, nous démontrons qu'en raison de la nature non linéaire des relations entre le climat et la société, la dynamique régionale joue un rôle essentiel dans les projections d'impact climatique : les agrégations temporelles et spatiales modifient le coût agrégé et la distribution des impacts sur le bien-être futur, ainsi que le classement des risques entre les modèles climatiques. Ces différences sont dues à l'hétérogénéité régionale des dommages et des modèles de réchauffement. La désagrégation spatiale révèle comment les incertitudes des modèles climatiques concernant la distribution complète des résultats météorologiques futurs se répercutent en cascade sur les estimations des dommages régionaux. Nous nous concentrons sur la manière dont l'agrégation temporelle annuelle actuelle peut fausser les projections de l'impact climatique. En utilisant la distribution annuelle complète des températures moyennes quo-

tidien, nous saisirons les variations intra-annuelles des modèles de température, en évitant de nous appuyer sur des statistiques sommaires arbitraires du vecteur climatique à haute dimension, par exemple la moyenne annuelle ou le nombre de jours au-dessus d'un seuil. Nous pourrions aller plus loin en désagrégant davantage la dimension temporelle, par exemple en considérant séparément les températures diurnes et nocturnes, afin de mieux saisir des phénomènes tels que les jours de canicule.

Dans le chapitre 4, j'incorpore les impacts biophysiques régionaux des changements d'utilisation des terres dans un modèle spatial quantitatif dans le cadre du scénario SSP2-4.5. Ces impacts résultent des changements d'albédo, d'évapotranspiration et de rugosité de la surface, déclenchés par les changements d'usage des sols, notamment depuis et vers des terres agricoles et urbaines. D'autres impacts biophysiques et transitions dans l'utilisation des terres pourraient également être pris en compte. J'insiste sur l'importance de tenir compte des interactions entre les activités économiques régionales, les changements physiques mondiaux et régionaux et leurs impacts locaux. Ces impacts ont également des effets d'entraînement en raison des migrations, des changements dans les prix relatifs, de la spécialisation sectorielle et de la structure des échanges. Il est essentiel de tenir compte non seulement des incertitudes exogènes lors de la transposition du changement climatique mondial aux impacts locaux, mais aussi de la manière dont les décisions locales influencent ces processus de manière endogène. Les choix locaux en matière d'utilisation des sols déterminent de manière significative les impacts climatiques futurs et peuvent compromettre les avantages escomptés des mesures d'adaptation. De nombreuses incertitudes au-delà des effets primaires des émissions mondiales restent sous-étudiées. Bien que secondaires en termes globaux, ces mécanismes peuvent avoir des conséquences distributives importantes au niveau régional et des effets qualitatifs plus précis sur les modèles. Le fait de se concentrer uniquement sur des scénarios carbone-intensifs tels que le SSP5-8.5 limite notre capacité à examiner ces dynamiques plus complexes.

Cette thèse me permet de proposer quelques recommandations modestes en matière de politique publique.

Premièrement, tous les risques climatiques ne sont pas égaux. Les risques ayant des effets multiplicateurs et des conséquences irréversibles doivent être traités avec une plus grande urgence, ce qui justifie des réductions d'émissions substantielles dès aujourd'hui. Une conclusion similaire pourrait être tirée pour

les événements répétés mais réversibles qui entraînent des dommages irréversibles au fil du temps. Toutefois, les interactions non linéaires potentielles entre les systèmes humains et les événements climatiques répétés restent sous-explorées - tant dans les estimations de la fonction de dommage dans la littérature économétrique que dans les modèles théoriques, où les impacts sont généralement supposés être additifs.

Deuxièmement, je propose des politiques de gestion des grands sous-systèmes climatiques, tels que la forêt amazonienne. Je recommande de mesurer l'impact des émissions de carbone sur la dynamique de ces sous-systèmes afin de répartir plus équitablement la responsabilité des futurs changements. Cette approche pourrait également permettre de collecter des fonds pour soutenir les mécanismes d'incitation coasiens en vue d'une gestion de ces sous-systèmes au niveau régional. En outre, la prise en compte de la dynamique du système dans son ensemble peut améliorer la gestion régionale, par exemple dans les analyses coûts-avantages de la déforestation dans les forêts tropicales, en tenant compte de l'impact des changements marginaux sur la résilience à long terme du sous-système. Bien que ces mécanismes ne représentent qu'une petite partie du coût social du carbone, ils représentent des montants significatifs lorsqu'ils sont appliqués à la taxation mondiale de toutes les émissions de GES.

Troisièmement, je plaide en faveur d'une prise de décision régionale mieux informée sur l'incertitude climatique, en particulier lors de la réduction de l'échelle du changement climatique mondial en fonction des impacts locaux. Les plans d'adaptation à des échelles plus fines, du niveau national au niveau local, devraient être conçus pour être robustes à la distribution complète des futurs possibles, plutôt que de se concentrer sur un scénario moyen. Le scénario moyen masque des incertitudes significatives, qui non seulement persistent mais s'intensifient souvent à plus petite échelle. Surtout, il ne tient pas compte des diverses sources d'incertitude. La variance quantifiable des projections d'impact climatique régional est influencée par l'incertitude des scénarios (différences entre les SSP), l'incertitude des modèles climatiques (variations des réponses des modèles du système terrestre aux SSP), la variabilité interne (due à la nature chaotique du climat, qui varie dans l'espace et le temps), ainsi que par les décisions prises lors du traitement ou de la correction des biais des résultats des modèles climatiques. En outre, l'incertitude dans l'estimation des fonctions dose-réponse affecte les projections des dommages futurs. La différenciation et la hiérarchisation de ces sources d'incertitude peuvent fournir des orientations plus claires pour la prise de décision à l'échelle régionale.

Quatrièmement, j'appelle à des politiques d'adaptation qui soient robustes aux rétroactions négatives potentielles sur les impacts climatiques locaux. Les changements d'usage des sols ont des répercussions considérables sur la biodiversité et le changement climatique mondial. Ils ont également une incidence sur les impacts climatiques régionaux. Dans mon travail, je suggère d'examiner attentivement les effets de rétroaction que nos activités économiques et nos mesures d'adaptation à un scénario d'impact climatique donné peuvent avoir sur ces impacts régionaux, ainsi que les retombées potentielles. Ces rétroactions sont susceptibles d'inverser et de réduire les gains de bien-être attendus de l'adaptation dans le cadre d'un scénario de réchauffement. Des politiques d'adaptation robustes doivent tenir compte de ces interactions plus complexes entre l'activité économique, le changement climatique et les incidences climatiques à l'échelle régionale afin d'éviter toute mauvaise adaptation.

Cette recherche a plusieurs limites. Tout d'abord, les problèmes à haute dimension sont souvent numériquement difficiles à résoudre lorsqu'ils intègrent toutes les dimensions simultanément, ce qui nécessite une approche cloisonnée des différentes dimensions. Cette segmentation signifie que le coût total de ces incertitudes en termes de bien-être n'est pas entièrement pris en compte. Souvent, on suppose que les coûts de chaque nouvelle incertitude sont additifs, ce qui est peu probable en raison des interactions dynamiques et de l'interdépendance entre les sous-systèmes à l'interface des systèmes naturels et humains. Deuxièmement, alors que les connaissances physiques ont considérablement progressé grâce aux données maillées, les données socio-économiques à une échelle et une qualité comparables font généralement défaut, en particulier en dehors des pays de l'OCDE et de la Chine. L'établissement d'un centre de recherche à l'Université Paris-Saclay pour développer systématiquement des ensembles de données harmonisés ou mettre en œuvre des pratiques de réduction d'échelle harmonisées pour les données socio-économiques maillées à l'échelle mondiale pourrait fournir un bien public mondial substantiel et avoir un impact important sur la recherche. Certains chercheurs se penchent déjà sur ces questions ([Mikou et al., 2024](#)).

Ces études ouvrent la voie à de nombreuses possibilités de recherche futures. En m'appuyant sur les quatre dimensions examinées précédemment, je vise à développer une approche plus intégrée qui fait le lien entre les perspectives positives et normatives. Mon objectif est de conserver les données spatiales détaillées et évolutives de l'approche positive, ainsi que les informations sur les mécanismes d'adaptation endogènes. Simultanément, je souhaite préserver le cadre éthique inter-temporel optimal de l'approche normative, pour aborder le risque

économique, le risque climatique et d'autres questions cruciales telles que la perte de biodiversité et les limites planétaires, y compris leurs interactions complexes. Pour ce faire, nous devons modéliser des mécanismes géophysiques crédibles et leurs interactions avec l'activité économique. En outre, pour faire progresser cette approche, il faudra améliorer la modélisation de la robustesse, de l'adaptabilité et des propriétés émergentes des systèmes, qui résultent des interactions complexes entre les composants des systèmes, éléments qui ne peuvent être prédicts par l'analyse des composants pris isolément. Au-delà de l'espace, du temps, du risque et de l'incertitude scientifique, il existe d'autres aspects fascinants du défi climatique et de ses implications politiques à explorer. Il s'agit notamment de la complexité du système (par exemple, les interactions, les boucles de rétroaction), de notre attitude à l'égard de cette complexité et de son interaction avec les attitudes plus conventionnelles vis-à-vis du risque et de l'incertitude scientifique (Oprea, 2024). Enfin, il est nécessaire de mieux comprendre les préférences en matière de gestion de l'exposition inégale aux risques, y compris les incidences marchandes et non-marchandes à différentes échelles (telles que la santé) et les différentes capacités d'adaptation. Cette exploration pourrait conduire à mettre l'accent sur les politiques environnementales basées sur le lieu ("place-based") et *ex ante* (Gaubert et al., 2021; Conte et al., 2022), par exemple dans le cadre plus général de la politique de cohésion de l'Union Européenne. J'ai déjà commencé à plonger dans ces eaux intrigantes !

Bibliographie

- B. Conte, K. Desmet, and E. Rossi-Hansberg. On the geographic implications of carbon taxes. Technical report, National Bureau of Economic Research, 2022.
- C. Gaubert, P. M. Kline, and D. Yagan. Place-based redistribution. Technical report, National Bureau of Economic Research, 2021.
- M. Mikou, A. Vallet, and C. Guivarch. Harmonized disposable income dataset for europe at subnational level. *Scientific Data*, 11(1) :308, 2024.
- R. Oprea. Decisions under risk are decisions under complexity. *American Economic Review*, 2024.